

**APPROACHES TO THE DISCOVERY OF  
BIOMARKERS OF PROSTATE  
CARCINOGENESIS IN TRAMP MICE AND  
OF CHEMOPREVENTIVE EFFICACY OF  
TEA POLYPHENOLS**

Thesis submitted for the degree of Doctor of Philosophy at the  
University of Leicester

**Friederike Teichert**  
**Department of Cancer Studies and Molecular Medicine**  
**University of Leicester**

August 2008

# **APPROACHES TO THE DISCOVERY OF BIOMARKERS OF PROSTATE CARCINOGENESIS IN TRAMP MICE AND OF CHEMOPREVENTIVE EFFICACY OF TEA POLYPHENOLS**

Friederike Teichert

To improve prostate cancer management in humans who have, or are at risk of developing, the disease, biomarkers are required to aid early diagnosis and monitoring of response to chemotherapeutic or chemopreventive intervention.

In this project metabonomic and peptidomic approaches were used to study biological changes associated with prostate carcinogenesis in a transgenic mouse model (TRAMP, TRansgenic Adenocarcinoma of the Mouse Prostate). Observed changes were compared with pathological alterations. Metabolome and peptidome analyses were conducted in TRAMP mice exposed to chemopreventive intervention with green tea polyphenols (GTP). Effects of consumption of GTP or black tea theaflavins on the plasma and urine metabonome/peptidome in patients with benign prostatic hyperplasia (BPH) were also investigated. Oxidative stress status reflected by urinary 8-oxo-7,8-dihydro-2'-deoxyguanosine (8-oxodG) was assessed in mice and humans on tea polyphenols.

Metabonomic profiling revealed that at early stages of carcinogenesis in mice, alterations of tumour levels of choline metabolites resembled the human disease. In contrast, in advanced stages of TRAMP prostate carcinogenesis, phospholipid metabolism is affected differently by malignancy than in its human counterpart. Disturbed prostate-specific citrate metabolism seems common to both human and TRAMP prostate tumours when compared to normal tissue. These results suggest that the TRAMP mouse may be a better model with respect to humans of early stage carcinogenesis with minor proliferative lesions than of more advanced stages of malignancy.

Urinary 8-oxodG levels were not affected by presence of prostate cancer or intervention with tea. Metabolic profiling gave evidence for an effect of GTP on energy metabolism in both mice and humans. Although TRAMP and GTP-group-specific metabonomic and peptidomic changes were found in plasma and urine, none of these metabolites or peptides could be unambiguously identified as biomarkers of carcinogenesis or GTP exposure. Among possible confounding factors which should be taken into consideration in future metabonomic/peptidomic studies is the host's gut microflora.

## **Acknowledgements**

This work would not have been possible without the help and support of many people. I have worked in many different labs in the last few years and was very lucky to only have met friendly and helpful people.

First of all I would like to thank my supervisors **Prof Andy Gescher** and **Prof Peter Farmer** for their support in every aspect and encouragement throughout the duration of my PhD. It has been a great pleasure to be your student. An extra thank you to Andy for being so positive and helpful no matter what trifles. A very special thank you to **Dr Richard Verschoyle** who has helped with all the animal work and was an endless source of advice even after his retirement. I would also like to express my gratitude to **Dr Don Jones** who has supervised the peptidomic analyses and was always full of enthusiasm no matter how bad it seemed. Big thanks to **Dr Richard Willingale** for sorting out the bioinformatic analysis of the peptide project and patiently answering all my questions and **John Lamb** for running most of the samples on the Q-Tof. The 8-oxodG analysis was supervised by **Dr Raj Singh**. Thank you for all your advice and encouragement. I am also very grateful to **Dr Peter Greaves** who has carried out the pathological assessment of the animal studies and has always given great advice. Many thanks to **Jenny Edwards** for processing all the pathology slides and also to **Richard Edwards** for carrying out the immunohistochemical staining. I am grateful to **Stephanie Euden** and **Sharon Platon** for carrying out the genotyping of the mice. I thank **Dr Timothy Gant** for making the microarray analysis possible and advising the experiment and **Dr Reginald Davies** and **Joan Riley** for help with the microarray and RT-PCR analysis. I would also like to thank all staff at the animal facility for their help with my studies.

At Imperial College in London **Dr Hector Keun** supervised the NMR based metabonomic work. Thank you very much for your help, support and patience; you have made a wonderful collaboration possible. I am very grateful to **Orla Teahan** who has helped me a lot in the lab and provided accommodation when I worked in London. I would also like to thank **Dr Muireann Coen** for help with assignments and everyone else in the group for helping me and making my stays in London a pleasurable time.

At AstraZeneca **Prof Ian Wilson** has supervised the LC-MS based metabonomic work. Thank you for your support and marvellous enthusiasm. Many thanks to **Timothy Sangster, Richard Payne, Dr Christopher Smith, Toby Athersuch, Dr Eleni Gika, Dr George Theodorides** and all the other lab members for their help and friendliness. I would like to thank **Dr Eva Lenz** for NMR analyses and **Dr Richard Gallagher** MS analyses. Thank you to **Dr Madeleine Brady and family** for giving me a warm temporary home during my visits at AstraZeneca.

I would like to make a special thank you to all the people I have met and worked with over the course of my PhD.

A very, very special thank you to **my parents, my sister and Raj**; you have always supported me and found the right words to bring me back on track when I was down (“Den Kampf aufnehmen und gewinnen!”, “Schackaaa”, “You can do it!”). I am so glad to have you.

To my friends **Christina, Iris and Colin**: Thank you for understanding and listening to my moaning. I am sorry to have neglected you a bit in the last year.

This thesis is dedicated to my wonderful family.

<b>Contents</b>	<b>Page</b>
Title	i
Abstract	ii
Acknowledgements	iii
Dedication	v
Content	vi
Figures	xiii
Tables	xix
Equations	xxi
Abbreviations	xxii
<b>Chapter 1: Introduction</b>	
1.1 Prostate cancer	2
1.1.1 Epidemiology and risk factors	2
1.1.2 Pathology, diagnosis, staging and treatment	4
1.1.3 Tumour metabolism	6
1.2 Prostate cancer chemoprevention	8
1.2.1 General concepts	8
1.2.2 Chemoprevention of prostate cancer by tea polyphenols	9
1.2.2.1 Green and black tea polyphenols	9
1.2.2.2 Epidemiological and clinical evidence for prostate cancer prevention by tea	11
1.3 The TRAMP mouse model of human prostate cancer	13
1.3.1 Chemoprevention by tea polyphenols in the TRAMP mouse model	17
1.4 Relevant analytical platforms for biomarker discovery	19
1.4.1 Metabonomic approaches in cancer research	19
1.4.1.1 <sup>1</sup> H-NMR based metabonomics in cancer research	20
1.4.1.2 LC-MS based metabonomics in cancer research	22
1.4.2 Peptidomic approaches in cancer research	24

1.4.3 Data analysis for global profiling approaches	27
1.5 Urinary 8-oxo-7,8-dihydro-2'-deoxyguanosine (8-oxodG) as a biomarker of oxidative stress status	29
1.6 Aims	32
1.6.1 Main aim	33
1.6.2 Specific objectives	33
<b>Chapter 2: Materials and Methods</b>	
2.1 Materials	37
2.1.1 General chemicals and kits	37
2.1.2 Animals	37
2.1.3 Animal diet	37
2.1.4 Green Tea Polyphenols (GTP)	37
2.1.5 Specimen collection	38
2.1.6 Muricholic acid (MCA) standards	38
2.2 Methods	
2.2.1 Studies and tissue collection	39
2.2.1.1 Maintenance of C57BL/6J TRAMP mouse colony	39
2.2.1.2 Determination of genotype	39
2.2.1.3 Study for method validation	39
2.2.1.4 TRAMP – C57BL/6J wild type study	40
2.2.1.5 TRAMP GTP intervention study	40
2.2.1.6 Clinical tea polyphenol intervention study	41
2.2.1.7 Plasma	42
2.2.1.8 Tissue and urine samples	42
2.2.1.9 Tissue processing and histology	42
2.2.2 Peptide profiling	42
2.2.2.1 Omix <sup>®</sup> peptide extraction	42
2.2.2.2 BOND ELUTE <sup>®</sup> peptide extraction	43
2.2.2.3 Strata <sup>™</sup> -X peptide extraction	43

2.2.2.4 Oasis <sup>®</sup> peptide extraction	44
2.2.2.5 Microcon <sup>®</sup> filtration	44
2.2.2.6 Precipitation method	44
2.2.2.7 Albumin / IgG removal	45
2.2.2.8 MALDI-Tof mass spectrometry	45
2.2.2.9 Mathematical data processing of MALDI-MS data	46
2.2.3 Urinary 8-oxodG	47
2.2.3.1 Synthesis of <sup>15</sup> N-labelled internal standard	47
2.2.3.2 Urine clean up method modified after Lin <i>et al.</i>	47
2.2.3.3 Urine clean up method HLB I	48
2.2.3.4 Urine clean up method HLB II	48
2.2.3.5 Determination of urinary 8-oxodG by HPLC-MS/MS	49
2.2.3.6 Determination of creatinine by Jaffé reaction	50
2.2.3.7 Determination of creatinine by LC-MS/MS	51
2.2.3.8 Determination of specific gravity	52
2.2.4 NMR-based metabolic profiling	52
2.2.4.1 Urine sample preparation for <sup>1</sup> H NMR analysis	52
2.2.4.2 Plasma sample preparation for <sup>1</sup> H NMR analysis	53
2.2.4.3 Preparation of aqueous tissue extracts	53
2.2.4.4 Tissue preparation for HRMAS <sup>1</sup> H NMR analysis	53
2.2.4.5 NMR data acquisition and processing	54
2.2.4.6 Spectral integration and statistical analyses	55
2.2.5 Immunohistochemical analysis for ChK	55
2.2.6 RNA extraction from prostate tissue	56
2.2.7 Real Time PCR analysis	57
2.2.8 Microarray analysis	57
2.2.9 HPLC-MS based metabolic profiling	58
2.2.9.1 Urine sample preparation	58
2.2.9.2 Plasma sample preparation	59
2.2.9.3 HPLC-MS analysis of urine and plasma (10min gradient)	59





<b>Chapter 5: Effect of green tea constituents on features of carcinogenesis in the TRAMP mouse model</b>	160
5.1 Effect of GTP on prostate tissue of TRAMP mice	160
5.1.1 Pathological assessment of prostate tissue	160
5.1.2 Effect of GTP on prostate weights in TRAMP mice	161
5.1.3 Effect of GTP on metabolic profile of prostate tissue of TRAMP and wild type mice	162
5.1.4 Discussion	165
5.2. GTP effects on the urinary metabolic profile of TRAMP mice	168
5.2.1 <sup>1</sup> H-NMR metabolic profiling of urine	168
5.2.1.1 Effect of GTP on urinary metabolite profile of TRAMP mice	168
5.2.1.2 Effect of TRAMP genotype on urinary metabolite profile	174
5.2.1.3 Age related changes of the urinary metabolic profile	175
5.2.2 LC-MS metabolic profiling of urine	177
5.2.3 Discussion	179
5.3 GTP effects on the plasma metabolic profile of TRAMP mice	180
5.3.1 <sup>1</sup> H-NMR metabolic profiling of plasma	180
5.3.2 Discussion	184
5.4 Effects of GTP on urine and plasma peptide profiles of TRAMP mice	186
5.4.1 Peptidomic profiling of urine	186
5.4.2 Peptidomic profiling of plasma	192
5.4.3 Discussion	196
5.5 Effect of GTP on levels of urinary 8-oxodG	197
5.5.1 Results	197
5.5.2 Discussion	200
5.6 Summary	201

<b>Chapter 6: Effect of tea constituents on patients with benign prostatic hyperplasia</b>	
6.1 Effects of tea polyphenols on the urinary and plasma metabonome	203
6.1.1 <sup>1</sup> H-NMR profiling of urine	203
6.1.2 <sup>1</sup> H-NMR profiling of plasma	209
6.1.3 Discussion	213
6.2 Effects of tea polyphenols on the urinary and plasma peptidome	217
6.2.1 Peptide profiling of urine	217
6.2.2 Peptide profiling of plasma	221
6.2.3 Discussion	223
6.3 Effects of tea polyphenols on urinary 8-oxodG levels	225
6.3.1 Results	225
6.3.2 Discussion	227
6.4 Summary	229
<b>Chapter 7: Final discussion</b>	
7.1 The use of TRAMP mice for chemoprevention studies	231
7.1.1 General aspects	231
7.1.2 GTP efficacy in the TRAMP mouse model	232
7.2 The role of the gut microflora in chemoprevention	234
7.3 Implications for clinical intervention studies	237
7.3 Summary	238
<b>Publications</b>	239
<b>Bibliography</b>	259

<b>Figures</b>	<b>Page</b>
<b>Chapter 1</b>	
1.1 Structures of theaflavins	10
1.2 Structures of tea catechins	11
1.3 Schematic image of the normal adult human prostate	15
1.4 Schematic image of the normal adult mouse prostate	16
1.6 Repair mechanisms that possibly contribute to 8-oxodG excreted in urine	31
1.6 Overview of studies conducted	35
<b>Chapter 3</b>	
3.1 MALDI-MS spectra of (A) mouse and (B) human plasma extracted with Omix <sup>®</sup> pipette tips	66
3.2 MALDI-MS spectrum of human plasma precipitated with 50% acetonitrile	67
3.3 MALDI-MS spectra of mouse plasma extracted with Oasis <sup>®</sup> HLB cartridges (A) with or (B) without subsequent Microcon <sup>®</sup> filtration	69
3.4 MALDI-MS spectra of human (A) and mouse (B) urine extracted with Oasis <sup>®</sup> HLB cartridges	71
3.5 Typical chromatogram obtained from human urine showing the SRM channels for (A) 8-oxodG and (B) [ <sup>15</sup> N <sub>5</sub> ]8-oxodG	74
3.6 Typical chromatogram obtained from mouse urine showing the SRM channels for (A) 8-oxodG and (B) [ <sup>15</sup> N <sub>5</sub> ]8-oxodG	75
3.7 Chromatogram of interfering peaks obtained from blank water injections	78
3.8 Typical chromatogram obtained from mouse urine showing the SRM channels for [ <sup>2</sup> H <sub>3</sub> ]creatinine and creatinine	79
3.9 Typical chromatogram obtained from human urine showing the SRM channels for [ <sup>2</sup> H <sub>3</sub> ]creatinine and creatinine	80

## Chapter 4

4.1 Prostatic tissue from TRAMP mice of 8 (A) or 28 weeks of age (B)	83
4.2 Typical <sup>1</sup> H-NMR spectrum of an aqueous prostate tissue extract	85
4.3 Hierarchical clustering of metabolite levels	88
4.4 Matrices of correlation coefficients (r) between metabolite levels	89
4.5 Individual metabolite levels for GPI, glutamate and GPI / glutamate ratio	90
4.6 Median <sup>1</sup> H-NMR spectra of aqueous tissue extracts and median HRMAS NMR spectra of intact tissue	91
4.7 Immunohistochemical staining for ChK-β	93
4.8 Expression levels of <i>ChK-α</i> and <i>ChK-β</i> mRNA	94
4.9 Pathways of phosphatidylcholine synthesis and degradation	95
4.10 Typical <sup>1</sup> H-NMR urine spectrum of a 28 week old wild type mouse	102
4.11 PCA scores plot of urine NMR spectra	103
4.12 Difference/correlation spectrum of urine spectra from 8 week old TRAMP and wild type mice	104
4.13 Difference/correlation spectrum of urine spectra from 28 week old TRAMP and wild type mice	105
4.14 Difference/correlation spectrum of urine spectra from 8 week and 28 week old TRAMP and wild type mice	106
4.15 Summary of changes in urinary metabolome	107
4.16 TIC chromatogram of urine from a 28 week old wild type mouse analysed in negative ionisation mode	109
4.17 PCA scores plots of urine samples analysed by LC-MS in negative ionisation mode	109
4.18 Negative ionisation TIC chromatograms of test mix injection prior and post sample analysis	110
4.19 Negative ionisation mass spectrum of theophylline	110
4.20 Scores and loadings plots of PLS-DA models for maximal separation between TRAMP and wild type mice	111
4.21 Intensity profiles of potentially related marker ions at (A) m/z 407.6 and (B) m/z 453.5 both eluting at 6.58min	114

4.22 Overlaid extracted ion chromatograms showing $^{13}\text{C}$ isotopes of a compound with the m/z 407	114
4.23 Aliphatic region of $^1\text{H}$ -NMR spectra of SPE extracts of pooled mouse urine samples	116
4.24 Overlaid extracted ion chromatograms of a mouse urine sample analysed in negative ionisation mode using a gradient over 32min	116
4.25 Overlaid extracted ion chromatograms (407.0-407.6m/z) of a urine sample and $5\mu\text{g/ml}$ standard solutions of $\alpha$ -, $\beta$ - and $\omega$ -muricholic acid and cholic acid	117
4.26 Overlaid extracted ion chromatograms of a mouse urine sample (TRAMP, 8 weeks), $\omega$ -MCA standard ( $5\mu\text{g/ml}$ ) and a mouse urine sample spiked with $\omega$ -MCA standard	118
4.27 Product ion spectra for $\omega$ -MCA peaks from (A) a mouse urine sample (TRAMP, 8 weeks), (B) $\omega$ -MCA standard ( $5\mu\text{g/ml}$ ) and (C) a urine sample spiked with $\omega$ -MCA standard	119
4.28 TIC chromatogram of urine from a 28 week old TRAMP mouse analysed in positive ionisation mode	120
4.29 PCA scores plots of urine samples analysed by LC-MS in positive ionisation mode	121
4.30 Synthesis of $\alpha$ -, $\beta$ - and $\omega$ -muricholic acids (MCA) in liver and intestine	124
4.31 Typical $^1\text{H}$ -NMR plasma spectrum of an 8 week old TRAMP mouse	127
4.32 PCA scores plot of plasma NMR spectra	128
4.33 TIC chromatogram of a plasma sample obtained from a 28 week old TRAMP mouse analysed in (A) negative and (B) positive ionisation mode	129
4.34 PCA scores plots of plasma samples analysed by LC-MS in negative ionisation mode	130
4.35 PCA scores plots of plasma samples analysed by LC-MS in positive ionisation mode	130
4.36 PCA scores plots of plasma samples analysed by LC-MS in (A) negative ionisation mode and (B) positive ionisation mode using a 30min gradient	132

4.37 Combined and binned mass spectra of all mouse urine samples analysed by MALDI-MS	135
4.38 Count values heat map of significant peaks of urine MALDI spectra	135
4.39 PCA scores plots of urine samples analysed by MALDI-MS	136
4.40 Scores and loadings plots of PLS-DA models for maximal separation between TRAMP and wild type mice at (A) 8 and (B) 28 weeks of age	137
4.41 Difference/correlation plots of TRAMP versus wild type mice at (A) 8 weeks and (B) 28 weeks of age	139
4.42 Combined and binned mass spectra of all mouse plasma samples analysed by MALDI-MS	140
4.43 Count values heat map of significant peaks of plasma MALDI spectra	141
4.44 PCA scores plots of plasma samples analysed by MALDI-MS	142
4.45 Scores and loadings plots of PLS-DA models for maximal separation between TRAMP and wild type mice at (A) 8 and (B) 28 weeks of age	143
4.46 Levels of urinary 8-oxodG in TRAMP and wild type mice	152
 <b>Chapter 5</b>	
5.1 Prostate weights in 8 week (A) and 29 week old (B) mice	161
5.2 PCA scores plot of all prostate extract NMR spectra	163
5.3 Scores plots of PLS-DA models generated to maximise the difference between TRAMP and wild type mice at (A) 8 and (B) 29 weeks of age regardless of treatment	163
5.4 Typical <sup>1</sup> H-NMR urine spectrum of a 28 week old TRAMP mouse receiving 0.05% GTP in the drinking water	169
5.5 PCA scores plot of all urine NMR spectra	170
5.6 Scores plot of a PLS-DA model generated to maximise the separation between 29 week old TRAMP and wild type mice	170
5.7 Median spectra of urine from 29 week old mice zoomed in on TRAMP specific regions that were TRAMP specifically affected by GTP	172
5.8 Median urine NMR spectra of all groups	174

5.9 Difference/correlation spectrum of urine spectra from 8 week and 28 week old TRAMP and wild type mice	176
5.10 PCA scores plots of all urine samples analysed in negative ionisation mode	178
5.11 PCA scores plots of all urine samples analysed in positive ionisation mode	178
5.12 Typical <sup>1</sup> H-NMR plasma spectrum of a 28 week old TRAMP mouse receiving 0.05% GTP in the drinking water	180
5.13 PCA scores plots of all plasma samples analysed by <sup>1</sup> H-NMR	181
5.14 Median <sup>1</sup> H-NMR spectra zoomed in on regions of plasma lipid signals	183/4
5.15 Combined and binned mass spectra of all mouse urine samples analysed by MALDI-MS	187
5.16 PCA scores plots of all urine samples analysed by MALDI-MS	187
5.17 Scores plot of a PLS-DA model generated to maximise separation between 29 week old TRAMP and wild type mice	188
5.18 Scores and loadings plots of PLS-DA models for maximal separation between GTP- and water-fed TRAMP mice at (A) 8 and (B) 29 weeks	189
5.19 Combined and binned mass spectra of all mouse plasma samples analysed by MALDI-MS	192
5.20 PCA scores plots of all plasma samples analysed by MALDI-MS	193
5.21 Scores and loadings plots of PLS-DA models for maximal separation between GTP- and water-fed TRAMP mice at (A) 8 and (B) 29 weeks	194
5.22 Urinary 8-oxodG levels for individual animals normalised to creatinine	198

## Chapter 6

6.1 Typical <sup>1</sup> H-NMR urine spectrum from a patient with BPH after four weeks of intervention with GTP	204
6.2 PCA scores plots of all urine samples analysed by <sup>1</sup> H-NMR	205
6.3 Median urine spectra of control, GTP and BTT samples zoomed in on the region of suspected GTP metabolites	205
6.4 Metabolite levels in individual samples pre or post treatment	208
6.5 <sup>1</sup> H-NMR spectrum of plasma from a patient with BPH after four weeks of GTP intervention	209
6.6 PCA scores plots of all plasma samples analysed by <sup>1</sup> H-NMR	210
6.7 Median NMR spectra of all treatment groups pre and post intervention zoomed in on the signal of CH <sub>3</sub> groups of the plasma lipids	212
6.8 Metabolite levels in individual samples pre or post treatment	212
6.9 Glucose-alanine-cycle	215
6.10 Combined and bucketed mass spectra of all urine samples analysed by MALDI-MS	217
6.11 PCA scores plots of all urine samples analysed by MALDI-MS	218
6.12 Section of difference/correlation plot of GTP and control samples after subtraction of the pre-dose from the post dose peak list in each individual sample	219
6.13 Combined and bucketed mass spectra of all plasma samples analysed by MALDI-MS	221
6.14 PCA scores plots of all plasma samples analysed by MALDI-MS	222
6.15 Concentrations of urinary 8-oxodG measured in patients with BPH before and after treatment with GTP, BTT, or no treatment	226

<b>Tables</b>	<b>Page</b>
<b>Chapter 3</b>	
3.1 Comparison of peptide extraction methods for plasma	68
3.2 Comparison of peptide extraction methods for urine	71
3.3 Comparison of SPE methods for urine for the determination of 8-oxodG	73
<b>Chapter 4</b>	
4.1 Median relative metabolite peak areas in prostate tissues of 8 week or 28 week old wild type or TRAMP mice	86
4.2 Median metabolite ratios in prostate tissues of 8 week or 28 week old wild type or TRAMP mice	87
4.3 Potential urinary biomarkers of TRAMP genotype disclosed by HPLC- MS analysis in negative ionisation mode	112
4.4 Potential urinary biomarkers of TRAMP genotype disclosed by HPLC- MS analysis in positive ionisation mode	122
4.5 Significant changes in the urinary peptide profile of TRAMP mice compared to age matched wild type mice	138
4.6 Significant changes in the plasma peptide profile of TRAMP mice compared to age-matched wild type mice	144
4.7 Marker ions which differentiate TRAMP and wild type mice, and similar marker ions found in human studies	146
4.8 Median values for urinary 8-oxodG across the four animal groups using different data normalisation techniques	151
4.9 Median values for measurements used for the normalisation of 8-oxodG concentrations	152
4.10 Changes in 8-oxodG levels between TRAMP and wild type mice	153

<b>Chapter 5</b>	
5.1 Effects of GTP on prostate tissue metabolite levels	165
5.2 TRAMP specific effects of GTP on urinary metabolite levels in 29 week old TRAMP mice	173
5.3 Effects of TRAMP genotype on urinary metabolite levels	175
5.4 Effect of aging on urinary metabolite levels	176
5.5 Significant changes in urinary peptide profile of GTP-fed TRAMP mice compared to age matched water-fed TRAMP mice	190
5.6 Significant changes in urinary peptide profile of TRAMP mice compared to age matched wild type mice	191
5.7 Significant changes in plasma peptide profile of GTP-fed TRAMP mice compared to age matched water-fed TRAMP mice	195
5.8 Significant changes in plasma peptide profile of TRAMP mice compared to age matched wild type mice	196
5.9 Median values for urinary 8-oxodG using different data normalisation techniques	198
5.10 Changes in 8-oxodG levels with respect to GTP treatment, transgenesis and age	199
 <b>Chapter 6</b>	
6.1 Levels of significance of urinary metabolite changes within one treatment group (Wilcoxon test)	207
6.2 Levels of significance of plasma metabolite changes within one treatment group (Wilcoxon test)	211
6.3 Statistically significant changes in the urinary peptide profile after four weeks of GTP or BTT intervention	220
6.4 Statistically significant changes in the plasma peptide profile after four weeks of GTP or BTT intervention	223
6.5 Median values for urinary 8-oxodG expressed in nmol/mmol creatinine and percent changes after tea polyphenol intervention	226
 <b>Chapter 7</b>	
7.1 Composition of GTP used in TRAMP chemoprevention studies	233

<b>Equations</b>	<b>Page</b>
1.1 Bio-energetic balance of net citrate production (A) versus normal glucose oxidation via the Krebs cycle (B)	6
2.1 Calculation of creatinine concentration	50

## Abbreviations

8-oxodG	8-oxo-7,8-dihydro-2'-deoxyguanosine
BPH	benign prostatic hyperplasia
BMI	body mass index
BTT	black tea theaflavins
ChK	choline kinase
Cho/Cit	choline to citrate ratio
DEPC	diethylpyrocarbonate
DRE	digital rectal examination
EGCG	(-)-epigallocatechin-3-gallate
ESI	prostatic intraepithelial neoplasia
FWHM	full width at half maximum
GPC	glycero-phosphocholine
GPI	glycero-phosphoinositol
GTP	green tea polyphenols
HEPES	4-(2-hydroxyethyl)-1-piperazineethanesulfonic acid
HG-PIN	high grade- prostatic intraepithelial neoplasia
HILIC	hydrophilic interaction liquid chromatography
HPLC	high performance liquid chromatography
HRMAS	high-resolution magic angle spinning
IGFBP-3	insulin-like growth factor binding protein 3
IGF-1	insulin-like growth factor-1
IgG	immunoglobulin G
LC	liquid chromatography
m/z	mass to charge ratio
MALDI	matrix-assisted laser desorption ionisation
MCA	muricholic acid
MRSI	magnetic resonance spectroscopic imaging
MS	mass spectrometry
MS/MS	tandem mass spectrometry
NER	nucleotide excision repair
NMR	nuclear magnetic resonance

PC	phosphocholine
PCA	principal component analysis
PCR	polymerase chain reaction
PEG	polyethylene glycol
PIN	prostatic intraepithelial neoplasia
PLS-DA	Partial Least Squares-Discriminate Analysis
ppm	parts per million
PSA	prostate-specific antigen
QC	quality control
ROS	reactive oxygen species
RP	reversed-phase
SBS	small bowel syndrome
SDS	sodium dodecyl sulphate
SELDI	surface enhanced laser desorption ionisation
SG	specific gravity
SIBO	small intestine bacterial overgrowth
SPE	solid phase extraction
SRM	selected reaction monitoring
SSC	saline – sodium citrate buffer
SV40	simian virus 40
TAg	SV40 large tumour antigen
tCho/Cit	total choline to citrate ratio
TFA	trifluoroacetic acid
TIC	total ion current
TMNO	trimethylamine-N-oxide
Tof	time of flight
TRAMP	TRansgenic Adenocarcinoma of the Mouse Prostate
TSP	3-(trimethylsilyl-2,2,3,3- <sup>2</sup> H <sub>4</sub> )-1-propionate
UDPx	UDP-linked sugars
UPLC	ultra performance liquid chromatography

# Chapter 1

## **1. Introduction**

This thesis describes work that focused on biological changes associated with prostate cancer in a transgenic mouse model and intervention with tea polyphenols with the aim of preventing it. The work encompasses metabolomic and peptidomic approaches as well as assessment of oxidative stress status as reflected by urinary 8-oxo-7,8-dihydro-2'-deoxyguanosine (8-oxodG). The effects of green tea polyphenols (GTP) and black tea theaflavins (BTT) on patients with benign prostatic hyperplasia (BPH) were investigated by the same approaches. The introduction provides an overview of chemoprevention of prostate cancer by tea in humans and in the TRAMP mouse model. The background for the analytical methods used here is also described.

### **1.1 Prostate Cancer**

#### **1.1.1 Epidemiology and risk factors**

With nearly a quarter (24%) of the total, prostate cancer is the most common male cancer in the UK and second leading cause of cancer related deaths after lung cancer. Indeed, 13% of all male cancer deaths are accounted for by prostate cancer. The chance that a man will be diagnosed with the disease at some stage in his life is currently 1:14 in the UK. Men under the age of fifty are rarely affected but the incidence increases exponentially with age. It is estimated that by the age of 80 up to 70% of men show histopathological evidence of cancer in the prostate. This makes age the greatest risk factor that a man will be diagnosed with prostate cancer (Cancer Research UK cancer statistics: <http://info.cancerresearchuk.org/cancerstats/types/prostate/>).

Apart from age, prostate cancer incidence is also greatly influenced by ethnicity and geography. While the incidence rate per 100000 is 137.0 amongst African Americans, it is 100.8 for white Americans and only 47.2 and 20.2 in Japanese and Chinese

Americans, respectively, (Los Angeles). In China (Tianjin), India (Bombay) and Japan (Hiroshima) these rates are only 1.9, 7.9 and 10.9, respectively. Interestingly, migrants from low risk countries tend to take on the risk of their adopted country, though not to a full extent. This shows that apart from environmental circumstances other population differences are also accountable for prostate cancer incidence (Gronberg, 2003).

An increased risk for the development of prostate cancer has also been assigned to the aggregation of the disease in the immediate family. In particular brothers and sons of patients with early-onset prostate cancer are also at a high risk of suffering from prostate cancer at an early age (9-40%). The risk increases with the number of immediate relatives affected. If three or more relatives are affected, an individual's risk of developing early onset prostate cancer is 15 times higher than that of a man with a negative family history of the disease. Hereditary prostate cancer is defined by either three affected generations from the paternal or maternal side, three affected family members in two subsequent generations or diagnosis before the age of 55 in two family members (Bratt, 2007). In 1996 Smith *et al.* mapped genes responsible for hereditary prostate cancer to the *HPC1* locus on chromosome 1 (Smith *et al.*, 1996). Despite intense research efforts to date no one high-risk gene has been identified unequivocally that would allow scanning of patient populations. Therefore familial anamnesis is still the only way to class prostate cancer as hereditary, familial (familial accumulation but less than hereditary) or sporadic (one case in the family). It has been estimated that 5 to 9% of all prostate cancers are hereditary prostate cancer. In recent years numerous genetic polymorphisms associated with a 1.5 to 2 fold risk increase have also been reported (Bratt, 2007).

As mentioned above migrant studies have delivered evidence that environmental factors play a significant role for the risk of developing prostate cancer. The observed increased

prostate cancer risk for migrants from low risk countries in their host countries may stem from new risk factors or the depletion of protective factors. Differences in dietary patterns have been intensely investigated and some studies suggest a positive correlation between prostate cancer incidence and the intake of dairy products, calcium, meat, fat and zinc. Other potential risk increasing lifestyle elements are smoking and low physical activity (Wolk, 2005).

Protective effects have been associated with tomatoes and tomato-based products (with lycopene as active component), vitamin E and D, selenium, soy, and green tea. Vitamin E, selenium, lycopene and soy are now being tested in major long term prevention studies (Fleshner and Zlotta, 2007).

The role of tea in the prevention of prostate cancer is described in more detail in section 1.2.

### **1.1.2 Pathology, diagnosis, staging and treatment**

The majority (95%) of all prostate cancers are adenocarcinomas; the remainder comprise transitional cell carcinoma of the epithelia of the urethra and glands, neuroendocrine carcinomas and sarcomas. The main site for the occurrence of prostate cancer is the peripheral zone of the prostate (Mazhar and Waxman, 2002).

High-grade prostatic intraepithelial neoplasia (HG-PIN) is regarded as the pre-neoplastic lesion with the best predictive value for the occurrence of cancer. The likelihood of being diagnosed with cancer at a follow-up biopsy after HG-PIN was found initially has been established at between 21 and 36%. However, HG-PIN does not always seem to be a necessary prerequisite step for carcinogenesis as some low grade cancers do not seem to be associated with areas of an HG-PIN. The cytological features

of HG-PIN lesion are very similar to those of adenocarcinomas. The main difference is the presence of the basal membrane in HG-PIN (DeMarzo *et al.*, 2003).

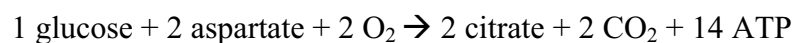
The grading of prostate tumours is performed using the Gleason system (Gleason and Mellinger, 1974) where the sum of the two most dominating grades gives the so called Gleason score. The grades range from 1 to 5, whereby 1 is well differentiated carcinoma with uniform gland pattern and 5 very poorly differentiated carcinoma with no or minimal gland formation. The treatment which a patient will receive is decided on the basis of Gleason scoring and the TNM staging system (updated 1997). The TNM staging scheme was developed by the International Union Against Cancer (UICC) and takes into account the presence, size and extent of the primary tumour (T 0-4), the absence or presence of pelvic nodal metastasis (N 0/1) and the absence or presence of distant metastasis (M 0/1) (Mazhar and Waxman, 2002).

The treatment options for organ confined prostate cancer range from active monitoring (“watchful waiting”) for low grade, low volume cancers to radical prostatectomy or radiotherapy for higher grades. Patient choice and physical fitness influence the decision for or against a certain treatment. Patients presenting with metastatic disease will initially receive androgen ablation therapy until after a period of about one year the prostate cancer inevitably becomes hormone-refractory. Chemotherapeutic approaches have hardly any impact on life expectancy. Hormone-independent prostate cancer remains incurable to date (Mazhar and Waxman, 2002).

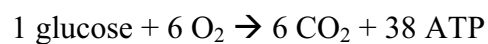
### 1.1.3 Tumour metabolism

In healthy human prostate tissue zinc accumulates and inhibits mitochondrial aconitase, an enzyme which recycles citrate to oxaloacetate in the Krebs cycle. Thus, in normal prostate, the cycle is truncated resulting in net citrate synthesis. This phenomenon is unique to prostatic tissue which is characterized by very high zinc and citrate levels. The accumulation of citrate and subsequent excretion into the prostatic fluid has considerable bio-energetic consequences. The cells lose approximate 60% of the energy that could be gained from complete oxidation of citrate (equation 1.1).

#### A) Normal prostate:



#### B) Normal mammalian cells and malignant prostate:



**Equation 1.1** Bio-energetic balance of net citrate production (A) versus normal glucose oxidation via the Krebs cycle (B).

In malignant prostate cells the accumulation of zinc is lost which consequently results in lower citrate levels compared to healthy prostatic tissue (Costello and Franklin, 1994; Costello and Franklin, 2001; Costello and Franklin, 2006). The underexpression of zinc uptake transporters has been identified as a reason for this metabolic shift. With a shift towards citrate oxidizing metabolism the cell has increased energetic resources which could be utilized for malignant cell growth. The genes encoding for the zinc uptake

transporters Zip 1-3 have been postulated to act as tumour suppressor genes in prostate carcinogenesis (Desouki *et al.*, 2007; Franklin *et al.*, 2005).

Increases in choline and choline related species, namely phosphocholine (PC) and glycerophosphocholine (GPC), are other metabolic changes associated with malignancies of the prostate (Glunde and Serkova, 2006; Griffin and Shockcor, 2004). Increased choline species are also inherent to other cancers, such as breast and colorectal cancer (Glunde *et al.*, 2006). Total choline species (choline, PC plus GPC), and individual components (choline and PC plus GPC), were reported to be elevated in human prostate samples containing at least 20 % malignant tissue, and these increases have been suggested to serve as markers of prostate cancer progression (Swanson *et al.*, 2003). Choline kinase (ChK), which catalyses the phosphorylation of choline, is overexpressed in human prostate cancer, and plays a major role in the mechanism leading to elevated levels of choline-derived species in malignant tissue (Ramírez de Molina *et al.*, 2002). Tumour levels of PC have been shown to be a pharmacodynamic marker of the chemotherapeutic efficacy of choline kinase inhibitors in experimental human breast and colon cancer models (Al-Saffar *et al.*, 2006). Measurement of citrate and total choline species using magnetic resonance spectroscopy imaging (MRSI) has been proven to be useful as a non-invasive tool to investigate the metabolic profile of the prostate *in situ*. This could help to diagnose and localize prostate cancer, aid staging and monitor treatment response (Heerschap *et al.*, 1997; Kurhanewicz *et al.*, 1996).

Other changes that have been postulated to occur in prostate cancer are increases in taurine, lactate, alanine and myo-inositol and a decrease in polyamines levels (Kurhanewicz *et al.*, 2002; Swanson, 2006).

## **1.2 Prostate cancer chemoprevention**

### **1.2.1 General concepts**

The term chemoprevention was coined in 1976 (Sporn *et al.*, 1976) and can be defined as the use of natural or synthetic chemical agents in order to suppress, prevent or reverse carcinogenesis (Lippman *et al.*, 1994). The fact that in the development of prostate cancer decades can lie between the occurrence of PIN lesions and clinically manifest tumours (Mazhar and Waxman, 2002) makes it an ideal target for chemopreventive strategies. As discussed above the treatment options, especially for hormone-refractory prostate cancer, are limited. It should therefore be the primary aim to avoid the development and progression of the disease.

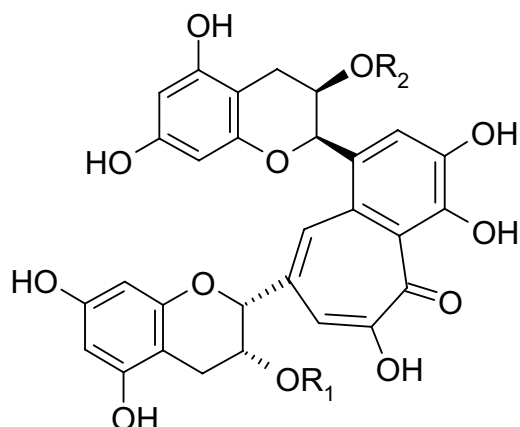
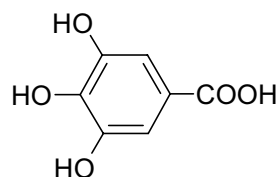
The recently completed Prostate Cancer Prevention Trial has proven that chemoprevention of prostate cancer is possible. In this large scale phase III placebo controlled trial the hypothesis was tested that finasteride can reduce the risk of developing prostate cancer. Finasteride is a 5- $\alpha$  reductase type II inhibitor and decreases the conversion of testosterone to dihydrotestosterone, which is the major androgen effector in the prostate. The trial was prematurely stopped as it could be shown that 5mg of finasteride daily reduced the risk of developing prostate cancer. While 24.4% in the placebo group were diagnosed with prostate cancer this number was reduced to 18.4% in the finasteride group (Thompson *et al.*, 2003).

## 1.2.2 Chemoprevention of prostate cancer by tea polyphenols

The high tea consumption in Asian countries has attracted much attention as a possible dietary factor responsible for the low incidence of prostate cancer in these regions (see section 1.1.1). Worldwide tea is a popular beverage and has long been thought to have health-beneficial attributes. It is almost certain that a drug derived from tea, may it be an extract or a single compound, would find acceptance and compliance within the population.

### 1.2.2.1 Green and black tea polyphenols

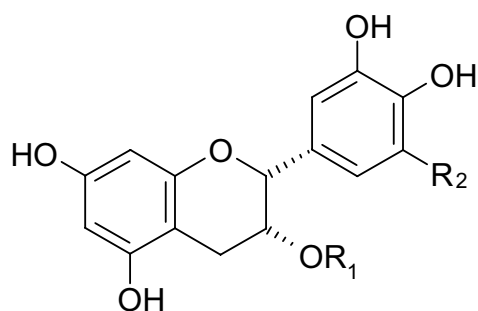
Green tea and black tea are both derived from *Camellia sinensis*. Black tea is produced from fully fermented leaves, while green tea originates from un- or only slightly fermented leaves. Tea fermentation is understood to be the natural browning process which is catalyzed by endogenous enzymes. Theaflavins are the products of this fermentation process and unique to black tea. They account for 3-5% of the extract solids. The characteristic benzotropolone ring structure results from a dimerisation of a catechin and a galliccatechin. This structure is responsible for the red-orange colour of black tea and also adds to the aroma. Figure 1.1 shows the structure of theaflavins. Thearubigens are oligomeric and polymeric fermentation products and account for more than 20% of the extract solids. They are chemically not as well characterised as the theaflavins. The remaining un-oxidised catechins account for around 9%. The given values are only estimates as the exact chemical composition of black tea polyphenols is always dependant upon the conditions and length of the fermentation process as well as the sub species of *Camellia sinensis* used.

**A****B**

compound	R <sub>1</sub>	R <sub>2</sub>
theaflavin	H	H
theaflavin-3-gallate	gallate	H
theaflavin-3'-gallate	H	gallate
teaflavin-3,3'- digallate	gallate	gallate

**Figure 1.1** Structure of (A) theaflavins and (B) gallic acid

For green tea the fresh leaves are fired or steamed at elevated temperatures to inactivate the fermenting enzymes and subsequently undergo drying and rolling steps. The chemical composition remains similar to that of the fresh leaves. Catechins account for 30% of the dry weight of the solids in brewed green tea. The main catechins in green tea are (-)-epicatechin-3-gallate (ECG), epigallocatechin (EGC), (-)-epigallocatechin-3-gallate (EGCG) and (-)-epicatechin (EC). Amongst these EGCG is the most abundant polyphenol (see figure 1.2). One cup (150ml) of green tea contains about 160mg catechins (Harbowy and Balentine, 1997).



compound	R <sub>1</sub>	R <sub>2</sub>
EC	H	H
ECG	gallate	H
EGC	H	OH
EGCG	gallate	OH

**Figure 1.2** Structures of tea catechins

Tea, especially green tea, has long been suggested to have antioxidant and chemopreventive properties. *In vitro* and preclinical studies provided evidence that the anti-carcinogenic effects of tea polyphenols are mediated via numerous molecular pathways which have been reviewed by Saleem *et al.* (Saleem *et al.*, 2003). Amongst others, GTP were shown to down regulate androgen synthesis, lower PSA levels and inhibit signalling pathways and enzymes associated with proliferation (Saleem *et al.*, 2003).

#### 1.2.2.2 Epidemiological and clinical evidence for prostate cancer prevention by tea

Epidemiological data about chemoprevention of prostate cancer by tea consumption are equivocal. A prospective cohort study which included nearly 8000 men of Japanese ancestry living in Hawaii, found a negative correlation between black tea consumption and prostate cancer incidence (Heilbrun *et al.*, 1986). Jain *et al.* found a decreased prostate cancer risk with the intake of more than 500g of unspecified tea (Jain *et al.*, 1998). Other studies did not find any correlation of prostate cancer risk and tea

consumption. This included an American case-control study (Slattery and West, 1993), an Italian case- control-study (Lavecchia *et al.*, 1992) and a Canadian retrospective cohort study (Ellison, 2000). While the above mentioned studies considered undefined tea preparations, mostly black tea, a case-control study from China investigated the effects of green tea consumption on prostate cancer risk. A dose dependent negative correlation of green tea consumption and the incidence of prostate cancer was shown (Jian *et al.*, 2004).

To my knowledge, clinical studies concerning BTT and prostate cancer prevention have yet to be published. Clinical trials in which the effects of GTP have been investigated delivered equivocal results. In a Phase II trial in which patients with androgen-independent metastatic prostate carcinoma were given 6g of green tea powder per day, only one out of 42 patients showed a transitional decrease in PSA (prostate-specific antigen), and no patient presented with a tumour response which could be radiographically or physically detected (Jatoi *et al.*, 2003). Another study, also carried out in patients with hormone-independent prostate cancer, used a dose of 500mg of green tea extract as a complementary alternative medicine. Nineteen patients completed the trial with a minimum duration of two months. No discernible clinical activity of green tea extract was found as determined by change of PSA levels and radiological disease progression (Choan *et al.*, 2005). Treatment of individuals presenting with high-grade prostate intraepithelial neoplasia with 600mg GTP per day over a period of one year, resulted in a 9-fold reduction of tumour occurrence (Bettuzzi *et al.*, 2006). In the GTC arm prostate cancer was only diagnosed once, compared to nine times in the placebo group. Each group consisted of 30 patients. These results indicate that GTP may be effective in the prevention or delay of early stage prostate cancer.

### 1.3 The TRAMP mouse model of human prostate cancer

The use of mouse models of prostate cancer is of great importance for the investigation of molecular mechanisms of carcinogenesis and of the effect of therapeutic or preventive agents on it. Autochthonous mouse models of prostate cancer are able to mimic interactions between cellular, tissue and hormonal compartments that constitute a complex organ system.

In 1994 the first transgenic mouse strain with susceptibility to prostate cancer was created. The so called TAg mouse model carries a recombinant gene expressing the early region of the simian virus 40 (SV40) large tumour antigen (TAg) using the 5'-flanking region of the rat prostatic steroid binding protein [C3(1)] gene as promoter. Female animals of this strain develop mammary adenocarcinoma (Maroulakou *et al.*, 1994).

The TRAMP (TRansgenic Adenocarcinoma of the Mouse Prostate) (Greenberg *et al.*, 1995) and so called *Lady* (Kasper *et al.*, 1998; Masumori *et al.*, 2001) transgenic mouse strains also use the prostate specific expression of this viral oncogene. While the TRAMP mouse expresses both the large T and small t-antigen, *Lady* transgenic mice only express the SV40 large T- antigen (Roy-Burman *et al.*, 2004).

The TRAMP mouse model of prostate cancer was introduced by Greenberg *et al.* in 1995. The regulatory elements of the rat probasin (rPB)-encoding gene is the promoter of this transgenic system leading to a prostate specific gene expression (Greenberg *et al.*, 1995).

The simian virus 40 (SV40) early-region tumour antigens are able to induce transformation *in vivo*. The SV40 large tumour T antigen (TAg) is an oncoprotein which interacts with the retinoblastoma (Rb) and p53 tumour-suppressor gene products, whereas the small t tumour antigen interacts with a protein phosphatase (Greenberg *et*

*al.*, 1995). It has been shown that the loss of wild type p53 and Rb is implicated in the development and progression of human prostate cancer (Bookstein *et al.*, 1990; Isaacs *et al.*, 1991). Therefore, the direct expression of the SV40 tumour antigens in the prostate is a logical step, creating an animal model which allows the investigation of molecular steps between early prostatic intraepithelial neoplasia (PIN) and progressive prostate cancer (Greenberg *et al.*, 1995). This genetically engineered mouse model facilitates the assessment of the efficacy of potential chemopreventive agents in a relative short time. In order to assess results obtained from studies with the TRAMP model, knowledge of the similarities and dissimilarities between human and murine prostate is absolutely vital.

There are major morphological and physiological differences between these species. The human prostate is one compact anatomical structure located between the base of the bladder and the rectum surrounding the proximal urethra, consisting of a central, transitional and peripheral zone (figure 1.3).

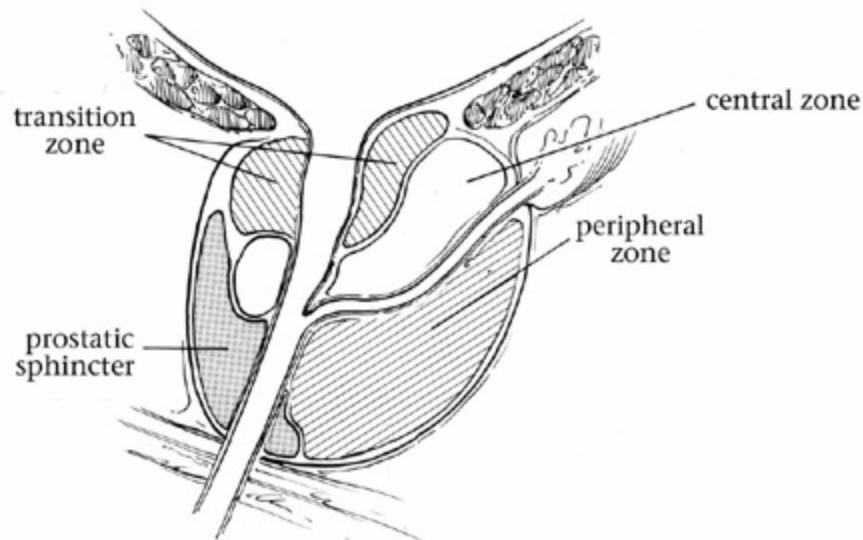


**Figure 1.3** Schematic image of the normal adult human prostate (sagittal section); adapted from “The Visible Mouse PROJECT” (available from: <http://tvmouse.compmc.ucdavis.edu/prostate/>)

The murine prostate on the other hand consists of four paired lobes situated around the urethra: anterior (AP), dorsal (DP), lateral (LP) and ventral (VP) prostate. DP and LP are often referred to as one structure (DLP) (figure 1.4). The DLP is considered to be analogous to the peripheral zone (PZ) of the human prostate, where most carcinomas arise. These anatomical differences between the murine and human prostate confound the ability to draw conclusions about local invasiveness in human prostate cancer from findings in mice.

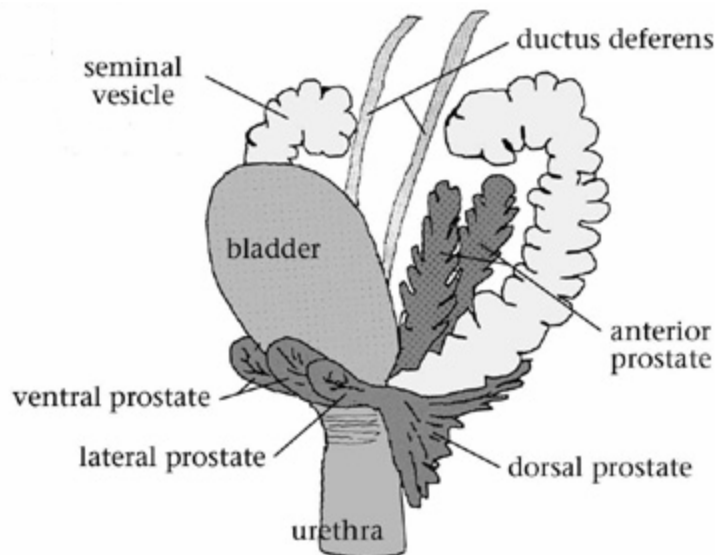


**Figure 1.4** Schematic image of the normal adult mouse prostate (lateral view); adapted from “The Visible Mouse PROJECT” (available from: <http://tvmouse.comped.ucdavis.edu/prostate/>)

However, at the cellular and microanatomic levels there are greater resemblances between the two species. Both human and murine epithelial prostate consist of basal, secretory and neuroendocrine cells, although in different ratios. It is assumed that these cells are responsible for the same physiological functions in both species. Ducts and glands are part of both human and murine prostate, but the stroma is very different. In human prostate it is a robust fibromuscular structure while it is only a very modest component of the mouse prostate.

While humans are very prone to spontaneously develop benign or malignant prostate pathology, especially with advanced age, this occurs rarely in mice, whereas the hormone responsiveness of the prostate is innate to both species. The loss of functional androgen receptors with progressing disease is a feature of prostate cancer in humans as well as in TRAMP mice. The increased nuclear p53 protein levels in neoplastic cells in

TRAMP mice mimics a feature often observed in high-grade human prostate cancer (Greenberg *et al.*, 1995).

The TRAMP transgenic mice develop prostatic intraepithelial hyperplasia by 10 weeks of age, 12 weeks later nearly all prostatic glands are hyperplastic but invasive adenocarcinoma can already be detected at 20 weeks of age (Greenberg *et al.*, 1995).

### **1.3.1 Chemoprevention by tea polyphenols in the TRAMP mouse model**

Green tea polyphenols (GTP) have been the subject of numerous chemoprevention studies in TRAMP mice. The landmark experiments were carried out by Gupta *et al.* In these experiments, the transgenic mice were, from week 8 of age, given a 0.1% GTP solution for 24 weeks. The control group received tap water. While 100% of the control group developed fully malignant, palpable tumours with distant site metastases in nearly all cases, tumour incidence and burden were significantly delayed in TRAMP mice on GTP. The incidence of metastasis was reduced from 95% in water-fed group to 0% in the GTP-fed TRAMP mice. Furthermore, the GTP fed animals showed a significant increase in time of tumour-free survival (up to 50%) as well as in life expectancy in general (68 weeks on average compared to 42 weeks for the control group). Observed molecular changes were reduced expression of proliferating cell nuclear antigen (PCNA), increased apoptosis and reduction of serum insulin-like growth factor-1 (IGF-1) levels in conjunction with restoration of insulin-like growth factor binding protein 3 (IGFBP-3) levels (Gupta *et al.*, 2001). Further investigations into the effects of GTP on the IGF/IGFBP-3 signalling pathway suggested it plays a major role in GTP-mediated chemoprevention in TRAMP mice (Adhami *et al.*, 2004).

The same group postulated metastasis-associated protein S100A4 (Mts 1) to be a biomarker of chemoprevention. Feeding of a 0.1% GTP solution resulted in a marked decrease in cancer progression which was associated with reduced mRNA and protein expression of S100A4 (Saleem *et al.*, 2005).

Caporali *et al.* and Scaltriti *et al.* have pointed out that only 80% of TRAMP mice are sensitive to GTP prevention. Failure to respond to GTP was accompanied by overexpression of histone H3 (H3) and growth arrest-specific gene 1 (Gas 1) plus downregulation of clusterin (Clu) (Caporali *et al.*, 2004). An 8-gene signature, which was found to be differentially expressed in human prostate cancer, could distinguish between GTP-sensitive and GTP-insensitive TRAMP mice. In particular, lower levels of Clu, and higher levels of ornithine decarboxylase antizyme (OAZ), H3 and glyceraldehyde 3-phosphate dehydrogenase (GAPDH) were found in non-responders (Scaltriti *et al.*, 2006).

The intervention with EGCG, the major catchin in green tea, was found to be efficient in early rather than late stage carcinogenesis in the TRAMP mouse as determined by histopathological assessment. The effect showed mainly in the ventral parts of the prostate (Harper *et al.*, 2007; Nyska *et al.*, 2003). The EGCG-induced reduction of proliferation observed after 5 weeks of treatment in animals of 12 weeks of age (Nyska *et al.*, 2003) was not matched by decreased 8-oxodG tissue levels as measured by immunohistochemistry. However, after 13 weeks of treatment (at 20 weeks of age) EGCG drastically reduced 8-oxodG in the prostate. The authors suggested additional “non-antioxidant” anti-tumour effects for EGCG (Tam *et al.*, 2006). A study from our laboratory has shown that GTP are able to reduce the tissue levels of malondialdehyde-deoxyguanosine (M<sub>1</sub>dG) in the TRAMP mouse prostate, a DNA adduct that is linked to lipid peroxidation (Thorpe *et al.*, 2007).

In summary, GTPs have shown good chemopreventive efficacy in the TRAMP mouse model of prostate cancer.

#### **1.4 Relevant analytical platforms for biomarker discovery**

The National Cancer Institute (NCI) defines a biomarker as *a biological molecule found in blood, other body fluids, or tissues that is a sign of a normal or abnormal process, or of a condition or disease. A biomarker may be used to see how well the body responds to a treatment for a disease or condition*

*(<http://www.cancer.gov/dictionary/?searchText=biomarker>).*

In recent years non-hypothesis driven “omic” approaches have become increasingly popular in the quest for new cancer biomarkers. The simultaneous measurements of as many gene expressions (genomics), proteins (proteomics), peptides (peptidomics), metabolites (metabonomics or metabolomics), lipids (lipidomics) etc. hold great promise for the discovery of new biomarkers and affected pathways. Therefore, a biomarker obtained from such studies is not restricted to a single molecule. It can also be an array of markers such as gene expression fingerprints (Santin *et al.*, 2005), combinations of up or down regulated mass to charge ratios (Willingale *et al.*, 2006) or metabolite profiles (Odunsi *et al.*, 2005).

##### **1.4.1 Metabonomic approaches in cancer research**

*“Metabonomics is the quantitative measurement of the multivariate metabolic responses of multicellular systems to pathophysiological stimuli or genetic modification. It is an approach to understanding global metabolic regulation of the organism and its commensal and symbiotic partners”* (Nicholson and Wilson, 2003).

Metabonomics is often differentiated from *metabolomics* which can be defined as *the measurement of metabolite concentration and fluxes and secretions in cells and tissues in which there is a direct connection between the genetic activity (gene expression) and the metabolic activity itself* (Nicholson and Wilson, 2003). The term metabolomics is widely used in the field of plant functional genomics.

Throughout this thesis, research involving methods that investigate metabolic patterns will be referred to as metabonomics.

The existence and abundance of metabolites present in biofluids and tissues is a result of the activity of metabolic pathways. Although alterations in the concentrations or activities of single enzymes (detected by proteomic approaches) mostly do not have an extensive impact on metabolite concentration (detected by metabonomics), changes in pathway activity will be detectable. The reason for this statement lies in the fact that the control of a metabolic flux is spread across all enzymes participating in a metabolic pathway (Griffin and Shockcor, 2004).

The up- and down-regulation of metabolic pathways is the body's response to all kinds of influences e.g. disease, medication, physiological processes and even diet. Metabolite levels reflect the final outcome of multiple changes in the genome and proteome. Therefore, the use of metabonomic approaches is a sophisticated way of investigating the process of carcinogenesis and the effect of dietary chemoprevention.

#### **1.4.1.1 $^1\text{H}$ -NMR based metabonomics in cancer research**

$^1\text{H}$  nuclear magnetic resonance (NMR) spectroscopy is a technique widely used in metabonomic research. It is based on the magnetic spin property of the  $^1\text{H}$  isotope. The hydrogen nucleus spins about its own axis. Since it has a positive charge its motion

builds up a weak local magnetic field (the so called magnetic moment). The orientation of the magnetic field depends on the spin state of the nucleus.

When a sample is subjected to a single strong magnetic field (static field) the nuclei are forced into a precession (referred to as Larmor precession) about the axis of the magnetic field. The Larmor precession occurs at the Larmor frequency  $\nu$  and is directly proportional to the applied magnetic field. It depends as well on the magnetogyric ratio  $\gamma$  (still often referred to as gyromagnetic ratio) which is a nuclide specific constant ( $^1\text{H}$ ,  $^2\text{H}$ ,  $^{13}\text{C}$  etc.) that indicates how “strongly magnetic” a nucleus is.

In the static magnetic field, the spin state where the nuclear magnetic field is aligned with the external field ( $\alpha$  state) has a lower energy than that spin state that gives rise to an opposing field ( $\beta$  state). The net magnetisation of the sample is the result of an excess of nuclei in the  $\alpha$  state. The  $\alpha$  state can be excited to the  $\beta$  state by electromagnetic radiation oscillating at the Larmor frequency. Protons of a molecule may precess at different Larmor frequencies, caused by the distinct chemical environment in which every proton is situated. A short (“hard”) radiofrequency pulse, which covers the range of the proton Larmor frequencies, applied at an angle perpendicular to the static magnetic field, results in excitement of the nuclear spins from the lower energy  $\alpha$  state to the higher energy  $\beta$  state. This can be conceived as rotation of the bulk magnetisation into the orthogonal plane. The resulting oscillating and decaying current which is induced in the receiver coil as the nuclear magnetisation precesses is detected as a function of time and is Fourier transformed to a NMR spectrum. The frequency scale in the spectrum is a relative scale which uses a reference substance, e.g. tetramethylsilane (TMS). Strictly speaking, the chemical shift ( $\delta$ ) is a dimensionless property but the units of parts per million (ppm) are used. Peak intensities in the spectrum of a given compound are proportional to the number of protons that give rise to the signal.

Splitting of resonance lines (peaks) is the result of coupling between nuclear spins. These “peak patterns” provide information about the structural properties of the analyte (Harwood and Claridge, 1997). This basic depiction of NMR principle by no means reflects the complex technology of modern NMR spectrometers.

Metabonomic profiling of serum has for example found successful application in the detection of epithelial ovarian cancer (Odunsi *et al.*, 2005) and coronary heart disease (Brindle *et al.*, 2002). It has also been proven to be useful for the determination of biochemical modifications in biofluids following dietary intervention (Solanky *et al.*, 2005; Solanky *et al.*, 2003a; Solanky *et al.*, 2003b).

Another technique, called high-resolution magic angle spinning (HRMAS)  $^1\text{H}$  NMR is used to obtain high-resolution spectra from intact tissue samples. With this approach both aqueous and lipid-soluble metabolites can be detected simultaneously. As the samples are not subjected to extraction procedures, the risk for metabolite modifications caused by the preparation method is eliminated. The analysis of intact prostatic tissue by HRMAS  $^1\text{H}$  NMR for the assessment of prostate cancer is one example of its successful application (Cheng *et al.*, 2005; Tomlins *et al.*, 1998).

#### **1.4.1.2 LC-MS based metabonomics in cancer research**

More recently, HPLC-MS (high performance liquid chromatography-MS) and UPLC-MS (ultra performance liquid chromatography) methods have found application in the field of metabonomics. The LC step prior to mass spectrometry is mostly performed on a reversed-phase (RP) column, although hydrophilic interaction liquid chromatography (HILIC) is gaining increasing popularity. The analyte flow from the column is directly subjected to electrospray ionisation (ESI). The mass analyser is typically a time of flight

(Tof) or quadrupole instrument. Ionisation occurs at atmospheric pressure and is achieved by applying a potential difference of several kV between the capillary, which conducts the eluent from the HPLC into the source and the counter electrode (0.3 – 2cm distance). The coaxial injection of a warmed nitrogen gas flow produces an aerosol of charged droplets. Subsequent desolvation and droplet rupture caused by repelling coulombic forces (exceeding the cohesion forces as droplet shrinks) leaves gas phase ions, or alternatively, desorption of ions from the droplet surface occurs. The exact mechanism of ESI ionisation is still not fully understood. The formed gas phase ions are conducted through focusing lenses with very small orifices into the low pressure compartment of the mass spectrometer leading to a mass analyser, e.g. a quadrupole (de Hoffmann and Stroobant, 2002).

Quadrupole mass analyzers consist of four parallel circular rods. The electric field within the analyser is composed of direct current voltages and superimposed radiofrequency (RF) voltages. Two diagonally opposite rods are regarded as one pair. To one pair of rods a positive direct current voltage is applied while the other pair receives a negative direct current voltage. The RF voltages are applied to each pair such that they are 180° out of phase. The ions entering the quadrupole undergo oscillation. At a given combination of RF and direct current voltages only those with a particular mass to charge ( $m/z$ ) ratio will experience a stable trajectory to reach the end of the quadrupole and the detector. The RF voltages are constantly varied to allow  $m/z$  scans across a defined range (de Hoffmann and Stroobant, 2002).

LC-MS based metabonomic approaches have been used in rodent toxicity studies (Lenz *et al.*, 2004a; Lenz *et al.*, 2004b) and also as a tool to investigate normal physiological variation (Plumb *et al.*, 2003).

As for metabonomics in general, the application of this technique to cancer research has been up to now rather limited. Kind *et al.* used a combination of RP-UPLC-MS, HILIC-HPLC-MS and GC-MS to mine the urinary metabolome for biomarkers of kidney cancer (Kind *et al.*, 2007).

In summary one can say that LC-MS is a promising tool for metabonomics. Direct comparisons between NMR and LC-MS analysis has shown that both techniques gave the same overall results, but the actual group-distinguishing markers were different (Lenz *et al.*, 2004a; Lenz *et al.*, 2004b). These findings imply that both platforms are suitable and complementary for metabonomic investigations. Therefore, using both techniques for sample analysis has been recommended (Nicholson and Wilson, 2003).

#### **1.4.2 Peptidomic approaches in cancer research**

Peptidomics is defined as “*the systematic, comprehensive analysis of native or endogenous peptides in a biological sample at a defined time point and location analyzed by multiplex assays*” (Tammen *et al.*, 2007).

The mining of biofluids such as plasma and urine for peptide biomarkers is justified by the insight that malignancies are often connected with alterations in protease expression or secretion. Changes in patterns of proteolytic products (peptides) may be more readily identified than the proteases themselves (Villanueva *et al.*, 2006).

Petricoin *et al.* (Petricoin *et al.*, 2002a) first introduced the concept of using information derived from serum protein patterns to diagnose ovarian cancer. Surface enhanced laser desorption ionisation-time of flight (SELDI-Tof) mass spectrometry was used in conjunction with pattern recognition software to diagnose women with ovarian cancer

(Petricoin *et al.*, 2002a). The selectivity of the method was also shown by its ability to differentiate between neoplastic and non-neoplastic ovarian disease.

SELDI-Tof mass spectrometry relies on affinity-based chromatographic separation of proteins on the precoated surface of the target plate and is a variation of MALDI-Tof mass spectrometry. SELDI chips are commercially available in a variety of different matrices (sometimes referred to as baits) e.g. hydrophobic, ion exchange or metal affinity (Hamdan and Righetti, 2005). The principle of ionisation in SELDI is matrix-assisted laser desorption ionisation (MALDI): The compound is dissolved in a matrix that has a strong absorption at the laser wavelength. This mixture is applied to a target plate and, when crystallized, subjected to laser irradiation. Through the absorbed energy, matrix molecules locally sublime and entrain compound molecules in their plume into the gas phase. One proposed mechanism of the actual molecule ionisation is a proton transfer in the expanding plume. The mass to charge ( $m/z$ ) ratio of the ion is then calculated by a time of flight analyzer: The ion is accelerated by a determined potential between source and detector. The time that the ion needs to fly a fixed distance is measured (de Hoffmann and Stroobant, 2002). The obtained raw data are processed using bioinformatic tools of data reduction and pattern recognition.

Adam *et al.* first reported the utility of this approach in prostate cancer research (Adam *et al.*, 2002). Using SELDI-MS of serum in combination with a decision tree classification algorithm, the investigators could distinguish between healthy controls, BPH and prostate cancer with high sensitivity and specificity. Several others studies (Pan *et al.*, 2006; Petricoin *et al.*, 2002b; Qu *et al.*, 2002), also using spectral patterns of serum proteins, supported the possibility of a more accurate prostate cancer diagnosis method than the measurement of prostate specific antigen. The method has also been applied to assess the effect of vitamin E, selenium and lycopene on the serum

peptidome of *Lady* mice, a transgenic mouse model for prostate cancer (Venkateswaran *et al.*, 2003).

However, the initial enthusiasm about SELDI-MS profiling as a diagnostic tool in oncology has diminished (Skytt *et al.*, 2007), and questions have been raised concerning the diagnostic potential and the reliability of protein profiles gained from SELDI-Tof mass spectrometry (Baggerly *et al.*, 2004; Check, 2004; Diamandis, 2003; Diamandis, 2004). Further investigation of this issue has shown that inter-laboratory reproducibility of SELDI-Tof-MS profiling can be achieved (Semmes *et al.*, 2005), but it has become clear that consistency of protocols, procedures and instrument performance at all stages of the experiment is crucial (Baggerly *et al.*, 2004; Semmes *et al.*, 2005). These prerequisites probably apply to any protein profiling technique.

A similar approach to investigate the peptide pattern in biological matrices is analysis by MALDI-Tof mass spectrometry (MS) after extraction of the peptides in a separate step. The application of this technique has some advantages. MALDI instruments are capable of producing spectra with resolution in excess of 10,000, mass accuracy within 20ppm and sensitivity in the femtomolar range.

In 2004 Villanueva *et al.* validated MALDI-Tof mass spectrometry as a suitable method for differential serum peptide profiling investigating the serum peptide pattern of patients with brain tumours compared to healthy controls (Villanueva *et al.*, 2004). MALDI-Tof mass spectrometry has also been used to obtain peptide patterns for diagnostic purposes in patients with asthma (Zhang *et al.*, 2004), prostate cancer (Mobley *et al.*, 2004) and colorectal cancer (Seraglia *et al.*, 2005). This technique was also applied in a prostate cancer chemoprevention study to detect changes in serum proteomic patterns before and after treatment (Kim *et al.*, 2005).

SELDI-MS based profiling approaches have also been applied in investigations of urinary peptidomic and proteomic patterns in medical research, including cancer research (Clarke *et al.*, 2003; Hampel *et al.*, 2001; Rogers *et al.*, 2003; Schaub *et al.*, 2004; Vlahou *et al.*, 2001; Ye *et al.*, 2006). Urine samples can be obtained non-invasively in relatively high quantities, and therefore constitute an advantage over blood and tissue specimens. The usefulness of urinary peptide patterns for prostate cancer detection and biomarker development has been demonstrated by a study employing capillary electrophoresis online coupled to a mass spectrometer (Theodorescu *et al.*, 2005). M'Koma *et al.* have shown that MALDI-MS based profiling is a suitable analytical platform to distinguish and investigate the urinary peptidomic patterns of men with normal prostate, BPH, HGPIN and prostate cancer (M'Koma *et al.*, 2007).

### **1.4.3 Data analysis for global profiling approaches**

All global profiling approaches have in common a requirement for multivariate statistical analysis for data evaluation, as the sheer number of acquired data points prohibits evaluation by conventional statistics. Pattern recognition methods of an unsupervised or supervised nature allow the determination of inherent and group specific variation in the data set and the identification of responsible signals as well as dimensional reduction for easy visual evaluation of separation trends, similarities or outliers.

Principal Component Analysis (PCA) is an unsupervised pattern recognition method which finds lines, planes and hyperplanes (principal components) in a multidimensional data space. Each variable (e.g. a certain  $m/z$  value) represents one dimension of that data space while each observation (=sample) is a point in that data space. The first

principle component will describe the largest variation within the data and each successive principal component describes the greatest possible portion of the remaining variation, whereby all principal components are orthogonal to each other and therefore independent from each other. Usually, most of the variation within a certain data set is described by the first few principal components which allow a good overview. The principal components can be plotted either as loadings or scores. In the latter, each sample is represented by a point in the coordinate system of the principal components, which are the newly created variables of the data space. In the loadings plot the points represent variables. The position of each variable in the loadings plot reflects the way in which the original variables are linearly combined to form the principal components. The location of a variable in a loadings plot indicates the weight in determining the position of a sample, or sample group, in the corresponding scores plot. In other words, the loadings plot allows for the identification of  $m/z$  values or spectral regions which are responsible for the separation observed in the scores plot (Eriksson *et al.*, 2001; Lindon *et al.*, 2007).

Partial Least Squares-Discriminate Analysis (PLS-DA) is a supervised pattern recognition method which maximises the separation between samples according to group affiliation. The scores and loadings plots of the calculated PLS components can be interpreted in the same way as described for PCA. PLS-DA is a useful tool to identify group-specific differences in data sets which are overlaid by a larger variation of a group-unspecific nature, and would therefore not show up in PCA (Eriksson *et al.*, 2001; Lindon *et al.*, 2007).

## 1.5 Urinary 8-oxo-7,8-dihydro-2'-deoxyguanosine (8-oxodG) as a biomarker of oxidative stress status

8-OxodG is formed by the hydroxylation of the C-8 position of guanine (Kasai, 1997) by reaction with reactive oxygen species (ROS) such as the superoxide radical ( $O_2^{\cdot-}$ ), singlet oxygen ( $^1O_2$ ), hydrogen peroxide ( $H_2O_2$ ) and the hydroxyl radical ( $\cdot OH$ ).  $^1O_2$  and  $\cdot OH$  are the only ROS capable of directly damaging DNA, and  $H_2O_2$  and  $O_2^{\cdot-}$  act as precursors (Halliwell and Cross, 1994; Halliwell and Gutteridge, 1984). The sources of ROS are endogenous, e.g. mitochondrial metabolism and inflammatory responses, or exogenous exposure to ionizing radiation or chemicals such as methylene blue. Aging and diseases like cancer, diabetes and rheumatism, all involving inflammation, have been linked to ROS (Ames *et al.*, 1993; Evans *et al.*, 2004; Loft and Poulsen, 1996; Wu *et al.*, 2004). 8-OxodG can lead to chromosomal aberrations and the induction of mutations, which mainly involve GC to TA transversions (Grollman and Moriya, 1993; Joenje, 1989).

The detection of 8-oxodG in urine of humans and rodents, which was first described in 1989 by Shigenaga *et al.*, represented the possibility of non-invasive analysis of a biomarker for the determination of oxidative DNA damage (Shigenaga *et al.*, 1989). The potential sources of 8-oxodG in urine are diet, cell death/turnover, DNA repair and the nucleotide pool (Cooke *et al.*, 2002). The contribution of diet and cell death / turnover to the presence of 8-oxodG in urine appears to be minimal (Cooke *et al.*, 2005). Recent evidence suggests that the occurrence of 8-oxodG in urine results from nucleotide excision repair (NER) of cellular DNA or from the action of nudix hydrolases on the nucleotide pool (Haghdoost *et al.*, 2006; Jaiswal *et al.*, 1998; Nakabeppu *et al.*, 2006; Reardon *et al.*, 1997; Tsuzuki *et al.*, 2001). The repair of 8-oxodG in cellular DNA by N-glycosylases has been well characterised resulting in the

cleavage of the glycosidic bond and formation of 8-oxoguanine. 8-Oxoguanine DNA glycosylase 1 (OGG1) is the major enzyme involved in the removal of 8-oxoguanine from cellular DNA and excretion into urine (Boiteux and Radicella, 1999; Croteau and Bohr, 1997). The repair of bulky lesions (adducts) by NER has been well defined (Friedberg, 2001), however there is also evidence that NER may repair 8-oxodG present in cellular DNA which is excised as a single stranded oligomer and further metabolised by endonucleases to yield 8-oxodG (Reardon *et al.*, 1997).

The function of nudix hydrolases is to prevent the incorporation of oxidatively damaged nucleotides present in the nucleotide pool into newly synthesised cellular DNA. The enzyme NUDT1 (MutT homologue, MTH1), which has 8-oxo-2'-deoxyguanosine triphosphatase activity, catalyses the hydrolysis of 8-oxo-2'-deoxyguanosine triphosphate to 8-oxo-2'-deoxyguanosine monophosphate (8-oxodGMP) (Hayakawa *et al.*, 1995). The 8-oxodGMP may then be further metabolised by nucleotidases to yield 8-oxodG, which is excreted into the urine.

The enzyme 8-oxodG-endonuclease has also been described to catalyse the simultaneous cleavage of the phosphodiester bonds on either side of the 8-oxodG residue in DNA, resulting in the generation of 8-oxodG diphosphate (8-oxodGDP), which can potentially undergo further metabolism by nucleotidases to 8-oxodG. The contribution of this pathway to the presence of 8-oxodG in urine has not yet been clarified (Bessho *et al.*, 1993).

Figure 1.5 provides a summary of the possible mechanisms/pathways that can lead to the excretion of 8-oxodG into the urine originating from both nuclear and mitochondrial DNA in cells.

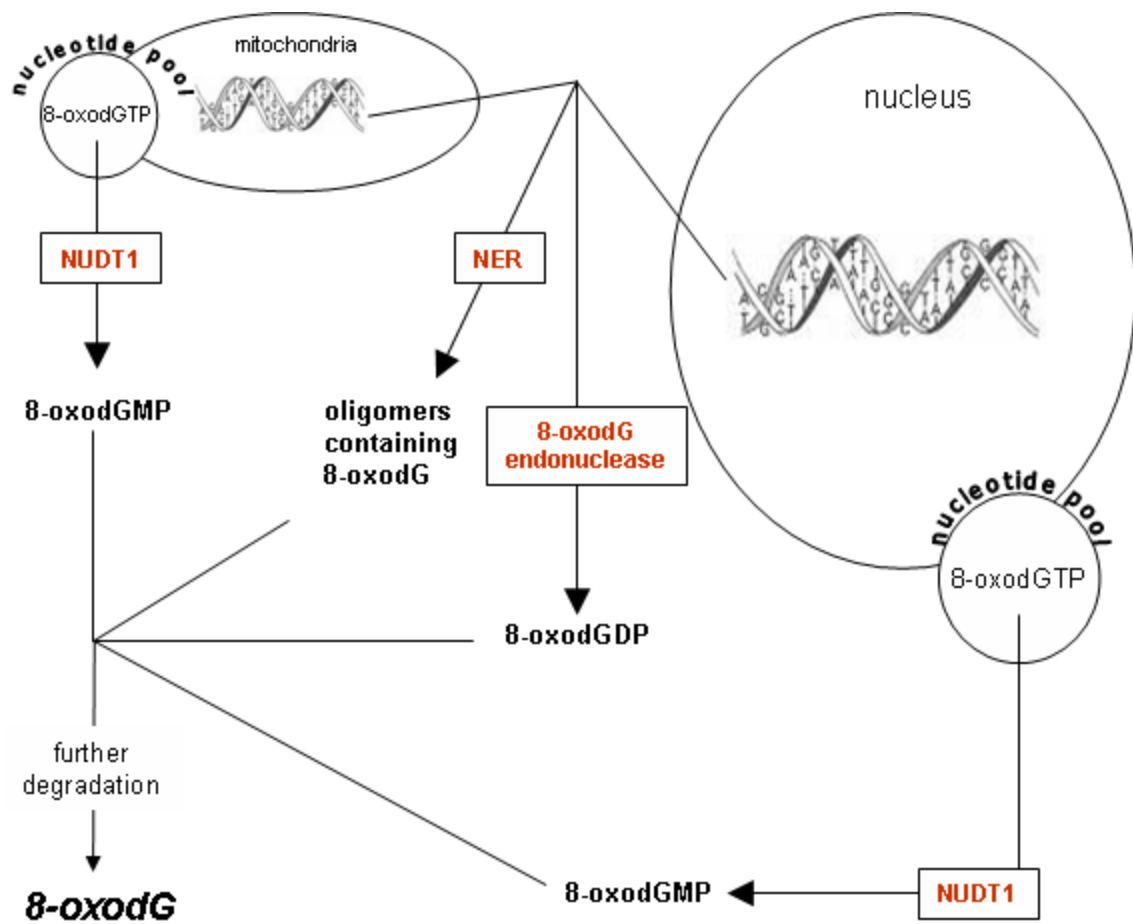


**Figure 1.5** Repair mechanisms that possibly contribute to 8-oxodG excreted in urine. NER, nucleotide excision repair; NUDT1, nudix hydrolase

## 1.6 Aims

At present serum prostate-specific antigen (PSA) is the only clinically approved non-invasive marker for the diagnosis of prostate cancer and the assessment of success of its treatment. PSA is a glycoprotein excreted by epithelial prostate cells. The fact that it is prostate-specific but not prostate cancer-specific, gives rise to issues of low sensitivity and specificity, especially in the case of values near the commonly used “normal” baseline cut-off of 4ng/ml (Thompson and Ankerst, 2007). Measurement of serum PSA in combination with digital rectal examination (DRE) is the standard in screening tests for prostate cancer. On the one hand it has been reported that 15% of men with PSA <4ng/ml and normal DRE have prostate cancer as determined by biopsy (Thompson *et al.*, 2003), on the other hand, the issue of over-detection has been raised. In the US, where a screening program for prostate cancer has been established, the lifetime risk of diagnosis is reported to be 18%, whereas the chance of death from prostate cancer is only 3% (Thompson and Ankerst, 2007). Serum PSA is not a dichotomous biomarker, and so far no convincing evidence has been provided that screening programs lower prostate cancer mortality rates. This notion includes PSA related measures such as PSA velocity, PSA density and percent free PSA (Lim and Sherin, 2008).

Biomarkers to aid early diagnosis and monitoring of response to chemotherapeutic or chemopreventive intervention are urgently needed to improve prostate cancer management in humans who have, or are at risk of developing, the disease.

### 1.6.1 Main aim

The overall aim of this project was the evaluation of biomarkers of prostate carcinogenesis and of the efficacy of chemopreventive intervention with GTP in the TRAMP mouse model. To achieve this aim, non-hypothesis driven metabonomic and peptidomic profiling approaches and measurement of urinary 8-oxodG levels, reflecting oxidative stress status, were applied.

### 1.6.2 Specific objectives

- I. Metabolism in human prostate tumours greatly differs from that in normal tissue (see section 1.1.3). The first aim of this work was to characterise the metabolic profile of TRAMP mouse prostate tumours using  $^1\text{H}$  NMR analysis of aqueous tissue extracts, as well as high resolution magic angle spinning  $^1\text{H}$  NMR analysis of intact tissue. Significant changes were investigated further by genomic means such as microarray and real time PCR analysis. All findings were correlated to general histopathological analysis of prostate tissue.
  
- II. The metabolic profiles of plasma and urine reflect influences on the organism, of either an external (e.g. lifestyle, medication) or endogenous nature (e.g. age, disease; see section 1.4.1). The second aim of this work was to search for changes in the metabolic profile that are related to cancer progression and chemoprevention by GTPs. The metabolic profiles of urine and plasma from TRAMP mice were evaluated at early and late stages of their life and compared to age-matched wild type controls. LC-MS and  $^1\text{H}$  NMR metabonomic platforms were used to achieve this aim.

- III. Differential patterns of plasma and urine peptides have been employed successfully to distinguish patients with cancer from healthy individuals (see section 1.4.2). The third aim of this work was to subject plasma and urine from TRAMP mice to peptide analysis by MALDI-MS to detect changes relating to carcinogenesis and GTP intervention.
- IV. 8-OxodG is a marker for oxidative damage in blood and tissues (see section 1.5). The hypothesis was tested that levels of urinary 8-oxodG reflect stages of carcinogenesis in TRAMP mice and can serve as a biomarker for GTP chemoprevention. 8-OxodG was measured using liquid chromatography – tandem mass spectrometry (LC-MS/MS).
- V. BPH, a common disease in men, is regarded as a precursor lesion for prostate cancer (see section 1.1.2). The hypothesis was tested that changes in metabolite and peptide patterns seen in TRAMP mice upon treatment with tea polyphenols resemble those in humans. Urine and plasma samples from patients with BPH were analysed by peptidomic and metabonomic means, and urinary levels of 8-oxodG were determined prior and post treatment with GTP or BTT.

Figure 1.6 shows an overview of the studies undertaken for the work described in this thesis.

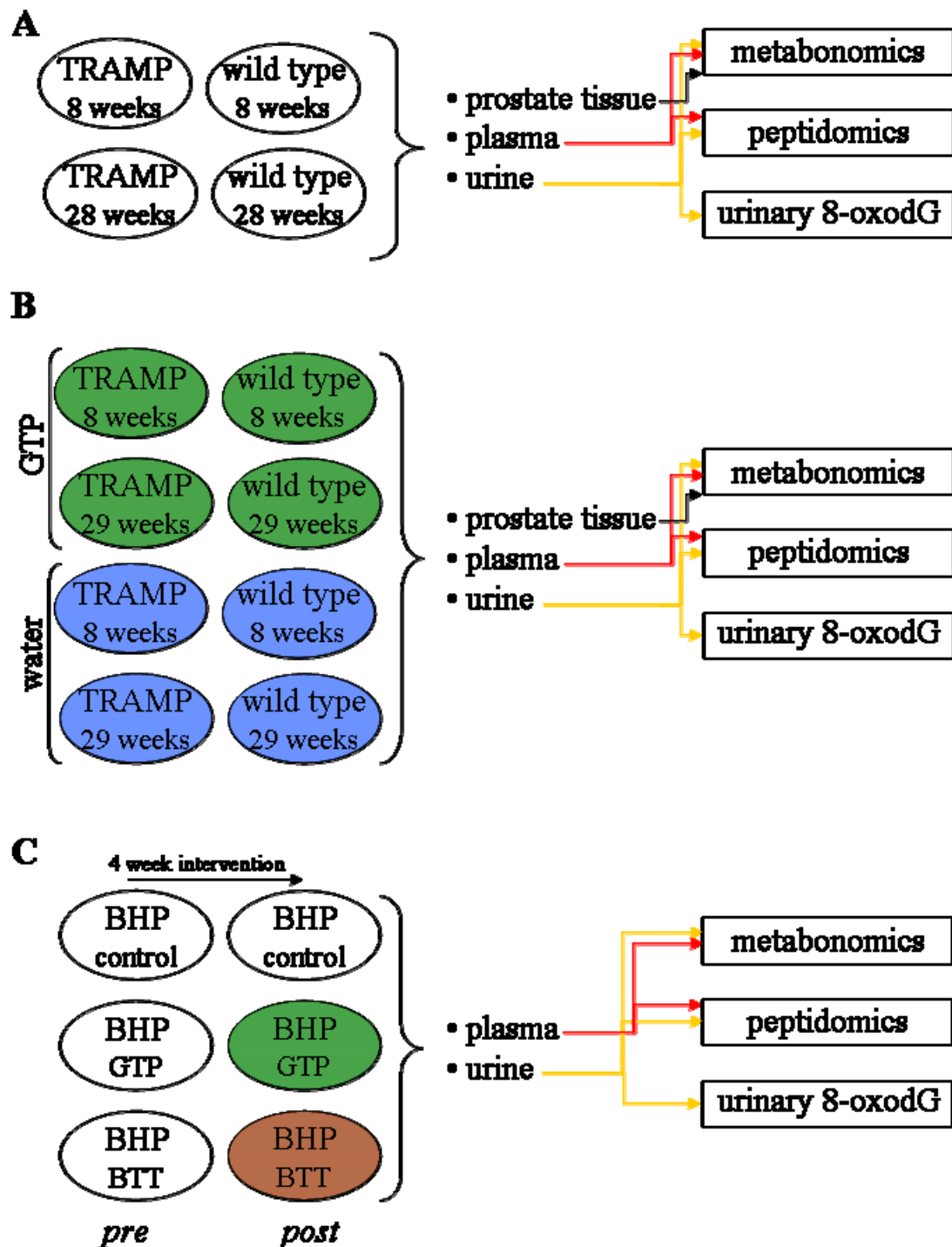


**Figure 1.6** Overview of studies conducted. **A:** Features of carcinogenesis in the TRAMP mouse model (study is described in Chapter 4). **B:** Effect of tea constituents on features of carcinogenesis in the TRAMP mouse model (described in Chapter 5). **C:** Effect of tea constituents on patients with BPH (described in Chapter 6). BPH = benign prostatic hyperplasia, GTP = green tea polyphenols, BTT = black tea theaflavins

# Chapter 2

## **2. Materials and methods**

### **2.1 Materials**

#### **2.1.1 General chemicals and kits**

All chemicals and reagents were purchased from Sigma-Aldrich Company Ltd (Gillingham, UK) and solvents from Fisher Scientific, Inc. (Loughborough, UK), unless stated otherwise.

#### **2.1.2 Animals**

Mice were bred in the Leicester University Biomedical Services facility using female hemizygous transgenic mice on a C57BL/6J background, originally obtained from the NCI Mouse Repository (NCI Frederick, USA) and male wild type C57BL/6J mice. Terminal anaesthesia was induced *via* inhalation of isoflurane (Isocare, Animalcare Ltd, York, UK) 3% in 1m<sup>3</sup>/ min nitric oxide : 0.5m<sup>3</sup>/ min oxygen.

#### **2.1.3 Animal diet**

All animals were fed AIN93g standard diet (DYETS, Inc., USA).

#### **2.1.4 Green Tea Polyphenols (GTP)**

Greenselect was purchased from Indena S.p.A, Milan, Italy.

### **2.1.5 Specimen collection**

Li-Heparin micro tubes (1.3ml) and sterile 2ml, 5ml and 15ml polypropylene screw top tubes and were purchased from Sarstedt, Leicester, UK.

Li-Heparin BD vacutainer<sup>®</sup> tubes (2ml) were obtained from Becton, Dickinson and Co., Oxford, UK.

### **2.1.6 Muricholic acid (MCA) standards**

$\alpha$ -,  $\beta$ - and  $\omega$ -MCA standards were purchased from Steraloids Inc., Newport, RI, USA

## **2.2 Methods**

### **2.2.1 Studies and tissue collection**

#### **2.2.1.1 Maintenance of C57BL/6J TRAMP mouse colony**

Biomedical Services, University of Leicester, carried out the general animal husbandry. The animals had unlimited access to AIN93g standard diet and water, unless stated otherwise. Ear punching of each animal at approximately 3 weeks of age allowed identification. The superfluous tissue was used for genotyping (see section 2.2.1.2).

All animal work was carried out under the Project Licence 40/2496 granted by the UK Home Office. The University of Leicester Ethical Committee for Animal Experimentation gave approval for all animal studies conducted.

#### **2.2.1.2 Determination of genotype**

Genotype determination was carried out by Sharon Platon and Stephanie Euden, Department of Cancer Studies and Molecular Medicine, University of Leicester. The presence of the transgene was detected in DNA extracted from ear punch tissue, obtained during cage identification at weaning, using an allele-specific polymerase chain reaction (PCR) assay published on The Jackson Laboratory website:

[http://jaxmice.jax.org/pubcgi/protocols/protocols.sh?objtype=protocol&protocol\\_id=18](http://jaxmice.jax.org/pubcgi/protocols/protocols.sh?objtype=protocol&protocol_id=18)

8

#### **2.2.1.3 Study for method validation**

Seven female C57BL/6J mice were used. To reduce the number of experimental animals employed, ex-breeders that were due to be culled were used. All mice were held in metabolism cages for 16 hours under food deprivation. Urine was collected in tubes

cooled with dry ice. Upon removal from the metabolism cages the animals were returned to normal holding cages with unlimited access to diet and water for 24 hours before being sacrificed. The blood was collected into BD vacutainer<sup>®</sup> Li-heparin tubes and placed on ice until further processed.

#### **2.2.1.4 TRAMP – C57BL/6J wild type study**

Each of 22 male TRAMP mice was paired with a C57BL/6J wild type control from the same litter or from a litter with the same father. At 4 weeks of age the animals were weaned and received AIN93g standard diet. At 8 weeks of age, 10 TRAMP mice and their matched controls were held in metabolism cages over night for 16h under food deprivation. Urine was collected in 15ml tubes at room temperature. Each tube contained 10µl of a 0.1% Na-azide solution and 10µl of protease inhibitor cocktail for mammalian tissue. Upon removal from the metabolism cages the animals were placed back in normal cages with unlimited access to diet and water for 24h before being sacrificed. Blood was collected by cardiac exsanguination into Sarstedt Li-heparin micro tubes and placed on ice until further processed. Prostates were dissected with the avoidance of seminal vesicles and weighed. One half was transferred to 2ml screw top tubes and frozen in liquid nitrogen and the other half was preserved in neutral buffered formalin for pathological analysis.

#### **2.2.1.5 TRAMP GTP intervention study**

Each of 44 male TRAMP mice was paired with a C57BL/6J wild type control from the same litter or from a litter with the same father. At 4 weeks of age the animals were weaned and received AIN93g standard diet, 22 TRAMP and 22 wild type mice received drinking water supplemented with 0.05% (w/v) GTP. The GTP water was kept in black drinking bottles to protect it from light and was freshly prepared three times per week.

At 8 weeks of age 10 TRAMP mice and their matched controls, and at 29 weeks of age the remaining animals, were held in metabolism cages for 16 hours under food deprivation. Urine was collected in 15ml tubes cooled with dry ice. Upon removal from the metabolism cages the animals were returned to normal holding cages with unlimited access to diet and water for 24 hours before sacrifice. The blood was collected into Li-Heparin BD vacutainer<sup>®</sup> tubes and placed on ice until further processed. Prostates were dissected avoiding the seminal vesicles and weighed. One half was transferred to 2ml screw top tubes and frozen in liquid nitrogen. The other half was preserved for pathological analysis.

#### **2.2.1.6 Clinical tea polyphenol intervention study**

The clinical pilot study was conducted by Dr James Thorpe, Department of Cancer Studies and Molecular Medicine, University of Leicester. In total, 18 patients, diagnosed with BPH, who required a prostate biopsy and a transurethral prostate resection as part of their ordinary clinical care were enrolled in the trial. The men received 1g/day GTP, 1g/day BTT or no polyphenols, for four weeks prior to their surgery. GTP polyphenols were encapsulated by Nova Laboratories, Leicester, UK. The black tea theaflavin mixture capsules were obtained from Beverages GTC (Unilever), Bedford, UK. For the work presented here plasma and spot urine samples were used. Samples were collected at recruitment before treatment started and at the day of surgery. Blood was collected into BD vacutainer<sup>®</sup> tubes. Urine was stored at -80°C within 2h after collection. Patients were not required to follow any dietary restrictions prior to or during the intervention period.

### **2.2.1.7 Plasma**

The blood (stored on ice immediately after collection) was centrifuged for 10min at 2000g and 4°C. The supernatant (plasma) was taken off, divided in aliquots for each analysis and stored at -80°C.

### **2.2.1.8 Tissue and urine samples**

The tissue was stored at -80°C. After collection urine samples were thawed and divided into aliquots for each analysis prior to storage at -80°C.

### **2.2.1.9 Tissue processing and histology**

The dissected tissues were fixed in 10% neutral buffered formalin. Further tissue processing and generation of haematoxylin and eosin stained paraffin sections was performed by Jennifer M. Edwards, MRC Toxicology Unit, Leicester.

The histological assessment was performed by Dr Peter Greaves, Department of Cancer Studies and Molecular Medicine, University of Leicester.

## **2.2.2 Peptide profiling**

### **2.2.2.1 Omix<sup>®</sup> peptide extraction**

The samples were adjusted with 2.5% trifluoroacetic acid (TFA) to give a final concentration of 1% TFA (10µl 2.5% TFA + 15µl plasma). The Omix<sup>®</sup> tips (Omix<sup>®</sup> pipette tips C18, 10µl, Varian Inc., Walton-on-Thames, UK) were wetted twice with 50% acetonitrile in water. After repeated equilibration with 0.1% TFA the sample was applied onto the Omix<sup>®</sup> tip by aspirating and re-dispensing it ten times. The tip was then washed with 0.1% TFA twice and the peptides eluted with 50% acetonitrile in 0.1% TFA. All steps were carried out using a pipette volume of 10µl.

### 2.2.2.2 BOND ELUTE<sup>®</sup> peptide extraction

BOND ELUTE<sup>®</sup> C18 EWP, 100mg, 1ml columns (Varian Inc., Walton-on-Thames, UK) were used for peptide extraction on a vacuum manifold maintained at a vacuum of 5mmHg. The columns were twice primed with 1ml of methanol and then twice washed with 1ml HPLC grade water followed by a repeated wash with 1ml 0.1% TFA. Plasma or urine samples (50µl) were diluted with 1ml of 1% TFA and left on ice for 20min before being applied to the column. After washing twice with 1ml of 0.1% TFA, two subsequent elution steps with 1ml of acetonitrile/1% TFA (60:40, v/v) and 1ml of acetonitrile/1% TFA (90:10, v/v) were carried out. After approximately 30min in the centrifugal evaporator the reduced volume eluates were combined, freeze dried, and reconstituted in 50µl of 0.1% TFA.

### 2.2.2.3 Strata<sup>™</sup>-X peptide extraction

Strata<sup>™</sup>-X columns (30mg/1ml, Phenomenex, Inc.) were used for peptide extraction on a vacuum manifold maintained at a vacuum of 5mmHg. Prior to extraction, each 50µl sample (either plasma or urine) was acidified with 0.8µl glacial acetic acid. The column was washed with 1ml methanol and equilibrated with 1ml of 0.1% acetic acid before the sample (50µl) was loaded onto the column. Following repeated washing with 1ml of 0.1% acetic acid, the peptides were eluted from the column with 1ml of 1% acetic acid in water/acetonitrile (40:60, v/v). After approximately 30min reduction in the centrifugal evaporator, the eluate was freeze dried, and reconstituted in 50µl of 0.1% TFA. This extraction is an adaptation of the method published by Hortin *et al.* (Hortin *et al.*, 2004).

#### **2.2.2.4 Oasis<sup>®</sup> peptide extraction**

Oasis<sup>®</sup> HLB cartridges, 1cc/30mg (Waters Ltd, Thermo Electron, Elstree, UK) were used for peptide extraction on a vacuum manifold maintained at a vacuum of 5mmHg following the manufacturer's guidelines for peptides (Waters, 2003). Plasma or urine samples (50µl) were acidified with 50ul of 4% phosphoric acid. The column was conditioned with 1ml methanol and 1ml HPLC grade water before application of the sample. After a wash step with 1ml of acetonitrile/0.1% TFA (10:90, v/v), the peptides were eluted with acetonitrile/0.1% TFA (80:20, v/v). After approximately 30min reduction in the centrifugal evaporator the eluate was freeze dried, and reconstituted in 50µl of 0.1% TFA.

#### **2.2.2.5 Microcon<sup>®</sup> filtration**

The Microcon<sup>®</sup> YM-30 centrifugal filter device (30,000 molecular weight cut-off) (Millipore Ltd, Watford, UK) was used, unless stated otherwise. For filter preparation 500µl HPLC grade water were centrifuged for 12min at 14,000g at 4°C twice. The samples were centrifuged for 80min at 14,000g and 4°C. Plasma samples from all studies underwent Microcon<sup>®</sup> filtration following Oasis<sup>®</sup> peptide extraction (section 2.2.2.4).

#### **2.2.2.6 Precipitation method**

The general principle of the method was obtained from a publication in the Millipore Technical Library (Gutierrez *et al.*, 2003). Plasma samples were diluted to 20% or 50% acetonitrile and left on ice for 20min. 50µl of that mixture was spun through Microcon<sup>®</sup> filters as described in section 2.2.2.5, using 30,000 or 100,000 molecular weight cut-off filters. The filtrates were freeze dried and reconstituted in HPLC grade water to the

volume of the original plasma sample and extracted using the Omix<sup>®</sup> method (see section 2.2.2.1).

#### **2.2.2.7 Albumin / IgG removal**

Plasma samples were depleted of albumin and IgG using the ProteoExtract<sup>®</sup> Albumin/IgG Removal Kit (Calbiochem<sup>®</sup>, Merck, Nottingham, UK). Plasma samples (35 $\mu$ l) were mixed with 315 $\mu$ l binding buffer and processed according to the manufacture's instructions. The eluents were further extracted using the Omix<sup>®</sup> method described in section 2.2.2.1.

#### **2.2.2.8 MALDI-Tof mass spectrometry**

The MALDI-Tof mass spectrometry was performed on a Q-ToF Ultima Global instrument (Waters, Manchester, UK) operating in positive ionisation mode.  $\alpha$ -cyano-4-hydroxy-cinnamic acid dissolved in acetonitrile/methanol (50:50, v/v, 2mg/ml) was used as matrix. Equal volumes of sample and matrix were mixed, 1 $\mu$ l of this mixture spotted to each well (referred to as spots in the following text) of a MALDI target plate (12x1 wells, Waters, Manchester, UK) and left to dry. For method development, four spots were analysed for each sample. For the analysis of study samples the number of spots analysed was increased to 8 for plasma samples from the TRAMP GTP intervention study (see section 2.2.1.5) and to 12 for all other plasma and urine samples. These adjustments were made to maximise the number of peaks detected in case the laser power diminished over time. The m/z range was from 1000 to 10000. Each spot was subjected to 100 laser ablations. The data were processed using Mass Lynx software (Waters, Manchester, UK).

### 2.2.2.9 Mathematical data processing of MALDI-MS data

Following the conversion of the raw data to text files, processing of the data was performed by Dr Richard Willingale, Department of Physics and Astronomy, University of Leicester as published previously (Willingale *et al.*, 2006). Briefly, the data obtained from each individual spot were binned with  $\Delta m/z = 1$  resulting in 9000 bins per analysis. Subsequently, spots for one sample were combined and the unresolved background continuum was removed. Peaks were detected from the Gaussian smoothed, summed spectrum over all individuals (samples) by detecting local maxima. Peaks were integrated by summing bins left and right to the centroid point of the peak corresponding to the full width at half maximum (FWHM). The significance of each peak was estimated using Poisson counting statistics. A significance cut-off of  $\sigma < 7$  was applied. Spectra of individual samples were then normalised using a set of stable and ubiquitous peaks, characterised by a fractional relative mean square scatter  $\sigma_S/S < 0.5$  and a mean total count  $S$  between 50 and 6000. For human plasma the fractional scatter was set to  $\sigma_S/S < 0.4$  and the total count to 100-10000. For human urine peaks in the same total count range was used for normalisation but the fractional scatter was set to  $\sigma_S/S < 0.25$ . For further data analysis the peak lists were exported to SIMCA-P 11.5 (Umetrics, Umea, Sweden) and MatLab (Mathworks, Natick, MA, USA).

For comparison of extraction methods during method development the number of significant peaks ( $\sigma > 5$ , detected as described above from the smoothed, summed spectrum over all samples) and the number of significant bins ( $\sigma > 5$ , detected from the unsmoothed, summed spectrum over all samples) was used.

### 2.2.3 Urinary 8-oxodG

#### 2.2.3.1 Synthesis of $^{15}\text{N}$ -labelled internal standard

The [ $^{15}\text{N}_5$ ]8-oxodG stable isotope internal standard was synthesised as described previously (Singh *et al.*, 2003). In brief, 5mg [ $^{15}\text{N}_5$ ]deoxyguanosine (Spectra Stable Isotopes, Columbia, MD, USA) were dissolved in 5.0ml HPLC grade water and 350 $\mu\text{l}$  of freshly prepared 170mM ascorbic acid solution, 350 $\mu\text{l}$  of 20mM copper(II)sulphate and 250 $\mu\text{l}$  of 30% hydrogen peroxide were added. The reaction mixture was incubated in the dark for 15min at room temperature, dried down using a centrifugal vacuum evaporator and redissolved in 500 $\mu\text{l}$  HPLC grade water. The [ $^{15}\text{N}_5$ ]8-oxodG was purified by HPLC with UV detection (254nm) using a Hypersil C18 BDS column (250 x 10mm, 5 $\mu\text{m}$ , Thermo Electron Corporation, Runcorn, UK). The flow rate was set to 3ml/min, solvent A was HPLC grade water and solvent B was methanol. Over 20min B was increased from 2% to 15%, to 20% at 25min and returned to 2% at 30min. The fractions corresponding to [ $^{15}\text{N}_5$ ]8-oxodG were collected and combined, evaporated to dryness and reconstituted in HPLC grade water. The concentration was determined by UV spectroscopy (293nm, extinction coefficient  $\epsilon = 10300$ ).

#### 2.2.3.2 Urine clean up method modified after Lin *et al.*

The method described here is a modification of the SPE method published by Lin *et al.* (Lin *et al.*, 2004). To 200 $\mu\text{l}$  of each urine sample 21 $\mu\text{l}$  10% formic acid and 10pmol of the internal standard [ $^{15}\text{N}_5$ ]8-oxodG (1pmol/ $\mu\text{l}$ ) were added. The mixture was incubated at 4°C for 1h and subsequently centrifuged at 10000g for 10min at 4°C. The supernatant was diluted to 1ml with 20mM formic acid. The samples were subjected to SPE using Oasis HLB columns (1 cc, 30 mg, Waters Ltd., Elstree UK) connected to a vacuum manifold maintained at a vacuum of 5mmHg (Phenomenex, Macclesfield, UK). After

initiating the cartridge with 1ml methanol followed by 1ml 20mM formic acid the sample was applied. A wash step with 1ml 20mM formic acid was followed by elution of 8-oxodG from the column with 1ml of 17.5% methanol in 20mM formic acid. The eluent was dried down in a centrifugal vacuum evaporator and reconstituted in 100 $\mu$ l HPLC grade water.

### **2.2.3.3 Urine clean up method HLB I**

A 200 $\mu$ l aliquot of each urine sample was diluted with 790 $\mu$ l of 0.1% TFA and spiked with 10pmol of the stable isotope internal standard, [ $^{15}\text{N}_5$ ]8-oxodG (1pmol/ $\mu$ l). The urine samples were subjected to SPE using Oasis HLB columns (1 cc, 30 mg, Waters Ltd., Elstree UK) connected to a vacuum manifold maintained at a vacuum of 5mmHg (Phenomenex, Macclesfield, UK). The columns were initially conditioned with 1ml of methanol followed by 1ml of 0.1% TFA. The urines samples (1ml) were then loaded onto the columns and washed with 1ml HPLC grade water. The 8-oxodG was eluted from the columns with 1ml of acetonitrile/0.1% TFA (80:20, v/v), dried down using a centrifugal vacuum evaporator and redissolved in 100 $\mu$ l of HPLC grade water.

### **2.2.3.4 Urine clean up method HLB II**

A 100 $\mu$ l aliquot of each urine sample (200 $\mu$ l for method testing) was diluted with 890 $\mu$ l (790 $\mu$ l) of HPLC grade water and spiked with 10pmol of the stable isotope internal standard, [ $^{15}\text{N}_5$ ]8-oxodG (1pmol/ $\mu$ l). The urine samples were subjected to SPE using Oasis HLB columns (1 cc, 30 mg, Waters Ltd., Elstree UK) connected to a vacuum manifold maintained at a vacuum of 5mmHg (Phenomenex, Macclesfield, UK). The columns were initially conditioned with 1ml of methanol followed by 1ml of HPLC grade water. The urines samples (1ml) were then loaded onto the columns and washed

with 1ml HPLC grade water. The 8-oxodG was eluted from the columns with 1ml of acetonitrile/HPLC grade water (80:20, v/v), dried down using a centrifugal vacuum evaporator and redissolved in 50 $\mu$ l (100 $\mu$ l) of HPLC grade water.

### 2.2.3.5 Determination of urinary 8-oxodG by HPLC-MS/MS

The LC-MS system consisted of a Waters Alliance 2695 separations module connected to a Micromass Quattro Ultima Platinum (Waters-Micromass Ltd., Manchester, UK) tandem quadrupole mass spectrometer with an electrospray interface. The temperature of the electrospray source was maintained at 110 °C and the desolvation temperature at 350 °C. Nitrogen gas was used as the desolvation gas (approximately 650 l/h) and the cone gas was set to 25l/h. The capillary, cone and RF1 lens voltages and the collision energy were optimized with a 8-oxodG tuning standard (10pmol/ $\mu$ l) dissolved in 0.1% acetic acid in water/methanol (92:8, v/v) introduced by continuous infusion at a flow rate of 10  $\mu$ L/min with a Harvard model 22 syringe pump (Harvard Apparatus Ltd., Edenbridge, UK). The dwell time was set to 200 ms and the resolution was two  $m/z$  units at peak base. Selected reaction monitoring (SRM) analysis was performed for the  $[M+H]^+$  ion to oxidised base  $[B+H_2]^+$  transitions of 8-oxodG ( $m/z$  284 to 168) and the stable isotope internal standard  $[^{15}N_5]8$ -oxodG ( $m/z$  289 to 173). A 10 $\mu$ L aliquot of the purified sample was injected onto a HyPurity C<sub>18</sub>, (3  $\mu$ m, 2.1  $\times$  150 mm, Thermo Electron Corporation, Runcorn, UK) column connected to a Uniguard HyPurity C<sub>18</sub> (3  $\mu$ m, 2.1  $\times$  10 mm) guard cartridge attached to a KrudKatcher disposable pre-column (0.5  $\mu$ m) filter. The column was eluted isocratically with 0.1% acetic acid in water/methanol (92:8, v/v) at a flow rate of 120 $\mu$ l/min and then washed with 100% methanol from 20 to 25 min before being finally re-equilibrated to starting condition for 20min. The level of 8-oxodG in each sample was determined from the ratio of the peak

area of 8-oxodG to that of the internal standard [ $^{15}\text{N}_5$ ]8-oxodG. The method described here is adapted from Cooke *et al.* (Cooke *et al.*, 2006a).

### 2.2.3.6 Determination of creatinine by Jaffé reaction

Creatinine concentrations in murine and human urine samples were determined using the Creatinine FS kit (DiaSys Diagnostic Systems, Holzheim, Germany). The kit consisted of a 160mM sodium hydroxide solution (R1), a 4mM picric acid solution (R2) and 177 $\mu\text{M}$  creatinine standard. Human and mouse urine samples were diluted with HPLC grade water 1:50 and 1:5, respectively. The sample, standard or water (=blank) (50 $\mu\text{l}$ ) was mixed with 1.0ml R1 and incubated for 2min at room temperature before 250 $\mu\text{l}$  of R2 were added. After 60s incubation the absorbance A1 was measured and after further 120s the absorbance A2 (492nm, Hitachi U-3010 spectrophotometer). The level of creatinine in each sample was determined as shown in equation 2.1.

$$\text{I} \quad \Delta A = [(A2-A1) \text{ sample or standard}] - [(A2-A1) \text{ blank}]$$

$$\text{IIa} \quad \text{Creatinine } [\mu\text{M}] = (\Delta A \text{ sample} / \Delta A \text{ standard}) \times 177\mu\text{M} \times 50$$

$$\text{IIb} \quad \text{Creatinine } [\mu\text{M}] = (\Delta A \text{ sample} / \Delta A \text{ standard}) \times 177\mu\text{M} \times 5$$

**Equation 2.1** Calculation of creatinine concentration in human urine (I and IIa) and mouse urine (I and IIb)

### 2.2.3.7 Determination of creatinine by LC-MS/MS

Concentrations of [ $^2\text{H}_3$ ]creatinine (Cambridge Stable Isotope Laboratories, Andover, MA, USA) and creatinine standards were determined by UV spectroscopy (235nm, extinction coefficient  $\epsilon = 6900$ ) (Rikitake *et al.*, 1979). Mouse and human urine samples were diluted with HPLC grade water 1:1000 and 1:10000, respectively. The diluted urine samples (100 $\mu\text{l}$ ) were transferred to a new vial and 50 $\mu\text{mol}$  of [ $^2\text{H}_3$ ]creatinine stable isotope internal standard (1 $\mu\text{mol}/\mu\text{l}$  dissolved in acetonitrile/water (2:98, v/v)) followed by 1ml ice-cold acetonitrile were added. After vortex mixing and centrifugation for 15min at 14000g and 4 $^\circ\text{C}$ , the supernatant was transferred to a new vial and dried down using a centrifugal vacuum evaporator, reconstituted in 100 $\mu\text{l}$  acetonitrile/water (2:98, v/v) and transferred to HPLC vials.

The LC-MS system consisted of a Waters Alliance 2695 separations module connected to a Micromass Quattro Ultima Platinum (Waters-Micromass Ltd., Manchester, UK) tandem quadrupole mass spectrometer with an electrospray interface. The temperature of the electrospray source was maintained at 110  $^\circ\text{C}$  and the desolvation temperature at 350  $^\circ\text{C}$ . Nitrogen gas was used as the desolvation gas (approximately 650l/h) and the cone gas was set to 25l/h. The capillary, cone and RF1 lens voltages and the collision energy were optimized with a creatinine tuning standard (20 $\mu\text{mol}/\mu\text{l}$ ) dissolved in water/acetonitrile (98:2, v/v) introduced by continuous infusion at a flow rate of 10  $\mu\text{l}/\text{min}$  with a Havard model 22 syringe pump (Havard Apparatus Ltd., Edenbridge, UK). The dwell time was set to 200 ms and the resolution was one  $m/z$  unit at peak base. SRM analysis was performed for transitions  $m/z$  114 to 86 and  $m/z$  114 to 44 for creatinine and  $m/z$  117 to 89 and  $m/z$  117 to 47 for [ $^2\text{H}_3$ ]creatinine. A 10 $\mu\text{l}$  aliquot of the purified sample was injected onto a HyPurity C<sub>18</sub>, (3  $\mu\text{m}$ , 2.1  $\times$  150 mm, Thermo Electron Corporation, Runcorn, UK) column connected to a Uniguard HyPurity C<sub>18</sub> (3

$\mu\text{m}$ ,  $2.1 \times 10 \text{ mm}$ ) guard cartridge attached to a KrudKatcher disposable pre-column ( $0.5 \mu\text{m}$ ) filter. Solvent A was 0.1% formic acid in 10mM ammonium acetate and solvent B was 0.1% formic acid in acetonitrile. The flow rate was set to  $120 \mu\text{l}/\text{min}$ . B was increased from 2% to 35% in 10min and returned to 2% at 10.1min. The column was left to equilibrate for a further 10min. The level of creatinine in each sample was determined from the ratio of the peak area of creatinine to that of the internal standard [ $^2\text{H}_3$ ]creatinine using the SRM transitions  $m/z$  114 to 86 and  $m/z$  117 to 89, respectively. The result was multiplied by a response factor of 1.750 (see section 3.2.2).

#### **2.2.3.8 Determination of specific gravity**

Specific gravity in urine samples was determined using Reichert TS 400 refractometer (Reichert Analytical Instruments, Depew, USA).

#### **2.2.4 NMR-based metabolic profiling**

##### **2.2.4.1 Urine sample preparation for $^1\text{H}$ NMR analysis**

Each NMR sample was prepared by addition of  $200 \mu\text{l}$  phosphate buffer (40mM  $\text{NaH}_2\text{PO}_4$ , 200mM  $\text{Na}_2\text{HPO}_4$ , 0.36mM  $\text{NaN}_3$ , 1.4mM sodium 3-(trimethylsilyl)-2,2,3,3- $^2\text{H}_4$ -1-propionate (TSP) in 20:80  $\text{D}_2\text{O}:\text{H}_2\text{O}$ ) to  $400 \mu\text{l}$  human urine or a mixture of  $150 \mu\text{l}$  mouse urine and  $250 \mu\text{l}$   $\text{D}_2\text{O}$ . After vortex mixing the samples were centrifuged at  $15000g$  for 5min at room temperature. A  $550 \mu\text{l}$  aliquot of the supernatant was transferred to a NMR tube (GPE-S-5-400, length 175mm, GPE Limited, Leighton Buzzard, UK).

#### **2.2.4.2 Plasma sample preparation for $^1\text{H}$ NMR analysis**

A solution of saline containing 0.9% NaCl (w/v) dissolved in  $\text{D}_2\text{O}$ /water (10:90, v/v) was prepared. Mouse plasma (100 $\mu\text{l}$ ) or human plasma (200 $\mu\text{l}$ ) were mixed with 500 $\mu\text{l}$  or 400 $\mu\text{l}$  of saline solution, respectively. After vortex mixing the samples were centrifuged at 15000g for 5min at room temperature. A 550 $\mu\text{l}$  aliquot of the supernatant was transferred to a NMR tube (GPE-S-5-400, length 175mm, GPE Limited, Leighton Buzzard, UK).

#### **2.2.4.3 Preparation of aqueous tissue extracts**

The frozen tissue (20-40mg) was homogenized in 300 $\mu\text{l}$  of a mixture of chloroform and methanol (2:1, v/v). After the addition of 30 $\mu\text{l}$  HPLC grade water and further mixing, the homogenate was centrifuged for 5min at 15000g and room temperature. The aqueous and organic phases were separated, and the tissue pellet was re-extracted. Both aqueous phases were combined, freeze dried and re-dissolved in 575 $\mu\text{l}$  of phosphate buffer ( $\text{D}_2\text{O}$  with 8mM  $\text{NaH}_2\text{PO}_4$ , 40mM  $\text{Na}_2\text{HPO}_4$ , 1.4mM TSP, 0.58mM sodium azide, 5%  $\text{H}_2\text{O}$ ). Following vortex mixing the samples were centrifuged at 15000g for 5min at room temperature. A 550 $\mu\text{l}$  aliquot of the supernatant was transferred to a NMR tube (GPE-S-5-400, length 175mm, GPE Limited, Leighton Buzzard, UK).

#### **2.2.4.4 Tissue preparation for HRMAS $^1\text{H}$ NMR analysis**

Intact tissue samples (30-50 mg) of prostate or prostate tumour from three TRAMP and five wild type mice (28 weeks of age) were used. Tissues were defrosted immediately before analysis, dipped in  $\text{D}_2\text{O}$  and placed into a 3 mm zirconium rotor.

#### 2.2.4.5 NMR data acquisition and processing

$^1\text{H}$  NMR spectra of aqueous extracts, intact tissue, urine and plasma were acquired using a Bruker DRX600 spectrometer (Bruker BioSpin GmbH, Rheinstetten, Germany) operating at a frequency of 600.13 MHz and a temperature of 300 K. Tissue extracts and urine samples were analysed using a 1-D NOESY (Nuclear Overhauser Effect Spectroscopy) pulse sequence (RD-90°- $t_1$ -90°- $\tau_m$ -90° acquire) with  $t_1 = 3\mu\text{s}$  and  $\tau_m = 100\text{ms}$ . Intact tissue and plasma samples were analysed using a CPMG (Carr-Purcell-Meiboom-Gill) pulse frequency (RD-90°- $\{\tau-180^\circ-\tau\}_n$ -acquire) with  $n = 250$  and  $\tau = 400\mu\text{s}$ . For HRMAS analysis a Magic Angle Spinning probe with a rotation speed of 5kHz was used. For all spectra, 128 free induction decays (FIDs) were collected into 32 K complex data points, using a spectral width of 12,019 Hz and a 2 s relaxation delay (RD) between pulses. A water presaturation pulse was applied throughout the RD. All FIDs were zero filled by a factor of 2 and multiplied by an exponential weighting function equivalent to a line broadening of 1 Hz prior to Fourier transformation (XWINNMR, Bruker). All subsequent data processing and analysis was conducted using in-house software developed in MATLAB (Mathworks) written and compiled by Drs TMD Ebbels, HC Keun, JT Pearce and O Cloarec (Imperial College, London). The acquired spectra were corrected for phase and baseline distortions and referenced internally to the anomeric proton signal of  $\alpha$ -glucose at  $\delta$  5.23 (plasma and intact tissue) or to TSP at  $\delta$  0 (urine and tissue extracts). Spectra were interpolated to a common ppm scale from 32K to 42K data points prior to visualisation and integration.

#### 2.2.4.6 Spectral integration and statistical analyses

Visualisation, normalisation and integration of NMR spectra were performed in MatLab (Mathworks, Natick, MA, USA). The same normalisation method was applied to spectra obtained for tissue extract, urine and plasma samples. Spectra of all groups were averaged to generate an overall median spectrum (reference spectrum). Each individual spectrum was then divided by the reference spectrum to obtain the fold change for each spectral data point. The median of these fold changes was used to normalise each individual spectrum (Dieterle *et al.*, 2006). HRMAS  $^1\text{H}$  NMR spectra were normalised to creatine (singlet at 3.04ppm).

For PCA and PLS-DA analysis data were exported to SIMCA-P 11.5 (Umetrics, Umea, Sweden) following binning with  $\Delta\text{ppm} = 0.01$ . Prior to PCA and PLS-DA analysis data were mean centred and scaled to unit variance.

#### 2.2.5 Immunohistochemical analysis for ChK

Formalin-fixed, paraffin sections (5 $\mu\text{m}$ ) of prostate and a lymph node metastasis were de-waxed in xylene and taken to water through descending concentrations of industrial methylated spirit. They were then placed in 0.01M citrate buffer (pH 6.0) and microwaved (20min, 700 W). Sections were placed in distilled water, and endogenous peroxidase activity was blocked with 3%  $\text{H}_2\text{O}_2$  in water (v/v) (20 min). ChK was detected using polyclonal antibodies for murine ChK- $\alpha$  and ChK- $\beta$  (Aoyama *et al.*, 2002) at a dilution of 1:800. For control staining normal rabbit serum lacking ChK reactivity was used. The primary antibodies were applied to sections and incubated at room temperature (3 h). Detection was by the DAKO Duet detection system (DAKO,

Ely, UK) using 3,3'-diaminobenzidine for visualization. Sections were counterstained with haematoxylin prior to dehydration and mounting.

### **2.2.6 RNA extraction from prostate tissue**

Total RNA was extracted from prostate tumours obtained from four TRAMP mice, a lymph node metastasis from one TRAMP mouse and normal prostates from two C57BL/6J wild-type mice, all 28 weeks of age. In the case of three tumors and both normal prostates, tissue was taken from two different sites, yielding seven tumour and four normal samples in total. Tissue (40-60 mg) was homogenised in 1ml TRI reagent for 40s and incubated at room temperature for 5min. Following the addition of 200µl of 1-bromo-3-chloropropane the mixture was vortex mixed, incubated at room temperature for 2min and centrifuged for 15min at 12000g and 4°C. The upper aqueous layer was transferred to a new tube and 600µl isopropanol were added. The mixture was incubated at room temperature for 10min and centrifuged at 12000g and 4°C for 10min. The supernatant was removed and the RNA pellet washed with 2ml ice-cold ethanol/water (75:25, v/v) and centrifuged at 12000g and 4°C for 5min prior to removal of the supernatant. The wash step was repeated and the RNA pellet was re-dissolved in 25µl DEPC-treated water (diethylpyrocarbonate; 0.1%, v/v). RNA was used for Real Time PCR and microarray analysis.

### 2.2.7 Real Time PCR analysis

Primers were designed to cross exon-exon boundaries to eliminate the detection of any contaminating genomic DNA using Primer Express software v2.0 (Applied Biosystems, Warrington, UK). Total RNA (500 ng) was reverse-transcribed using Superscript III RT (Invitrogen, Paisley, UK). The resulting cDNA product was amplified with SYBR Green Mastermix (Applied Biosystems, Warrington, UK) using an ABI PRISM 7700 RT-PCR Sequence Detection System (Applied Biosystems) and the following optimized primers: 900nM forward primer and 900nM reverse primer for ChK- $\alpha$  or ChK- $\beta$  and 900nM and 300nM of forward and reverse primer for  $\beta$ -actin, respectively. The sequences (forward primer/reverse primer) were CTCCTGCCAGACTCCATAGC / CTCATCTTTAAGATTGCCCCATAGAG for ChK- $\alpha$  and CTAGGGCCCCAGCTTTACG / CCGGCTTGGGAGGTACTGT for ChK- $\beta$ . Expression levels were normalized to those of  $\beta$ -actin. Relative quantification of ChK gene expression was performed with the comparative cycle threshold method (Applied Biosystems, User Bulletin no 2, 1997). The mean expression level of ChK- $\alpha$  or ChK- $\beta$  in normal prostate samples was used as calibrator.

### 2.2.8 Microarray analysis

cDNA microarrays were made on aldehyde slides (Genetix, New Milton, UK) using a Stanford type microarray spotter. Targets were the MEEBO set designed in the laboratory of Alizadeh (<http://alizadehlab.stanford.edu/>) and obtained from Invitrogen (Paisley, UK). Targets were printed from a 10 $\mu$ M solution in 1.5M Betaine/3 X SSC (Saline - Sodium Citrate; 450mM NaCl, 45mM Na-citrate, pH 7.0). After printing microarrays were processed according to the manufacturer's (Invitrogen) instructions.

RNA (10µg) was labelled using an indirect technique of incorporation of aminoallyl-dUTP (Ambion, Warrington, UK) in the reverse transcription reactions, which were primed using both a locked oligodT<sub>25</sub> primer and pentadecamers. Superscript III (Invitrogen) was used to generate cDNA. After synthesis of labelled cDNA, it was coupled to the Alexa 555 or 647 dyes (Invitrogen). Labelling efficiency was checked using a Nanodrop spectrophotometer. Each experimental sample was hybridised against a common reference, which was a mixture of all samples. Hybridization was performed under coverslips in a humidified chamber (Genetix, New Hamilton, UK) at 42°C in a hybridisation buffer, which contained 50 % deionized formamide. After hybridisation overnight, microarrays were washed to a stringency of 0.05 X SSC (7.5mM NaCl, 0.75mM Na-citrate, pH 7.0) before drying by centrifugation and scanning using an Axon 4200A scanner and GenePix 5.10.19 (Molecular Devices Coop, Sunnyvale, CA, USA). Data was acquired from the image using GenePix. Data was processed using NorTT and statistical methods published previously (Zhang and Gant, 2004).

## **2.2.9 HPLC-MS based metabolic profiling**

### **2.2.9.1 Urine sample preparation**

Urine (20µl) was mixed with 80µl of 0.1% formic acid and transferred to HPLC vials. Prior to analysis the HPLC vials were centrifuged at 3000 rpm for 3min (centrifuge: Sorval RT 7 plus). A quality control (QC) sample was obtained by mixing equal amounts of each sample.

### **2.2.9.2 Plasma sample preparation**

Each plasma sample (50µl) was transferred to a reaction tube and mixed with 250µl ice-cold acetonitrile. After brief vortex mixing the tubes were centrifuged at 14000 rpm for 15min (Centrifuge 5417C, Eppendorf). The supernatant (200µl) was transferred to a glass tube and blown to dryness under a stream of nitrogen for 15min at 40°C (TurboVap LV Evaporator, Zymark). The samples were redissolved in 100µl of 0.1% formic acid/acetonitrile (90:10, v/v). The QC sample was treated in the same way.

### **2.2.9.3 HPLC-MS analysis of urine and plasma (10min gradient)**

HPLC was performed using a CTC HTC PAL autosampler (CTC analytics) and two series 200 Micro pumps (PerkinElmer). A 2.1 x 100mm Symmetry C18 column, particle size 3.5µm, was maintained at 30°C. The flow rate was set to 0.4ml/min. Samples were maintained at 4°C in the auto sampler. The injection volume was 10µl. Elution solvents were A: 0.1% formic acid in water and B: 0.1% formic acid in acetonitrile. Initial conditions were 100% A for 0.5 minutes. This then changed to 20% B at 4 minutes and 95% B at 8 minutes. The mobile phase remained at 95% B for 1min before returning to the starting conditions. Mass spectrometry was performed using a 4000 Q TRAP instrument (AB Sciex Instruments, Toronto, Canada) operating in enhanced mass spectrometry scan mode, set either to positive or negative ionisation mode. The mass range was set 100 – 1000m/z. The electrospray source temperature was 350°C. The cone voltage was set to -4500V in negative ionisation mode and 5500V in positive ionisation mode. The ion trap was set to dynamic fill mode. The scan rate was 1000 amu/s with a step size of 0.08 amu. Instrument operation and data processing was performed with Analyst software version 1.4.1 (AB Sciex Instruments, Toronto, Canada).

#### 2.2.9.4 HPLC-MS analysis of plasma (30min gradient)

The same HPLC-MS system, including the same column, as described in section 2.2.9.3 was used. Samples were maintained at 4°C in the auto sampler. The injection volume was 10µl. The flow rate was 0.2ml/min and the column was maintained at 30°C. Solvents were A: 0.1% formic acid and B: 0.1% formic acid in acetonitrile. B was increased from 0 to 95% with a linear gradient over 30min and held at 95% for 2min. Subsequently, two cycles of washing that switched from 100% A to 95% B after 0.2min were applied, before the column was left to equilibrate at 100% A until 35min. The mass spectrometer was operating in enhanced mass spectrometry scan mode, set either to positive or negative ionisation mode. The mass range was set 100 – 1000m/z. The electrospray source temperature was 350°C. The cone voltage was set to -4000V in negative ionisation mode and 5500V in positive ionisation mode. The ion trap was set to dynamic fill mode. The scan rate was 1000 amu/s with a step size of 0.08 amu.

#### 2.2.9.5 Peak finding, integration and statistical analyses

For data reduction and peak finding, the raw data were exported to MarkerView™ software Version 1.1.0.3 (Applied Biosystems, Toronto, Canada). The method by which peaks were detected and integrated has been described previously (Sangster *et al.*, 2007). For the analyses described here the subtraction offset was set to 10 scans multiplied by a factor of 1.3. The noise threshold was 10000 counts per second and the minimum peak width 0.25amu. The retention time peak width was set to be between 2 and 60 scans. Peak alignment parameters were 0.1min retention time and 1amu mass tolerance. Peaks were integrated from the raw data. For PCA and PLS-DA analysis peak list were exported to SIMCA-P 11.5 (Umetrics, Umea, Sweden). Prior to PCA and PLS-DA analysis data were mean centred and Pareto scaled.

#### **2.2.9.6 SPE method for purification of unknown compound**

A total of 100 $\mu$ l mouse urine (combined from three samples) was mixed with 900 $\mu$ l 0.1% formic acid and subjected to SPE using Oasis HLB columns (1 cc, 30 mg, Waters Ltd., Elstree UK). Positive pressure was manually applied to the column via a syringe with a rubber adaptor. The column was primed with 1ml methanol and 1ml 0.1% formic acid before the sample (1ml) was applied. The sample flow through and all subsequent elutions were collected separately. Further elution steps were 20% acetonitrile in 0.1% formic acid, increasing to 40%, 60%, 80%, and finally 100% acetonitrile. Fractions were evaporated to dryness under a constant stream of nitrogen at 40°C. Each fraction was redissolved in 200 $\mu$ l 0.1% formic acid prior to HPLC-MS analysis.

#### **2.2.9.7 HPLC-MS analysis for identification of muricholic acids**

The same HPLC-MS system, including the same column, as described in section 2.2.9.3 was used. Samples were maintained at 4°C in the auto sampler. The injection volume was 10 $\mu$ l. The flow rate was 0.4ml/min and the column was maintained at 30°C. Solvents were A: 0.1% formic acid and B: 0.1% formic acid in acetonitrile. The starting condition was 100% A which were held for 0.5min. From 0.5 to 4.0min B was increased to 20%, to reach 40% at 8.0min, 75% at 28min and 95% at 32.0min. After 1.0min at 95% B the gradient returned to starting conditions and was left to equilibrate for a further 3min. The mass spectrometer was operated in enhanced mass spectrometry scan mode, with negative ionisation mode. The mass range was set to 100 – 1000m/z. The electrospray source temperature was 350°C. The cone voltage was set to -4500V. The ion trap was set to dynamic fill mode. The scan rate was 1000amu/s with a step size of 0.08amu.

### **2.2.9.8 HPLC-MS method for comparison of fragment patterns of cholic acid isomers**

The HPLC-MS system, including the column, was identical to that described in section 2.2.9.3 and the HPLC gradient was as described in section 2.2.9.7. Samples were maintained at 4°C in the auto sampler. The injection volume was 10µl. The mass spectrometer was operating in enhanced product ion scan mode set to negative ionisation mode. Production of the precursor ions  $m/z$  453 (muricholic acids) or  $m/z$  407 (cholic acid) were monitored using four different collision energies: -10V, -30V, -60V and -80V. The electrospray source temperature was 350°C. The cone voltage was set to -4500V. The ion trap was set to dynamic fill mode. The scan rate was 1000 amu/s with a step size of 0.08 amu.

# Chapter 3

### 3. Method development

The objective was to develop analytical methods for peptide profiling and urinary 8-oxodG measurement which were suitable for murine samples. In the case of urinary 8-oxodG the limited amount of sample volume available from mice required adaptations of existing methods. For peptide profiling two considerations were taken into account: i) The SPE extraction method needed to be suitable for plasma derived from blood collection tubes containing Li-heparin, as samples were also analysed by NMR for which only heparinised plasma can be used. ii) The method should be equally suitable for human and murine samples in order to facilitate direct comparison of the two species.

#### 3.1 Peptide extraction for MALDI MS profiling

##### 3.1.1 Peptide extraction method for plasma

The analysis of the plasma peptides was carried out using a MALDI-MS method that has been described previously (Willingale *et al.*, 2006), spanning a range from 1000 – 10000m/z. Preliminary extraction experiments were carried out with mouse plasma provided by Dr Richard Verschoyle, Department of Cancer Studies and Molecular Medicine, University of Leicester. Samples prepared with Omix<sup>®</sup> extraction tips (see section 2.2.2.1) showed spectra with numerous peaks and good signal intensity (figure 3.1 A). However, in subsequent experiments carried out on human plasma the extraction with Omix<sup>®</sup> pipette tips failed to yield any measurable signals (figure 3.1 B). This failure was observed for plasma derived from blood collected into tubes containing either Li-Heparin or EDTA. Sample pre-treatment such as protein precipitation with acetonitrile (figure 3.2) as investigated by Gutierrez *et al.* (Gutierrez *et al.*, 2003) (see

section 2.2.2.6) or removal of Immunoglobulin G (IgG) and albumin with affinity columns (see section 2.2.2.7.) did not lead to an improvement in the results. Omix<sup>®</sup> pipette tips were not considered further for the extraction of peptides from plasma. Although the reason for the failure of the Omix<sup>®</sup> extraction method for human samples is not known, the conditions of sample handling and storage could potentially have contributed to the failure of the method. Sample degradation occurs relative quickly at room temperature and therefore influences the peptide profile (Banks *et al.*, 2005; Findeisen *et al.*, 2005). The mouse blood samples were stored at room temperature for a few hours prior to centrifugation and long term storage was at -20°C, in contrast, the human blood samples were immediately stored at 4°C and the plasma was stored at -80°C. A lower degree of degradation might be a reason for the lack of success with human plasma samples prepared with the Omix<sup>®</sup> extraction method.

Sample degradation is more readily controllable and easier to standardise with cooling of the samples immediately after collection and long term storage at -80°C. Therefore, the extraction method was optimized for samples collected in a way to minimise degradation (see section 2.2.1.7). New mouse plasma samples were prepared according to this protocol.

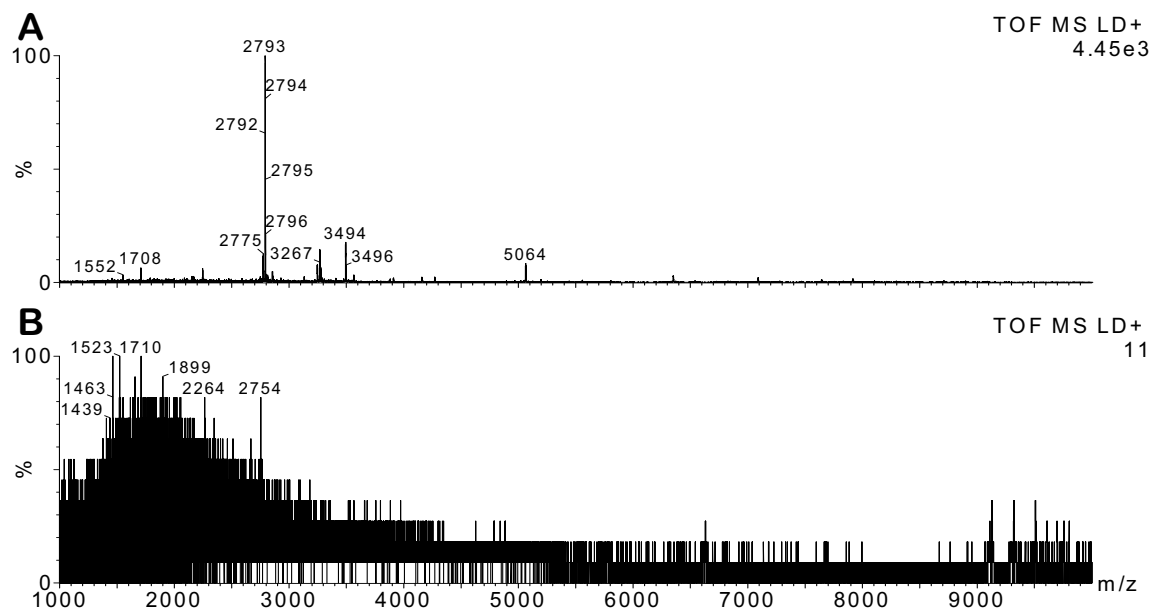


**Figure 3.1** MALDI MS spectra of (A) mouse and (B) human plasma extracted with Omix<sup>®</sup> pipette tips.

Another issue encountered during method development was the occurrence of ion patterns with mass differences of 44m/z between each ion (figure 3.2), indicative of the presence of polyethylene glycol (PEG) in the sample (Thuermer *et al.*, 1998). This effect seemed to be enhanced whenever acetonitrile was used in the sample preparation (e.g. precipitation). Therefore, Eppendorfs and Sarstedt blood collection tubes (microtubes<sup>®</sup>) containing 1ml of 50% acetonitrile were incubated for 24h then the solution was analysed by MALDI mass spectrometry (see section 2.2.2.8). A series of experiments identified the beads of the blood collection tubes as the source of the contamination. The problem of PEG contamination in samples arising from blood collection tubes has previously been reported in the literature (Weaver and Riley, 2006). The protocol for future blood collection was altered to use BD vacutainer<sup>®</sup> tubes which were shown not to contain PEG. However, for the first animal study, from which some

animals had already been sacrificed, the use of Sarsted microtubes<sup>®</sup> was continued in order to minimize any variation.

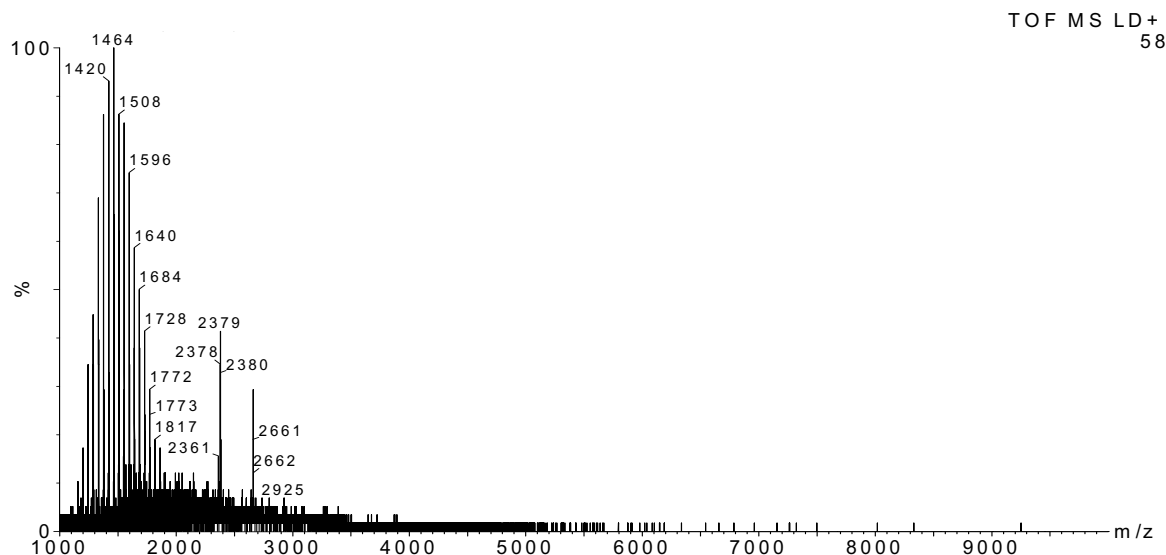


**Figure 3.2** MALDI-MS spectrum of human plasma precipitated with 50% acetonitrile, spun through 30,000 molecular weight cut-off Microcon<sup>®</sup> filter, and extracted with Omix<sup>®</sup> pipette tips. The dominating ion pattern arose from PEG contamination.

The final step of method development involved the comparison of three extraction methods from the literature: BOND ELUT<sup>®</sup>, Strata-X<sup>®</sup>, and Oasis<sup>®</sup> (see sections 2.2.2.2 – 2.2.2.4). The effect of subsequent filtration with Microcon<sup>®</sup> centrifugal filters (molecular weight cut-off 30,000Da, see section 2.2.2.5), in order to remove abundant high molecular weight proteins such as IgG and albumin, was also tested for each method. Murine and human blood samples were collected into BD vacutainer<sup>®</sup> tubes and immediately placed on ice until centrifugation. Plasma samples were stored at -80°C. All methods were tested in triplicate using aliquots of the same sample. Raw data were evaluated as described in section 2.2.2.9. The quantity of peptides present in a sample was assessed by using the number of significant peaks and bins ( $\sigma > 5$ ). These

values give an overview of the number of signals that can be evaluated present in the spectrum. Means of these values were used for comparison (see table 3.1).

**Table 3.1** Comparison of peptide extraction methods for plasma

<i>extraction method</i>	<i>number of significant bins (<math>\sigma &gt; 5</math>)</i>	<i>number of significant peaks (<math>\sigma &gt; 5</math>)</i>
<b>Human plasma</b>		
<b>Oasis<sup>®</sup> HLB</b>	2	0
<b>Oasis<sup>®</sup> HLB + Micron<sup>®</sup> filter</b>	988	132
<b>BOND ELUTE<sup>®</sup></b>	2	0
<b>BOND ELUTE<sup>®</sup> + Microcon<sup>®</sup> filter</b>	730	102
<b>Strata<sup>™</sup>-X</b>	15	1
<b>Strata<sup>™</sup>-X + Microcon<sup>®</sup> filter</b>	565	84
<b>Murine plasma</b>		
<b>Oasis<sup>®</sup> HLB</b>	25	4
<b>Oasis<sup>®</sup> HLB + Micron<sup>®</sup> filter</b>	1188	153
<b>BOND ELUTE<sup>®</sup></b>	9	0
<b>BOND ELUTE<sup>®</sup> + Microcon<sup>®</sup> filter</b>	861	115
<b>Strata<sup>™</sup>-X</b>	21	3
<b>Strata<sup>™</sup>-X + Microcon<sup>®</sup> filter</b>	1215	161

Values represent means of three analyses from aliquots of the same sample.

From the results shown above it is clear that size exclusion filtration is an essential step for each method to improve the signal intensity for lower molecular weight species, on which the applied method focuses. Figure 3.3 demonstrates the effect of filtration on the spectrum.

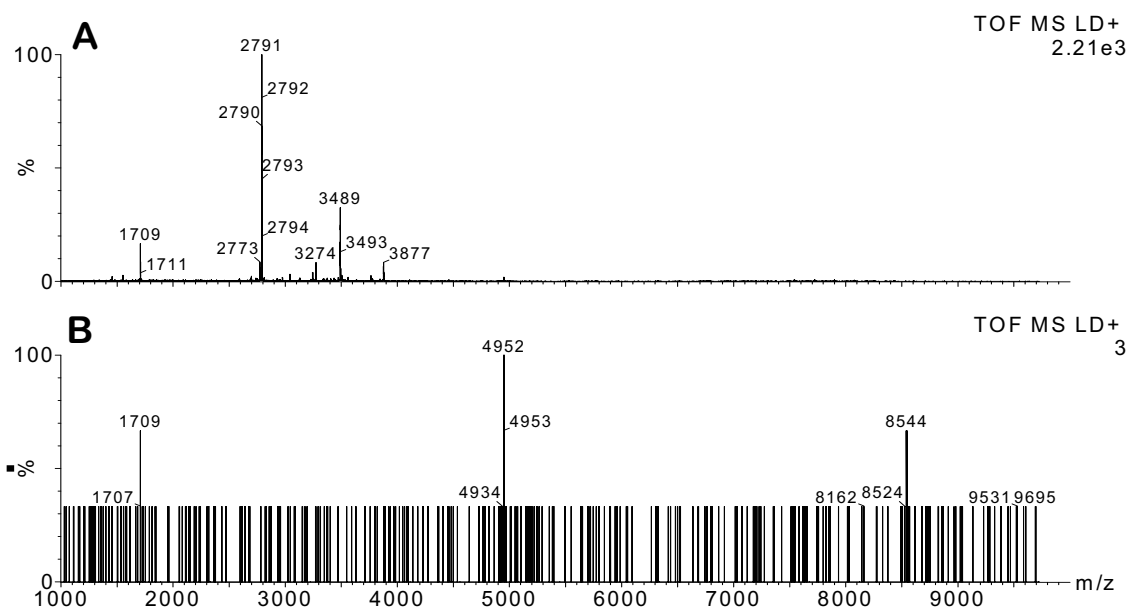


**Figure 3.3** MALDI-MS spectra of mouse plasma extracted with Oasis<sup>®</sup> HLB cartridges (A) with or (B) without subsequent Microcon<sup>®</sup> filtration.

For human plasma the Oasis<sup>®</sup> HLB method gave by far the most information rich spectra, while Strata-X<sup>®</sup> was marginally superior for mouse plasma. As mentioned above, it was necessary to choose a method that is suitable for plasma from both species. Therefore, due to its clear advantages over the other methods for human plasma, the Oasis<sup>®</sup> HLB method was chosen for all peptide extractions from plasma.

### 3.1.2 Peptide extraction method for urine

As in the case of the plasma peptide extraction method an extraction method was required that was suitable for urine samples of both human and murine origin, in order to create a basis for comparability.

To minimise sample degradation mouse urine samples were collected over dry ice in metabolism cages over night and then stored at  $-80^{\circ}\text{C}$ . Human urine samples were aliquoted and stored at  $-80^{\circ}\text{C}$  immediately after collection. Oasis<sup>®</sup> HLB, BOND ELUT<sup>®</sup>, and Strata-X<sup>®</sup> were compared using the same mathematical measures as described above (section 3.1.1 and sections 2.2.2.2-2.2.2.4). All methods were tested in triplicate using aliquots of the same sample. Preliminary results showed that additional Microcon<sup>®</sup> filtration did not improve the signal intensity for urine samples. Table 3.2 shows the results of the mathematical comparison of the three extraction methods. Consistent with the results for the plasma peptide extraction (see section 3.1.1), Oasis<sup>®</sup> HLB extraction showed the best overall performance and was chosen for all future urine peptide extractions. Figure 3.4 shows MALDI-MS spectra obtained from human and mouse urine extracted using Oasis<sup>®</sup> HLB cartridges

**Table 3.2** Comparison of peptide extraction methods for urine

<i>extraction method</i>	<i>number of significant bins (<math>\sigma &gt; 5</math>)</i>	<i>number of significant peaks (<math>\sigma &gt; 5</math>)</i>
<b>Human urine</b>		
<b>Oasis<sup>®</sup> HLB</b>	382	52
<b>BOND ELUTE<sup>®</sup></b>	377	63
<b>Strata<sup>™</sup>-X</b>	284	46
<b>Murine urine</b>		
<b>Oasis<sup>®</sup> HLB</b>	779	109
<b>BOND ELUTE<sup>®</sup></b>	601	88
<b>Strata<sup>™</sup>-X</b>	696	102

Values represent means of three analyses from aliquots of the same sample.

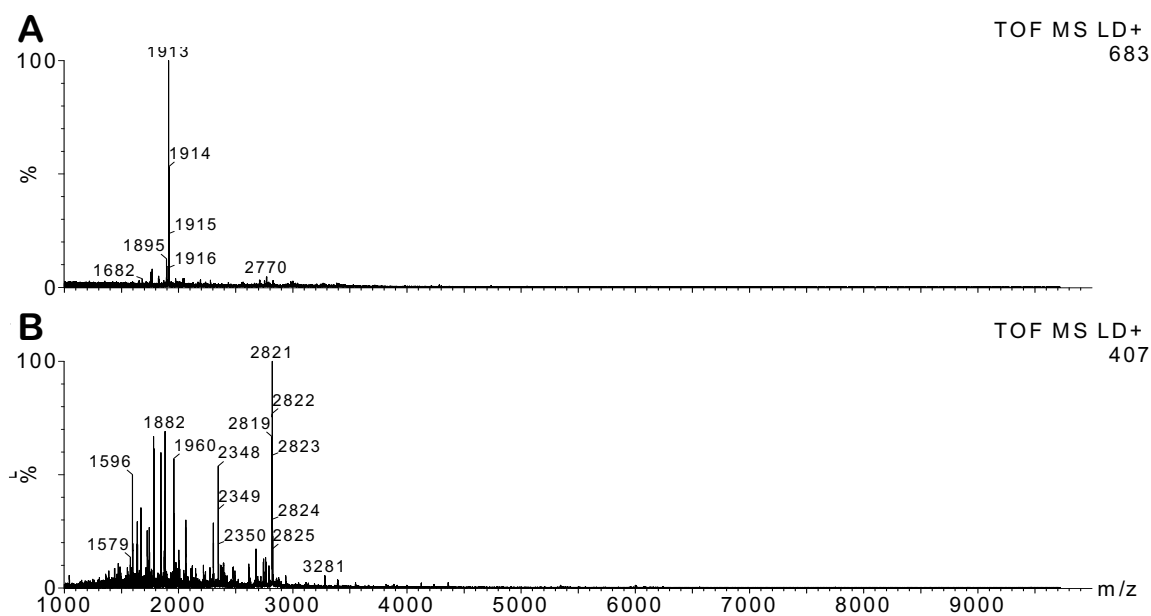


**Figure 3.4** MALDI-MS spectra of human (A) and mouse (B) urine extracted with Oasis<sup>®</sup> HLB cartridges.

## 3.2 Measurement of urinary 8-oxodG

### 3.2.1 SPE of urine samples

The objective was to determine the concentration of 8-oxodG in mouse and human urine samples. The LC-MS/MS method used for the quantification has been described previously (Cooke *et al.*, 2006a). However, the method required alterations due to the limited volume available from the mice.

In order to investigate whether the determination of 8-oxodG was feasible using smaller urine volumes, 200µl aliquots of a human urine sample were processed with different SPE methods. For each method three aliquots were extracted and analysed in duplicates. Firstly, the sample preparation method by Lin *et al.* (2004), which was also used by Cooke *et al.* (2006a) was adjusted to use a smaller sample volume (see section 2.2.3.2). Modifications of the Water Oasis<sup>®</sup> HLB guidelines for peptide extraction (Waters, 2003) were also tested (see sections 2.2.3.3 and 2.2.3.4). All three methods used Oasis<sup>®</sup> HLB columns (30mg). Other than the method by Lin *et al.* the HLB methods did not involve acid incubation and centrifugation steps. The difference between the HLB I and HLB II method is that HLB II uses non-acidified solvents while in HLB I all wash and elution solvents contain 0.1% formic acid. None of the three methods tested showed any major differences for the detected amount of 8-oxodG. However, the values for the peak areas suggested that the HLB II method had a better recovery than the other two methods (table 3.3).

**Table 3.3** Comparison of SPE methods for urine for the determination of 8-oxodG

<i>extraction method</i>	<i>peak area [counts]</i>		<i>8-oxodG [pmol/ml]</i>
	<i>8-oxodG</i>	<i>[<sup>15</sup>N<sub>5</sub>]8-oxodG</i>	
<b>mod. paper method</b>	18833 (1560)	40419 (4440)	23.4 (0.8)
<b>HLB I</b>	17415 (2347)	37562 (4974)	23.2 (0.3)
<b>HLB II</b>	25857 (2161)	55423 (4879)	23.3 (0.6)

Values given are means from all 6 analyses; standard deviation in brackets.

Sample volumes were further reduced to 100µl for both murine and human urine and the reconstitution volume was therefore changed to 50µl instead of 100µl. HLB II showed significantly higher peak areas than the other two methods and was therefore chosen for final validation. The recovery of 8-oxodG following SPE was 93 to 98% for mouse urine and 94 to 104% for human urine as determined by the addition of 8-oxodG standard ranging from 0.5 to 20pmol to 100µl aliquots of the same mouse urine sample before or after SPE purification and the addition of 10pmol of [<sup>15</sup>N<sub>5</sub>]8-oxodG following SPE. Linearity for the detection of 8-oxodG was tested by plotting the 8-oxodG peak area / [<sup>15</sup>N<sub>5</sub>]8-oxodG peak area ratio against 8-oxodG standard ranging from 0 to 25pmol on column spiked into aliquots of the same mouse urine sample and subsequent subjection to the entire analysis procedure. For both murine and human urine the response was linear to the amount of added standard with correlation coefficients (R<sup>2</sup>) of 0.9999 and 0.9994, respectively. The average coefficient of variation for the determination of 8-oxodG was 2.2% in mouse urine and 4.6% in human urine, which was obtained by the analysis of aliquots of the same urine sample five times. The limit of detection for the analysis of 8-oxodG by LC-MS/MS was 5fmol on column (signal-to-noise ratio, S/N = 3) for pure 8-oxodG standard and 10fmol in matrix (100µl of urine

subjected to SPE) ( $S/N, = 4$ ), for both human and mouse urine. Figure 3.5 and 3.6 show typical chromatograms from human and mouse urine in the SRM channels of 8-oxodG and [ $^{15}\text{N}_5$ ]8-oxodG.

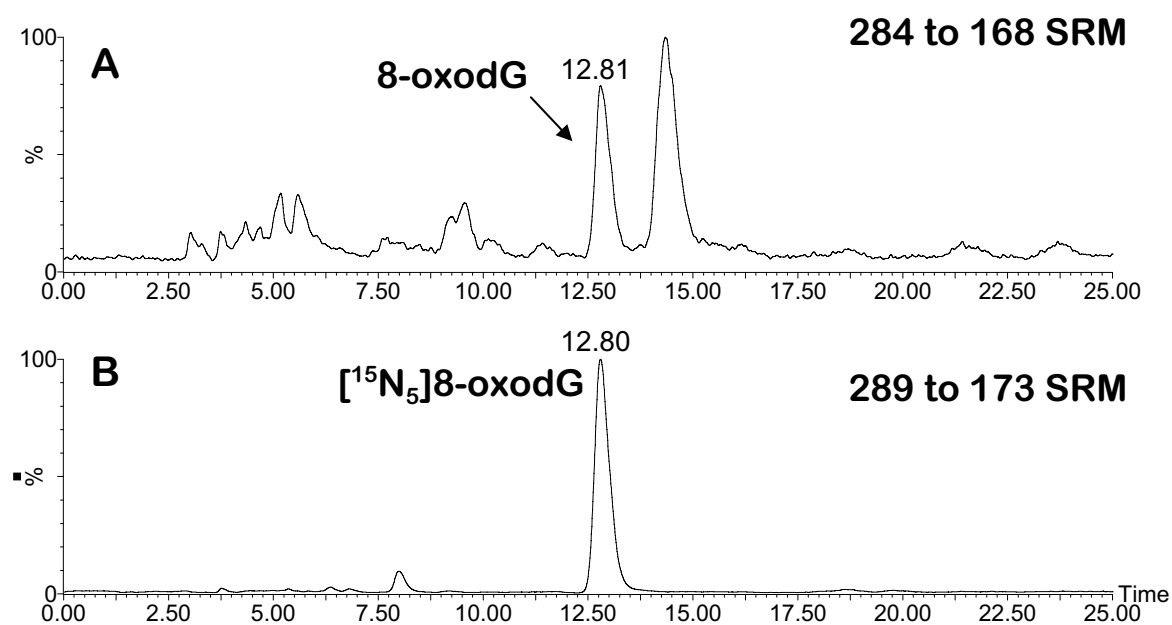


**Figure 3.5** Typical chromatogram obtained from human urine showing the SRM channels for (A) 8-oxodG and (B) [ $^{15}\text{N}_5$ ]8-oxodG.

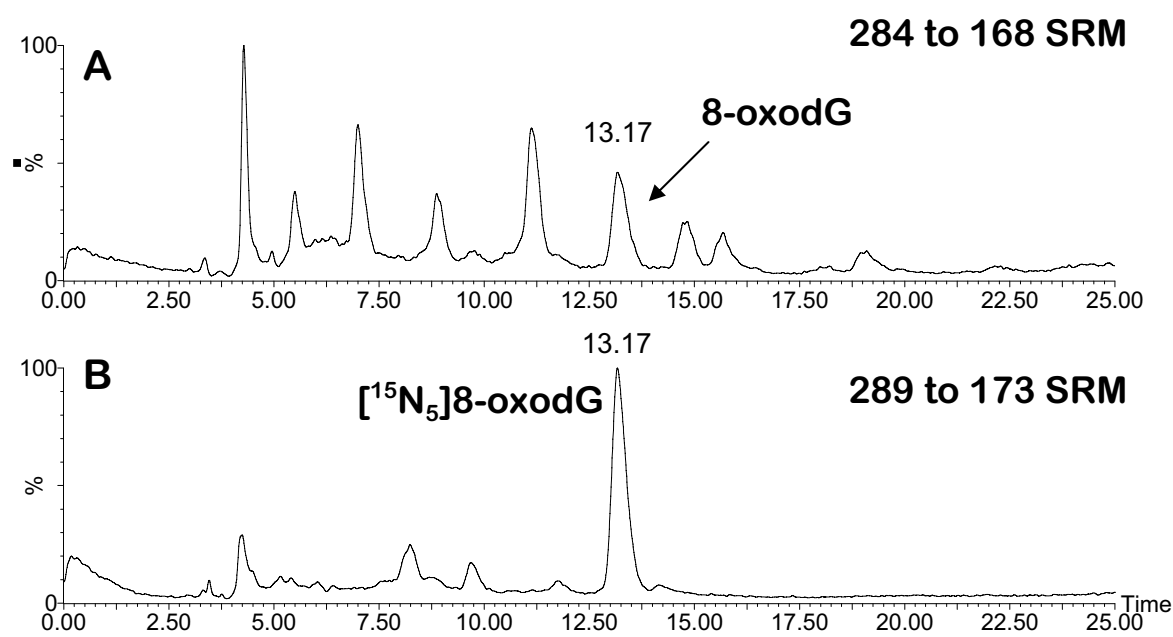


**Figure 3.6** Typical chromatogram obtained from mouse urine showing the SRM channels for (A) 8-oxodG and (B)  $[^{15}\text{N}_5]$ 8-oxodG.

### 3.2.2 Determination of urinary creatinine by LC-MS/MS

Urinary creatinine is derived from phosphocreatine degradation in muscle tissue. It is filtered through the glomeruli and is not reabsorbed by the tubules (Narayanan and Appleton, 1980). It is frequently used as normalisation factor for endogenous and exogenous substances measured in urine (Heavner *et al.*, 2006). The most commonly used method to determine urinary creatinine in the clinic is the Jaffé reaction with picric acid in alkaline medium (Jaffé, 1886). However, this method has its limitations as it is very sensitive to changes in experimental conditions such as temperature and pH. In addition to that the assay suffers from cross reactivity with carbonyl compounds (Narayanan and Appleton, 1980; Weber and Vanzanten, 1991).

For mouse urine samples a maximum of 50 µl was available for the creatinine measurement which was too little for the automated measurement in the clinic. The manual determination of creatinine using a creatinine kit (see section 2.2.3.6) proved to be very time consuming and the reliability was questionable, since the difference between the replicate analyses was in some cases up to 50%. Therefore it was decided to develop a method to determine creatinine by LC-MS/MS using SRM and a stable isotope internal standard.

Creatinine can be measured using two different transitions in positive ionisation mode mass spectrometry: 114 m/z to 86 m/z or 114 m/z to 44 m/z; with corresponding transitions of 117 m/z to 89 m/z and 117 m/z to 47 m/z for the [<sup>2</sup>H<sub>3</sub>]creatinine stable isotope internal standard. Both SRM transitions have been employed previously for the determination of creatinine by LC-MS/MS (Husková *et al.*, 2004; Takahashi *et al.*, 2007) and were therefore both investigated for their suitability.

The HPLC conditions are described in section 2.2.3.7. In brief, the acetonitrile was increased from 2% to 35% over 10 min before returning to starting conditions. The

column was then left to re-equilibrate for 10 min. The sample preparation (section 2.2.3.7) was a simple protein precipitation following dilution of 1:1000 for mouse urine and 1:10000 for human urine since the creatinine concentration in human urine is approximately ten times higher. A similar method of sample preparation has previously been used by Takahashi *et al.* (2007).

During method development an interfering contamination peak at the same retention time as creatinine was observed in blank injections using HPLC grade water (figure 3.7). This contamination peak also persisted following the switch from laboratory purified HPLC grade water to bottled HPLC grade water. Injections with acetonitrile did not show any interfering peak, neither did 2% acetonitrile in water. It was therefore decided to use 2% acetonitrile as solvent for standards and samples as well as for blank injections. Another phenomenon observed was the persistence of the creatinine and [<sup>2</sup>H<sub>3</sub>]creatinine peaks in blank injections after the first sample or standard injections. This problem was solved by injecting a sample containing creatinine five times prior to the analysis of study samples. Figures 3.8 and 3.9 show SRM chromatograms obtained from murine and human urine, respectively.

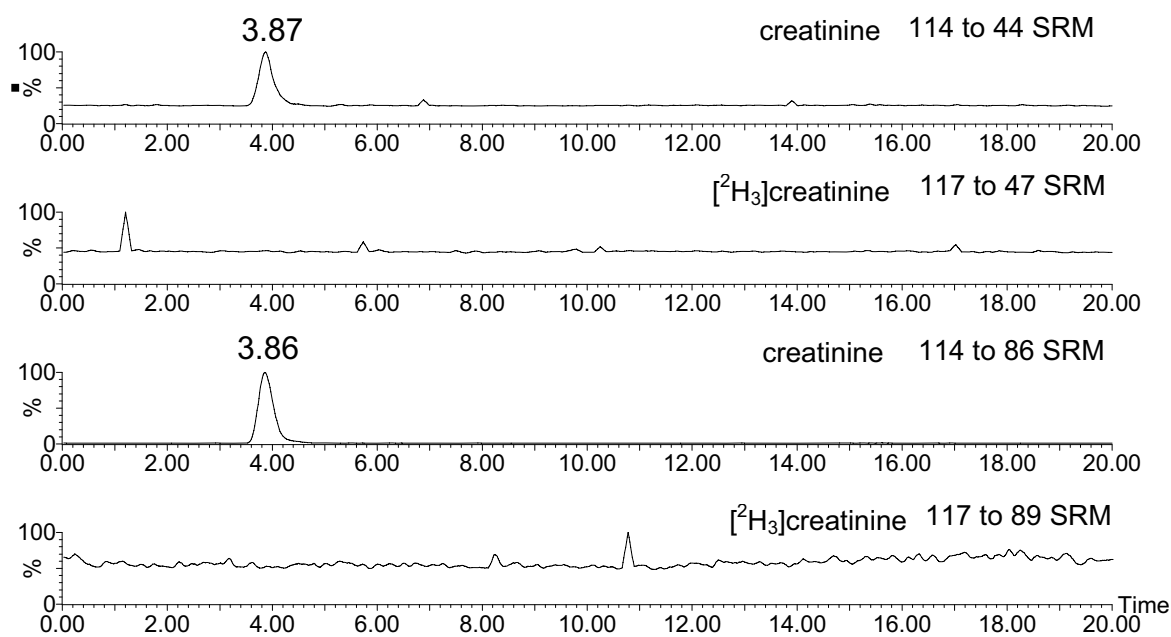


**Figure 3.7** Chromatogram of interfering peaks obtained from blank water injections showing the different SRM channels for creatinine and [ $^2\text{H}_3$ ]creatinine.

The ionisation properties of deuterated compounds are different from natural isotope containing compounds due to altered electronegativities of the covalent bonds (Haskins, 1982). The use of deuterated internal standards therefore requires the determination of a response factor. To calculate this factor, mixtures of equal amounts of labelled and unlabelled creatinine standard ranging from 0.5 to 10fmol on column, were injected onto the mass spectrometer. The peak area of the [ $^2\text{H}_3$ ]creatinine was then divided by the peak area of creatinine. For the 117 m/z to 89 m/z SRM transition the response factor for [ $^2\text{H}_3$ ]creatinine was 0.854 and 1.750 in the 117 m/z to 47 m/z SRM transition. Linearity for the detection of creatinine was tested by plotting the creatinine peak area / [ $^2\text{H}_3$ ]creatinine peak area ratio against creatinine standard ranging from 0 to 50pmol on column spiked into aliquots of the same urine sample prior to sample extraction. For mouse urine the correlation coefficients ( $R^2$ ) were 1.000 and 0.9999 for the 114 to 86

m/z and 114 to 44 m/z SRM transitions, respectively. For human urine the correlation coefficients ( $R^2$ ) were 0.9998 and 0.9996 for the 114 to 86 m/z and 114 to 44 m/z SRM transitions, respectively. The average coefficient of variation (CV) was obtained by the analysis of aliquots of the same urine sample five times. The CV for the 114 to 89 m/z SRM transition was 1.8% in human and 4.9% in mouse urine and 1.0% and 4.7% for 114 to 44 m/z in human and mouse urine, respectively. For determination of creatinine the 114 to 86 m/z SRM transition was used since it gave a higher response when compared to the 114 to 44 m/z SRM transition.

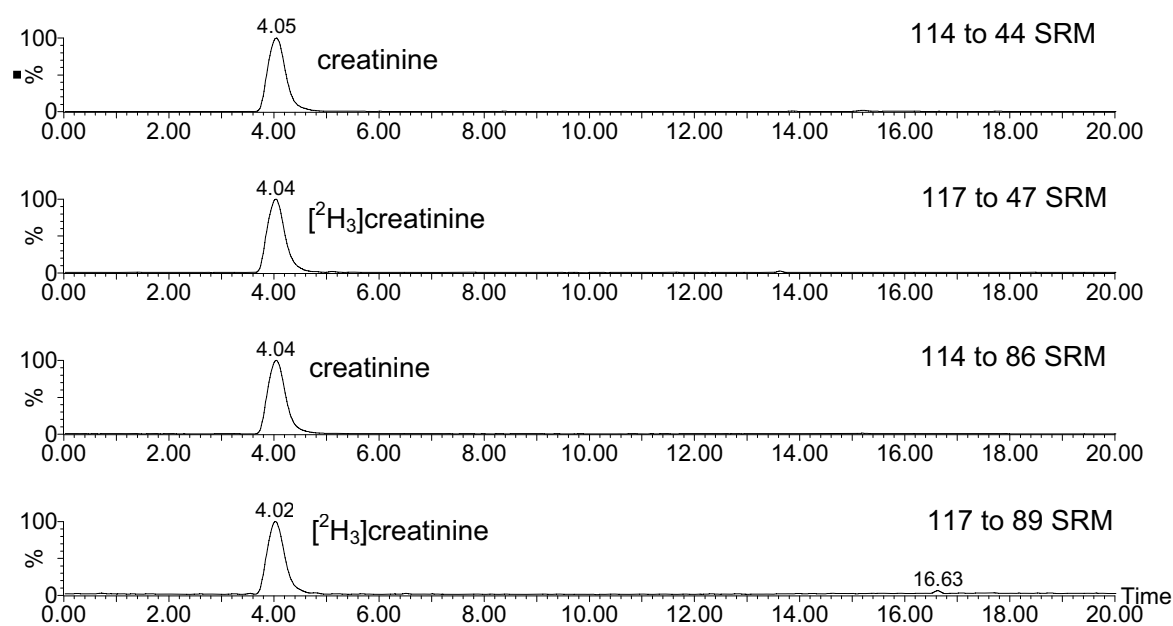


**Figure 3.8** Typical chromatogram obtained from mouse urine showing the SRM channels for [ $^2\text{H}_3$ ]creatinine and creatinine.

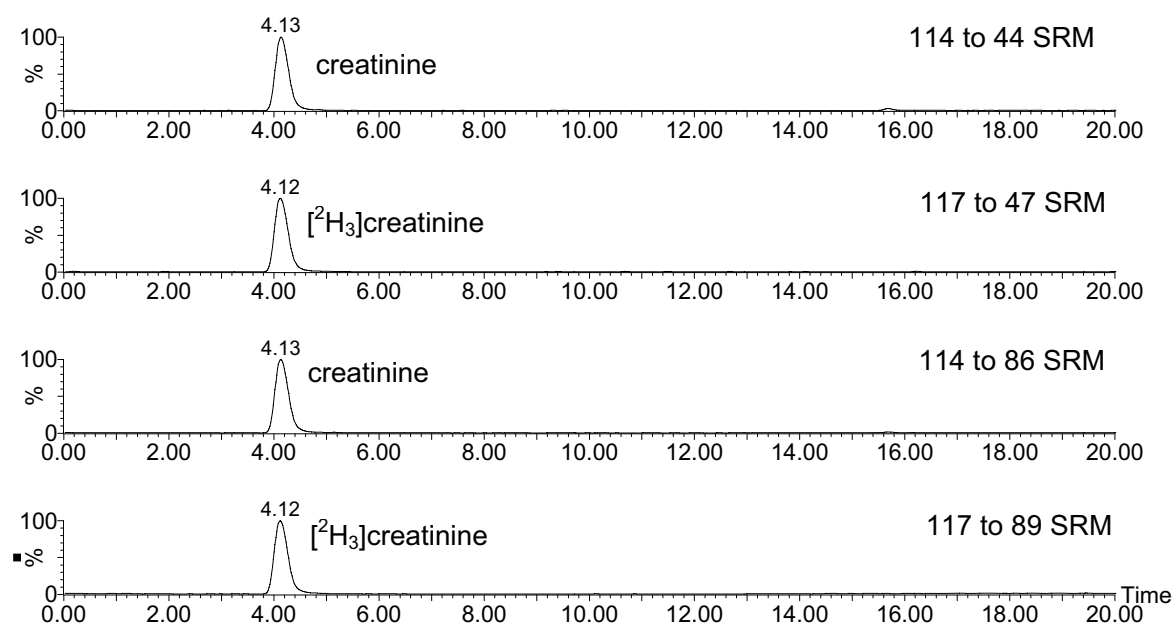


**Figure 3.9** Typical chromatogram obtained from human urine showing the SRM channels for [<sup>2</sup>H<sub>3</sub>]creatinine and creatinine.

# Chapter 4

## **4. Search for biochemical features of carcinogenesis in the TRAMP mouse model of prostate cancer**

It was the aim of this study (see section 2.2.1.4) to search for biomarkers related to the process of carcinogenesis in the TRAMP mouse model of prostate cancer and to elucidate further its mechanism. Age matched TRAMP and wild type mice were sacrificed at an early and a late stage of carcinogenesis; 8 and 28 weeks of age, respectively. In the following text the 8 week old mice are referred to as “young” and the 28 week old as “old”. Urine, plasma and prostate tissue samples were collected as described in sections 2.2.1.4 and 2.2.1.7 – 2.2.1.9.

### **4.1 Metabolic and pathological changes in prostate tissue of TRAMP mice**

Metabolic changes accompanying human prostate carcinogenesis are already used in the clinic as a diagnostic feature (see Chapter 1). It was the aim of this experiment to compare the TRAMP mouse tumour metabolite profile to that in humans with prostate cancer.

#### **4.1.1 Histopathological changes in prostate tissue of TRAMP mice**

Young TRAMP mice presented with small and scattered foci of hyperplasia characterised by the presence of dense hyperchromatic epithelial cells. These were the earliest proliferative lesions observed. Figure 4.1 A shows a photograph of prostate tissue from an 8 week old TRAMP mouse with a hyperplastic focus. Glands in old TRAMP mice were characterised by varying degrees of glandular hyperplasia and atypical hyperplasia (prostatic intraepithelial neoplasia, PIN), carcinomas with

microinvasion through to overtly invasive well-differentiated adenocarcinomas (figure 4.1 B) In a small proportion of the animals poorly differentiated carcinomas were found. Wild type mice did not show any discernible malignant change at either time point.

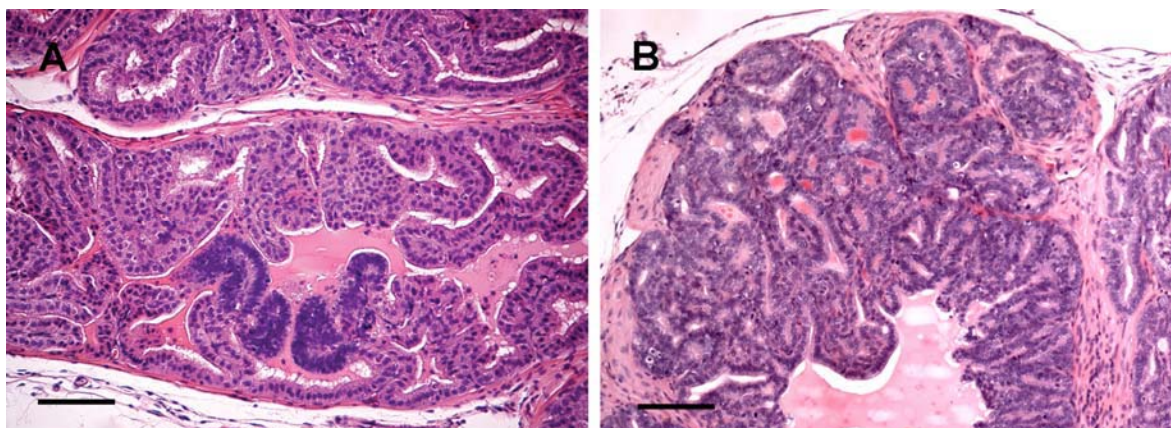


**Figure 4.1** Prostatic tissue from TRAMP mice of 8 (A) or 28 weeks of age (B) stained with haematoxylin and eosin. Dark staining reflects elevated chromatin levels indicating an above-average cell division rate. Note early focal zone of hyperplasia in A, and edge of a large well differentiated carcinoma showing the disordered glandular structure and tumour cells pushing through to the edge of the fibrous capsule at the periphery, features of microinvasion in B. Bar: 100  $\mu\text{m}$ .

#### 4.1.2 $^1\text{H}$ -NMR metabolic profiling of aqueous tissue extracts

The results described here are for a combination of aqueous tissue extracts from both TRAMP studies (see sections 2.2.1.4 and 2.2.1.5); only water-fed animals from the second study were included. Sample preparation, acquisition method and data handling are described in sections 2.2.4.3, 2.2.4.5 and 2.2.4.6. Spectral assignments were made with a combination of homonuclear COSY experiments (carried out by Dr Hector Keun, Imperial College, London), literature (Bollard *et al.*, 2005; Nicholson *et al.*, 1989), the

BMRB database (<http://www.bmrb.wisc.edu/>) (Seavey *et al.*, 1991) and advice from Drs Hector Keun and Muireann Coen, Imperial College, London. Glycero-phosphoinositol (GPI) was assigned by additional analysis of extracts by  $^1\text{H}$ - $^{31}\text{P}$  correlation spectroscopy (HMQC) using a QXI probe and a Bruker Avance 800 MHz spectrometer, carried out by Dr Hector Keun, and by comparison to spectra of phosphoinositol standards and literature data (van der Rest *et al.*, 2002).

Changes in metabolite levels were calculated from the medians and significance was established using the Mann-Whitney U-test.

Figure 4.2 shows a representative  $^1\text{H}$ -NMR spectrum of an aqueous prostate tissue extract from an old wild type mouse. Signals of citrate, choline, phosphocholine (PC), glycerophosphocholine (GPC), GPI, lactate, taurine, glucose, UDP-linked sugars (UDPx), tyrosine, aspartate, glutamate, and alanine were integrated for comparative quantitative evaluation.

In the young animal groups there were no significant differences in single metabolite levels between transgenic and non-transgenic mice. In contrast, old TRAMP mice presented with decreased levels of citrate, choline, PC, GPC, GPI, glucose and UDPx by 49, 33, 57, 66, 61, 54 and 45%, respectively, as compared to normal prostate in age-matched wild type mice. An increase was observed for taurine, tyrosine, alanine, glutamate and aspartate by 27, 28, 18, 39 and 12%, respectively, in tumour tissue when compared to wild type prostate. The difference was statistically significant only in the case of aspartate. No group difference was observed in lactate tissue levels (table 4.1).

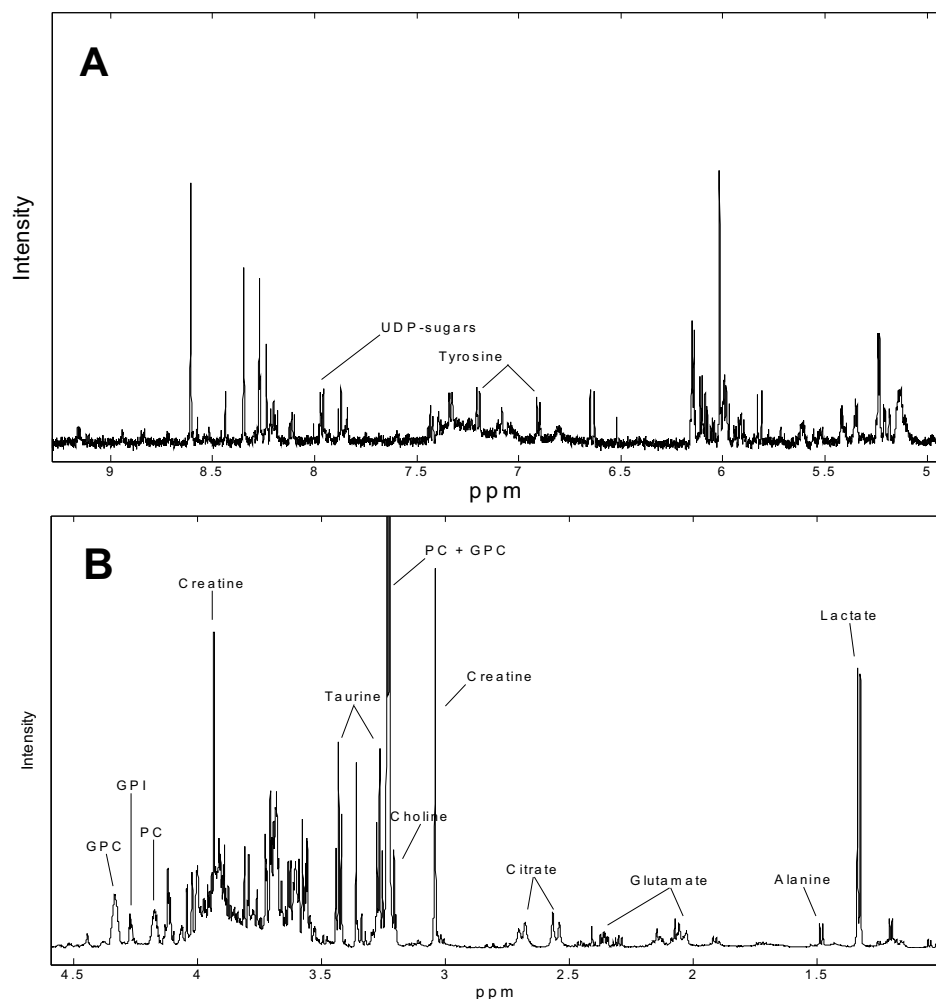


**Figure 4.2** Typical  $^1\text{H-NMR}$  spectrum of an aqueous prostate tissue extract from a 28 week old wild type mouse in the (A) aromatic and (B) aliphatic region.

Results very similar to those shown in Table 4.1 were obtained when metabolite levels were normalised to creatine (singlet 3.04 ppm) (results not shown), which has been used previously to normalise metabolite data in human studies (Swanson *et al.*, 2003). This finding reflects the robustness of the results obtained.

**Table 4.1** Median relative metabolite peak areas in prostate tissues of 8 week or 28 week old wild type or TRAMP mice

<i>metabolite</i>	<i>wild type</i> 8 weeks	<i>TRAMP</i> 8 weeks	<i>wild type</i> 28 weeks	<i>TRAMP</i> 28 weeks
<b>citrate</b> (d 2.55ppm)	1.21x10 <sup>9</sup> (0.54x10 <sup>9</sup> / 1.76x10 <sup>9</sup> )	1.27x10 <sup>9</sup> (0.52x0 <sup>9</sup> / 2.14x10 <sup>9</sup> )	1.72x10 <sup>9</sup> (0.58x10 <sup>9</sup> / 2.61x10 <sup>9</sup> )	★★ 0.88x10 <sup>9</sup> (0.33x10 <sup>9</sup> / 1.61x10 <sup>9</sup> )
<b>choline</b> (s 3.20ppm)	1.13x10 <sup>9</sup> (0.32x10 <sup>9</sup> / 2.72x10 <sup>9</sup> )	0.87x10 <sup>9</sup> (0.47x10 <sup>9</sup> / 1.65x10 <sup>9</sup> )	0.81x10 <sup>9</sup> (0.57x10 <sup>9</sup> / 0.96x10 <sup>9</sup> )	★ 0.54x10 <sup>9</sup> (0.13x10 <sup>9</sup> / 0.93x10 <sup>9</sup> )
<b>PC</b> (s 3.23ppm)	2.36x10 <sup>9</sup> (1.60x10 <sup>9</sup> / 4.31x10 <sup>9</sup> )	3.44x10 <sup>9</sup> (1.53x10 <sup>9</sup> / 4.87x10 <sup>9</sup> )	5.90x10 <sup>9</sup> (2.62x10 <sup>9</sup> / 6.78x10 <sup>9</sup> )	★★ 2.53x10 <sup>9</sup> (0.39x10 <sup>9</sup> / 6.44x10 <sup>9</sup> )
<b>GPC</b> (s 3.24ppm)	5.22x10 <sup>9</sup> (2.92x10 <sup>9</sup> / 10.44x10 <sup>9</sup> )	6.34x10 <sup>9</sup> (1.34x10 <sup>9</sup> / 9.87x10 <sup>9</sup> )	8.02x10 <sup>9</sup> (4.92x10 <sup>9</sup> / 11.23x10 <sup>9</sup> )	★★★ 2.75x10 <sup>9</sup> (0.39x10 <sup>9</sup> / 5.44x10 <sup>9</sup> )
<b>GPI</b> (t 4.247ppm)	2.87x10 <sup>8</sup> (2.30x10 <sup>8</sup> / 5.45x10 <sup>8</sup> )	3.34x10 <sup>8</sup> (1.87x10 <sup>8</sup> / 5.76x10 <sup>8</sup> )	5.24x10 <sup>8</sup> (4.13x10 <sup>8</sup> / 5.80x10 <sup>8</sup> )	★★★ 2.07x10 <sup>8</sup> (1.16x10 <sup>8</sup> / 4.07x10 <sup>8</sup> )
<b>taurine</b> (t 3.43ppm)	3.07x10 <sup>9</sup> (1.64x10 <sup>9</sup> / 4.72x10 <sup>9</sup> )	3.03x10 <sup>9</sup> (1.37x10 <sup>9</sup> / 4.16x10 <sup>9</sup> )	2.75x10 <sup>9</sup> (1.87x10 <sup>9</sup> / 3.28x10 <sup>9</sup> )	3.50x10 <sup>9</sup> (1.40x10 <sup>9</sup> / 6.10x10 <sup>9</sup> )
<b>lactate</b> (d 1.33ppm)	2.52x10 <sup>9</sup> (1.28x10 <sup>9</sup> / 4.61x10 <sup>9</sup> )	2.88x10 <sup>9</sup> (1.01x10 <sup>9</sup> / 3.90x10 <sup>9</sup> )	1.90x10 <sup>9</sup> (1.44x10 <sup>9</sup> / 3.27x10 <sup>9</sup> )	1.96x10 <sup>9</sup> (1.08x10 <sup>9</sup> / 3.47x10 <sup>9</sup> )
<b>glucose</b> (d 5.23ppm)	0.84x10 <sup>8</sup> (0.45x10 <sup>8</sup> / 1.88x10 <sup>8</sup> )	0.70x10 <sup>8</sup> (0.52x10 <sup>8</sup> / 1.13x10 <sup>8</sup> )	0.83x10 <sup>8</sup> (0.60x10 <sup>8</sup> / 1.22x10 <sup>8</sup> )	★★★ 0.38x10 <sup>8</sup> (0.18x10 <sup>8</sup> / 0.59x10 <sup>8</sup> )
<b>tyrosine</b> (d 6.90ppm)	3.82x10 <sup>7</sup> (2.54x10 <sup>7</sup> / 5.33x10 <sup>7</sup> )	3.11x10 <sup>7</sup> (2.10x10 <sup>7</sup> / 4.51x10 <sup>7</sup> )	2.79x10 <sup>7</sup> (2.20x10 <sup>7</sup> / 4.91x10 <sup>7</sup> )	3.57x10 <sup>7</sup> (2.02x10 <sup>7</sup> / 7.60x10 <sup>7</sup> )
<b>aspartate</b> (d 2.82ppm)	1.78x10 <sup>8</sup> (1.17x10 <sup>8</sup> / 2.26x10 <sup>8</sup> )	1.71x10 <sup>8</sup> (1.42x10 <sup>8</sup> / 2.25x10 <sup>8</sup> )	1.80x10 <sup>8</sup> (1.44x10 <sup>8</sup> / 1.93x10 <sup>8</sup> )	★ 2.02x10 <sup>8</sup> (1.58x10 <sup>8</sup> / 3.63x10 <sup>8</sup> )
<b>glutamate</b> (td 2.36ppm)	7.91x10 <sup>8</sup> (5.84x10 <sup>8</sup> / 9.25x10 <sup>8</sup> )	7.40x10 <sup>8</sup> (5.44x10 <sup>8</sup> / 9.03x10 <sup>8</sup> )	5.99x10 <sup>8</sup> (4.81x10 <sup>8</sup> / 7.19x10 <sup>8</sup> )	8.32x10 <sup>8</sup> (4.68x10 <sup>8</sup> / 12.73x10 <sup>8</sup> )
<b>alanine</b> (d 1.48ppm)	7.25x10 <sup>8</sup> (3.90x10 <sup>8</sup> / 8.99x10 <sup>8</sup> )	6.07x10 <sup>8</sup> (3.28x10 <sup>8</sup> / 8.36x10 <sup>8</sup> )	4.16x10 <sup>8</sup> (3.93x10 <sup>8</sup> / 6.03x10 <sup>8</sup> )	4.90x10 <sup>8</sup> (3.07x10 <sup>8</sup> / 7.15x10 <sup>8</sup> )
<b>UDP-sugars</b> (d 7.96ppm)	0.59x10 <sup>8</sup> (0.07x10 <sup>8</sup> / 1.53x10 <sup>8</sup> )	0.58x10 <sup>8</sup> (0.08x10 <sup>8</sup> / 1.26x10 <sup>8</sup> )	0.63x10 <sup>8</sup> (0.41x10 <sup>8</sup> / 1.51x10 <sup>8</sup> )	★ 0.34x10 <sup>8</sup> (0.14x10 <sup>8</sup> / 0.59x10 <sup>8</sup> )
<b>creatine</b> (s 3.04ppm)	1.73x10 <sup>9</sup> (0.66x10 <sup>9</sup> / 3.28x10 <sup>9</sup> )	1.76x10 <sup>9</sup> (0.66x10 <sup>9</sup> / 2.96x10 <sup>9</sup> )	1.56x10 <sup>9</sup> (1.03x10 <sup>9</sup> / 2.74x10 <sup>9</sup> )	2.10x10 <sup>9</sup> (0.39x10 <sup>9</sup> / 8.42x10 <sup>9</sup> )

Stars indicate that differences between median metabolite levels were significant according to Mann-Whitney U-test, ★ p<0.05; ★★ p<0.01; ★★★ p<0.001. Values in brackets are minima and maxima. ppm values under the metabolite denote the signal that has been integrated.

Peak ratios of choline to citrate (Cho/Cit) and total choline (choline+PC+GPC) to citrate (tCho/Cit) can be used to distinguish malignant from normal prostate in humans (Kurhanewicz *et al.*, 1996). These ratios did not show a significant change between TRAMP and wild type mice at either time point. However, the GPC to PC ratio (GPC/PC) was decreased by 22% in young TRAMP mice compared to age matched wild type mice (table 4.2).

**Table 4.2** Median metabolite ratios in prostate tissues of 8 week or 28 week old wild type or TRAMP mice

<i>metabolite ratio</i>	<i>wild type 8 weeks</i>	<i>TRAMP 8 weeks</i>	<i>wild type 8 weeks</i>	<i>TRAMP 8 weeks</i>
<b>Cho/Cit</b>	0.79 (0.36 / 5.07)	0.88 (0.22 / 3.20)	0.50 (0.24 / 0.98)	0.56 (0.25 / 1.12)
<b>tCho/Cit</b>	9.35 (4.30 / 16.06)	9.03 (3.96 / 13.35)	9.17 (4.17 / 20.48)	6.76 (2.73 / 16.89)
<b>GPC/PC</b>	2.40 ★ (1.23 / 3.55)	1.88 (0.87 / 2.36)	1.33 (0.92 / 3.33)	1.03 (0.42 / 2.23)
<b>aspartate/PC</b>	0.062 (0.052 / 0.11)	0.056 (0.041 / 0.11)	0.032 ★ ★ ★ (0.027 / 0.055)	0.057 (0.056 / 0.46)
<b>GPI/glutamate</b>	0.48 (0.28 / 0.61)	0.42 (0.26 / 0.69)	0.89 ★ ★ ★ (0.69 / 1.08)	0.25 (0.18 / 0.32)

Stars indicate that differences between median metabolite levels were significant according to Mann-Whitney U-test, ★ p<0.05; ★★ p<0.01; ★★★ p<0.001. Values in brackets are minima and maxima.

Hierarchical cluster analysis (carried out by Dr Hector Keun) of metabolite levels showed that at 28 weeks of age the metabolite profiles of TRAMP mice formed distinct clusters from those of wild type mice (figure 4.3 B). Young animals revealed no group specific clustering (figure 4.3 A), hence, the clustering was driven by natural variation

and not by the presence of the TRAMP genotype. In this analysis metabolites separated into two main groups. In the old animals one group consisted of phospholipid related species (PC, GPC, GPI, choline), citrate, UDPx and glucose, which were present at lower levels in tumour tissue compared to normal tissue. The other group contained amino acids, which were more abundant in tumour tissue than in normal prostate. In young animals the pattern of metabolite clustering was broadly similar, with the exception of glucose and aspartate. These two metabolites changed the clusters in conjunction with the presence of malignancy. At 28 weeks, when the TRAMP mice have fully developed tumours, glucose is associated with the phospholipid group and aspartate with the amino acid group (figure 4.3 B), whereas the reverse scenario is observed in 8 week old mice (figure 4.3 A). This finding suggests that glucose and aspartate are related to different metabolic events in tumour and normal tissue.

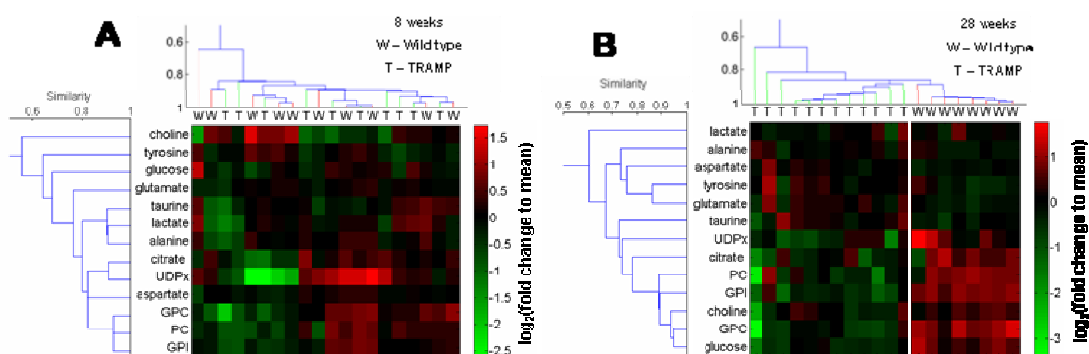


**Figure 4.3** Hierarchical clustering of metabolite levels showing that TRAMP and wild type mice can be distinguished by prostate metabolic profile at 28 weeks of age (**B**) but not at 8 weeks of age (**A**). Data are presented as mean-centred  $\log_2$  values, such that a value of 1 indicates a 2-fold change from the average amount of each metabolite across all samples from the same age group.

This apparent shift in metabolism was also observed when inter-metabolite correlations (carried out by Dr Hector Keun) for TRAMP mice were compared with those in wild type mice (figure 4.4). These correlations were calculated using data from young and old mice combined, hence patterns obtained reflect variation due to the normal process of aging in wild type mice and tumourigenesis in TRAMP mice. This analysis suggests that normal prostate tissue development is characterised by a positive correlation between levels of aspartate and citrate, with both metabolites sharing a common correlation pattern, and by a negative correlation between levels of citrate and glucose. The reverse scenario was observed in TRAMP mice, in which there was a positive correlation between levels of citrate and glucose, and both constituted part of the same cluster. In TRAMP mice aspartate was not correlated to citrate and clustered with other amino acids.

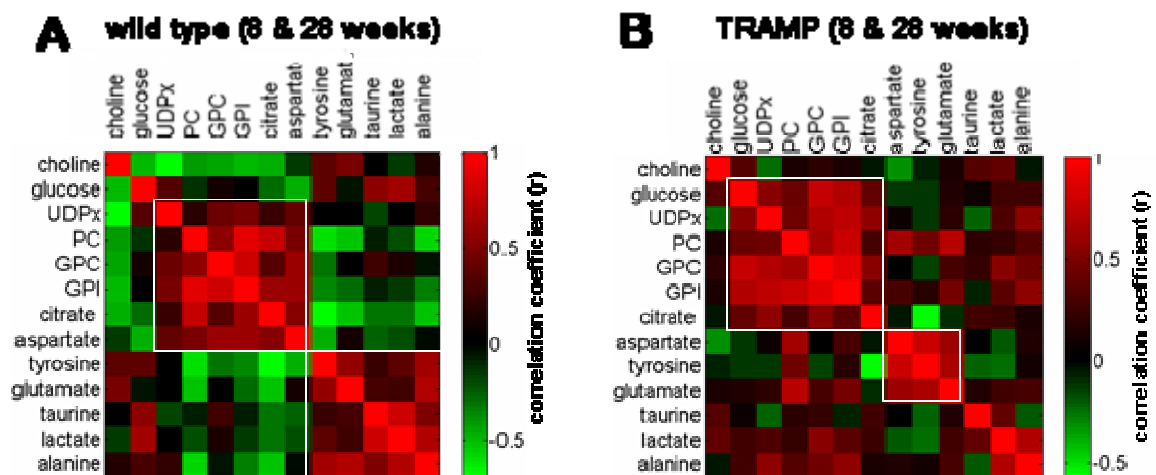


**Figure 4.4** Matrices of correlation coefficients ( $r$ ) between metabolite levels in extracts of prostate from wild type mice at either age (**A**), or in extracts of prostate from TRAMP mice at either age (**B**), showing a difference in metabolite clustering between prostate carcinogenesis and normal prostate aging.

The hypothesis was tested that ratios of metabolites allow better discrimination between TRAMP and wild type animals than levels of individual metabolites. Hierarchical clustering analysis suggests that metabolites from each cluster provides similar information regarding the presence of malignancy, and hence that the evaluation of combinations of metabolites from different clusters could be potentially more informative. For example, the aspartate/PC ratio was completely discriminatory between the two groups, whereas levels of the individual species were not (table 4.2). GPI levels separated between old TRAMP and wild type mice, but the GPI/glutamate ratio improved separation considerably: For GPI alone the difference between the lowest value for wild type tissue and the highest value for tumour tissue was only 1.3% of the combined wild type and tumour tissue value range, whilst for the GPI/glutamate ratio this value was 41.1% (Table 4.2, figure 4.5). Collectively, the results of the metabolite ratio and clustering analyses provide evidence for an effect of malignancy on the production and/or utilisation of metabolites, even when the difference in absolute concentration between wild type and TRAMP mice was, in some cases, not statistically significant.

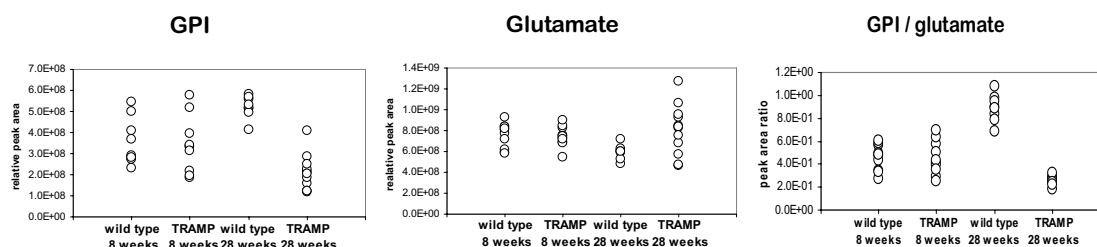


**Figure 4.5** Individual metabolite levels for GPI, glutamate and GPI / glutamate ratio

#### 4.1.3 High-Resolution Magic Angle Spinning (HRMAS) $^1\text{H}$ -NMR analysis of intact tissue

Human prostate cancer is associated with increased levels of choline metabolites as compared to healthy prostate tissue (see Introduction, section 1.1.3). In TRAMP mouse tumours choline species were lower than in healthy wild type prostates (see above). In order to verify the unexpected results for choline species in tissue extracts, intact prostate tissue samples from old mice were analysed by HRMAS  $^1\text{H}$ -NMR (see sections 2.2.4.4 and 2.2.4.5). Median levels of PC plus GPC, as reflected by relative peak areas, were 4.33 in tumour samples (minimum 3.21, maximum 4.93) and 9.41 in normal prostate (minimum 2.77, maximum 15.79,  $p=0.101$ , figure 4.6), suggesting tumour levels were 54 % below controls, even though the difference was not significant. No discrepancy was found in choline levels between normal and malignant tissue.

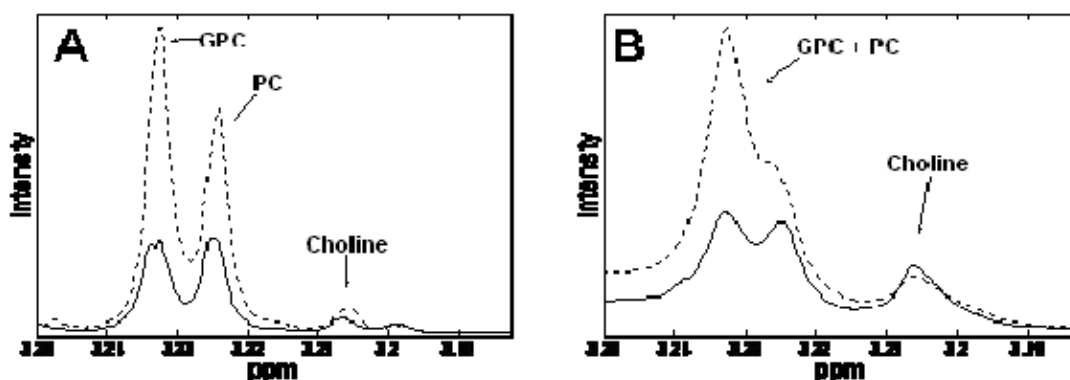


**Figure 4.6** Median  $^1\text{H}$ -NMR spectra of aqueous tissue extracts (A; wild type  $n = 8$ , TRAMP  $n = 12$ ) and median HRMAS NMR spectra of intact tissue (B; wild type  $n = 5$ , TRAMP  $n = 3$ ) of normal prostate from 28 week old wild type mice (broken line) or TRAMP mouse tumours (solid lines). Spectra focus on the choline metabolite region.

#### **4.1.4 Comparison of choline kinase (ChK) expression in prostate of 28 week old TRAMP and wild type mice**

Immunohistochemistry and RT-PCR analysis for murine ChK- $\alpha$  and - $\beta$  in normal or malignant prostate from old mice was carried out as described in sections 2.2.5 – 2.2.7. Expression of ChK- $\beta$  protein was present in the cytoplasm of glandular epithelial cells in the prostate gland (figure 4.7). In wild type animals, the staining intensity varied between different lobes of the gland; intense expression was only observed in the ventral regions (figure 4.7 A). Hyperplastic glands and well-differentiated carcinomas generally showed low expression (figure 4.7 B). Even less or no expression of ChK- $\beta$  was seen in poorly differentiated carcinomas, either in primary tumours or in a lymph node metastasis (figure 4.7 C, D). The antibody against ChK- $\alpha$  failed to generate significant staining in any of the tissues studied.

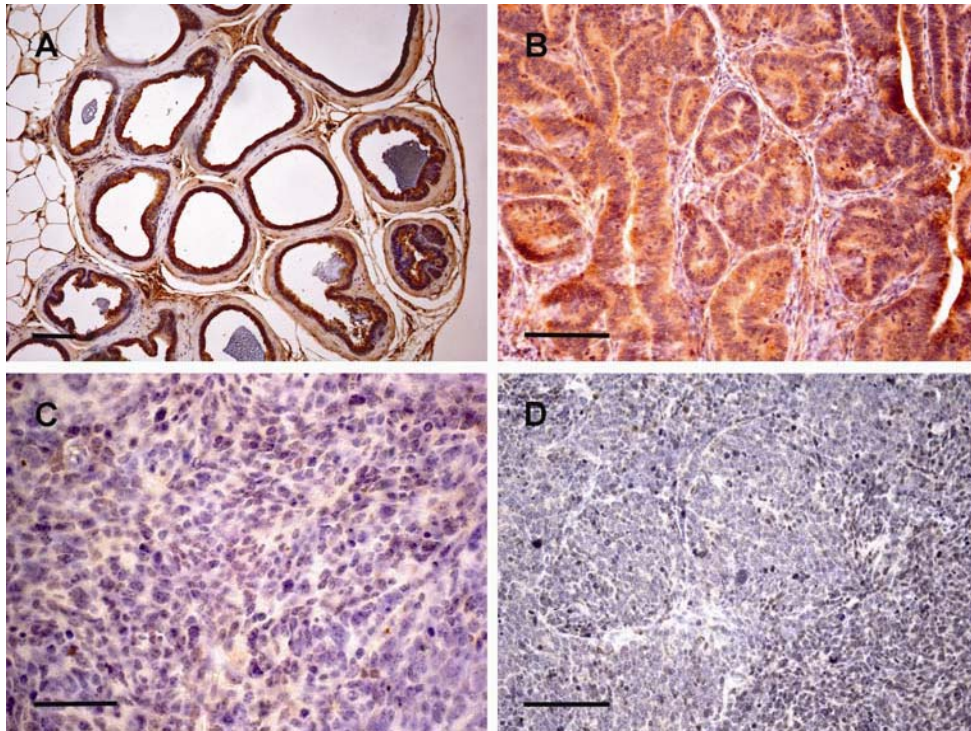


**Figure 4.7** Immunohistochemical staining for ChK- $\beta$  in normal ventral prostate (**A**) of C57BL/6J wild type mice, and in prostate tumours, well-differentiated (**B**) and poorly differentiated (**C**), or in a pelvic lymph node metastasis (**D**) in TRAMP mice. All mice were 28 weeks of age. Brown staining intensity reflects presence of enzyme. Bar: 100  $\mu\text{m}$ .

There was no difference in mean expression levels of *ChK-a* or *ChK- $\beta$*  mRNA between wild type prostate and TRAMP prostate tumour tissue as determined by RT-PCR. In contrast, in the lymph node metastasis sample *ChK-a* and *- $\beta$*  mRNA levels were only 8 and 50%, respectively, of those found in normal tissue (figure 4.8).

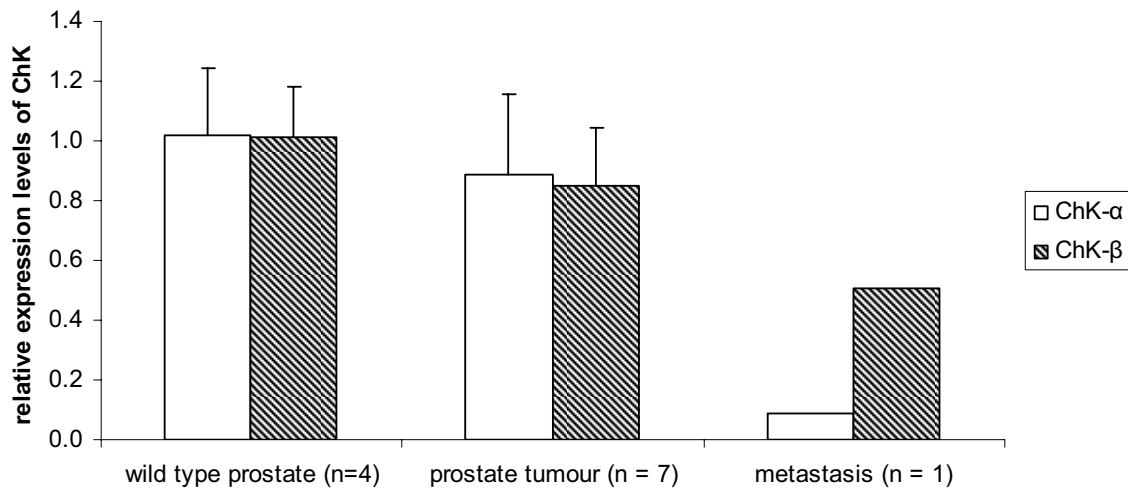


**Figure 4.8** Mean expression levels of *ChK-α* (open bar) and *ChK-β* (textured bar) mRNA normalised to  $\beta$ -actin expression, in prostatic tissue from 28 week old mice. The values for each gene have been expressed as fold change compared to the wild type prostate samples expression levels. Error bars indicate standard deviation.

#### 4.1.5 Comparison of gene expression linked to phospholipid metabolism in prostate of 28 week old TRAMP and wild type mice

cDNA microarray analysis (see sections 2.2.6 and 2.2.8) focused on changes in genes specifically linked to metabolic pathways related to phosphatidylcholine synthesis (Kennedy pathway) and degradation. In prostate tumour tissue of old TRAMP mice, mRNA expression levels of choline phosphotransferase 1 (*Chpt1*) and lysophospholipase 3 (*Lypla3*) were reduced as compared to normal prostate. Fold reduction was 0.47 for *Chpt1* (n=5 TRAMP and 4 wild type, p=0.008) and 0.57 for *Lypla3* (n=7 TRAMP and 4 wild type, p=0.028). Other significant changes in the expression of genes germane to these pathways, including *ChK*, were not observed, consistent with the results obtained by RT-PCR. Figure 4.9 illustrates and integrates the



#### 4.1.6 Discussion

This is the first report of the tumour metabolome in the TRAMP mouse model of prostate cancer. When compared to normal prostate, tumour tissue displayed decreased levels of citrate, choline, PC and GPC, GPI and increased levels of taurine, aspartate, tyrosine and glutamate. These changes were observed in old mice, which presented with histopathologically well established tumours. In young mice, in which histopathological investigation detected subtle preneoplastic lesions, the only metabolic feature which allowed discrimination between TRAMP and wild type mice was a reduction in the GPC/PC ratio. In the following, the differences in levels of metabolites between TRAMP tumours and normal prostate described here are juxtaposed with those reported in humans.

#### Amino acids and citrate

The changes in citrate and taurine in TRAMP tumours described above mimic those reported in humans. In healthy human prostate tissue zinc accumulates and inhibits malic dehydrogenase, an enzyme which recycles citrate to oxaloacetate in the Krebs cycle. Thus, in normal prostate, the cycle is truncated resulting in net citrate synthesis (see Introduction). In prostate cancer such truncation does not exist, which explains why it harbours lower citrate levels than normal prostate. The decrease in citrate observed here in TRAMP tumours is consistent with results in the murine DU-145 prostate xenograft and PB-ErbB-2 $\Delta$  x Pten<sup>+/-</sup> models (Fricke *et al.*, 2006; Kurhanewicz *et al.*, 1993). Reduced recycling of citrate in normal prostate means that alternative sources for oxaloacetate are utilised, namely transamination of aspartate, hence prostate tissue contains high levels of this metabolite (Costello and Franklin, 2005). According to the results described above, in normal prostate tissue from C57BL/6J mice aspartate

concentrations were directly correlated to citrate levels, whilst in TRAMP tumour tissue aspartate was increased and citrate reduced. These observations suggest that in TRAMP tumours a greater proportion of citrate produced from aspartate is consumed by the Krebs cycle than in normal prostate, mimicking the biochemistry of the human counterpart. The observed increase in other amino acids in tumour, relative to normal prostate, is consistent with a general enhancement in amino acid catabolism *via* the Krebs cycle.

### **Choline Species**

Human prostate cancer is characterised by increased choline and choline metabolites when compared to healthy prostate (see Introduction). Total choline species (choline, PC plus GPC), and the individual components (choline and PC plus GPC), were reported to be elevated in human prostate samples containing at least 20 % malignant tissue, and these measures have been suggested to serve as markers of prostate cancer progression (Swanson *et al.*, 2003). In contrast to human prostate cancer, prostate tumours from old TRAMP mice with well-established malignancy are shown here to harbour lower choline, PC and GPC than normal prostate. Furthermore, the GPC/PC and total choline/citrate species ratios did not differ between the two tissue types. These results are consistent with a recent analysis in which the total choline/citrate species ratio was measured in TRAMP mouse tumour using  $^1\text{H}$ -MR spectroscopic imaging, which did not resolve individual choline species (Fricke *et al.*, 2006). The authors reported that in contrast to the finding in TRAMP mice, in PB-ErbB-2 $\Delta$ xPten<sup>+/-</sup> mouse tumours the total choline/citrate species ratio was increased, consistent with observations in human prostate cancer.

The observed decrease in GPC/PC ratio in young TRAMP mice, which showed only minor signs of dysplasia, is consistent with changes demonstrated in human cancer (Glunde and Serkova, 2006). This finding suggests that at an early stage of carcinogenesis TRAMP mice may be subject to metabolic alterations similar to those observed in the human disease. However, as carcinogenesis progresses, secondary processes are engaged, which differ between TRAMP mice and humans.

### **GPI**

Altered levels of GPI have hitherto not been associated with prostate cancer, and the finding presented here, that levels of GPI in TRAMP tumours were lower than in normal prostate, is novel. GPI is generated by deacylation of membrane phosphoinositides (PIs). PIs occur at micromolar concentrations in most cell types (Alonso *et al.*, 1988; Falasca *et al.*, 1997). GPI has been found to be elevated in Ras-transformed cell lines (Alonso *et al.*, 1988; Valitutti *et al.*, 1991), and exposure to exogenous GPI inhibits tumour cell invasion of the extracellular matrix (Buccione *et al.*, 2005). The difference in GPI levels observed here between normal murine prostate and prostate tumour was strongly correlated to differences in levels of PC and GPC, implying commonality in the source of variation or mechanism of regulation. The phospholipid metabolism profile in TRAMP tumours, in which malignancy is driven by SV40 T/t-antigen mediated inactivation of p53 and Rb, may conceivably be influenced by events associated with p53 and/or Rb inactivation. Loss of normal p53 function has been shown to increase glycolysis (Bensaad *et al.*, 2006; Matoba *et al.*, 2006), and our observation that TRAMP tumours had lower glucose levels than normal prostate is consistent with this finding.

### Enzymes affecting choline metabolite levels

Altered choline phospholipid metabolism in human prostate cancer, as compared to normal tissue, has been linked to overexpression of ChK (Ramírez de Molina *et al.*, 2002), and overexpression of ChK has been postulated to be a critical requirement for malignant disease progression in breast cancer (Ramírez de Molina *et al.*, 2004). Here, ChK overexpression, or a link between ChK expression and PC levels, was not found in TRAMP mice. Regional or lobe-specific differences in enzyme expression might have confounded detection of subtle differences. These results are consistent with a recent gene expression study in which *ChK* expression was demonstrated to be decreased in advanced stage TRAMP tumours (Morgenbesser *et al.*, 2006). These results imply that ChK overexpression is not a necessary consequence of, nor a requirement for, TRAMP tumour development, as suggested for mammary tumours (Ramírez de Molina *et al.*, 2004). The decrease in GPC observed here in TRAMP tumour as compared to normal prostate might be explained by transcriptional down-regulation of lysophospholipase *Lypla3* (figure 4.9). Malignancy-related underexpression of lysophospholipase has been demonstrated in breast cancer cells (Glunde *et al.*, 2004). The underexpression of choline phosphotransferase *Chpt1* mRNA shown here in TRAMP tumour, compared to normal prostate, contrasts with overexpression of this enzyme reported in mammary tumours (Akech *et al.*, 2005; Ghosh *et al.*, 2002).

In summary, the results show both similarities and differences between metabolic profiles associated with prostate cancer in humans and in TRAMP mice. Whilst perturbation in prostate-specific citrate metabolism seems to be conserved in prostate tumours between rodent prostate carcinogenesis models including TRAMP and humans, regulation of choline metabolism differs between them. NMR methodology has been used before to show that cancer chemotherapeutic intervention changes choline

phospholipid metabolite levels (Al-Saffar *et al.*, 2006), and choline kinase inhibition has been suggested as a potential prostate cancer chemotherapeutic approach (Ramírez de Molina *et al.*, 2002). Hence, the observations presented here imply that the TRAMP model may respond to chemotherapeutic or chemopreventive strategies impinging on choline phospholipid metabolism in a fashion which differs from other rodent models and humans. The results shown here demonstrate that NMR spectroscopy is an eminently suitable tool for the detection of metabolic differences between normal prostate and prostate tumours and for the characterisation of biochemical connections between these differences. The results also exemplify the power of the profiling approach, which allows combined measurement of two or more species and their correlation, as it can provide more discriminatory and process-specific biomarkers than single metabolites.

## 4.2 Metabolic changes in urine of TRAMP mice

### 4.2.1 <sup>1</sup>H-NMR metabolic profiling of urine

In this experiment urine samples from young and old TRAMP and wild type mice were subjected to <sup>1</sup>H-NMR analysis in order to identify biomarkers relating to the TRAMP genotype. Sample preparation and analysis and data processing are described in sections 2.2.4.1, 2.2.4.5 and 2.2.4.6. Spectral assignments were made with homonuclear COSY experiments (carried out by Dr Hector Keun), literature (Bollard *et al.*, 2005; Nicholson *et al.*, 1989), the BMRB database (<http://www.bmrwisc.edu/>) (Seavey *et al.*, 1991) and advice from Dr Hector Keun. Changes in metabolite levels were calculated from the medians and significance was established using the Mann-Whitney U-test with  $p < 0.05$ . Figure 4.10 shows a typical urine spectrum obtained from an old wild type mouse.

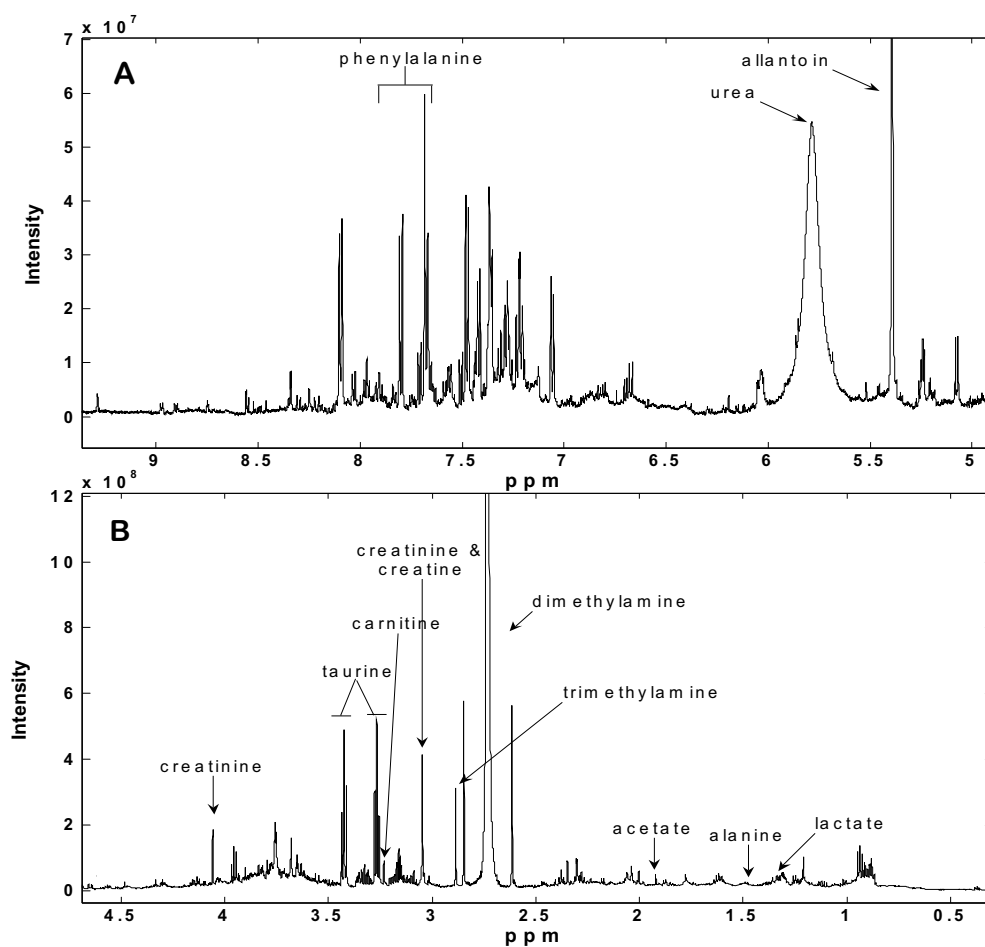


**Figure 4.10** Typical  $^1\text{H-NMR}$  urine spectrum of a 28 week old wild type mouse in the (A) aromatic and (B) aliphatic region.

Predominant separation of the urine spectra was related to age as shown by the Principal Component Analysis (PCA) scores plot (figure 4.11).

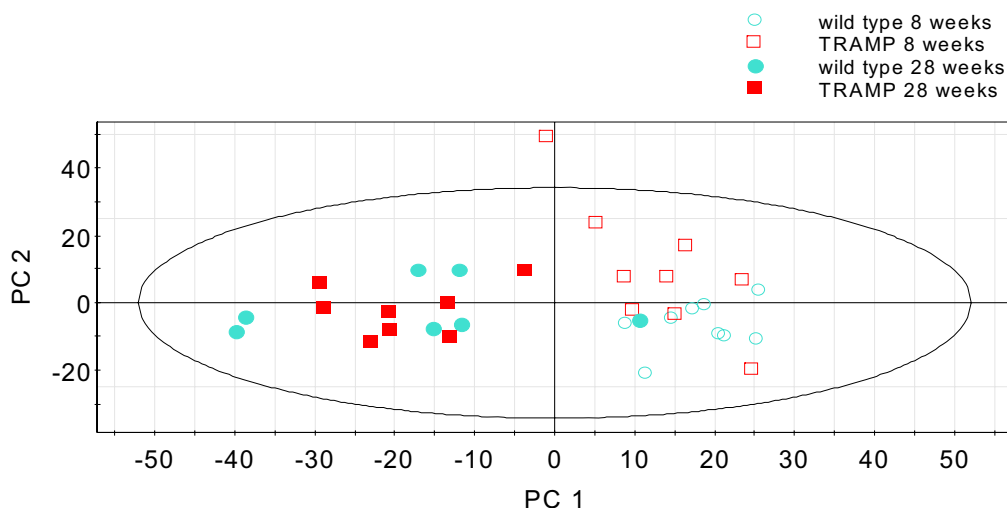


**Figure 4.11** PCA scores plot of urine NMR spectra showing the first and second principal component (PC). The data are scaled to unit variance.

In order to identify differences that are related to the TRAMP genotype, difference/correlation spectra from TRAMP and wild type mice of 8 and 28 weeks of age were generated. Metabolite decreases in TRAMP compared to wild type mice are shown as negative peaks and increases as positive peaks. The absolute peak height depicts the average group difference and the colour indicates the magnitude of correlation to the groups, with red being highly correlated. Mathematically this plot equals an orthogonal partial least square discriminate analysis (O-PLS-DA) loadings plot (Cloarec *et al.*, 2005). Young TRAMP mice showed significantly increased excretion of lactate, alanine, acetate and an unknown compound (multiplet at 0.96ppm) by 18, 11, 30 and 2%, respectively, as compared to young wild type mice (figure 4.12 A).

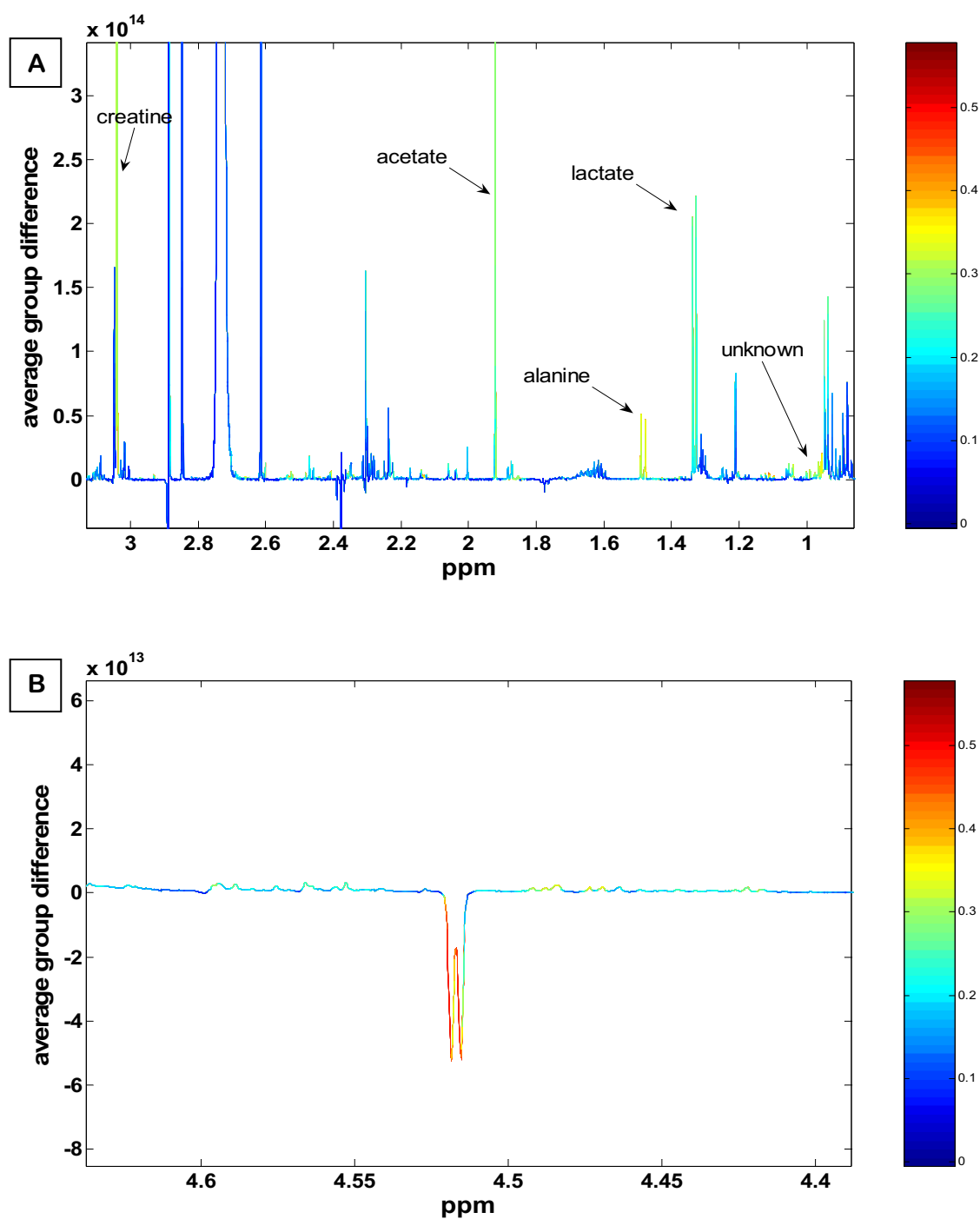


**Figure 4.12** Difference/correlation spectrum of urine spectra from 8 week old TRAMP and wild type mice. **A:** Elevated metabolite levels in TRAMP mice compared to wild type mice. **B:** Decreased unknown compound in TRAMP mice compared to wild type mice.

A decrease of an unidentified compound (d 4.52ppm) by 31% was observed in the urine of young TRAMP mice when compared to age matched wild type mice (figure 4.12 B). In a homonuclear COSY experiment the doublet at 4.52ppm coupled with a doublet at 3.51ppm. It is therefore likely that the unknown compound is a sugar. Figure 4.15 at the end of this section shows the individual levels for most of the metabolites discussed. In the difference/correlation plot of the 28 week old animals the most prominent peak was a singlet at 6.74ppm, showing an increase in TRAMP mice by 43% compared to wild type mice. Other signals that were increased in TRAMP mice included doublets at 5.27ppm (+29%), 7.50ppm (+13%, not significant), 7.63ppm (+25%), 7.70ppm (+25%) and 8.16ppm (+32%) (figure 4.13).

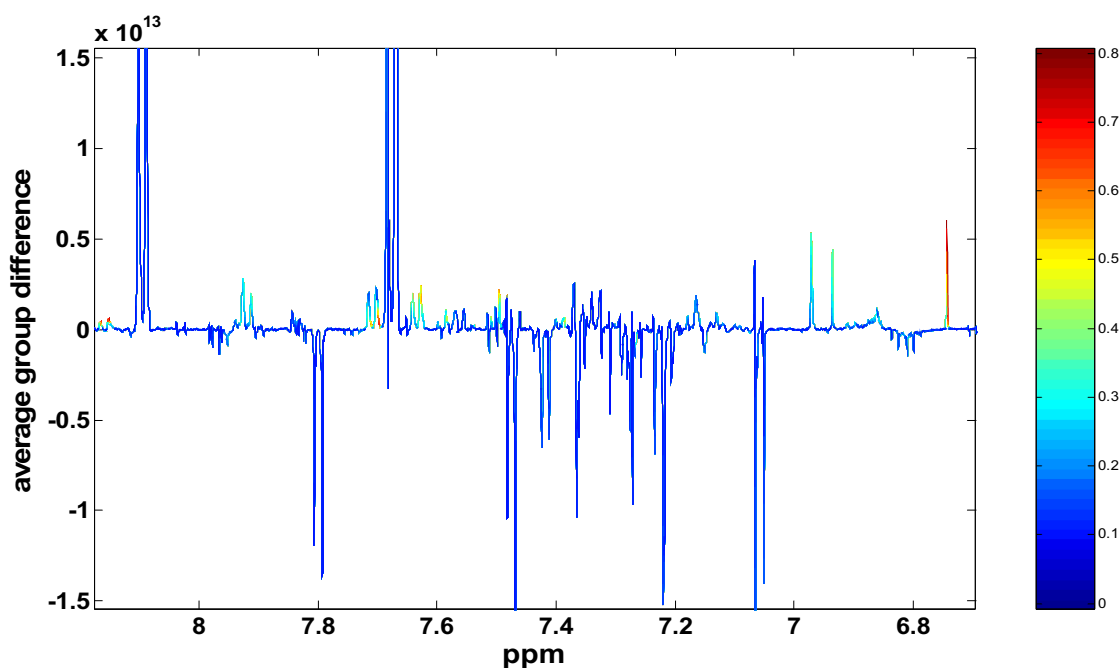


**Figure 4.13** Difference/correlation spectrum of urine spectra from 28 week old TRAMP and wild type mice showing TRAMP related increases in unknown metabolites as indicated by green to red colouration.

Additional visual inspection of overlaid raw spectra (coloured according to groups) and PLS-DA analysis did not highlight further differentially excreted metabolites in TRAMP or wild type mice. PCA showed that the main variance in the data set was due to age related changes. In agreement with this observation, the difference/correlation spectrum of young and old animals revealed more discriminatory signals than the difference/correlation spectra for TRAMP and wild type mice at each time point. The strongest group-correlated changes were increases in creatinine and carnitine excretion in old compared to young mice, of 95 and 76%, respectively. Isoleucine and phenylalanine excretion increased by 65 and 80%, respectively (figure 4.14).

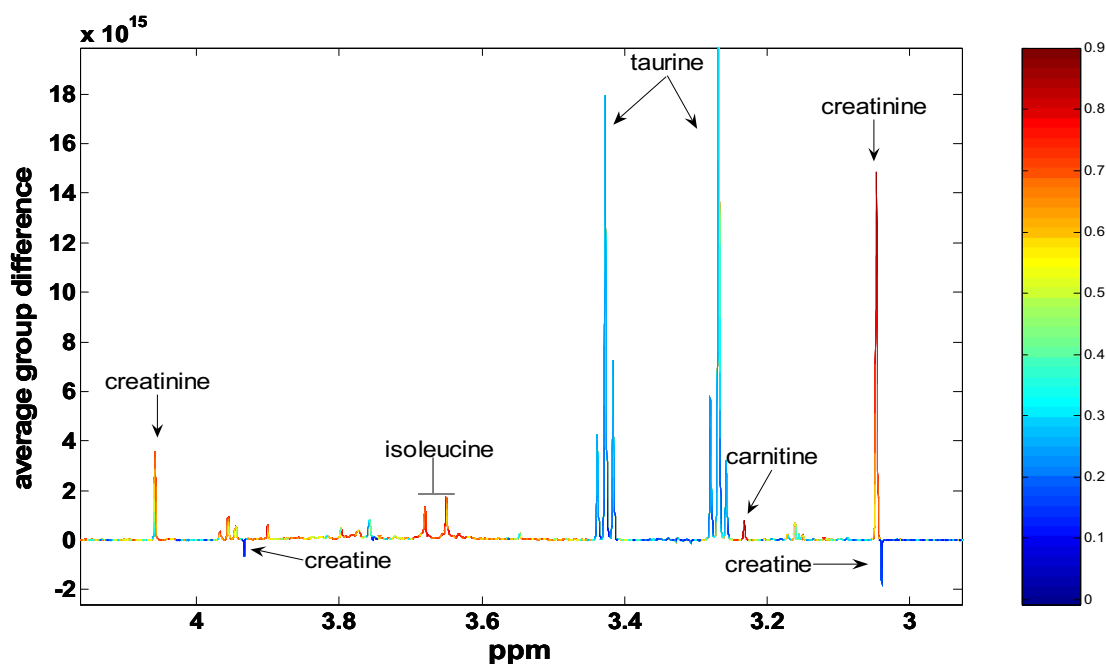


**Figure 4.14** Difference/correlation spectrum of urine spectra from 8 week and 28 week old TRAMP and wild type mice. Differences related to age were established regardless of genotype.

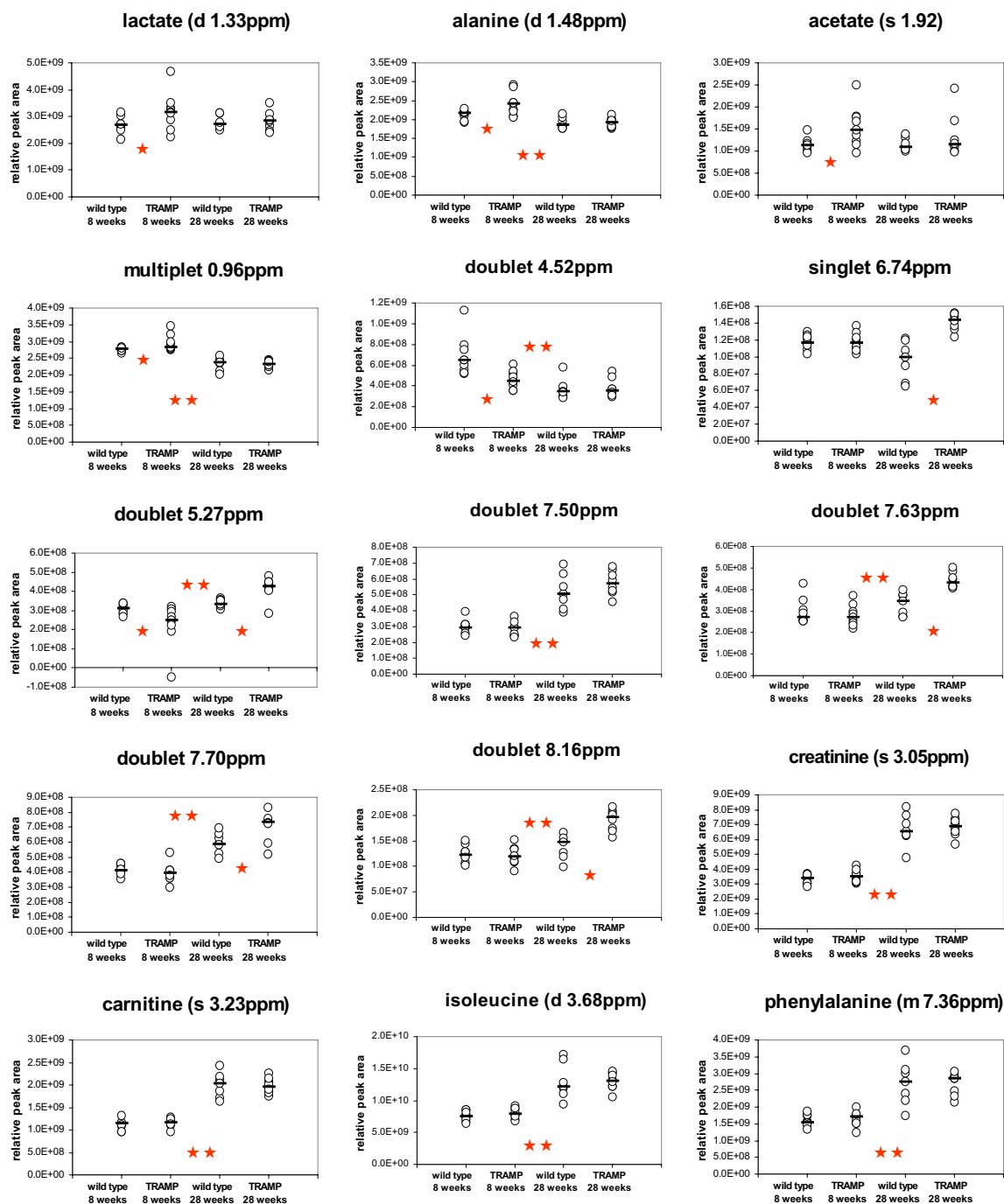


**Figure 4.15** Summary of changes in urinary metabolome. Circles indicate metabolite levels of individual samples and the black bars the group medians. ★ = significant difference between TRAMP and wild type mice at either 8 or 28 weeks of age; ★★ = significant difference between young and old animals, regardless of genotype. Significance was established with the Mann-Whitney U-test with  $p < 0.05$ .

## 4.2.2 Metabolic profiling of urine by LC-MS

Urine samples from young and old TRAMP and wild type mice were prepared and analysed as described in sections 2.2.9.1, 2.2.9.3 and 2.2.9.5. The chemical properties of a compound will determine whether it is more susceptible to ionisation in an environment of either positive or negative voltage. In order to enhance the chances for the discovery of a potential biomarker the samples were analysed in positive as well as negative ionisation mode.

### 4.2.2.1 Analysis in negative ionisation mode

A typical total ion current (TIC) chromatogram obtained for a wild type mouse urine sample is shown in figure 4.16. The scores plots of the PCA analysis show that variation unrelated to the groups dominates the data set (figure 4.17 A). The spread of the quality control (QC) samples provides a measure for the analytical variation. The QC sample consisted of a mixture of equal volumes of all the samples and was injected throughout the analysis procedure after every fifth sample in order to monitor the performance and stability of the LC-MS system. The scores plot of the second and third principal component (figure 4.17 B) shows that the QC samples are grouped closely together and located in the middle of the data space, which reflects the fact that it is a mixture of all analysed samples. A metabonomics test mix, containing theophylline, caffeine, nortriptyline, 4-nitrobenzoic acid, and hippuric acid (Waters Ltd.) was run before and after the sample set in order to verify the performance of chromatography and mass spectrometry. In negative ionisation mode, theophylline, 4-nitrobenzoic acid and hippuric acid were detected. The mass spectrum of each peak confirmed the identity of the detected compound. Figure 4.19 shows the mass spectrum of theophylline. The TIC chromatograms of the test mix run before and after the samples are shown in figure

4.18. The retention times and peak intensities were consistent before and after running the complete sample set. QC samples and the test mix confirmed the validity of the sample analysis.

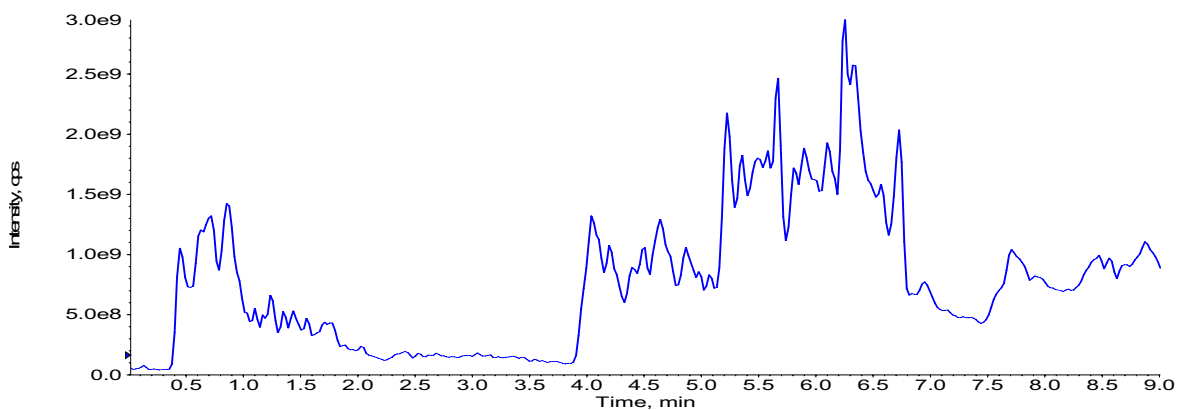


**Figure 4.16** TIC chromatogram of urine from a 28 week old wild type mouse analysed in negative ionisation mode.

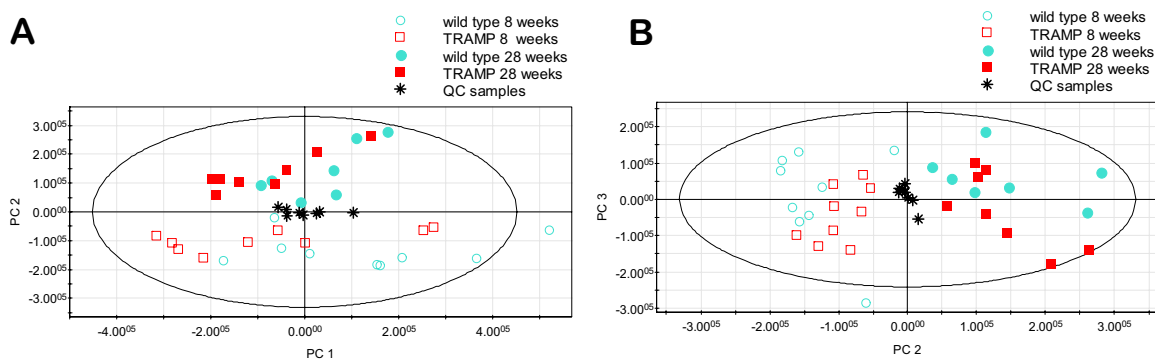


**Figure 4.17** PCA scores plots of urine samples analysed by LC-MS in negative ionisation mode showing (A) the first and second and (B) the second and third principal component (PC). The data are Pareto scaled.

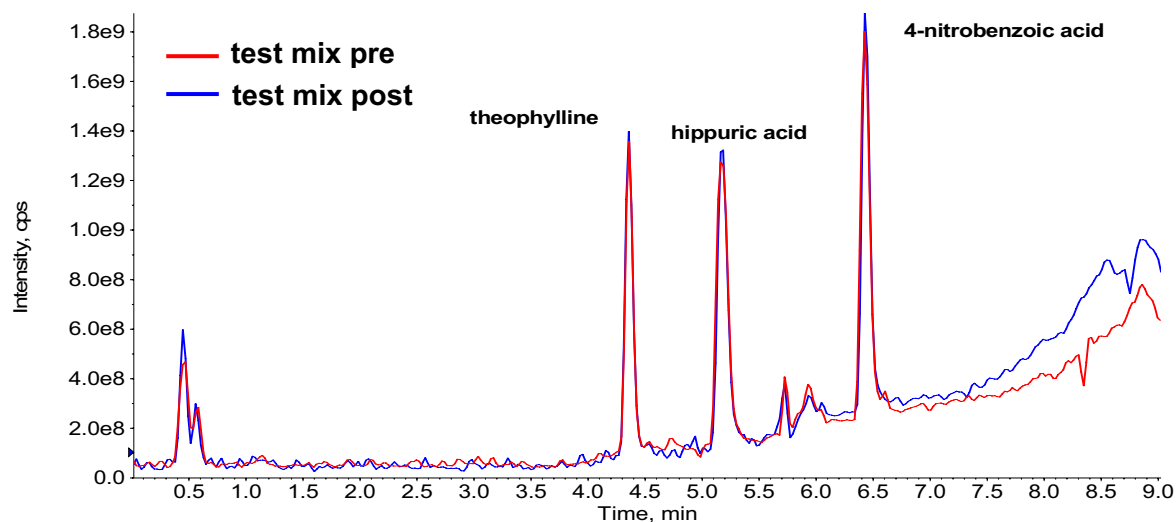


**Figure 4.18** Negative ionisation TIC chromatograms of test mix injection prior (red trace) and post sample analysis (blue trace).

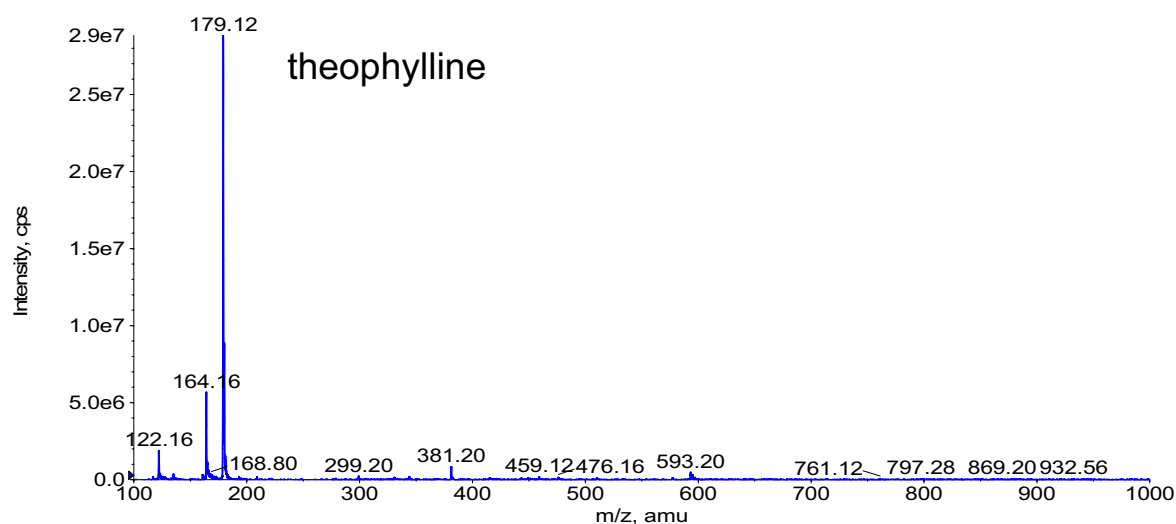


**Figure 4.19** Negative ionisation mass spectrum of theophylline peak in the test mix chromatogram (figure 4.18).

In order to identify potential biomarkers related to the TRAMP phenotype, PLS-DA models were generated for each time point. Figure 4.20 shows the scores and loadings

plots for each time point. Table 4.3 lists potential biomarkers revealed by PLS-DA analysis. The group differences of the listed ions were significantly different as established by Mann-Whitney U-test. Furthermore, peak values were only considered to be indicative of potential markers when the value for the QC samples was consistent throughout the entire sample analysis.

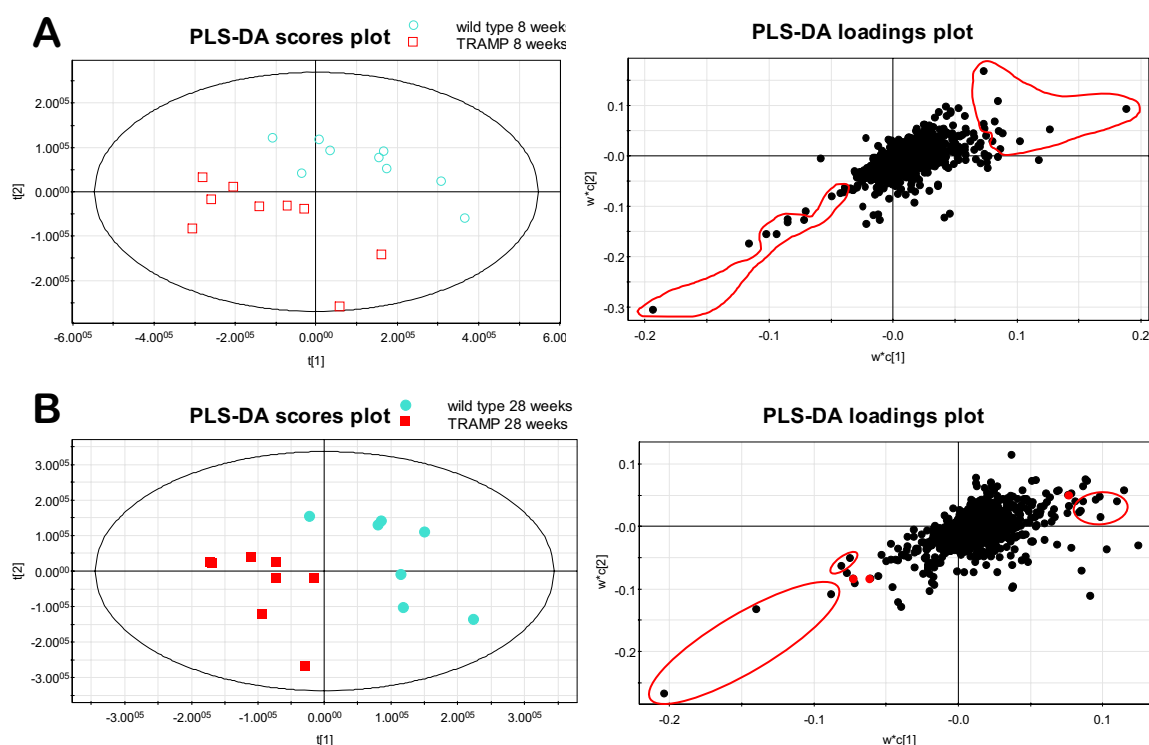


**Figure 4.20** Scores and loadings plots of PLS-DA models for maximal separation between TRAMP and wild type mice at (A) 8 and (B) 28 weeks of age. The dots in the areas of the loadings plots marked red are ions which were significantly different between the groups. The data are Pareto scaled.

The effect of urine concentration on group differences was investigated by normalising the peaks to specific gravity (SG) (see section 2.2.3.8). Colours in table 4.3 indicate which peaks were significantly different unnormalised or normalised or both ways.

**Table 4.3** Potential urinary biomarkers of TRAMP genotype disclosed by HPLC-MS analysis in negative ionisation mode

Peak [m/z / min]	Change in TRAMP vs. wild type (unnormalised data)	Peak [m/z / min]	Change in TRAMP vs. wild type (unnormalised data)
<i>8 weeks</i>		201.2 / 6.24	-24%
407.6 / 6.58●	+119%	177.0 / 0.76	-21%
408.7 / 6.56●	+86%	225.3 / 6.58	-36%
409.4 / 6.56●	+119%	294.3 / 6.45	-34%
453.5 / 6.58●	+216%	187.2 / 5.99	-15%
454.4 / 6.56●	+167%	408.2 / 5.10	-45%
475.8 / 6.56●	+75%	195.0 / 0.74	-17%
815.8 / 6.56●	+864%	<i>28 weeks</i>	
407.6 / 6.71●	+278%	380.2 / 4.88	+69%
408.8 / 6.73●	+231%	380.2 / 5.19	+64%
409.4 / 6.73●	+171%	380.2 / 4.99	+114%
405.4 / 6.69●	+283%	775.4 / 5.68	+157%
451.4 / 6.95	+360%	381.2 / 5.21	+55%
423.3 / 6.20	+60%	303.3 / 4.18	+44%
405.4 / 6.61	+71%	321.4 / 5.27	-43%
391.4 / 7.11	+156%	337.4 / 4.67	-27%
365.2 / 6.37	+57%	319.4 / 5.18	-45%
383.3 / 7.53	+163%	222.2 / 6.70	-16%
391.4 / 7.69	+330%	187.2 / 5.99	-18%
389.4 / 7.35	+396%	415.4 / 6.24	-14%
630.6 / 6.70	+111%	317.3 / 5.63	-28%
404.3 / 5.35	-33%	201.2 / 6.24	-20%
405.6 / 5.22	-45%		

— group difference significant in unnormalised and SG-normalised data

— group difference only significant in SG-normalised data

— group difference only significant in unnormalised data

● Ions labelled with a dot of the same colour are likely to originate from the same compound.

#### 4.2.2.1.1 Identification of marker ion 407

PLS-DA analysis revealed that the ion with  $m/z$  407.6 at 6.58min was significantly increased in 8 week old TRAMP mice as compared to age-matched wild type mice. Comparison of intensity profiles of the potential markers eluting at the same time, provided evidence that different ions originated from the same compound. Figure 4.21 exemplifies this conclusion for ions with  $m/z$  407.6 and 453.5 eluting at 6.58min. The difference of 46 in the  $m/z$  value can be explained by the loss of a formic acid from the formate adduct ion  $[M+HCOO]^-$ . Formic acid was used in sample preparation and as part of the HPLC solvent. The formate plus sodium adduct ion  $[M-H+HCOONa]^-$  of the compound has a  $m/z$  of 475.8. The intensity profiles for ions at 407 $m/z$ , 408 $m/z$  and 409 $m/z$  as well as ions at 453 $m/z$  and 454 $m/z$  also suggest a common origin for the ion. The intensity ratio was  $407 : 408 : 409 = 100 : 27 : 4$  which is a typical  $^{13}C$  isotope pattern for a molecule with 24 to 26 C atoms (figure 4.22). An ion at  $m/z$  815 also showed a similar ion intensity profile as the ion with  $m/z$  407 at the same elution time, suggesting the formation of a dimer. From the findings described above it was assumed that one compound with different stereoisomers produced the marker ions highlighted by dots in table 4.3. Further efforts for biomarker identification were focused on this compound.

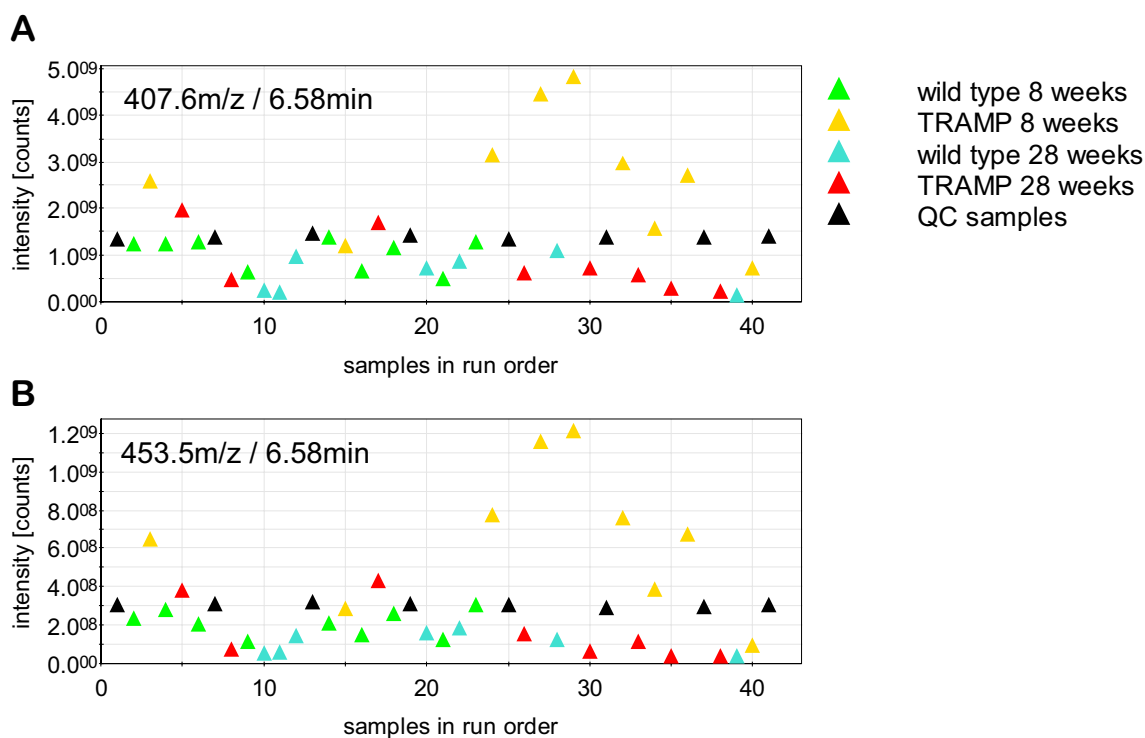


**Figure 4.21** Intensity profiles of potentially related marker ions at (A) m/z 407.6 and (B) m/z 453.5 both eluting at 6.58min

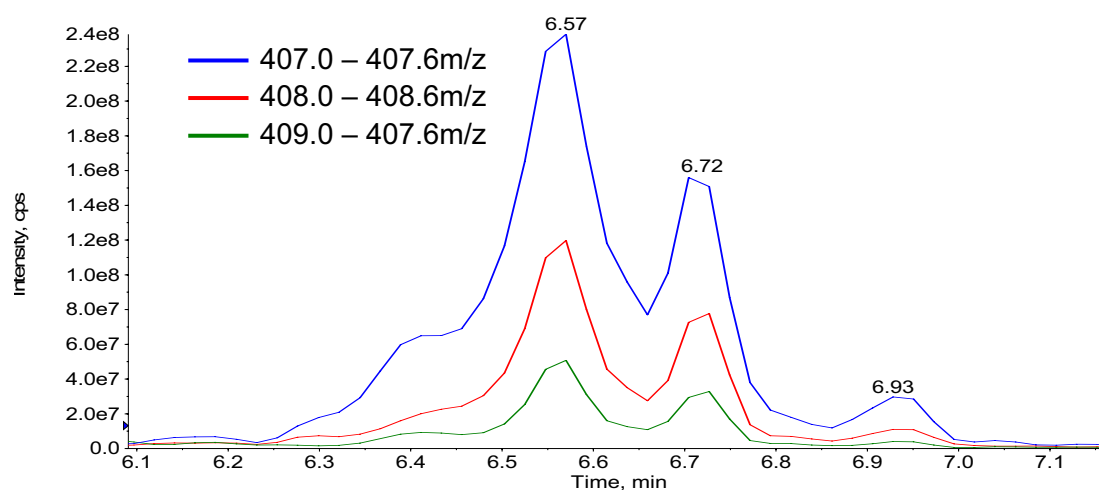


**Figure 4.22** Overlaid extracted ion chromatograms showing  $^{13}\text{C}$  isotopes of a compound with the m/z 407

In order to purify and concentrate the unknown compound with a  $m/z$  at 407 and retention time at 6.58min, a pooled urine sample was subjected to SPE fractionation (see section 2.2.9.6), and each fraction was initially analysed by the HPLC-MS method used in the original sample analysis. The compound of interest was mainly found in the 40% and 60% acetonitrile fractions.

For determination of the elemental composition of the unknown compound accurate mass measurements were carried out using a Finnigan hybrid linear ion trap-Fourier transform mass spectrometer (Thermo Electron Corp.). The 60% acetonitrile SPE fraction was analysed by the same LC conditions used for the original sample analysis. The analysis was performed by Dr Richard Gallagher, DMPK, AstraZeneca, Alderley Park, Macclesfield. The accurate  $m/z$  for the 407 ion was 407.28043. The most likely elemental composition for the  $[M-H]^-$  ion was determined to be  $C_{24}H_{39}O_5$ . This was in agreement with the observed  $^{13}C$  isotope pattern (see above). A search of the Metlin database (<http://metlin.scripps.edu/>), (Smith *et al.*, 2005) for compounds with the formula  $C_{24}H_{40}O_5$  returned unconjugated cholic acid derivatives as the most likely identity for this compound.

Both the 40% and 60% acetonitrile SPE fractions were subjected to  $^1H$ -NMR analysis using a Bruker AV600 spectrometer in order to structurally identify the cholic acid isomers. The analysis was carried out by Dr Eva Maria Lenz, DMPK, AstraZeneca, Alderley Park, Macclesfield. The spectrum of the 40% acetonitrile fraction (figure 4.23 A) was dominated by broad, unresolved signals in the aliphatic region which confounded confirmation for the presence of cholic acid derivatives in the urine samples. Equally, the 60% acetonitrile fraction failed to show the three singlets around 1ppm typical of cholic acid derivatives, probably due to an insufficient concentration of the compound in the sample.

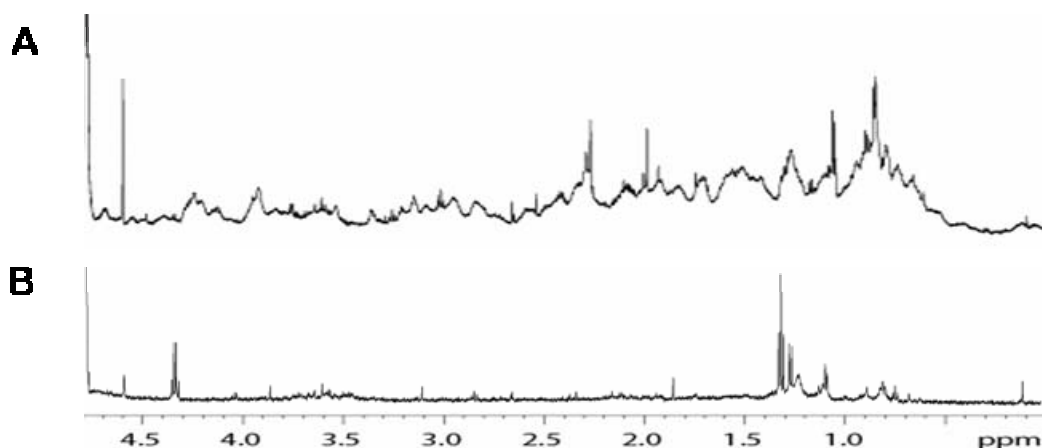


**Figure 4.23** Aliphatic region of  $^1\text{H}$ -NMR spectra of SPE extracts of pooled mouse urine samples; **A**: 40% acetonitrile fraction; **B**: 60% acetonitrile fraction

For identification of the cholic acid isomers by HPLC-MS a more shallow HPLC gradient was employed, which went up to 95% acetonitrile in 32min rather than 10min, in order to facilitate better separation (see section 2.2.9.7). This prolonged gradient resulted in the 6.57min peak being eluted at around 9.4min (figure 4.24). It was also observed that the original two peaks were now further resolved into four peaks.

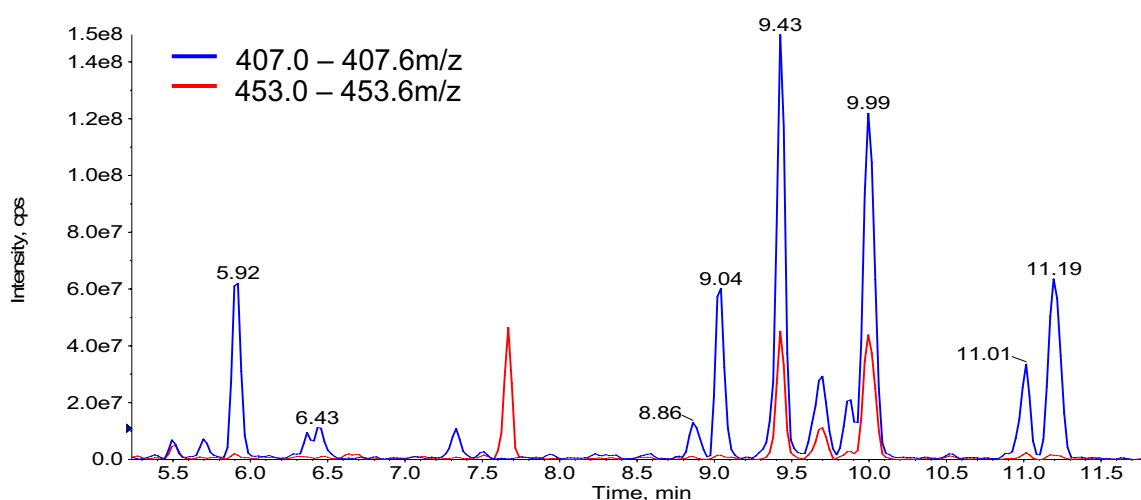


**Figure 4.24** Overlaid extracted ion chromatograms of a mouse urine sample (TRAMP, 8 weeks) analysed in negative ionisation mode using a gradient over 32min instead of 10min.

A recently published study has investigated bile acids in the ileal content of mice and identified bile acids with a molecular weight of 408Da which were cholic acid, hyocholic acid and  $\alpha$ -,  $\beta$ - and  $\omega$ -muricholic acid (MCA) (Martin *et al.*, 2007). The latter three eluted closely together with the HPLC conditions used by the authors. Comparison of retention times of standard solutions of MCAs and cholic acid strongly suggested the presence of all four cholic acid isomers in mouse urine (figure 4.25).

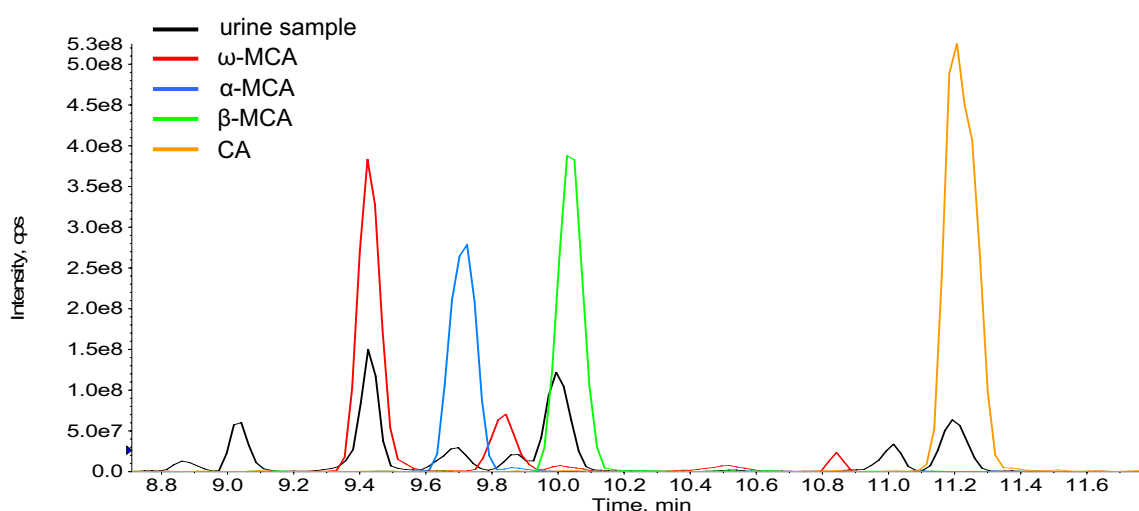


**Figure 4.25** Overlaid extracted ion chromatograms (407.0-407.6m/z) of a urine sample and 5 $\mu$ g/ml standard solutions of  $\alpha$ -,  $\beta$ - and  $\omega$ -muricholic acid (MCA) and cholic acid (CA).

The identity of all four cholic acid isomers was confirmed by spiking urine samples with standards as well as comparison of fragment patterns for the sample, standard and spiked sample. To compare the fragments of the cholic acid isomers, an enhanced precursor ion scan method with four different collision energies (-10V, -30V -60V and -80V) was used (see section 2.2.9.8). For the MCAs and cholic acid the product ions of m/z 453 and 407 were analysed, respectively. Collision energies of -10V and -30V led to loss of formic acid in the MCAs, while at -80V the precursor ions were fragmented to many low molecular weight fragments with low intensity, which were unsuitable for

fragmentation pattern comparison. Identification was made from patterns generated with -60V collision energy. Figures 4.26 to 4.28 exemplify the identification process for  $\omega$ -MCA. In both sample and the standard, an additional minor peak eluting 0.4min after the main peak was observed. This may be due to isomerisation in solution.

Due to the fact that in the original sample analysis  $\alpha$ -,  $\beta$ - and  $\omega$ -MCA were not chromatographically separated, it was difficult to conclude by how much exactly each compound was elevated in urine of young TRAMP mice as compared to their wild type counterparts. It was only possible to deduce that  $\omega$ - and  $\beta$ - MCA and probably  $\alpha$ -MCA excretion was greater in young TRAMP mice than in young wild type mice.

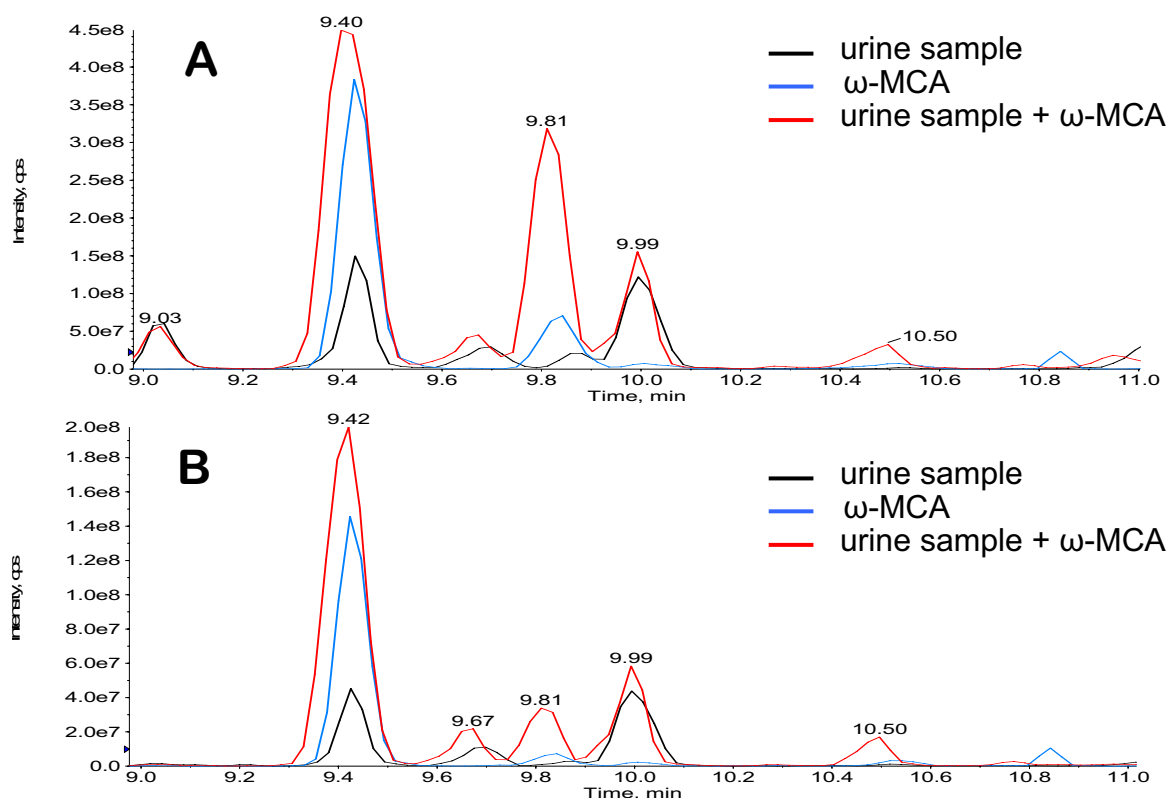


**Figure 4.26** Overlaid extracted ion chromatograms of a mouse urine sample (TRAMP, 8 weeks),  $\omega$ -MCA standard (5  $\mu$ g/ml) and a mouse urine sample spiked with  $\omega$ -MCA standard; A: 407.0 – 407.6 m/z; B: 453.0 – 453.6 m/z.

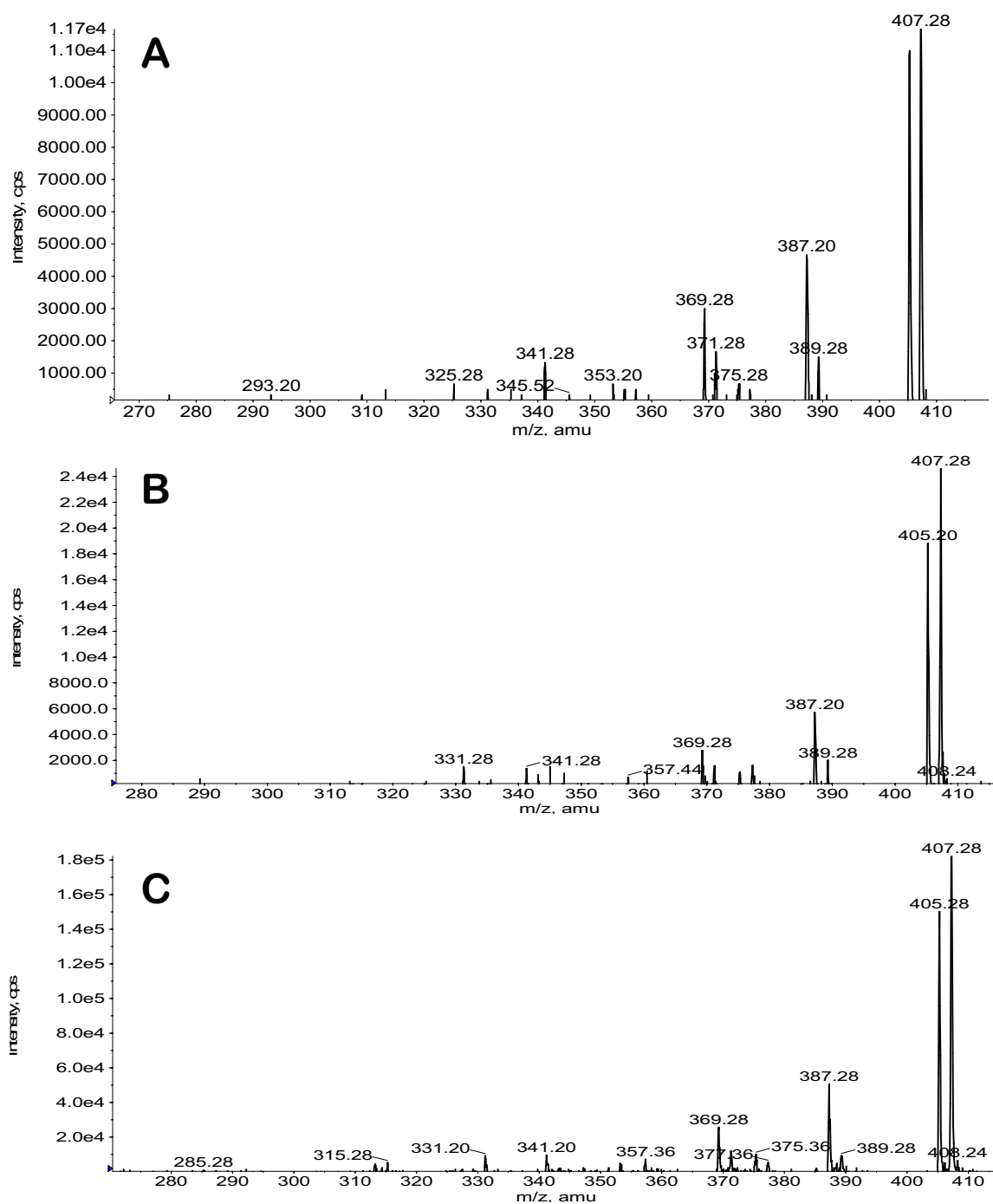


**Figure 4.27** Product ion spectra for  $\omega$ -MCA peaks from (A) a mouse urine sample (TRAMP, 8 weeks), (B)  $\omega$ -MCA standard (5  $\mu$ g/ml) and (C) a urine sample spiked with  $\omega$ -MCA standard. The collision energy employed was -60V, the instrument was set to scan for product ions of the precursor ion at 453m/z.

#### 4.2.2.2 Analysis in positive ionisation mode

A typical TIC chromatogram obtained from a mouse urine sample (TRAMP, 8 weeks) acquired in positive ionisation mode is shown in figure 4.28. The same HPLC gradient as used for negative ionisation mode was employed. The sample analysis was deemed to be valid, as the chromatograms of the test mixes, run before and after the sample set, were congruent without shift in retention time or intensity. Also the QC samples clustered reasonably close together in the second and third principal component (figure 4.29). However, the variation in the data set due to group-unspecific differences is more pronounced than in negative ionisation mode. The spread of the QC samples in the first principal component indicates the extent of the analytical variation. Only in the third principal component did group specific differences become apparent.

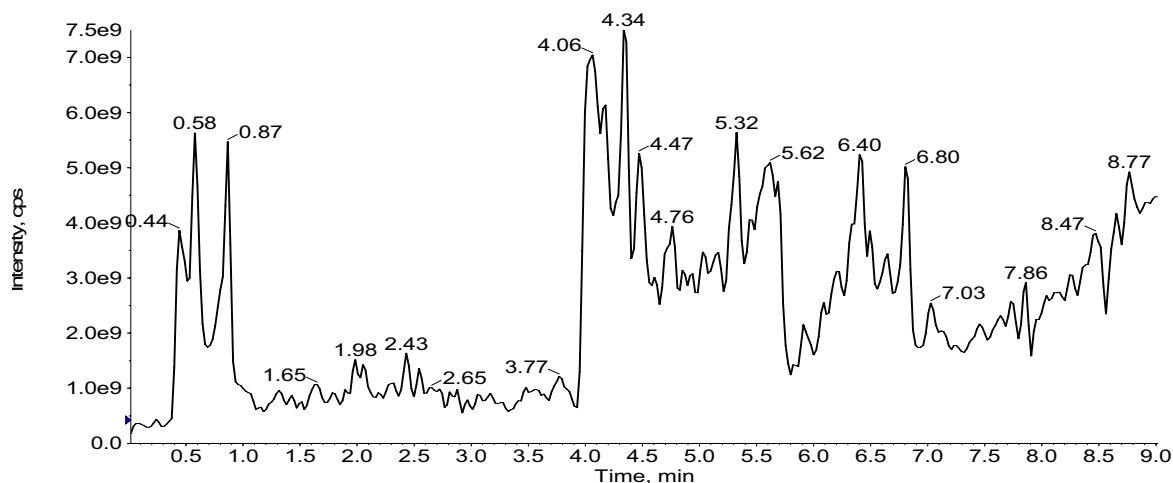


**Figure 4.28** TIC chromatogram of urine from a 28 week old TRAMP mouse analysed in positive ionisation mode.

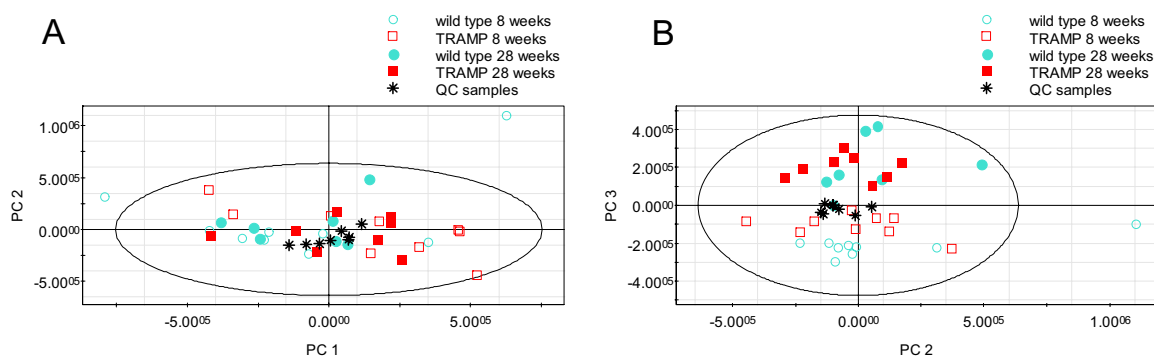


**Figure 4.29** PCA scores plots of urine samples analysed by LC-MS in positive ionisation mode showing (A) the first and second and (B) the second and third principal component (PC). The data are Pareto scaled.

In general, electrospray ionisation in positive ionisation mode leads to ionisation of more molecules than negative ionisation mode. For metabolic profiling this fact can mean higher variation due to increased background noise as well as increased ionisation suppression. The number of ions extracted after data processing was 12064 as compared to 8062 in negative ionisation mode using identical peak extraction parameters (see section 2.2.9.5).

For the identification of potential marker ions PLS-DA models were generated to maximise the difference between TRAMP and wild type animals at either time point (not shown). Ions significantly different in TRAMP and age-matched wild type mice were only considered when the QC samples were consistent throughout the run. To exclude dilution effects as a source of group differences, significance testing was repeated on the data normalised to specific gravity, and only ions which were significantly different in the raw and normalised data were considered. Table 4.4 lists all ions passing the criteria described above. A considerable number of potential marker ions had to be rejected due to inconsistent intensity values for the QC samples. There were no overlapping marker ions between the two age groups.

**Table 4.4** Potential urinary biomarkers of TRAMP genotype disclosed by HPLC-MS analysis in positive ionisation mode

Peak [m/z / min]	Change in TRAMP vs. wild type (unnormalised data)	Peak [m/z / min]	Change in TRAMP vs. wild type (unnormalised data)
<i>8 weeks</i>		<i>28 weeks</i>	
355.3 / 6.66●	+66%	381.9 / 5.04●	+84%
356.5 / 6.66●	+180%	383.1 / 5.03●	+129%
373.4 / 6.66●	+90%	384.1 / 5.03●	+93%
355.7 / 6.81	+204%	763.0 / 5.04●	+391%
593.5 / 5.68	+234%	206.0 / 5.05●	+104%
372.7 / 6.32●	+38%	205.0 / 5.76	+56%
372.9 / 6.32●	+47%	442.2 / 4.62	+47%

● Ions labelled with a dot of the same colour potentially originate from the same compound.

### 4.2.3 Discussion

The urinary metabolic profile of TRAMP and wild type mice at 8 and 28 weeks of age was investigated using <sup>1</sup>H-NMR and LC-MS analysis. Both analytical platforms showed that metabolic changes related to age are much greater than those related to the TRAMP phenotype. NMR analysis showed that old mice excrete more creatinine, carnitine, phenylalanine and isoleucine than young mice, which is due to differences in the body mass.

Differences between TRAMP and wild type mice were more pronounced at 8 weeks of age than at 28 weeks. The PCA scores plots revealed a trend of separation for the young but not the old animals.

The urinary metabolic profile of young TRAMP mice was characterised amongst others by elevated levels of lactate, acetate,  $\omega$ -,  $\beta$  and possibly  $\alpha$ -MCA.  $\alpha$ - and  $\beta$ -MCA are primary bile acids which are synthesised in the liver, while  $\omega$ -MCA, which is a secondary bile acid, is the product of bacterial C-6 epimerisation in the gut microflora (see figure 4.30). Intestinal bacteria are responsible for a variety of other bile acid modifications, including deconjugation (Cummings and Macfarlane, 1997). The observation of increased renal excretion of MCAs together with elevated levels of lactate and acetate may be indicative of an altered gut microflora in TRAMP compared to wild type mice. Previous metabonomic investigations have shown that the urinary metabolic profile of rodents is greatly influenced by the composition of the gut microflora (Martin *et al.*, 2007; Robosky *et al.*, 2005; Rohde *et al.*, 2007). High levels of lactate in urine are commonly described in patients with small bowel syndrome (SBS) as a consequence of dominating, lactate producing lactobacilli in the gut microflora (Bongaerts *et al.*, 1997). Similarly, patients with small intestine bacterial overgrowth (SIBO) have been reported to present with higher levels of lactate, acetate and formate as well as unconjugated bile acids in upper-gut aspirate (Bala *et al.*, 2006). Enhanced bacterial bile acid deconjugation due to bacterial overgrowth in the gut has been suggested to play a role in dietary fat malabsorption (Tabaqchali *et al.*, 1968). With regard to the findings described above and the fact that the 8 week old TRAMP mice in this study had a 7% lower bodyweight than the age matched controls (statistically significant, see section 4.5), it is conceivable that the young TRAMP mice, but not their wild type litter mates, suffered from malabsorption due to bacterial overgrowth or a gut microflora imbalance. Other possible explanations for differences in the gut microflora of young TRAMP and wild type mice could be different rates of maturation of the gut microflora in transgenic and non – transgenic mice, or the influence of different

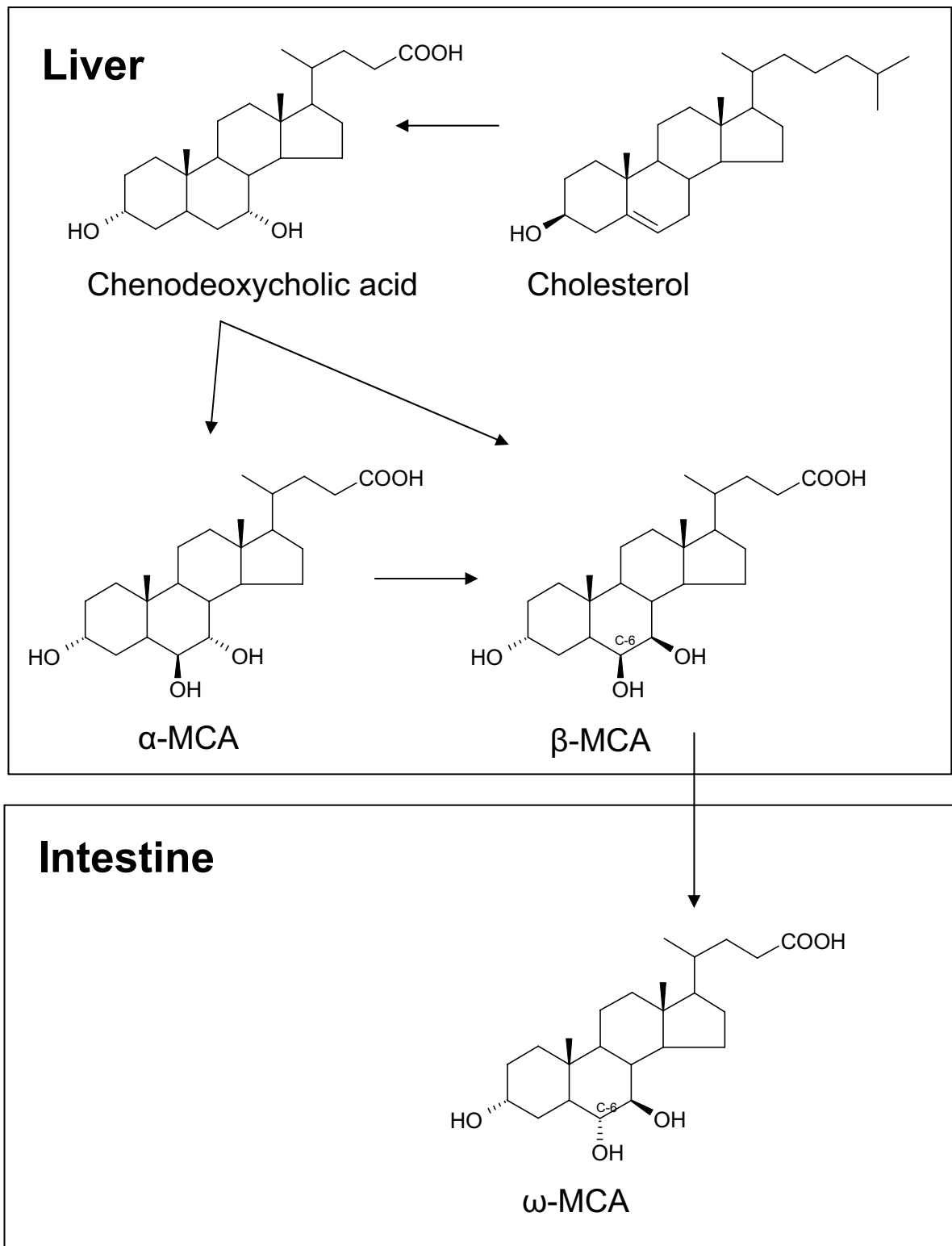


**Figure 4.30** Synthesis of  $\alpha$ -,  $\beta$ - and  $\omega$ -muricholic acids (MCA) in liver and intestine

microenvironments, e.g. the cage position in the isolator. In the 28 week old animals there were no group differences in any of the discussed metabolites, and levels were comparable to those observed in young wild type mice. If, and in what way, the TRAMP genotype influences the bacterial composition in the gut remains unclear. It should be noted, however, that the gut microflora is of great importance for the host's health (Nicholson *et al.*, 2005). An unhealthy gut microflora can impose enormous stress on the host organism and therefore might contribute to cancer development. Bile acids, for example, are known to have endocrine functions and play a role in energy, triglyceride, cholesterol and glucose metabolism (Houten *et al.*, 2006). The gut microorganisms modify bile acids, and some of those bacterial products re-enter the host's bile acid circulation. Therefore, it is not surprising that the gut microflora has been suggested to play a role in obesity and the onset of Type II diabetes (Cani and Delzenne, 2007).

None of the TRAMP and wild type differences observed in 8 week old mice were found in 28 week old animals. Therefore, none of the compounds identified to be differentiating at either time point can unambiguously be linked to prostate carcinogenesis in TRAMP mice.

It was mentioned earlier that differences in the old mice were less pronounced than those in young animals, and that there was no evidence for a difference in the bacterial composition of the gut in the old TRAMP or wild type mice, suggesting that changes in the gut microflora have a greater impact on the urinary metabolome than an advanced prostate tumour.

### 4.3 Metabolic changes in plasma of TRAMP mice

#### 4.3.1 $^1\text{H}$ -NMR metabolic profiling of plasma

Plasma samples were prepared and analysed as described in sections 2.2.4.2, 2.2.4.5 and 2.2.4.6. Spectral assignments were made based on the literature (Nicholson *et al.*, 1995; Teahan *et al.*, 2006), the BMRB database (<http://www.bmrwisc.edu/>), (Seavey *et al.*, 1991) and personal communication with Dr Hector Keun. Figure 4.31 shows a typical  $^1\text{H}$ -NMR spectrum of plasma from an 8 week old TRAMP mouse acquired using a Carr-Purcell-Maiboom-Gill (CPMG) pulse frequency.

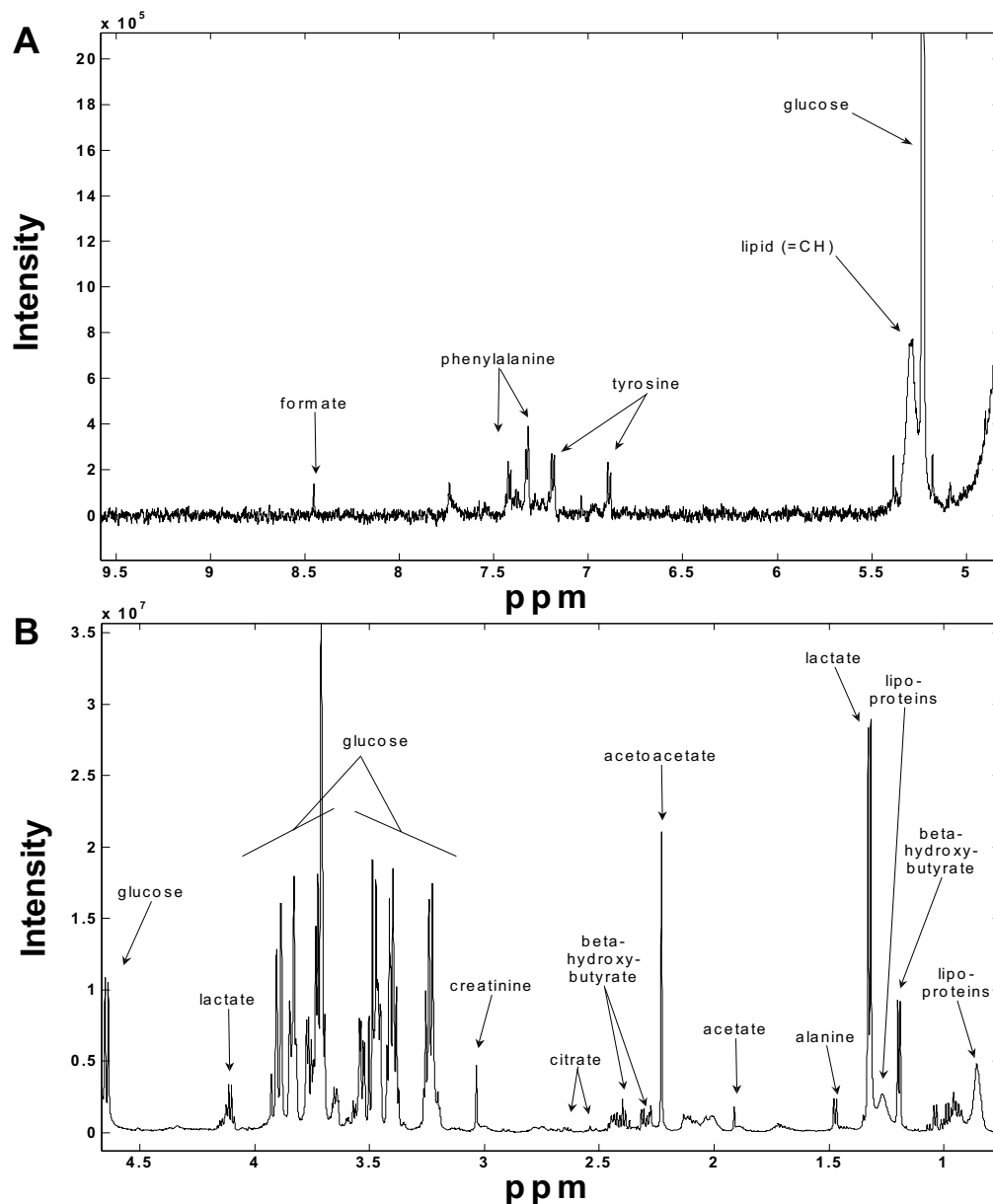


**Figure 4.31** Typical  $^1\text{H-NMR}$  plasma spectrum of an 8 week old TRAMP mouse in the (A) aromatic and (B) aliphatic region.

PCA analysis of the data set revealed that, as for urine, the main variance arose from age related changes (figure 4.32). Difference/correlation spectra of TRAMP versus wild type mice at either 8 or 28 weeks of age did not reveal any group-specific metabolic alterations. Equally, visual inspection of overlaid spectra coloured according to group,

and PLS-DA analysis did not disclose any TRAMP genotype-related differences in the plasma metabolic profile at either time point. Phenylalanine (m 7.42ppm), valine (d 1.04ppm), isoleucine (t 0.96ppm), creatine (s 3.02ppm) and creatinine (s 3.03ppm) levels were decreased by 27, 37, 30, 29 and 25% respectively, in older mice, regardless of genotype. A multiplet at 1.72ppm showed 36% lower intensity in old animals. Signals from fatty acid =CH (m 5.29ppm) and terminal CH<sub>3</sub> groups (m 0.86ppm) were increased by 30 and 23%, respectively, in 28 week old mice compared to 8 week old mice. All changes described above were highly statistically significant, with  $p < 0.001$  according to the Mann-Whitney U-test.

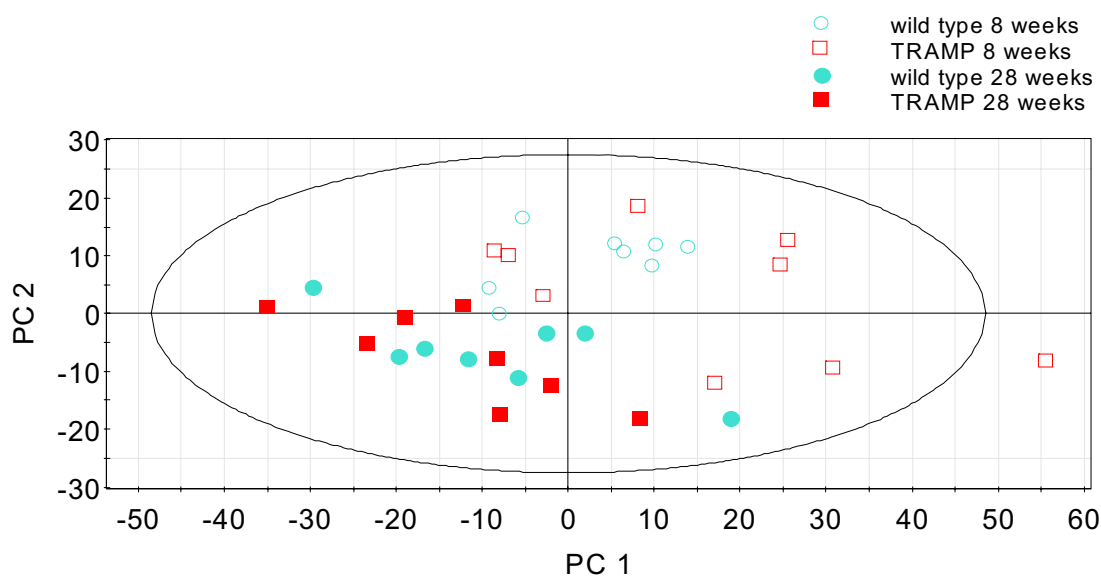


**Figure 4.32** PCA scores plot of plasma NMR spectra showing the first and second principal component (PC). The data are scaled to unit variance.

### 4.3.2 LC-MS metabolic profiling of plasma

The plasma samples were prepared as described in section 2.2.9.2. The LC-MS method used was identical to the method employed for the urine samples (see sections 2.2.9.3 and 2.2.9.5). Samples were analysed in both negative and positive ionisation mode. Figure 4.33 shows TIC chromatograms obtained for both ionisation modes. Although the test mixes did not show any retention time shift or signal intensity change, PCA analysis of the data set revealed substantial analytical variation (figure 4.34 and 4.35).

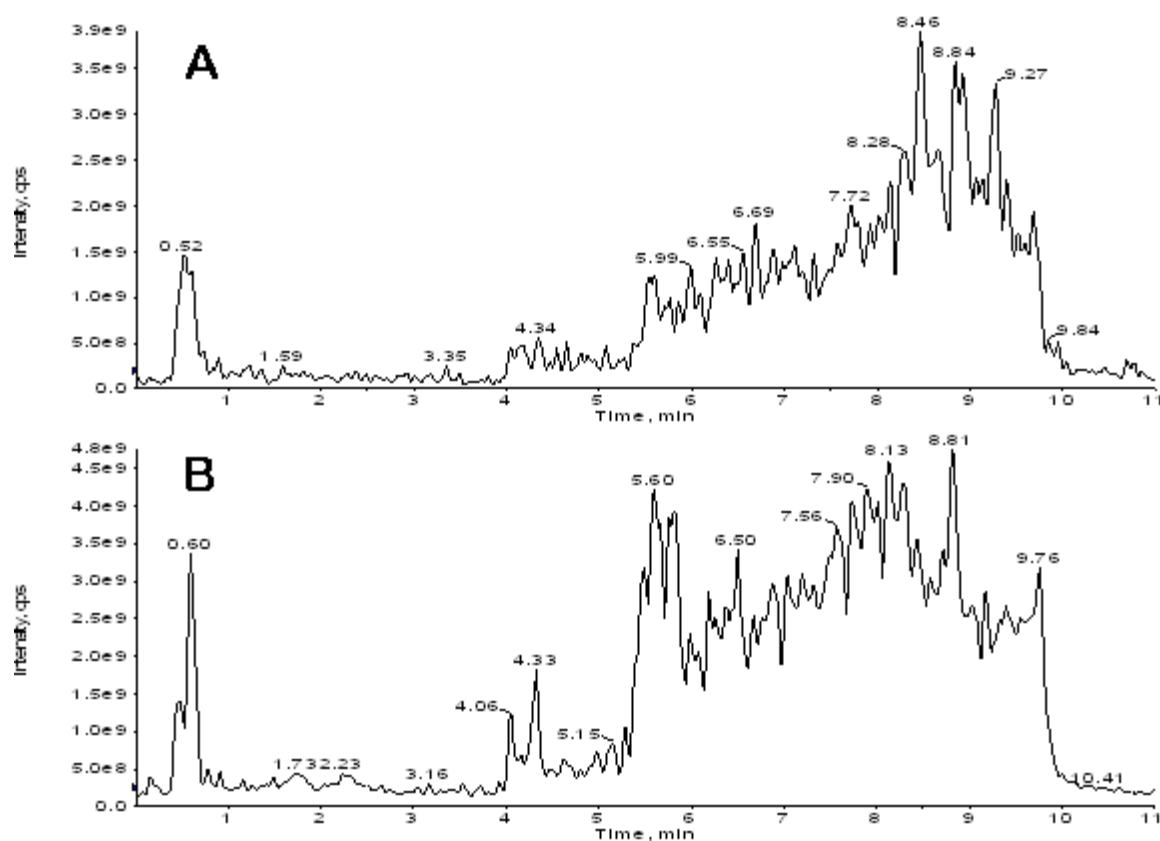


**Figure 4.33** TIC chromatogram of a plasma sample obtained from a 28 week old TRAMP mouse analysed in (A) negative and (B) positive ionisation mode.

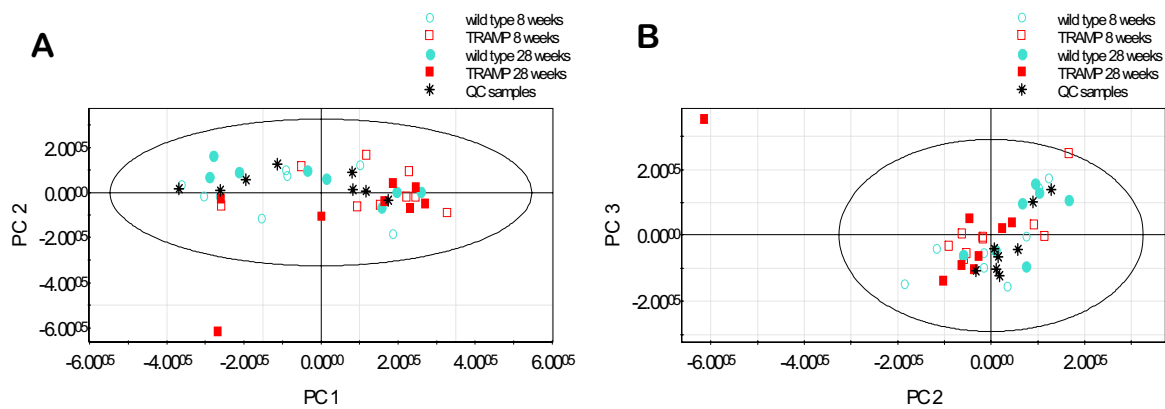


**Figure 4.34** PCA scores plots of plasma samples analysed by LC-MS in negative ionisation mode showing (A) the first and second and (B) the second and third principal component (PC). The data are Pareto scaled.

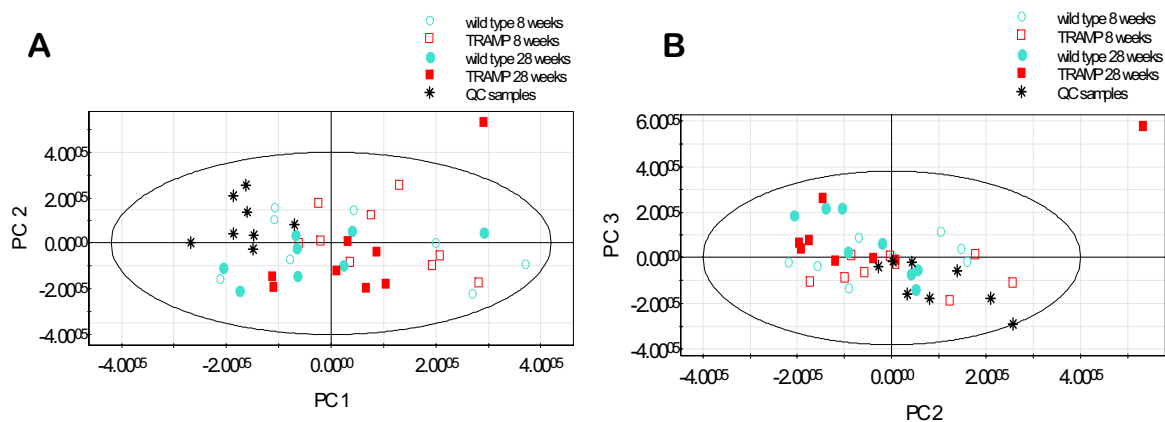


**Figure 4.35** PCA scores plots of plasma samples analysed by LC-MS in positive ionisation mode showing (A) the first and second and (B) the second and third principal component (PC). The data are Pareto scaled.

The high content of lipophilic compounds in plasma results in the majority eluting at the high organic phase end of the gradient (see figure 4.33). The increased number of co-eluting substances might lead to ionisation suppression effects, which may cause the observed analytical variation. In order to circumvent such a potential effect, a prolonged gradient increasing the organic phase over 30min rather than 10min was employed (see section 2.2.9.4) using both, negative and positive ionisation mode. PCA analysis showed that for positive, but not negative ionisation mode, the modified gradient has reduced the analytical variation (figure 4.36). In positive ionisation mode the QC samples moved closer together, apart from one outlier, and an age related difference became apparent. However, for both gradients, in negative and positive ionisation mode, the QC samples were not situated in the middle of the samples, but as a group in the periphery of the multivariate data space. This indicated that the composition of the QCs differed from that of the other samples. Procedures during sample preparation might have introduced these differences. Nevertheless, the QC samples could still be used to judge the extent of the analytical variation as long as there was no time trajectory visible. To what extent the sample preparation differently influenced the other samples is unclear, but as the preparation and run order was randomised, it should not have biased the result.

On the basis of the results from the PCA analysis, the data obtained from sample analysis using the 10min gradient in positive and negative ionisation mode, as well as data from the 30min gradient in negative ionisation mode, were rejected for further data analysis. For the positive ionisation mode data, PLS-DA models were generated for maximal separation of TRAMP and wild type mice at both time points. However, no potential markers were found due to the fact that, none of the ions suspected of separating as judged by their position on the loadings plot, showed a stable QC sample

profile and were therefore not considered further. All in all, the data obtained from the plasma samples were rejected due to inordinately large analytical variation.

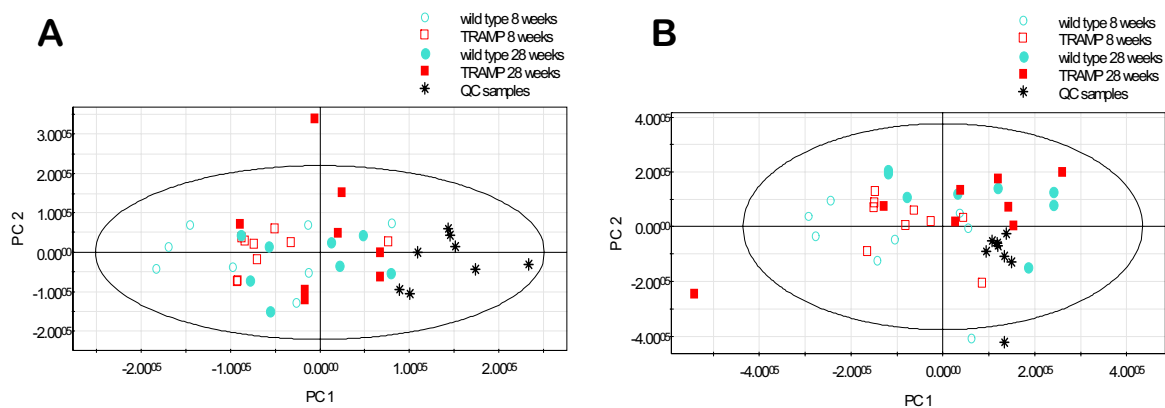


**Figure 4.36** PCA scores plots of plasma samples analysed by LC-MS in (A) negative ionisation mode and (B) positive ionisation mode using a 30min gradient showing the first and second principal component (PC). The data are Pareto scaled.

### 4.3.3 Discussion

The analytical variation in the LC-MS analysis of plasma samples from 8 and 28 week old TRAMP and wild type mice confounded the disclosure of potential biomarkers. The literature contains a large number of LC-MS metabonomic studies for urine, but studies using LC-MS metabolic profiling of plasma or serum are less common (Lenz and Wilson, 2007; Wilson *et al.*, 2005). Although successful application of plasma profiling with only protein precipitation as sample pre-treatment has been reported for UPLC-MS (Plumb *et al.*, 2006; Williams *et al.*, 2006), additional phospholipid capture was shown to enhance the detection of metabolites by HPLC-MS profiling of serum (Want *et al.*,

2006). The conclusion from this study is that the methods employed here for sample preparation and chromatographic separation need to undergo further development before they can be suitably applied to other studies.

In the case of NMR analysis, TRAMP-specific differences were not found in plasma, while age differences were readily detected. These findings do not reflect results from plasma metabonomic profiling of the PC3 xenograft model for prostate cancer (Rantalainen *et al.*, 2006). The authors detected decreased amino acid levels and increased levels of  $\beta$ -OH-butyrate, acetate and glucose in tumour-bearing mice compared to controls. A reason for the discrepancy between the two studies might lie in the fact that PC3 cells are derived from prostate cancer metastatic to the bone (Kaighn *et al.*, 1979) while the tumours in the TRAMP mice were not necessarily metastatic and presented a wide range of pathological stages (see section 4.1.1). Furthermore, PC3 tumours are likely to have a greater impact on the hosts metabolism than TRAMP tumours because they are faster growing.

All metabonomic techniques employed in the present study showed aging to be the major reason for changes in metabolic profiles in plasma. The changes observed are not further discussed here as they are not related to carcinogenesis. The fact that urine, but not plasma, revealed TRAMP-related differences may be related to the fact that urine is an excreted body fluid, while blood remains in the body, and its composition is tightly controlled e.g. by excretion of unwanted compounds into the urine.

#### **4.4 Peptide profiling of plasma and urine of TRAMP mice**

Samples were prepared and analysed as described in sections 2.2.2.4, 2.2.2.5 and 2.2.2.8. Data reduction and normalisation are described in section 2.2.2.9. The obtained peak lists were exported to SIMCA and MatLab software for detailed evaluation. Changes in m/z intensities were calculated from the group medians, and significance was established using the Mann-Whitney U-test with  $p < 0.05$ .

##### **4.4.1 Peptidomic changes in urine of TRAMP mice**

Figure 4.37 shows the binned, combined mass spectra of all urine samples with the green line indicating the unresolved background continuum which was subtracted before data evaluation. From the background-subtracted spectrum 344 significant peaks were extracted for further analysis. Figure 4.38 shows the heat map of count values of the significant peaks for all samples. The majority of the high intensity signals can be found in the lower molecular weight region.

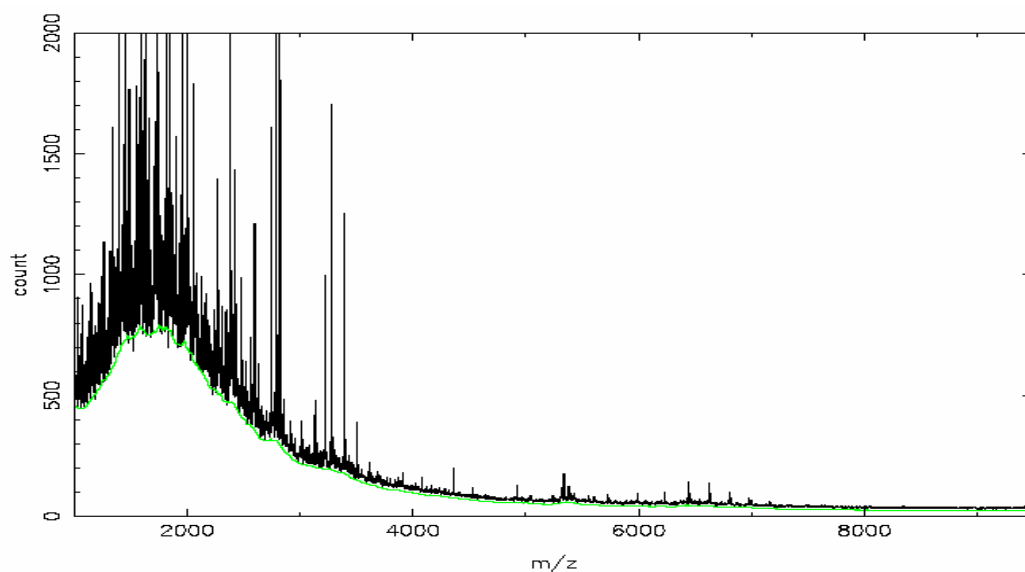


**Figure 4.37** Combined and binned mass spectra of all mouse urine samples analysed by MALDI-MS. The green line indicates the unresolved background continuum which is subtracted prior to data evaluation.

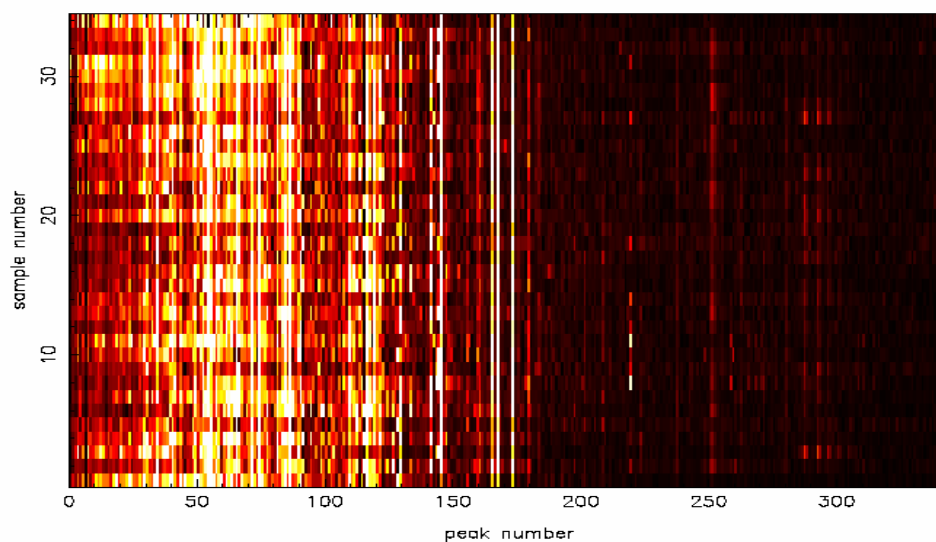


**Figure 4.38** Count values heat map of significant peaks of urine MALDI spectra. The peaks are sorted in ascending order of  $m/z$  values. The brightness is proportional to signal intensity. Samples are listed in run order.

PCA analysis revealed that the major variation in the data set is unrelated to groups (figure 4.39 A). Age differences were revealed in the third principal component (figure 4.39 B).

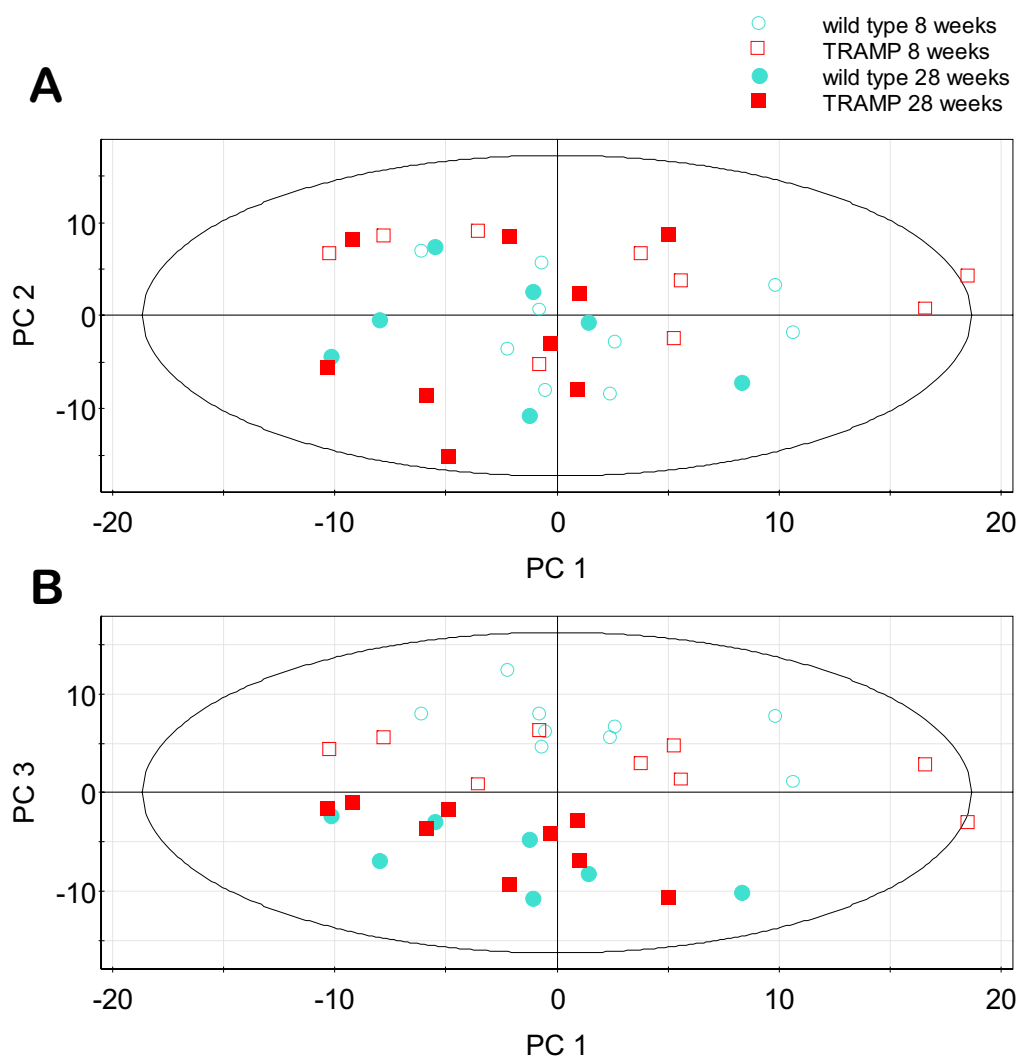


**Figure 4.39** PCA scores plots of urine samples analysed by MALDI-MS showing (A) the first and second and (B) the first and third principal component (PC). The data are scaled to unit variance.

In order to identify changes related to the TRAMP genotype, a PLS-DA model for each time point was generated. Although the model for the old mice did not pass the validation test, five ions significantly different between old TRAMP and wild type mice were identified. Figure 4.40 shows scores and loadings plots for young and old animals. Table 4.5 lists all significant changes in the urinary peptide profile of TRAMP and wild type mice at either time point. None of the ions that differentiated TRAMP and wild type mice were common to both age groups.

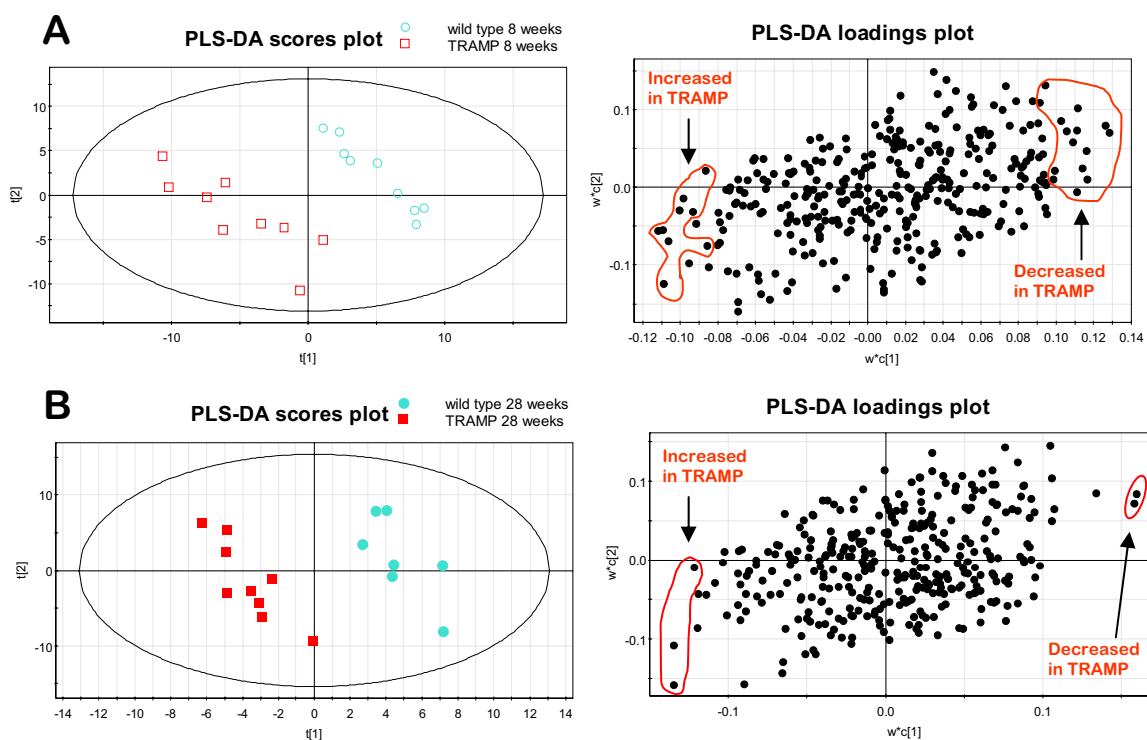


**Figure 4.40** Scores and loadings plots of PLS-DA models for maximal separation between TRAMP and wild type mice at (A) 8 and (B) 28 weeks of age. The dots in the red marked areas of the loadings plots are  $m/z$  ratios which were significantly different between the groups. The data are scaled to unit variance.

**Table 4.5** Significant changes in the urinary peptide profile of TRAMP mice compared to age matched wild type mice

<b>m/z</b>	<b>Change in TRAMP vs. wild type</b>	<b>m/z</b>	<b>Change in TRAMP vs. wild type</b>
<i>8 weeks</i>			
1744.0	-69%	1291.0	+41%
2073.9	-27%	1322.3	+134%
2090.1	-46%	1433.0	+118%
2257.1	-21%	1435.0	+176%
2273.0	-38%	2100.9	+115%
2393.0	-34%	2184.9	+38%
2424.2	-25%	2211.9	+219%
2998.0	-19%	2592.0	+358%
3008.0	-60%	8223.1	+45%
3505.0	-44%	<i>28 weeks</i>	
4006.0	-37%	4406.0	-3%
4236.0	-21%	8510.0	-13%
4317.0	-44%	5839.0	+9%
4528.0	-50%	7703.0	+14%
6469.0	-33%	9250.0	+17%

From table 4.5 and figure 4.40 it is evident that differences in the urinary peptide pattern between TRAMP and wild type mice were much more pronounced in the young animals compared to the older group. In agreement with the PLS-DA analysis, the difference/correlation plots (figure 4.41) highlight the most significant changes in TRAMP mice. While in the young animals group differences were mostly concentrated on the lower molecular weight range, in the old animals changes were found at the upper end of the investigated m/z range.

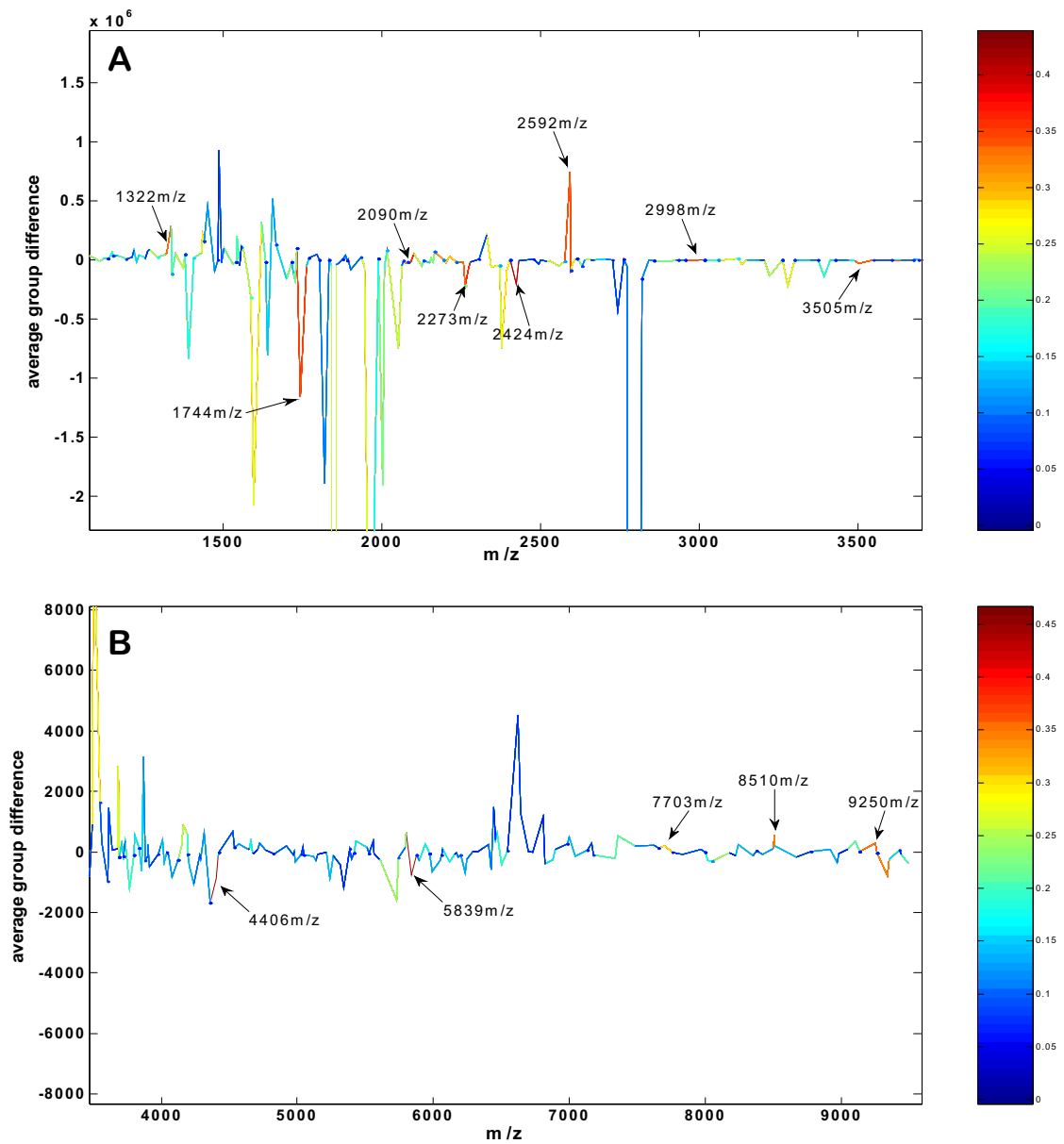


**Figure 4.41** Difference/correlation plots of TRAMP versus wild type mice at (A) 8 weeks and (B) 28 weeks of age.

#### 4.4.2 Peptidomic changes in plasma of TRAMP mice

Figure 4.42 shows the binned combined mass spectra of all plasma samples with the green line indicating the unresolved background continuum which was subtracted before data evaluation. From the background-subtracted spectrum 286 significant peaks were extracted for further analysis. The unresolved background signal only reached about 100 counts as compared to 500 counts in the urine spectra. The peaks were more evenly distributed across the first half of the  $m/z$  range than in the urine spectra. Figure 4.43 shows the heat map for count values of the significant peaks for all samples.

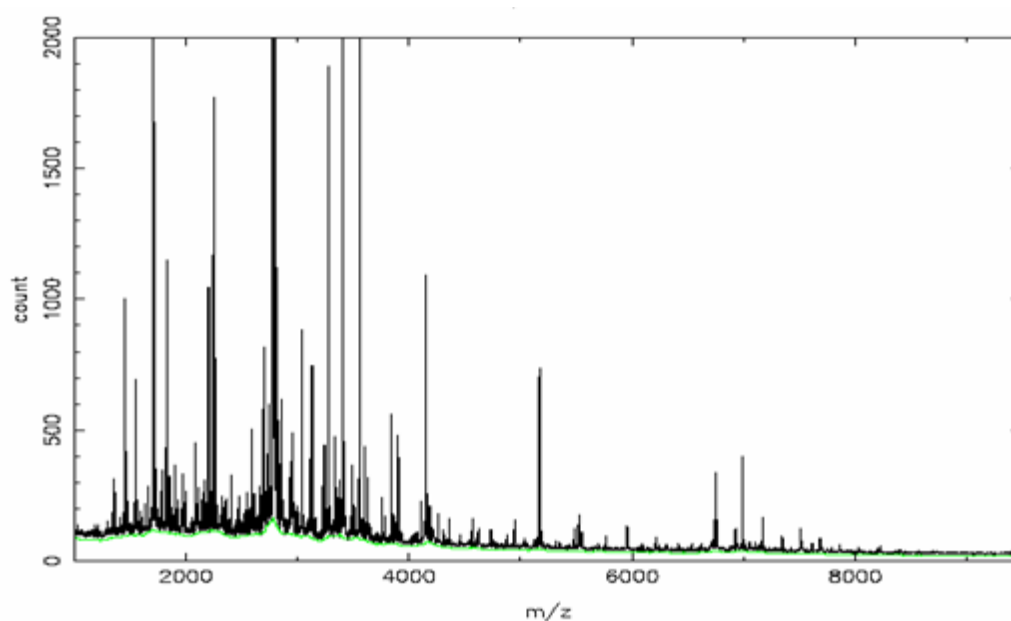


**Figure 4.42** Combined and binned mass spectra of all mouse plasma samples analysed by MALDI-MS. The green line indicates the unresolved background continuum which is subtracted prior to data evaluation.

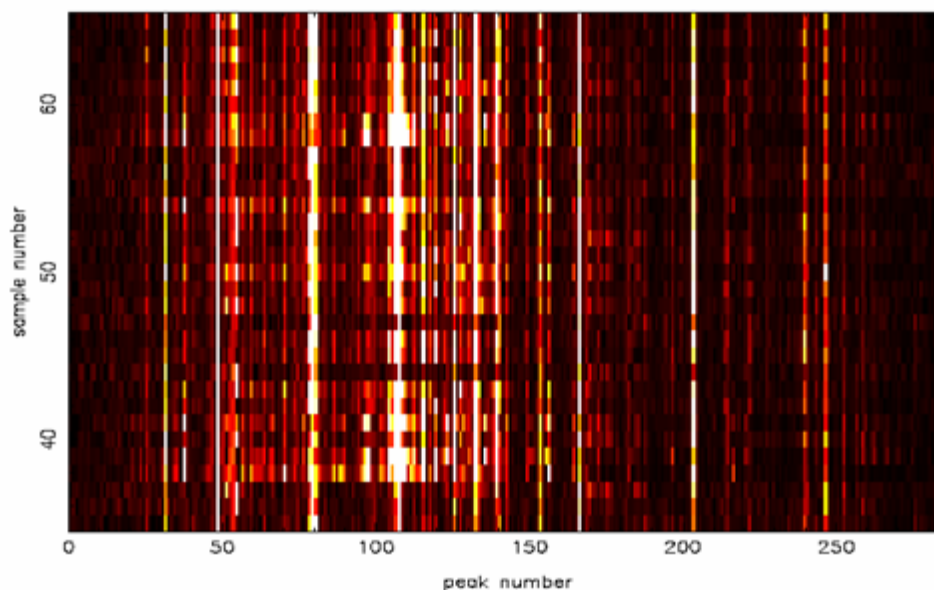


**Figure 4.43** Count values heat map of significant peaks of plasma MALDI spectra. The peaks are sorted in ascending order of  $m/z$  values. The brightness is proportional to signal intensity. Samples are listed in run order.

PCA analysis (figure 4.44) shows that age differences are the major contributors to variation in the data set. Differences related to the TRAMP genotype were established using PLS-DA models generated to maximise the separation between wild type and TRAMP at both time points. In contrast to the urine data, the differences were stronger in the old animals, in which tumours in TRAMP mice were fully developed. The PLS-DA model for the young animals did not pass the validation test. However, it was possible to identify five  $m/z$  values significantly different between TRAMP and wild type mice (figure 4.45, table 4.6).

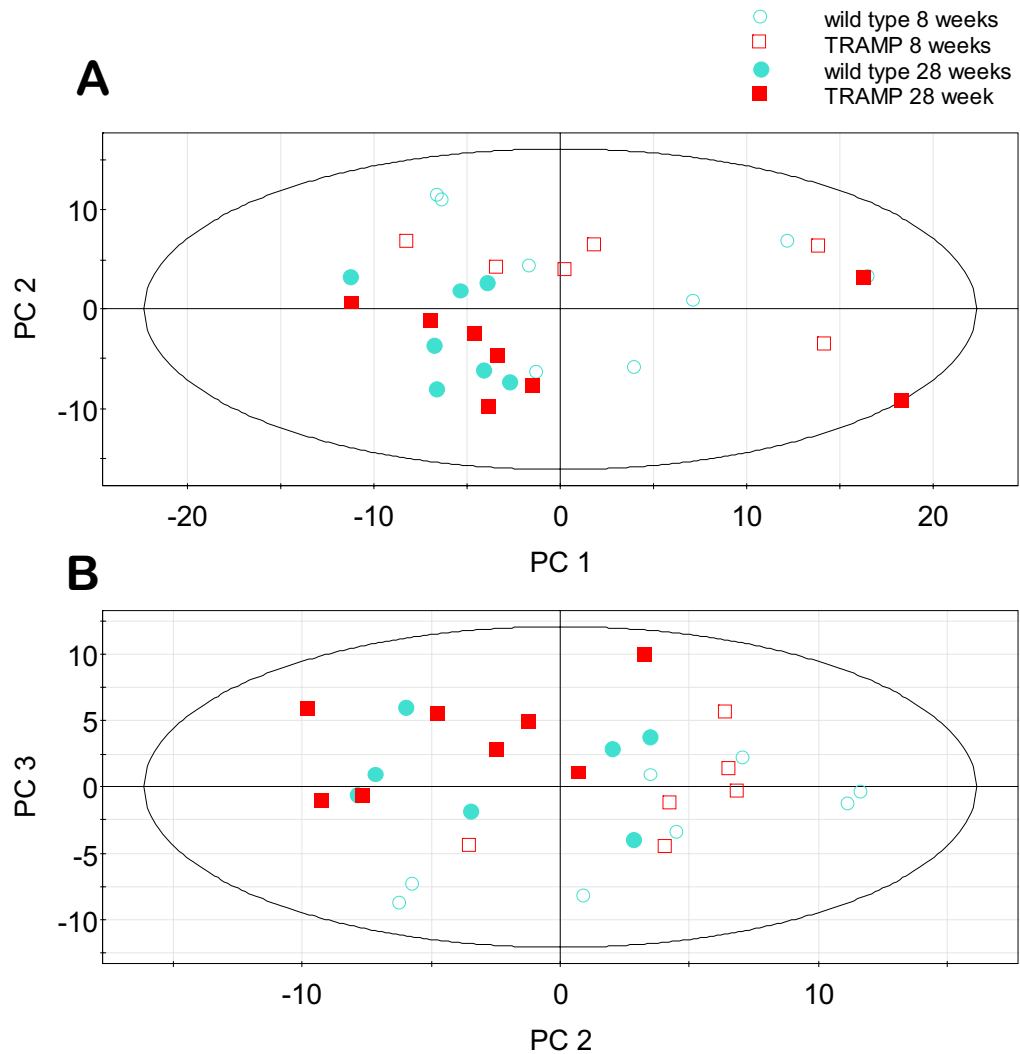


**Figure 4.44** PCA scores plots of plasma samples analysed by MALDI-MS showing (A) the first and second and (B) the second and third principal component (PC). The data are scaled to unit variance.

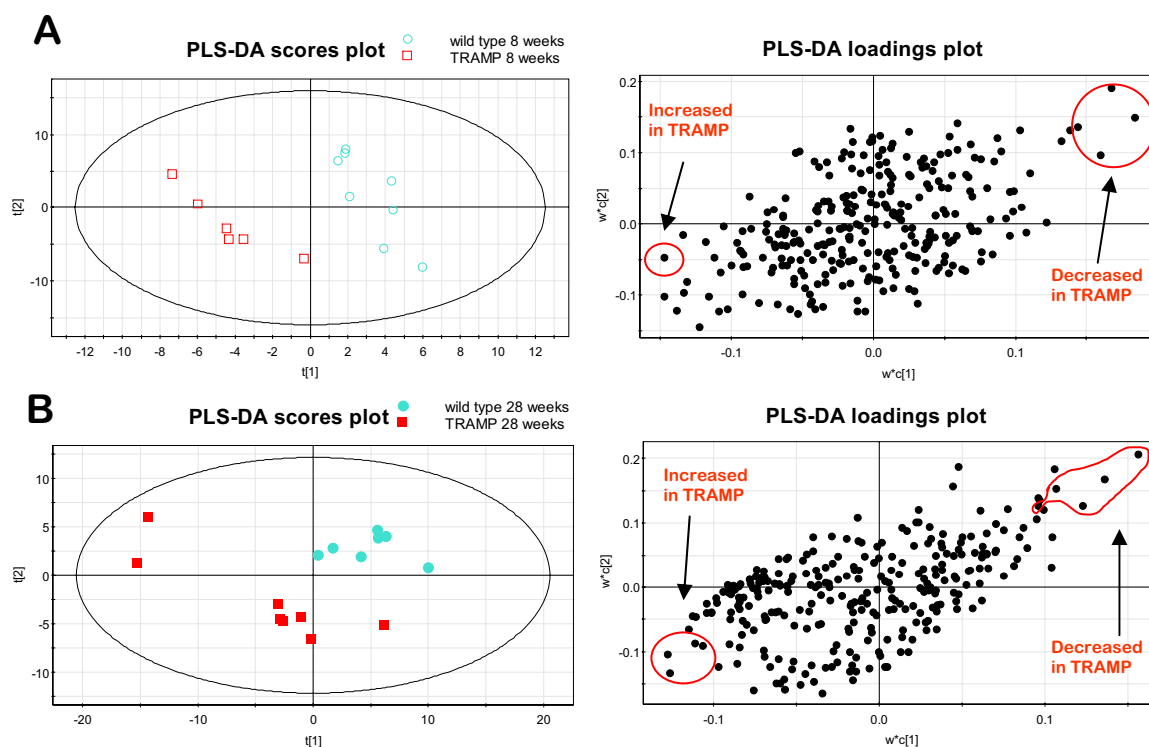


**Figure 4.45** Scores and loadings plots of PLS-DA models for maximal separation between TRAMP and wild type mice at (A) 8 and (B) 28 weeks of age. The dots in the red marked areas of the loadings plots are  $m/z$  ratios which were significantly different between the groups. The data are scaled to unit variance.

The difference/correlation plots generated for the separation of TRAMP and wild type mice at each time point confirmed the findings from the PLS-DA analysis (data not shown). As for the urine samples, there were no overlaps in the differing ions between the two age groups. Furthermore, there was no overlap found between urine and plasma samples.

**Table 4.6** Significant changes in the plasma peptide profile of TRAMP mice compared to age-matched wild type mice

<b>m/z</b>	<b>Change in TRAMP vs. wild type</b>	<b>m/z</b>	<b>Change in TRAMP vs. wild type</b>
<i>8 weeks</i>		3361.0	+25%
5539.0	+68%	4260.0	+89%
1030.3	-35%	5186.9	+15%
6066.0	-71%	1183.2	-51%
6517.0	-70%	1241.0	-37%
7430.0	-38%	1346.0	-44%
<i>28 weeks</i>		3713.9	-52%
2103.0	+40%	4072.2	-29%

#### 4.4.3 Discussion

Peptidomic profiling of urine and plasma from TRAMP and wild type mice at 8 and 28 weeks of age revealed group specific differences in both young and old animals. However, a marker ion common to both age groups was not detected in plasma or urine. Therefore, none of the differentially excreted ions can be unequivocally termed a marker for early detection or related to the process of prostate carcinogenesis in the TRAMP mouse. This finding is in agreement with the results obtained from the metabolic profiling. Also consistent with findings from the metabonomic investigations is the fact that the age of the animals is the major contributor to differences observed in urinary and plasma peptide profiles.

As for NMR analysis, urine samples showed a greater variation between TRAMP and wild type mice at 8 weeks of age compared to 28 weeks of age. This finding may be due to the suspected alteration in the gut microflora in 8 week old TRAMP mice (see section 4.2). It remains unclear which of these changes are related to the TRAMP phenotype or whether gut microfloral alterations and TRAMP phenotype are linked at 8 weeks of age. The presence of a prostate tumour had a less prominent effect on the urinary peptidome than aging or bacterial alterations in the gut. The plasma peptidome on the other hand showed more variation between TRAMP and wild type mice at 28 weeks. The plasma peptidome seems to be more influenced by the presence of a tumour than changes in the gut microflora. The reason for the better detection of the neoplasm in the plasma peptidome compared to the urine peptidome may either be explained by the “closeness” of the plasma to tumour or by bias due to sample preparation. Both samples types were prepared following the same SPE method (see section 2.2.2.4) which would allow for the detection of the same markers, if they were the same. However, “hydrophilising” metabolic changes, which the peptides might undergo prior to renal excretion, may lead to a poorer recovery using the applied SPE method. The heat map plots have shown that the peptide composition of urine and plasma is different with regard to mass distribution. An analogous situation might also apply to hydrophilic / hydrophobic properties. For future studies an additional SPE extraction for urine samples concentrating especially on hydrophilic species could be envisaged.

The literature (Adam *et al.*, 2002; Banez *et al.*, 2003; M'Koma *et al.*, 2007; Mobley *et al.*, 2004; Pan *et al.*, 2006; Petricoin *et al.*, 2002b; Qu *et al.*, 2002) was checked for peptide markers inherent to both human and TRAMP prostate cancer. Table 4.3 lists the peaks (+/- 15 mass units) that were also found to distinguish patients with prostate cancer (PCa) from healthy controls or patients with BPH.

**Table 4.7** Marker ions which differentiate TRAMP and wild type mice, and similar marker ions found in human studies

<b>Ion different between TRAMP and wild type (m/z)</b>	<b>Change TRAMP vs. wild type</b>	<b>Marker ion found in humans (m/z)</b>	<b>Type of change</b>	<b>Reference</b>
3714	decrease (plasma, 28 weeks)	3700	decrease in PCa (serum)	(Pan <i>et al.</i> , 2006)
4072	decrease (plasma, 28 weeks)	4071	differentiating BPH from normal (serum)	(Qu <i>et al.</i> , 2002)
4072	decrease (plasma, 28 weeks)	4079	differentiating PCa from normal (serum)	(Qu <i>et al.</i> , 2002)
2103	increase (plasma, 28 weeks)	2092	differentiating PCa from benign condition (serum)	(Petricoin <i>et al.</i> , 2002)
1433	increase (urine, 8 weeks)	1434	Increased in PCa vs. BPH (urine)	(M'Koma <i>et al.</i> , 2007)

Many reports state that SELDI or MALDI-MS profiling of serum samples can detect prostate cancer with better accuracy than PSA. Though it is remarkable that the overlap of markers between the different studies is only minimal (Mobley *et al.*, 2004). In this respect the work described here is no exception. It should be borne in mind though that murine and not human samples, and plasma rather than serum, were analysed. The great effects of sample preparation and handling on the composition of the mass spectra and the need for rigorous validation have been recognised (see Introduction, section 1.4.2). But even after inter-laboratory reproducibility has been established (Semmes *et al.*, 2005) and sources of sample bias identified (McLerran *et al.*, 2008a) and eliminated, correct classification of a sample cohort independent from the training set failed (McLerran *et al.*, 2008b). In agreement with these authors I conclude that a mass spectrometry approach measuring peptide signals in specimens of blood or urine is unlikely to succeed as a diagnostic tool for prostate cancer. However, the many reports, including the work presented here, that show differences in the peptide profile of prostate cancer and BPH patients, are good evidence that the peptidome of biofluids contains valuable diagnostic information. A peptidomics shotgun approach as is described here and in other studies, gives a snap-shot of a “peptidomic situation”, which is influenced by numerous pre-analytical factors. Bearing this scenario in mind, peptide profiling can be a valuable stepping stone for biomarker discovery. Marker ions have to be identified and assessed in their biological context, and then a robust testing method for a specific molecule can be developed.

## 4.5 Levels of urinary 8-oxodG in TRAMP mice

### 4.5.1 Results

#### 4.5.1.1 Data normalisation

The concentration of 8-oxodG in urine of TRAMP and wild type mice was determined by LC-MS/MS as described in sections 2.2.3.4 and 2.2.3.5. In order to assess dilution factors, normalisation to creatinine (see section 2.2.3.7 and 3.2.2), specific gravity (SG) (see section 2.2.3.8) and a combination of SG with the animal weight were investigated. Statistical significance was tested using the Mann-Whitney U-test with  $p < 0.05$ .

SG is the ratio of the density of a given substance or liquid to that of water. The value of (SG-1) has been shown to correlate with the total mass of dissolved solids (Levine and Fahy, 1945). In studies measuring urinary compounds SG is often used to account for the dilution of urine samples (Heavner *et al.*, 2006). The renal excretion of creatinine occurs in a relative constant relation to muscle mass (Narayanan and Appleton, 1980), and is therefore to a certain extent correlated to body mass, namely lean body mass. This fact makes creatinine a common point of reference in many research investigations and clinical measurements (Heavner *et al.*, 2006). The normalisation to SG and weight was chosen in order to account for dilution and body mass, respectively. Since oxidative damage does not only occur in muscle tissue, and the animals undergo substantial weight gain between 8 and 28 weeks of age, the influence of total body weight on levels of urinary 8-oxodG was investigated.

Table 4.8 shows the median values of urinary 8-oxodG for all four groups of mice using the described normalisation procedures. The median values of the factors used for normalisation are shown in table 4.9. Young wild type and TRAMP mice differed significantly in body weight (indicated by one dot). When all young versus all old

animals were compared, body weight and creatinine, but not SG, were significantly different. Table 4.10 presents the percent differences of median 8-oxodG levels between animal groups. The unnormalised and SG-normalised data show large age differences, since here body mass is not taken into account. The correction for creatinine reduces the differences since an older mouse will excrete more creatinine due to an increase of muscle mass. SG- and weight-adjusted data exhibit the least differences in relation to animal age. This finding reflects the fact that the median body weight of old animals was 97% higher than in young animals while the creatinine excretion was elevated by only 43%.

The values normalised by SG and weight did not confirm the significant increase of urinary 8-oxodG levels with age in TRAMP mice. This can be explained by the increase of 8-oxodG in young TRAMP mice compared to young wild type mice (table 4.10), which is caused by a significant weight difference between these two animal groups (table 4.9). However, this weight difference is not reflected by the difference in creatinine, suggesting that the cause for the weight difference is not related to the lean body mass. The source for the difference in body weight is unknown; however, fat and water deposits might play a role, both of which are unlikely to contribute to renally excreted 8-oxodG. Normalisation to creatinine seemed therefore the most appropriate for the analysis of the data. Previous studies in humans show evidence that urinary 8-oxodG is in fact formed in the lean body mass (Pilger *et al.*, 2001; Pourcelot *et al.*, 1999).

#### **4.5.1.2 Comparison of urinary 8-oxodG levels in TRAMP and wild type mice**

For data evaluation the creatinine-normalised data were used (marked yellow in tables 4.8 and 4.10). There is no significant difference in urinary 8-oxodG levels between TRAMP and wild type mice at either time point. However, a significant elevation was observed in old mice of both genotypes as compared to the young animals (table 4.10, figure 4.46). The general trend of these findings (no difference between TRAMP and wild type but a strong increase with age) was the same in the data that were normalised to SG or unnormalised. The reasons for the discrepancies in the SG- and weight-normalised data are discussed in the section above.

**Table 4.8** Median values for urinary 8-oxodG across the four animal groups using different data normalisation techniques.

	wild type 8 weeks	TRAMP 8 weeks	wild type 28 weeks	TRAMP 28 weeks
<b>unnormalised</b> [pmol/ml]	5.80 (2.35/12.71) (n=9)	5.71 (2.90/8.79) (n=9)	17.75 (13.95/26.54) (n=7)	16.59 (11.83/22.22) (n=8)
<b>creatinine-normalised</b> [nmol/mmol]	3.68 (2.22/4.24) (n=7)	4.00 (2.83/4.89) (n=8)	6.91 (6.46/16.66) (n=6)	6.73 (5.98/8.53) (n=8)
<b>SG-normalised</b> [pmol/ml]	5.01 (3.13/5.75) (n=9)	5.48 (3.58/10.31) (n=9)	12.34 (11.16/16.51) (n=7)	11.46 (10.33/15.15) (n=8)
<b>SG- &amp; weight normalised</b> [fmol/ml/g]	252 (168/338) (n=8)	318 (216/617) (n=8)	356 (326/479) (n=7)	356 (304/469) (n=8)

The numbers in brackets are the minima and maxima; n is the number of animals per group.

**Table 4.9** Median values for measurements used for the normalisation of 8-oxodG concentrations

	wild type 8 weeks	TRAMP 8 weeks	wild type 28 weeks	TRAMP 28 weeks
<b>animal weight</b> [g]	17.9 ♦ (16.98/20.84)	16.65 (16.26/19.47)	34.29 (31.3/37.3)	33.65 ♦♦ (30.3/38.4)
<b>creatinine</b> [μM]	1709 (1057/3282)	1648 (691/2480)	2613 (837/3267)	2176 ♦♦ (1822/3566)
<b>specific gravity</b>	1.026 (1.015/1.049)	1.017 (1.012/1.042)	1.0285 (1.024/1.039)	1.0265 (1.020/1.043)

Values in brackets are minima and maxima. ♦ = significant difference between animals within one age group; ♦♦ = significant difference between all young vs. all old animals (Mann-Whitney U test,  $P < 0.05$ )

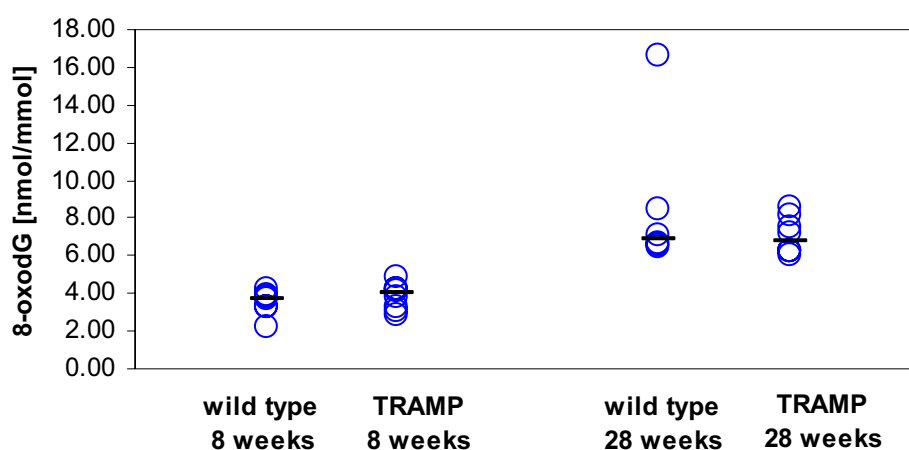


**Figure 4.46** Levels of urinary 8-oxodG in TRAMP and wild type mice. The circles represent the urinary 8-oxodG levels for individual animals normalised to creatinine. The black bars indicate the median value for each group.

**Table 4.10** Changes in 8-oxodG levels between TRAMP and wild type mice

	<b>wild type 8 weeks vs. TRAMP 8 weeks</b>	<b>wild type 28 weeks vs. TRAMP 28 weeks</b>	<b>wild type 8 weeks vs. wild type 28 weeks</b>	<b>TRAMP 8 weeks vs. TRAMP 28 weeks</b>
<b>unnormalised [pmol/ml]</b>	-2% (p=0.691)	-7% (p=0.298)	+206% (p=0.0009)	+191% (p=0.0005)
<b>creatinine-normalised [nmol/mmol]</b>	+9% (p=0.563)	-3% (p=0.366)	+88% (p=0.003)	+69% (p=0.0008)
<b>SG-normalised [pmol/ml]</b>	+9% (p=0.122)	-7% (p=0.298)	+146% (p=0.0009)	+109% (p=0.0005)
<b>SG- &amp; weight normalised [fmol/ml/g]</b>	+26% (p=0.074)	0% (p=0.772)	+41% (p=0.002)	+12% (p=0.401)

#### 4.5.2 Discussion

The initial aim was to test the hypothesis that animals which harbour the TRAMP genotype show higher levels of urinary 8-oxodG as a result of increased oxidative stress. Elevated levels of urinary 8-oxodG have been linked to human cancers in general (Wu *et al.*, 2004) and prostate cancer in particular (Chiou *et al.*, 2003; Miyake *et al.*, 2004). However, decreased urinary 8-oxodG levels in cancer patients have also been reported (Cooke *et al.*, 2006b). In the TRAMP mouse 8-oxodG was detected in prostate tissue by immunohistochemical staining, but it was not detectable in age matched wild

type mice (Tam *et al.*, 2006). However, the present study could not show an increase in urinary 8-oxodG in TRAMP compared to wild type mice at either 8 or 28 weeks of age. Bearing in mind that urinary 8-oxodG is a product of DNA repair or derived from the nucleotide pool (see Introduction, section 1.5) and assuming that the findings by Tam *et al.* (2006) are genuine, there are three possible explanations as to why 8-oxodG was not elevated in the urine of TRAMP mice: i) The contribution from the prostate tissue and tumour is only minor in comparison with 8-oxodG from other body compartments, and therefore changes do not register in urine. ii) The DNA repair mechanisms that remove 8-oxodG (see Introduction, section 1.5) are impaired in TRAMP prostate tissue leading to unchanged 8-oxodG levels in urine despite increased oxidative DNA damage in the prostate. McCabe *et al.* have shown that in TRAMP prostates hypermethylation leads to underexpression of O<sup>6</sup>-methylguanine-DNA methyltransferase (Mgmt) (McCabe *et al.*, 2006), which plays an important role in the repair of O<sup>6</sup>-methylguanine and other alkylation DNA damage (Margison and Santibanez-Koref, 2002). In this context, it is conceivable that hypermethylation also affects other DNA repair enzymes, e.g. nucleotide excision repair, 8-oxodG endonuclease, and 8-oxodGTPase, which are thought to be responsible for the excretion of 8-oxodG in urine (see Introduction, section 1.5). An impaired repair mechanism in cancer patients has also been postulated by Cooke *et al.* who found slightly decreased urinary 8-oxodG in colorectal and lung cancer patients (Cooke *et al.*, 2006b). iii) The accumulation of nuclear 8-oxodG in TRAMP prostate observed by Tam *et al.* (2006) does not contribute to 8-oxodG in urine. This possibility would favour the nucleotide pool as a major contributor to excreted 8-oxodG. Recently, the nucleotide pool has been suggested to be significantly affected by radiation-induced oxidative stress and to greatly contribute to extra-cellular 8-oxodG, as found in urine (Haghdoost *et al.*, 2005; Haghdoost *et al.*, 2006).

The other observation of this study was the increase of urinary 8-oxodG in 28 week old TRAMP and wild type mice compared to their 8 week old counterparts. Due to the confounding factors of normalisation, discussed in section 4.5.1.1, it is difficult to say by how much the value does exactly increase, but the general trend of increase with age is undeniable. The increase of oxidative damage with age has been intensely discussed in the literature. Various studies in mice and rats have shown that tissue levels of 8-oxodG increase with age, though to different extents in different tissues (Fraga *et al.*, 1990; Hamilton *et al.*, 2001; Sohal *et al.*, 1994). Studies on human subjects have demonstrated increases of 8-oxodG in skeletal muscles (Mecocci *et al.*, 1999) and leukocytes (Siomek *et al.*, 2007) from adulthood to old age. The latter study could also show that the renal excretion of 8-oxodG follows a similar pattern. Other researchers reported no or even a slightly negative correlation of urinary 8-oxodG to age in humans (Miwa *et al.*, 2004; Pilger *et al.*, 2001; Poulsen *et al.*, 1998). A significant decrease of urinary 8-oxodG with age has been shown for rats, despite increases in the 8-oxodG in tissues (Fraga *et al.*, 1990). The authors of this study postulated impaired repair mechanisms as the cause of decreased 8-oxodG excretion. However, more recently, Hamilton *et al.* demonstrated that the increase of 8-oxodG with age in various tissues of female C57BL/6 mice was not due to a diminished ability to remove these lesions (Hamilton *et al.*, 2001). Young and old animals, exposed to  $\gamma$ -irradiation, showed no difference in the rate of removal, but old animals exhibited much higher levels of 8-oxodG than young mice upon radiation exposure. The authors concluded that an enhanced sensitivity to oxidative stress is responsible for increasing 8-oxodG levels in aging. C57BL/6 is the background strain used for the TRAMP study here. It seems reasonable to assume that the observed increase of urinary 8-oxodG in 28 week old TRAMP and wild type mice compared to their 8 week old counterparts reflects the

increase in susceptibility to oxidative stress as described by Hamilton *et al.* It is interesting to note that these processes seem to start relatively early in the life of the mouse, as the group that is here marked “old” (28 weeks) is the “young” group in the study by Hamilton *et al.* (2001).

The changes in urinary 8-oxodG observed for mice, rats and humans during aging are quite different from each other, although an increase in tissue levels is common to all species. Further research is required to determine the source of urinary 8-oxodG and whether, and to what extent, differences in DNA and nucleotide pool repair in general, and during aging in particular, exist between these species. It seems important to be able to assess the transferability of data acquired in preclinical animal studies to humans.

## 4.6 Summary

The metabolic profiling of prostate tissue showed that the loss of prostate-specific citrate metabolism in prostate cancer is common to both TRAMP mice and men. The tumour phospholipid metabolism on the other hand was found to be different to that observed in human prostate cancer. The implications of these findings for the use of the TRAMP model in chemoprevention research will be discussed in Chapter 7.

Metabolic and peptidomic profiles of urine showed greater differences between 8 week old TRAMP and wild type mice than between 28 week old mice. In 8 week old mice gut microflora related alterations of the urinary metabolic profile were found to be the major contributors to group separation. These findings showed that the urinary metabolite and possibly peptide profile is greatly influenced by the composition of the gut microflora. This fact should be borne in mind for the design of future studies.

NMR based metabolic profiling of plasma did not reveal any TRAMP-specific changes, whereas peptidomic profiling was able to pick up TRAMP-specific alterations. None of the profiling approaches, however, detected TRAMP-specific markers consistent to both age groups. It was therefore not possible to identify a marker that could be assigned unambiguously to carcinogenesis. All profiling approaches have identified aging to be the most influential factor for the metabolic and peptidomic profiles. It is conceivable that these general underlying changes influence the way the organism deals with cancer related “threats”, which would make the detection of markers common to both age groups unlikely. Metabolic and peptidomic profiling studies investigating smaller time windows would be of great benefit to elucidate possible connections.

The urinary excretion of 8-oxodG was not different between TRAMP and wild type mice at either time point, but great increases were seen in old compared to young mice. This finding is consistent with the results from investigations mentioned above, that

aging is the major cause of changes in the organism. Reports for urinary 8-oxodG as cancer biomarkers are equivocal; increases as well as decreases have been reported. Since the origin of urinary 8-oxodG is currently not clear, it is not possible to define the role of urinary 8-oxodG in cancer. The present study showed that in a well controlled and – compared to humans – homogenous model organism the development of advanced prostate cancer did not lead to changes in levels of urinary 8-oxodG. Although the development of LC-MS/MS methods has given researchers a tool for the accurate determination of 8-oxodG, its use as biomarker has to be looked at with caution until the origin of its appearance in urine is elucidated.

# Chapter 5

## **5. Effect of green tea constituents on features of carcinogenesis in the TRAMP mouse model**

This study (see section 2.2.1.5) was conducted with the aim of assessing the effect of intervention with green tea polyphenols (GTP) on TRAMP mouse carcinogenesis and to find biomarkers to monitor possible effects. Age matched wild type and TRAMP mice were divided into tea treatment and control groups and sacrificed at either 8 or 29 weeks of age. Urine, plasma, and tissue samples were collected as described in sections 2.2.1.5, 2.2.1.7, 2.2.1.8 and 2.2.1.9. In the following the 8 week old mice are referred to as “young” and the 29 week old as “old”.

### **5.1 Effect of GTP on prostate tissue of TRAMP mice**

#### **5.1.1 Pathological assessment of prostate tissue**

At 8 weeks of age TRAMP mice presented with early focal hyperplastic alterations to the glandular epithelium of the prostate. In TRAMP mice receiving GTP these lesions seemed overall a little less extensive. However, accurate quantification was not possible due to the highly focal nature of these lesions their variable size and random distribution within the sections. As discussed previously (see Chapter 4.1.1), two histological types of carcinoma were present in old TRAMP mice: well-differentiated adenocarcinoma and poorly differentiated carcinoma (less common). The latter were much larger and more extensive tumours. Wild type mice did not present with any discernible malignant change at either time point.

### 5.1.2 Effect of GTP on prostate weights in TRAMP mice

Prostates and prostate tumours were dissected avoiding the seminal vesicles. For weight comparison two and three large central tumours (weighing from 1.2g to 10g) were excluded from the old TRAMP groups receiving GTP and water, respectively. Prostate weights were not significantly different (Mann-Whitney U-test,  $p < 0.05$ ) between water- and GTP-fed TRAMP or wild type mice at either time point (figure 5.1). At 8 weeks of age the prostates of TRAMP mice already showed a tendency to increased prostate weights compared to their wild type litter mates. In the case of the water-fed animals this difference (+12%) was significant ( $p = 0.0321$ , figure 5.1 A).

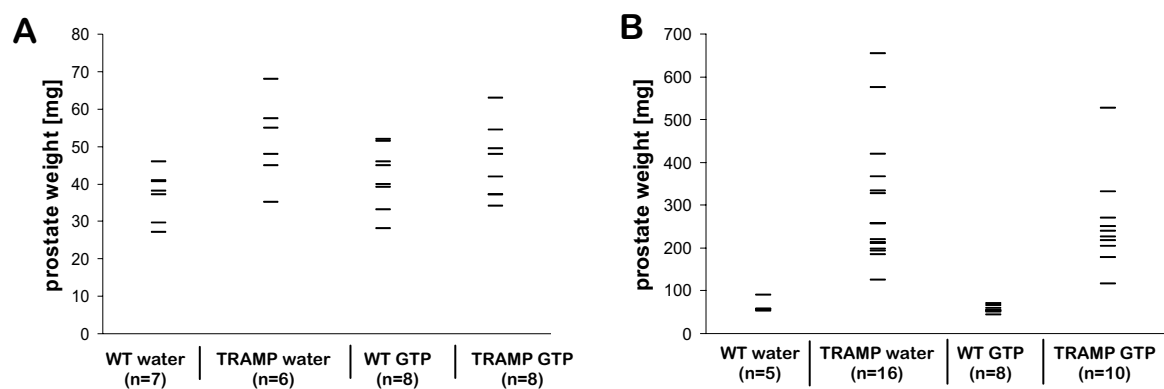


**Figure 5.1** Prostate weights in 8 week (A) and 29 week old (B) mice.

### 5.1.3 Effect of GTP on metabolic profile of prostate tissue of TRAMP and wild type mice

Prostate tissue was extracted and analysed as described in sections 2.2.4.3, 2.2.4.5 and 2.2.4.6. Spectral assignments were made with a combination of homonuclear COSY experiments (carried out by Dr Hector Keun, Imperial College, London), literature (Bollard *et al.*, 2005; Nicholson *et al.*, 1989), the BMRB database (<http://www.bmrwisc.edu/>) (Seavey *et al.*, 1991) and advice from Dr Hector Keun. Changes in metabolite levels were calculated from the group medians, and significance was established using the Mann-Whitney U-test.

Figure 5.2 shows the PCA scores plot of all tissue extracts analysed by  $^1\text{H-NMR}$ . The presence of tumours and the age of the animals are the greatest contributors to variation in the data set. In order to eliminate the aging effect, the young and old animals were evaluated separately. For each age group a PLS-DA model was generated such that the separation between wild type and TRAMP mice was maximised regardless of treatment. The validity of each model was tested by comparing the predictive ability of the model, summarised by  $Q^2$  statistics, with those of 20 models where the TRAMP and wild type mice were randomly assigned to different groups. Only in the case of the old animals was the model  $Q^2$  greater than all 'permuted' models, confirming the model predictivity as statistically significant ( $p < 0.05$ ). For both age groups a scores plot of the PLS-DA model was created which was coloured according to genotype and treatment (figure 5.3). This allowed the visualisation of the green tea effect on the profile in the TRAMP – wild type profile shift. However, GTP-fed mice did not form a separate cluster but were grouped together with water-fed animals.

To confirm this observation, the Y predictive values for water-fed TRAMP mice and GTP-fed TRAMP mice as well as water- and GTP-fed wild type mice were compared.

The values did not differ significantly (t-test), indicating that both TRAMP groups are equally distant to the wild type animals and vice versa. GTP did not have a global effect on the metabolic profile of prostate tissue in 8 and 28 week old TRAMP mice.

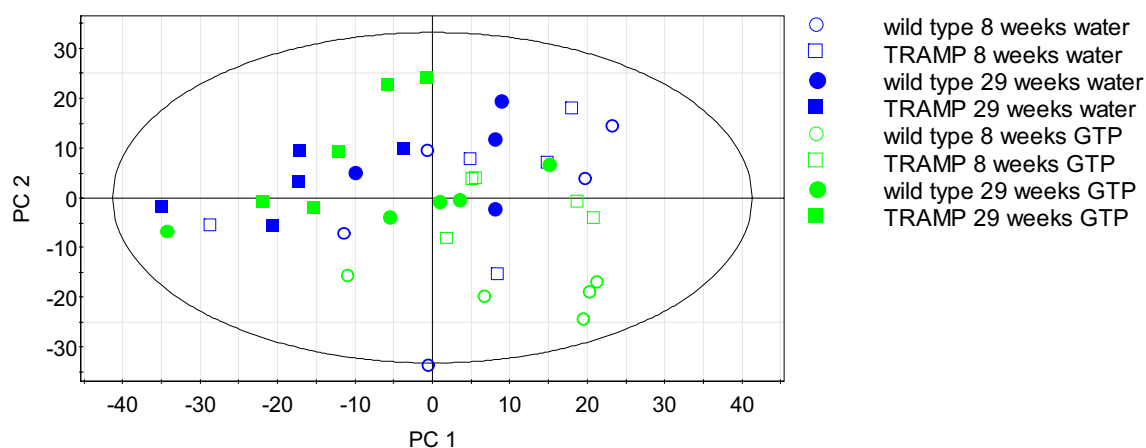


**Figure 5.2** PCA scores plot of all prostate extract NMR spectra showing the first and second principal component (PC). The data are scaled to unit variance.

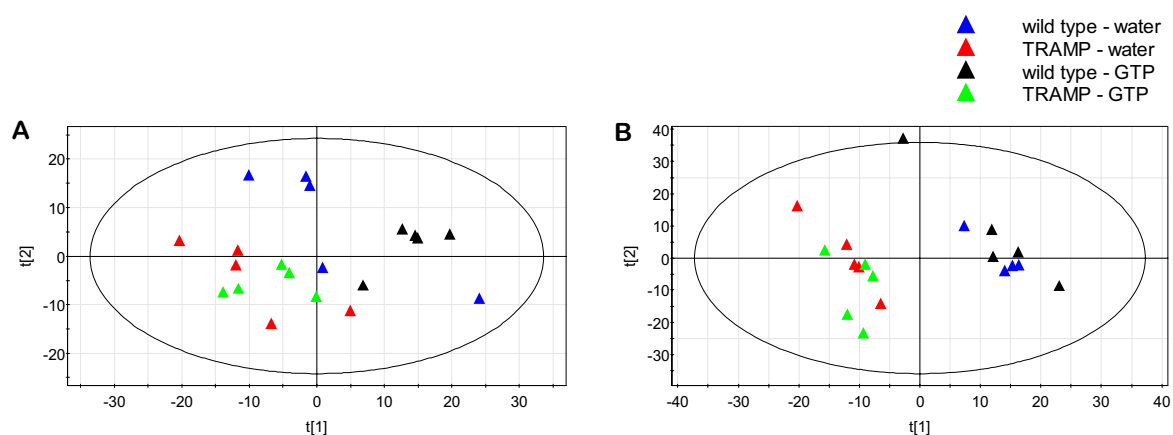


**Figure 5.3** Scores plots of PLS-DA models generated to maximise the difference between TRAMP and wild type mice at (A) 8 and (B) 29 weeks of age regardless treatment. The groups are coloured according to genotype and treatment. The data are scaled to unit variance.

Differences in the prostate metabolome of TRAMP and wild type mice at 8 and 28 weeks of age are described in Chapter 4. At 8 weeks of age the only discriminating feature was the GPC/PC ratio. In the old animals significant decreases of citrate, glucose, UDP-linked sugars, choline, PC, GPC and GPI were observed, while aspartate was significantly increased. GTP did not show an effect on any of these metabolites at either time point.

In order to mine the data set for more subtle GTP effects on prostate tissue, four difference/correlation plots were generated to visualise the differences between GTP- and water-receiving TRAMP and wild type mice at either time point. Additionally, overlaid spectra coloured according to groups were inspected for GTP related differences. Five spectral regions differed significantly between GTP- and water-fed animals (table 5.1). None of these differences were consistent throughout the animal groups.

**Table 5.1** Effects of GTP on prostate tissue metabolite levels

<i>metabolite or spectral region</i>	<i>change in GTP-fed compared to water-fed</i>	<i>p-value</i>
8 week old wild type mice ( $n_{\text{GTP}} = 5$ ; $n_{\text{water}} = 5$ )		
s 8.19ppm	-26%	0.0472
8 week old TRAMP mice ( $n_{\text{GTP}} = 5$ ; $n_{\text{water}} = 5$ )		
d 2.94ppm	+54%	0.0472
29 week old wild type mice ( $n_{\text{GTP}} = 5$ ; $n_{\text{water}} = 4$ )		
creatine (s 3.04ppm)	-46%	0.0143
s 1.92ppm	-14%	0.0143
s 2.92ppm	-17%	0.0192
29 week old TRAMP mice ( $n_{\text{GTP}} = 5$ ; $n_{\text{water}} = 5$ )		
s 3.36ppm	+279%	0.0472

ppm value in brackets indicate the signal that was used for integration; s = singlet, d = doublet. Changes were calculated from the group median values. Significance was established with the Mann-Whitney U-test.

#### 5.1.4 Discussion

Histopathological assessment of TRAMP prostate tissue suggested a slight anti-neoplastic effect of GTP at 8 weeks of age but not at 29 weeks of age (see section 5.1.1), while comparison of prostate weights did not provide evidence for chemopreventive efficacy of GTP at either time point (see section 5.1.2). In agreement with this observation, no global GTP effect diminishing the TRAMP phenotype at the metabolic level could be observed (see section 5.1.3). A small number of differences in signal intensities in tissue extract NMR spectra between GTP- and water-fed animals, which were discovered upon detailed data mining, were not consistent between the groups. Only in 29 week old wild type mice was more than one signal found to be

significantly different, suggesting that in this group the GTP effect on the prostate metabolome was more pronounced.

Although histopathological examination suggests a slight anti-neoplastic effect of GTP in 8 week old TRAMP mice, all the findings from prostate tissue examination taken together were unable to give sufficient evidence of chemopreventive efficacy of GTP in this study. This observation is in contrast to previously reported green tea mediated chemoprevention in the TRAMP mouse model (see Chapter 1, section 1.3.1). It should be emphasised, however, that the success rates for chemoprevention of prostate carcinogenesis in TRAMP mice with GTP or EGCG as reported in the literature, are very variable. Supplementation of drinking water with 0.1% and 0.3% GTP have been reported to lead to a 65 and 80% reduction in the development of palpable tumours, respectively (Caporali *et al.*, 2004; Gupta *et al.*, 2001). Treatment with EGCG, the major catechin in green tea, has been shown to exert an effect on the ventral prostatic lobes, but a significant reduction of hyperplasia in the whole of the prostate in animals older than 12 weeks was not found (Harper *et al.*, 2007; Nyska *et al.*, 2003). The observation by Harper *et al.* that EGCG was only effective in 12 week old but not 28 week old animals, is consistent with the less extensive lesions in the 8 week old GTP-fed TRAMP mice compared to water-fed TRAMP mice observed in this study. Comparison of the results from the studies published in the literature (see above) suggests that EGCG as a single compound is less effective than a mixture of GTP.

The study described here used 0.05% GTP dissolved in the drinking water, which is less GTP and equivalent EGCG compared to that used in previously published studies. It appears clear, that the dose administered here was not sufficient to exert a chemopreventive effect. In this context, it should also be considered that a possible oxidation of GTP in the drinking bottle (air bubbles introduced by drinking) could have

lowered the GTP-dose further. Miura *et al.* observed a nearly 60% decrease in the EGCG concentration over 24h in a GTP solution offered to rats, while the compound was relatively stable in the same bottle kept on the bench (Miura *et al.*, 2001).

## 5.2 GTP effects on the urinary metabolic profile of TRAMP mice

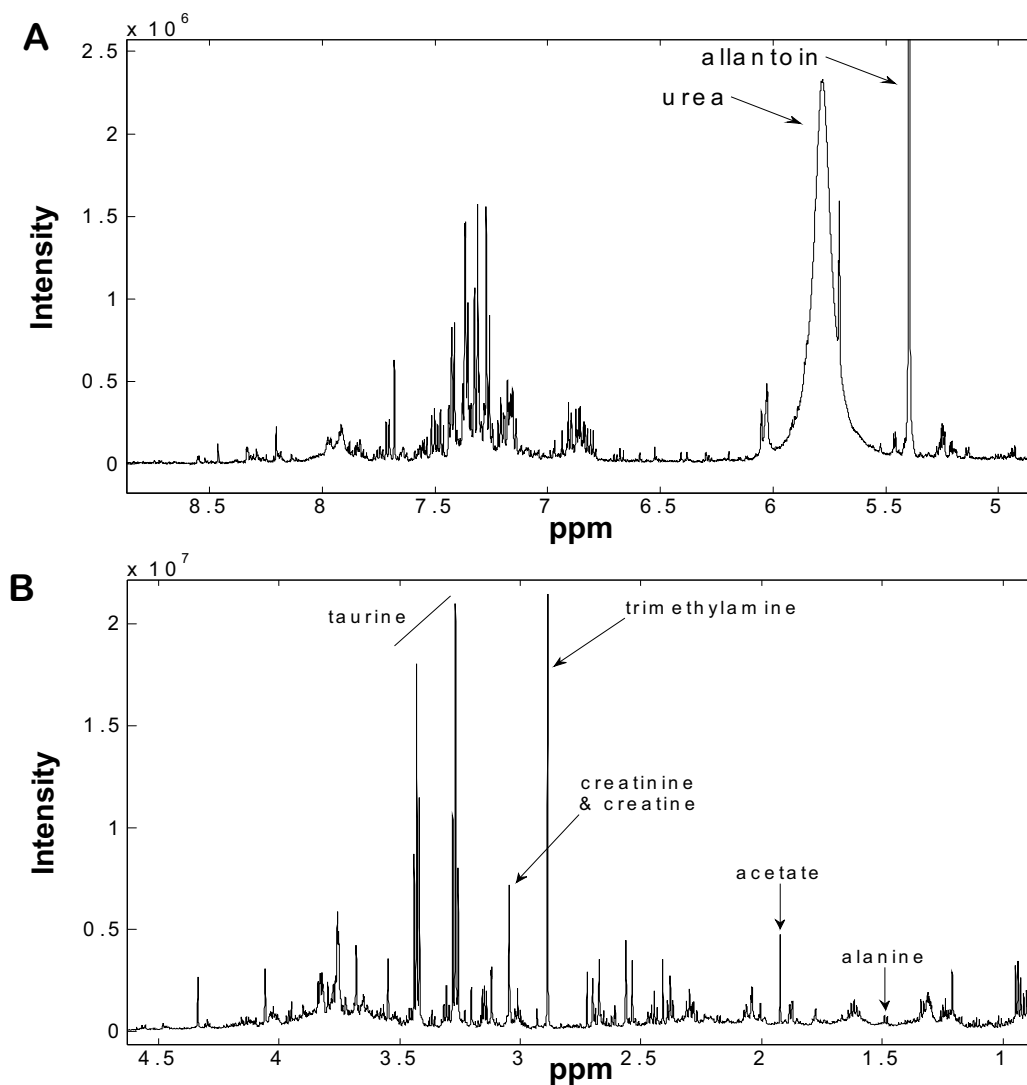
### 5.2.1 <sup>1</sup>H-NMR metabolic profiling of urine

Urine samples were prepared and analysed as described in sections 2.2.4.1, 2.2.4.5 and 2.2.4.6. Spectral assignments were made by comparison with the literature (Bollard *et al.*, 2005; Nicholson *et al.*, 1989), the BMRB database (<http://www.bmrbl.wisc.edu/>) (Seavey *et al.*, 1991) and personal communication with Dr Hector Keun (Imperial College, London). Changes in metabolite levels were calculated from the medians, and significance was established using the Mann-Whitney U-test. Figure 5.4 shows a urine NMR spectrum obtained from a GTP-fed 29 week old TRAMP mouse.

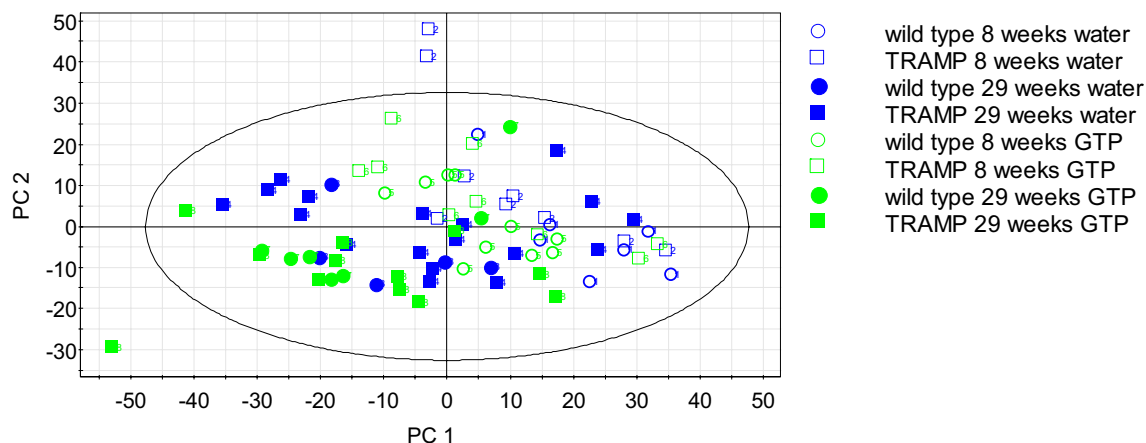
#### 5.2.1.1 Effect of GTP on urinary metabolite profile of TRAMP mice

Figure 5.5 shows a PCA scores plot for all urine NMR spectra. The trend of separation along the first principal component indicates that the main variation within the data set arises from the age difference. Subsequent data analysis was carried out for both age groups separately. As described in section 5.1.3 for tissue extract NMR data, PLS-DA models were generated to maximise the separation between TRAMP and wild type mice regardless of treatment. In the 29 week old animals the PLS-DA model could successfully separate (as tested against permuted models) wild type (WT) and TRAMP (T) mice (figure 5.6). However, the consumption of GTP did not show a global effect on the urinary metabolic profile of TRAMP mice. To confirm this observation the Y predictive values for water-fed TRAMP mice and GTP-fed TRAMP mice were compared. The values did not differ significantly (t-test), indicating that both TRAMP groups are equally distant to the wild type animals. Similarly, in the urine of the 8 week

old animals no global effect of GTP could be established (not shown). At neither time point could GTP metabolites be detected in the mouse urine.



**Figure 5.4** Typical  $^1\text{H-NMR}$  urine spectrum of a 28 week old TRAMP mouse receiving 0.05% GTP in the drinking water in the (A) aromatic and (B) aliphatic regions.



**Figure 5.5** PCA scores plot of all urine NMR spectra showing the first and second principal component (PC). The data are scaled to unit variance.

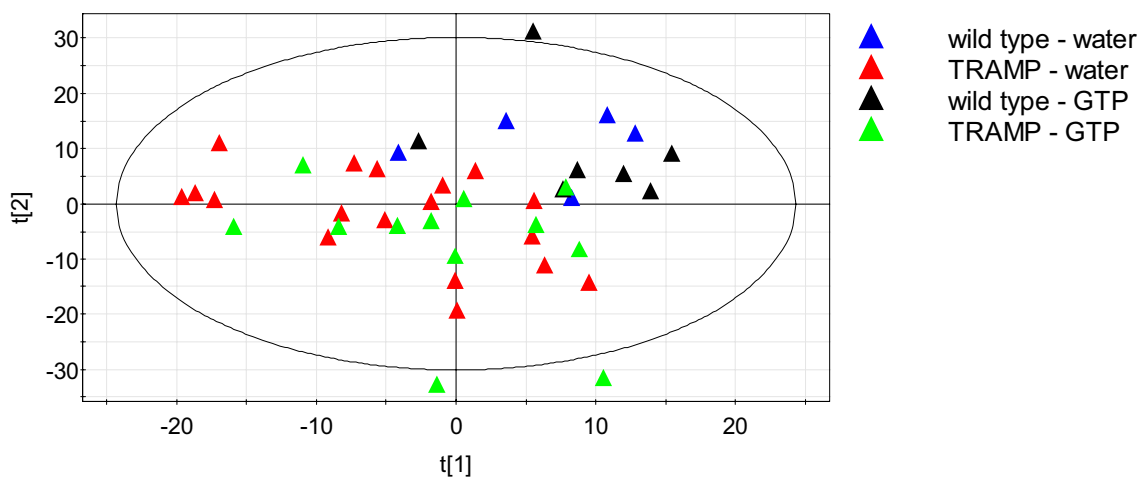


**Figure 5.6** Scores plot of a PLS-DA model generated to maximise the separation between 29 week old TRAMP (T; red & green) and wild type mice (WT; blue & black). The data are scaled to unit variance.

In order to mine the data set for differences in single metabolites, which might have been overlooked by the PLS-DA models described above, the following approaches were taken for each age group: 1. visual inspection of the NMR spectra, 2. calculation

of difference/correlation spectra from tea and water TRAMP samples at each age and 3. examination of loadings plots from PLS-DA models calculated to maximise the separation between GTP- and water-fed TRAMP mice at each time point.

In the urine of the young animals no metabolite changes indicating a TRAMP specific GTP effect could be found using any of the data mining techniques. However, in the urine of old mice signals for TRAMP specific GTP effects were identified. In all cases the difference between the water-fed TRAMP mice and those receiving GTP was statistically significant according to the Mann-Whitney U-test with  $p < 0.01$  (table 5.2), while no significant differences were observed for the wild type counter parts (U test with  $p < 0.05$ ). None of these signals was significantly changed in young TRAMP mice receiving GTP compared to the water group. Figure 5.7 shows the median spectra of each group. The effect of GTP on TRAMP mice seems such that it moves the metabolite levels closer to levels seen in the healthy wild type mice and reverses the effect of the TRAMP genotype.

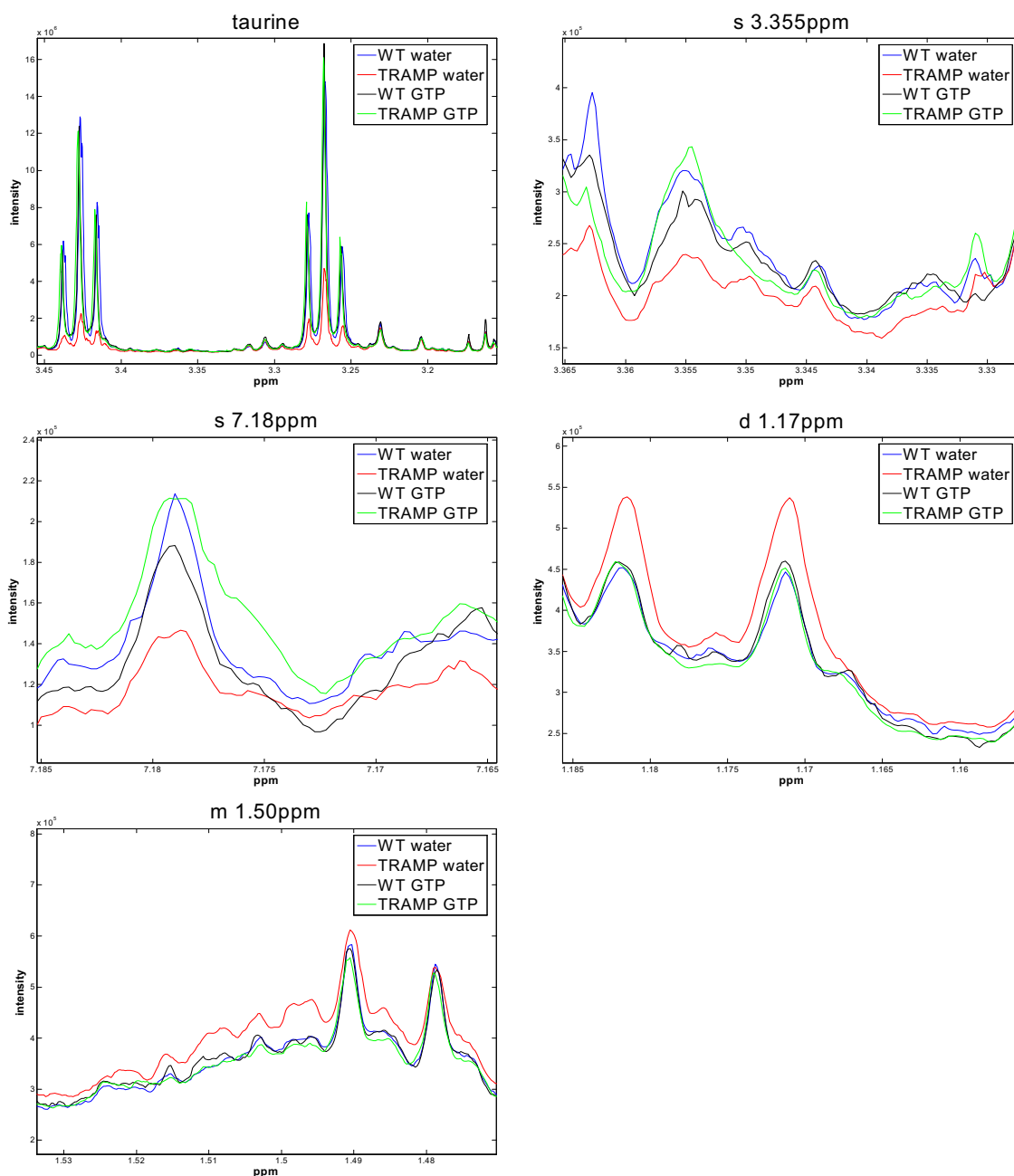


**Figure 5.7** Median spectra of urine from 29 week old mice (WT water, n=5; TRAMP water, n=18; WT GTP, n=7; TRAMP GTP, n=12) zoomed in on regions that were TRAMP specifically affected by GTP; WT = wild type

**Table 5.2** TRAMP specific effects of GTP on urinary metabolite levels in 29 week old TRAMP mice

<i>metabolite or spectral region</i>	<i>change in GTP-fed compared to water-fed</i>	<i>p-value</i>
taurine (t 3.43ppm)	+166%	0.0012
s 3.355ppm	+30%	0.0030
s 7.18ppm	+32%	0.0013
d 1.17ppm	-13%	0.0098
m 1.50ppm	-15%	0.0023

ppm value in brackets indicate the signal that was used for integration; s = singlet, d = doublet, t = triplet, m = multiplet. Changes were calculated from the group median values. Significance was established using the Mann-Whitney U-test.

Regions that were similarly changed in TRAMP and wild type mice were tryptophan and phenylalanine (figure 5.8). These changes were only observed in old animals and statistical significance was only reached when TRAMP and wild type mice were evaluated together. The excretion of tryptophan (d 7.71ppm) and phenylalanine (m 7.42ppm) increased by 59% and 26%, respectively. These changes have to my knowledge not previously been associated with GTP consumption.

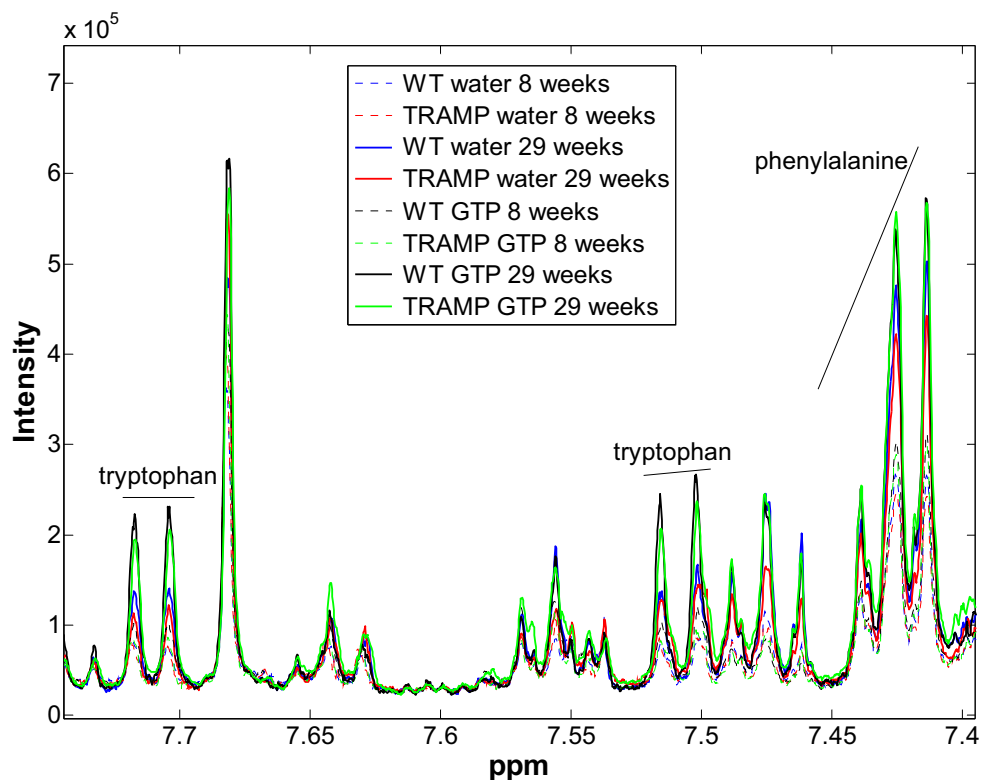


**Figure 5.8** Median urine NMR spectra of all groups (WT water 8 weeks, n=7; TRAMP water 8 weeks, n=9; WT water 29 weeks, n=5; TRAMP water 29 weeks, n=18; WT GTP 8 weeks, n=10; TRAMP GTP 8 weeks, n=9; WT GTP 29 weeks, n=7; TRAMP GTP 29 weeks, n=12); WT = wild type

### 5.2.1.2 Effect of TRAMP genotype on urinary metabolite profile

In order to establish whether metabolites, which were discriminating between TRAMP and wild type mice in the study described in Chapter 4, were also discriminatory in this study, a difference/correlation plot, which focused on spectral differences correlating to the TRAMP genotype, was calculated for each age group. The observed changes are listed in table 5.3. None of these differences between TRAMP and wild type mice were observed in the TRAMP study described in Chapter 4. NMR analysis did not show any evidence for differences in the gut microflora of 8 week old TRAMP and wild type

mice, as seen in the previous TRAMP study, thus ruling out this phenomenon as being generally linked to the TRAMP genotype.

**Table 5.3** Effects of TRAMP genotype on urinary metabolite levels

<i>metabolite or spectral region</i>	<i>change in TRAMP vs. wild type mice</i>	<i>p-value</i>
effect of TRAMP genotype in 8 week old mice receiving water		
s 2.93ppm	+5%	0.0172
s 4.72ppm	+58%	0.0129
effect of TRAMP genotype in 29 week old mice receiving water		
s 3.355ppm	-23%	0.0014
taurine (t 3.43ppm)	-52%	0.0091
m 1.50ppm	+15%	0.0369
d 1.17ppm	+14%	0.0442

ppm values in brackets indicate the signal that was used for integration; s = singlet, d = doublet, t = triplet, m = multiplet. Changes were calculated from the group median values. The p-value was determined using the Mann-Whitney U-test.

### 5.2.1.3 Age related changes of the urinary metabolic profile

Changes related to aging have been determined using a difference/correlation spectrum from all young versus all old animals (figure 5.9). Consistent with the study described in Chapter 4, differences between old and young animals were more pronounced than changes relating to GTP intake or TRAMP genotype. Table 5.4 summarises the effect of age on urinary metabolite levels. Creatinine, carnitine, isoleucine, phenylalanine and taurine have also been found to be elevated in older mice of the study described in Chapter 4.

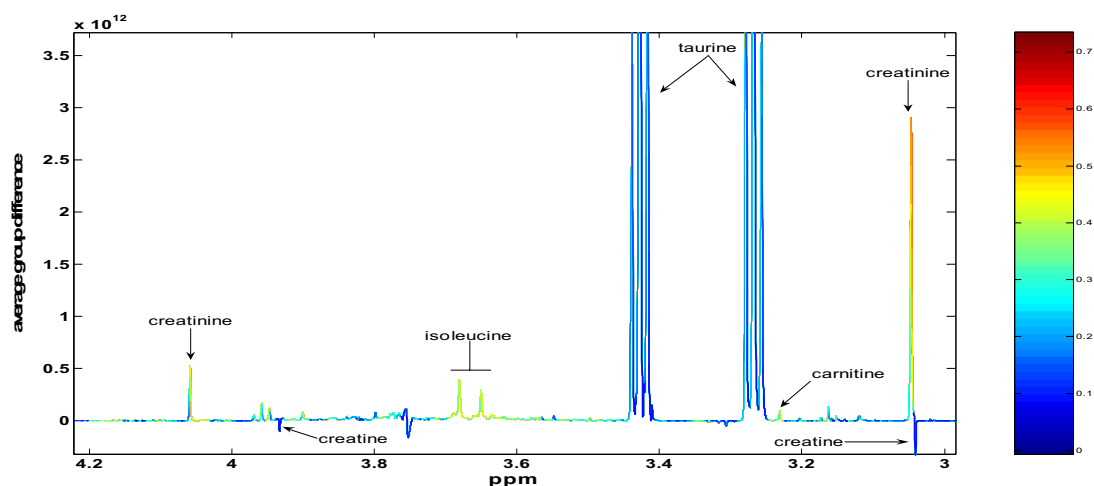


**Figure 5.9** Difference/correlation spectrum of urine spectra from 8 week and 28 week old TRAMP and wild type mice. Differences related to age were established regardless of genotype or treatment.

**Table 5.4** Effect of aging on urinary metabolite levels

<i>metabolite or spectral region</i>	<i>change</i>	<i>p-value</i>
creatinine (s 3.05ppm)	+58%	<0.0001
carnitine (s 3.23ppm)	+36%	<0.0001
isoleucine (d 3.66ppm)	+51%	<0.0001
phenylalanine (m 7.42ppm)	+52%	<0.0001
taurine (t 3.43ppm)	+51%	0.0102
creatine (s 3.04ppm)	-33%	0.0054
d 6.86ppm	-29%	<0.0001

ppm values in brackets indicate the signal that was used for integration; s = singlet, d = doublet, t = triplet, m = multiplet. Changes were calculated from the group median values of all young and old animals, regardless of genotype or treatment. Significance was established using the Mann Whitney U-Test

### **5.2.2 LC-MS metabolic profiling of urine**

Urine samples were prepared and analysed as described in sections 2.2.9.1, 2.2.9.3 and 2.2.9.5. Sample analysis was conducted in both negative and positive ionisation mode. The PCA scores plots of all urine samples from analysis in negative and positive ionisation mode are shown in figures 5.10 and 5.11, respectively. In both cases the QC samples were widely spread over the data space indicating that the analytical variation was very high. Even though in higher principal components the QC samples cluster closer together along an axis that roughly divides young and old animals, the analytical variation was still too great to distinguish TRAMP and wild type mice or treatment groups (figures 5.10 B and 5.11 B). The analytical instability had occurred after the LC-MS system had been relocated to another building. Repeated analysis after intensive cleaning of the mass spectrometer and the injection system as well as change of the HPLC column did not lead to improved analytical stability. Due to the unacceptably high variation the data set had to be discarded and further mining for biomarkers was not performed.

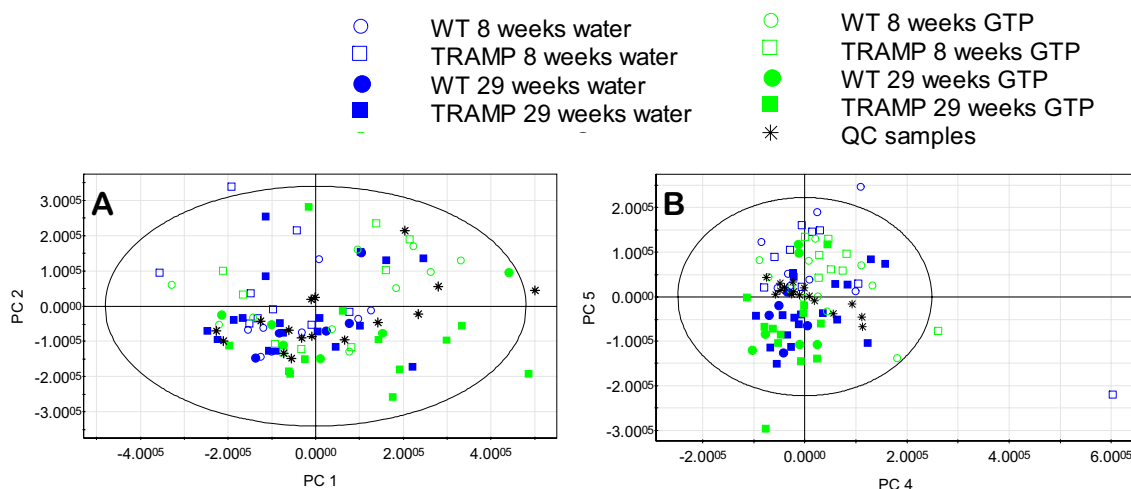


**Figure 5.10** PCA scores plots of all urine samples analysed in negative ionisation mode showing (A) the first and second and (B) the fourth and fifth principal component (PC).

The data are Pareto scaled.

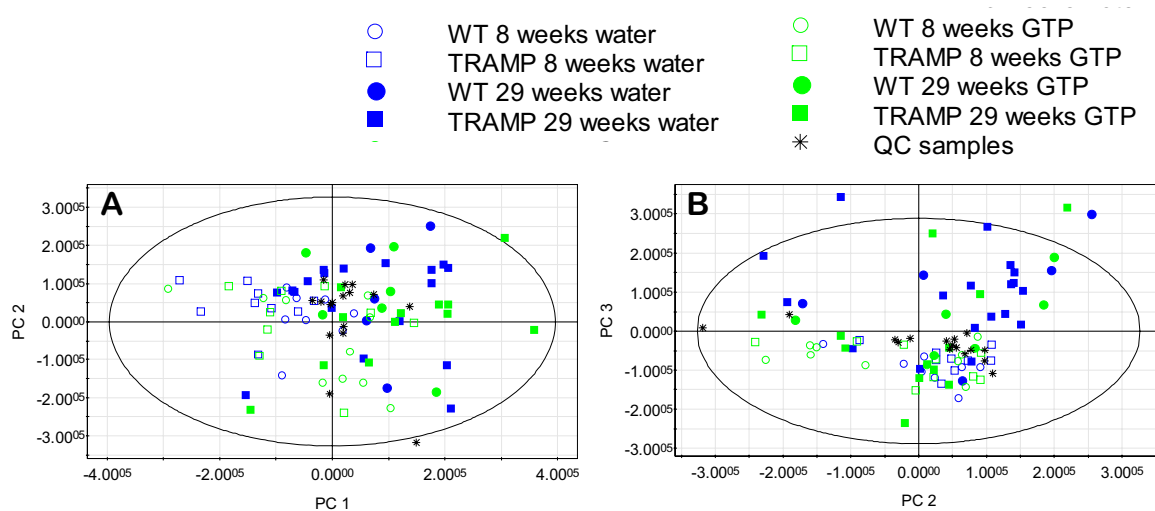


**Figure 5.11** PCA scores plots of all urine samples analysed in positive ionisation mode showing (A) the first and second and (B) the second and third Principal Component (PC).

The data are Pareto scaled.

### 5.2.3 Discussion

NMR analysis did not detect strong general effects of GTP consumption on the urinary metabolite profile, probably due to the low dose on the one hand and large physiological variation on the other. Multivariate data analysis showed that GTP-fed TRAMP mice were equally distant to the wild type phenotype as the water-fed counterparts. Only detailed inspection of the spectra of 29 week old animals revealed some signals, which were shifted in GTP-fed TRAMP mice towards the wild type level. However, these results have to be interpreted with caution, firstly because there is no other evidence of chemopreventive efficacy of GTP in the old TRAMP mice and secondly because none of the signals discriminating old TRAMP and wild type mice in this study were markers of the TRAMP phenotype in the study described in Chapter 4. The latter argument may be questionable, since urine collection conditions were different in the two studies (see section 2.2.1.4, 2.2.1.5 and 3.1).

Overall, urinary metabolic profiling did not provide convincing evidence for a general GTP effect and/or chemopreventive activity of GTP in TRAMP mice in this study.

### 5.3 GTP effects on the plasma metabolic profile of TRAMP mice

#### 5.3.1 $^1\text{H}$ -NMR metabolic profiling of plasma

Plasma samples were prepared and analysed as described in sections 2.2.4.2, 2.2.4.5 and 2.2.4.6. Spectral assignments were made based on the literature (Nicholson *et al.*, 1995; Teahan *et al.*, 2006), the BMRB database (<http://www.bmrbl.wisc.edu/>), (Seavey *et al.*, 1991) and communication with Dr Hector Keun. Figure 5.12 shows a typical  $^1\text{H}$ -NMR spectrum of plasma from an old wild type mouse receiving GTP.

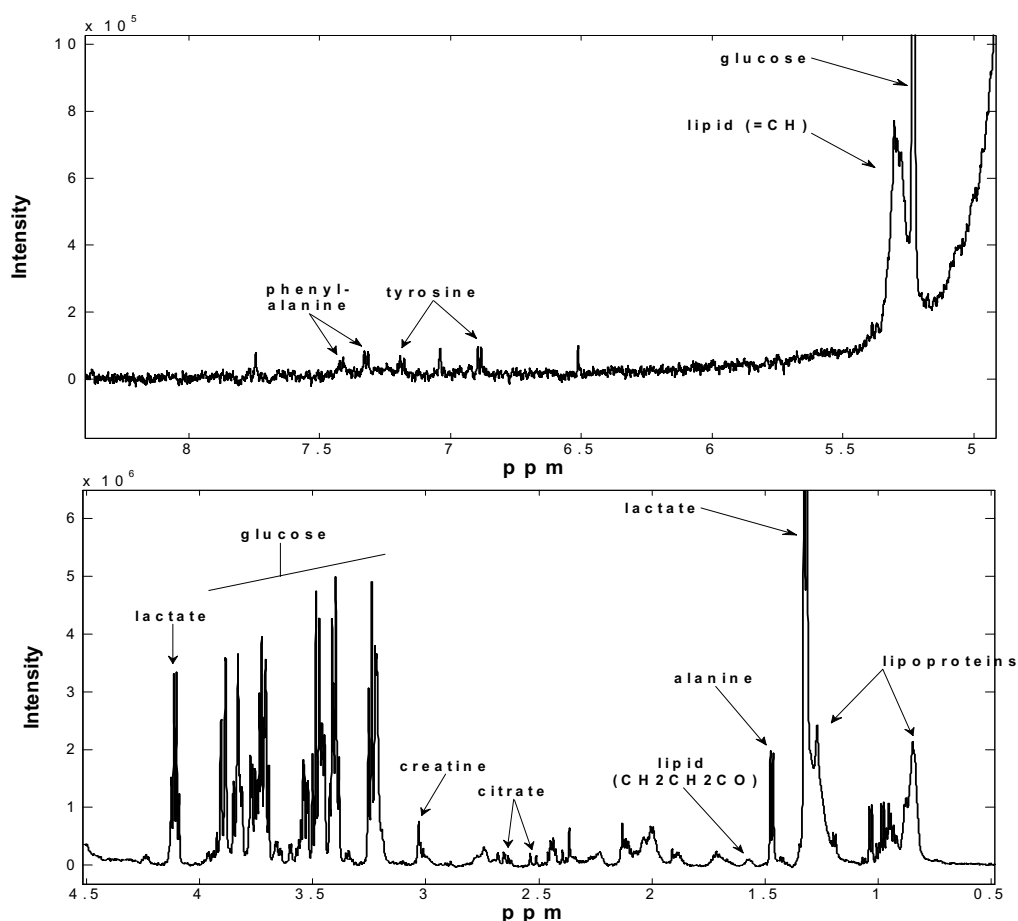


**Figure 5.12** Typical  $^1\text{H}$ -NMR plasma spectrum of a 28 week old TRAMP mouse receiving 0.05% GTP in the drinking water in the (A) aromatic and (B) aliphatic regions acquired using a Carr-Purcell-Maiboom-Gill (CPMG) pulse frequency.

The PCA scores plots of all samples (figure 5.13) show that the main variation, as represented by the first principal component, is unrelated to age, genotype or treatment. A trend of age separation is visible in the second principal component.

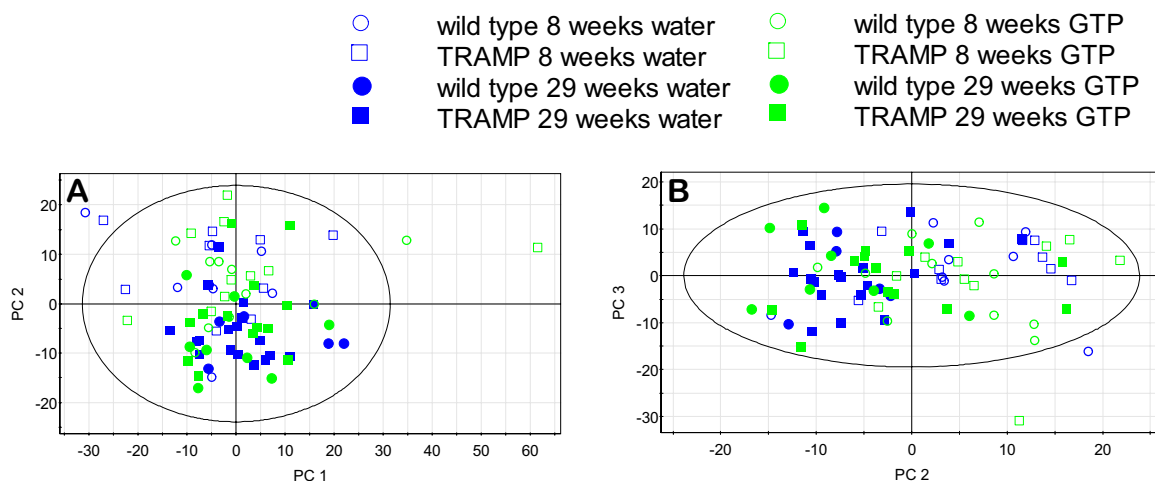


**Figure 5.13** PCA scores plots of all plasma samples analysed by  $^1\text{H-NMR}$  showing (A) the first and second and (B) the second and third principal component (PC). The data are scaled to unit variance.

To establish whether GTP had a global effect on the metabolic TRAMP phenotype in plasma, PLS-DA models maximising the separation between TRAMP and wild type mice, regardless of treatment, were generated for each time point. A valid PLS-DA model (as tested against permutation models, see above) could not be calculated for either the 8 or 29 week data. Further steps in the search for GTP effects on plasma metabolites included the examination of difference/correlation spectra and PLS-DA loadings plots of GTP- and water-fed TRAMP mice at either time point, as well as the examination of overlaid, group coloured, NMR spectra. Lower plasma lipid levels were observed in young animals receiving GTP-supplemented water compared to the control

groups (see figure 5.14). When TRAMP and wild type mice were evaluated together, significantly (Mann-Whitney U-test,  $p < 0.05$ ) lower intensities were observed for the signals from  $\text{CH}_2\text{CH}_2\text{C}=\text{C}$  (m 2.00ppm),  $\text{CH}_2\text{CH}_2\text{CO}$  (m 1.58ppm) and  $\text{CH}_2$  groups (m 1.26ppm) by 19, 61, and 27%, respectively.

Plasma metabolic profiling did not reveal any differences between TRAMP and wild type mice in the study described in Chapter 4. Here, difference/correlation spectra of TRAMP and wild type mice receiving water at either time were used to mine the data set for potential metabolic markers of the TRAMP genotype. The only significant difference observed was a 38% higher formate level (s 8.45ppm,  $p = 0.0307$ ) in old TRAMP mice compared to old wild type mice. In general, no metabolic difference was present between transgenic and non-transgenic mice, which is in agreement with finding from the previous study (see Chapter 4).

Age related changes were established using a difference/correlation spectrum of all young versus all old animals regardless of genotype and treatment. Old mice showed decreased levels of lactate (d 1.32ppm), isoleucine (t 0.95ppm) and phenylalanine (m 7.42ppm) by 12, 23 and 10%, respectively. The multiplet at 1.72ppm was decreased by 89% in old compared to young animals. Glucose (d 5.23ppm) was 11% higher in the old group. Signals from fatty acids at 2.00ppm ( $\text{CH}_2\text{CH}_2\text{C}=\text{C}$ ), 1.58ppm ( $\text{CH}_2\text{CH}_2\text{CO}$ ), 1.26ppm ( $\text{CH}_2$  groups) and 0.88ppm ( $\text{CH}_3$  groups) were decreased by 17, 94, 15 and 33%, respectively. Lower levels of phenylalanine, isoleucine and the multiplet at 1.72ppm are consistent with the findings from the study described in Chapter 4, while increases in plasma lipids ( $=\text{CH}$  groups, m 5.29ppm and  $\text{CH}_3$  groups, m 0.85ppm) and decreases in creatine (s 3.02ppm) and creatinine (s 3.03ppm) previously detected, could not be confirmed.

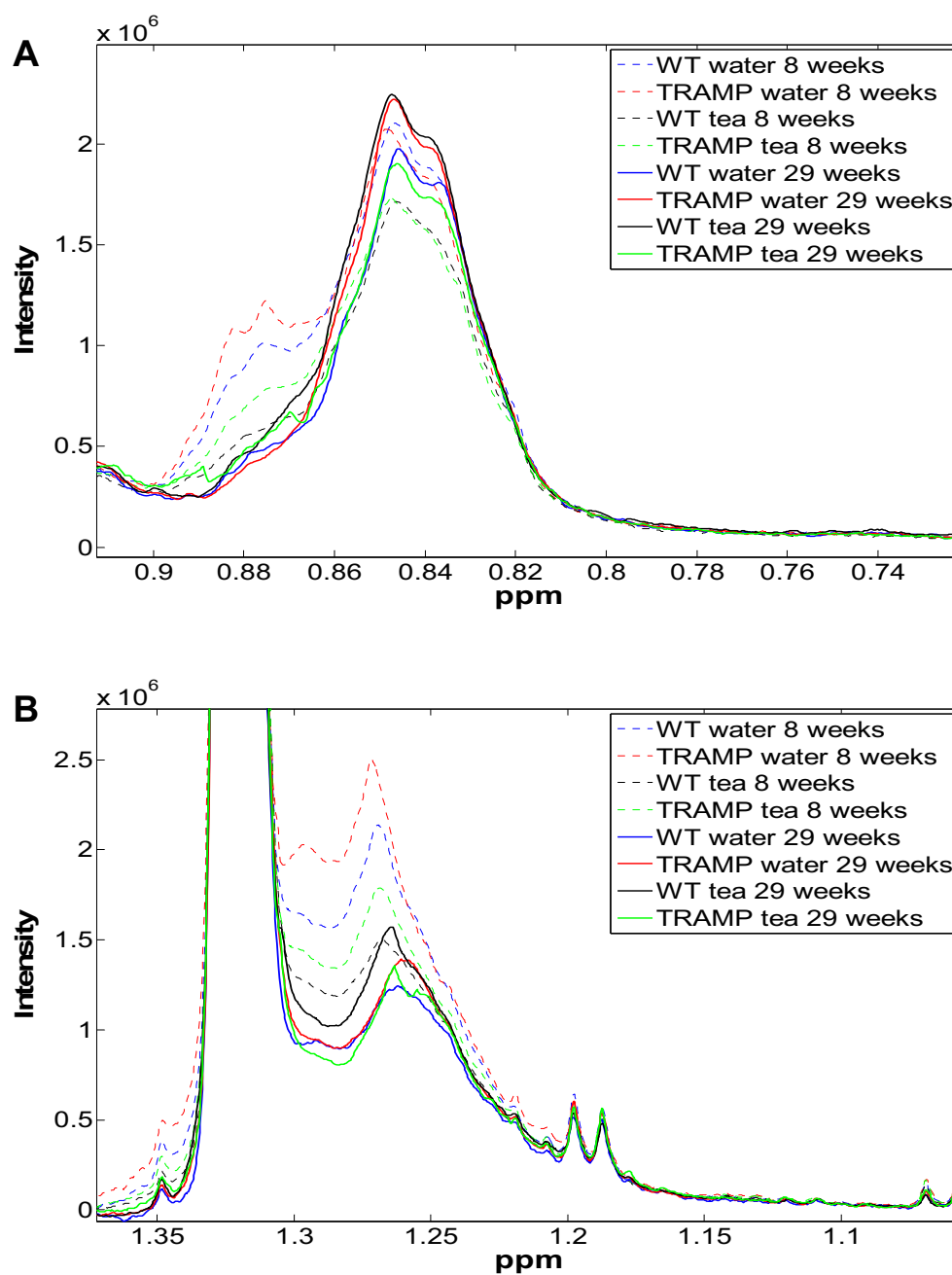


**Figure 5.14** Median  $^1\text{H-NMR}$  spectra zoomed in on regions of plasma lipid signals; (A)  $\text{CH}_3$  groups (mainly lipoproteins), (B)  $\text{CH}_2$  groups (mainly lipoproteins), (C) other  $\text{CH}_2$  groups of fatty acids

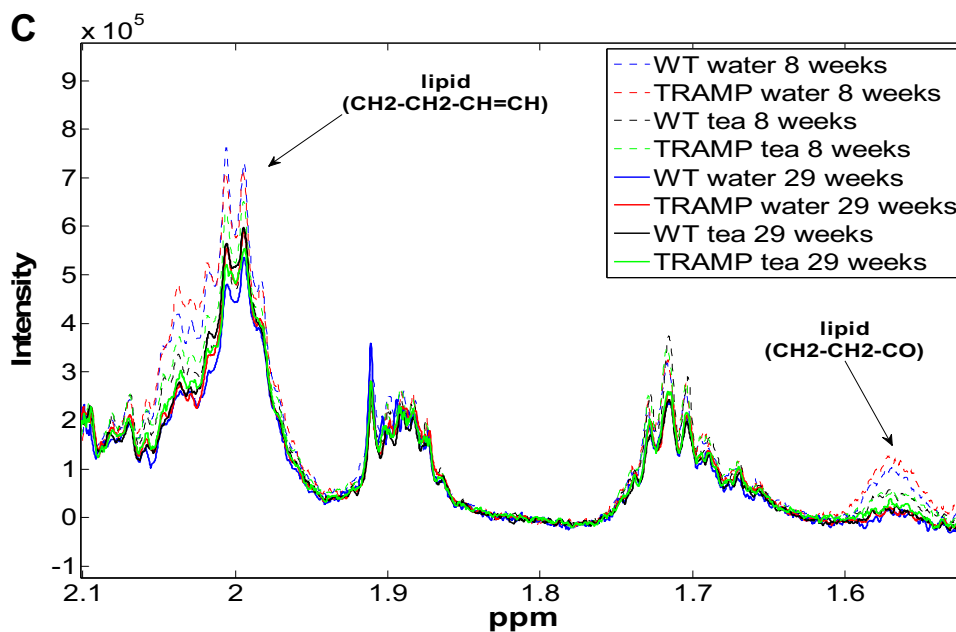


**Figure 5.14 continued** Median  $^1\text{H}$ -NMR spectra zoomed in on regions of plasma lipid signals; (A)  $\text{CH}_3$  groups (mainly lipoproteins), (B)  $\text{CH}_2$  groups (mainly lipoproteins), (C) other  $\text{CH}_2$  groups of fatty acids

### 5.3.2 Discussion

Plasma metabolic profiling did not reveal any TRAMP specific GTP effects or global shift of the TRAMP phenotype towards the wild type phenotype. However, in the young animals GTP-treated groups exhibited lower levels of some lipids compared to the water-fed groups. This effect was observed regardless of genotype. In the case of the young TRAMP mice this effect was accompanied by a significant lower body weight (-7%,  $p < 0.05$ ). But an unequivocal assignment of this weight difference to GTP is not possible, as the body weights were not different between young TRAMP and wild type mice on water or tea, respectively.

Recent studies have associated green tea consumption with increased fatty acid oxidation and energy expenditure in both humans and mice (Harada *et al.*, 2005; Murase *et al.*, 2005; Ota *et al.*, 2005; Shimotoyodome *et al.*, 2005). Decreases in plasma lipoproteins following green tea consumption have also been described and linked to an effect on energy metabolism (van Dorsten *et al.*, 2006). Increased energy expenditure has been shown to significantly lower the adenoma frequency in TRAMP mice (Huffman *et al.*, 2007). TRAMP mice housed at 22°C were shown to be leaner and develop fewer tumours than controls housed at 27°C receiving the same amount of food. No difference in tumour development between the two temperature groups was observed when the animals were fed *ad libitum*, which resulted in a 30% higher calorie intake in the 22°C housed mice. In the present study lower levels of plasma lipids observed in GTP-fed young animals is concurrent with slightly less pronounced preneoplastic lesions (see section 5.1.1). Although the data obtained are not strong enough to formulate a conclusive assumption, it is conceivable that chemopreventive efficacy of GTP in young TRAMP mice is mediated through effects on energy metabolism. Further work using higher GTP doses is required to test this hypothesis.

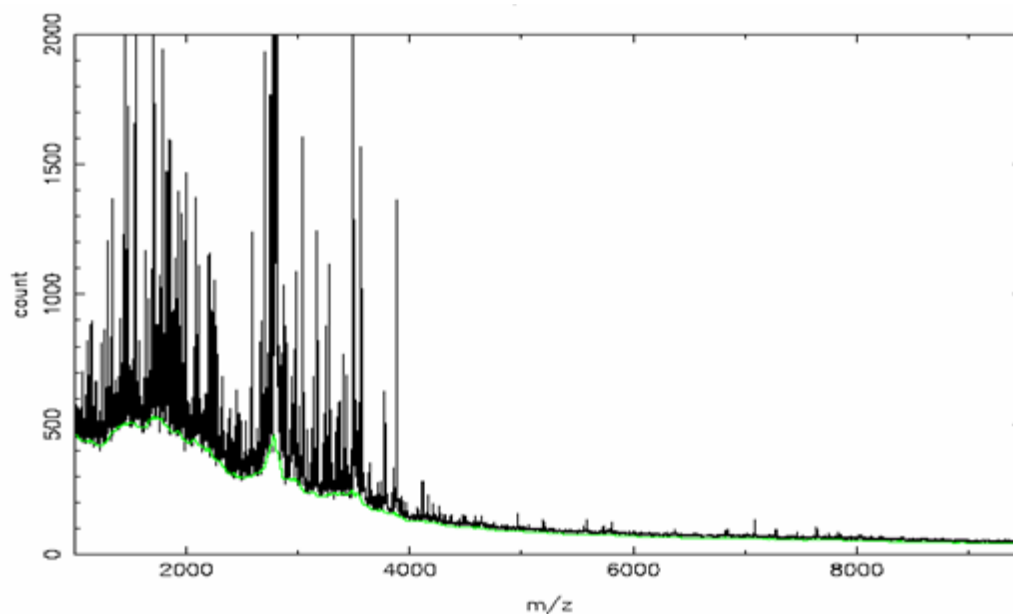
## 5.4 Effects of GTP on urine and plasma peptide profiles of TRAMP mice

Samples were prepared and analysed as described in section 2.2.2.4, 2.2.2.5 and 2.2.2.8. Data reduction and normalisation are described in section 2.2.2.9. The obtained peak lists were exported to SIMCA and MatLab software for detailed evaluation. Changes in  $m/z$  intensities were calculated from the group medians, and significance was established using the Mann-Whitney U-test with  $p < 0.05$ .

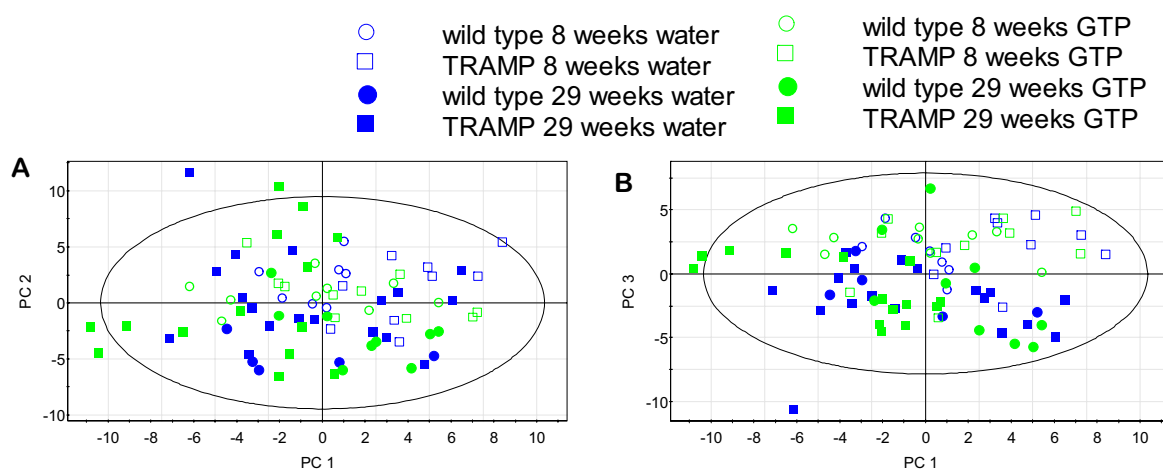
### 5.4.1 Peptidomic profiling of urine

Figure 5.15 shows the binned, combined mass spectra of all urine samples with the green line indicating the unresolved background continuum which was subtracted before data evaluation. From the background-subtracted spectrum 104 significant peaks were extracted for further analysis. The majority of the high intensity signals can be found in the lower molecular weight region up to 4000 $m/z$ .

PCA analysis indicated that the main variation in the data set was unrelated to age, genotype or treatment. In the second and third principal component trends of separation according to age, and in the young group, genotype, became apparent (figure 5.16). Further data analysis for the evaluation of GTP-feeding effects on the urinary peptide profile was carried out for each age group separately. As described in previous sections of this Chapter, an attempt was made to establish a global GTP effect on the TRAMP phenotype by generating PLS-DA models maximising the separation between TRAMP and wild type mice regardless of treatment, but colouring the scores plot by genotype and treatment. In the case of the 8 week old animals the PLS-DA model did not pass the validation test (see section 5.1.3) and was not used to test for a GTP effect.



**Figure 5.15** Combined and binned mass spectra of all mouse urine samples analysed by MALDI MS. The green line indicates the unresolved background continuum which is subtracted prior to data evaluation.



**Figure 5.16** PCA scores plots of all urine samples analysed by MALDI-MS showing (A) the first and second and (B) the first and third principal component (PC). The data are scaled to unit variance.

For the 29 week old animals the PLS-DA model was valid but GTP-treated mice did not cluster separately from water-fed TRAMP mice (figure 5.17). This observation was confirmed by comparison of the Y predictive values of GTP- and water-fed TRAMP mice. There was no difference between the two groups (t-test) indicating that both TRAMP groups were equally distant from the wild type phenotype.

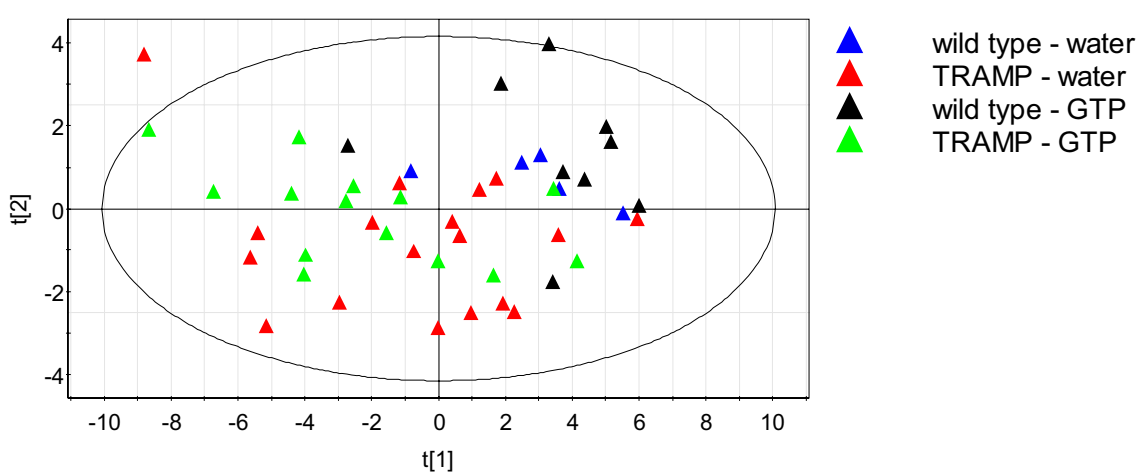


**Figure 5.17** Scores plot of a PLS-DA model generated to maximise separation between 29 week old TRAMP (T; red & green) and wild type mice (WT; blue & black). The data are scaled to unit variance.

In order to mine the data for more subtle TRAMP specific GTP effects, PLS-DA models and difference/correlation plots separating GTP-and water-fed TRAMP mice at both time points were generated. Figure 5.18 shows the scores and loadings plots for each age group. For the older TRAMP the PLS-DA model passed the validation test. Significant changes are marked red in the loadings plot and are summarised in table 5.5. The only commonly affected ion in 8 and 29 week old animals was at  $m/z$  1977.1. None

of the observed changes were found to be different in the wild type counter parts, indicating that they are not due to an overall GTP effect.

It was not possible to generate valid PLS-DA models for the separation of tea- and water-fed animals regardless of genotype at either time point. This finding suggests that GTP consumption did not exert a general effect on the urinary peptidome.

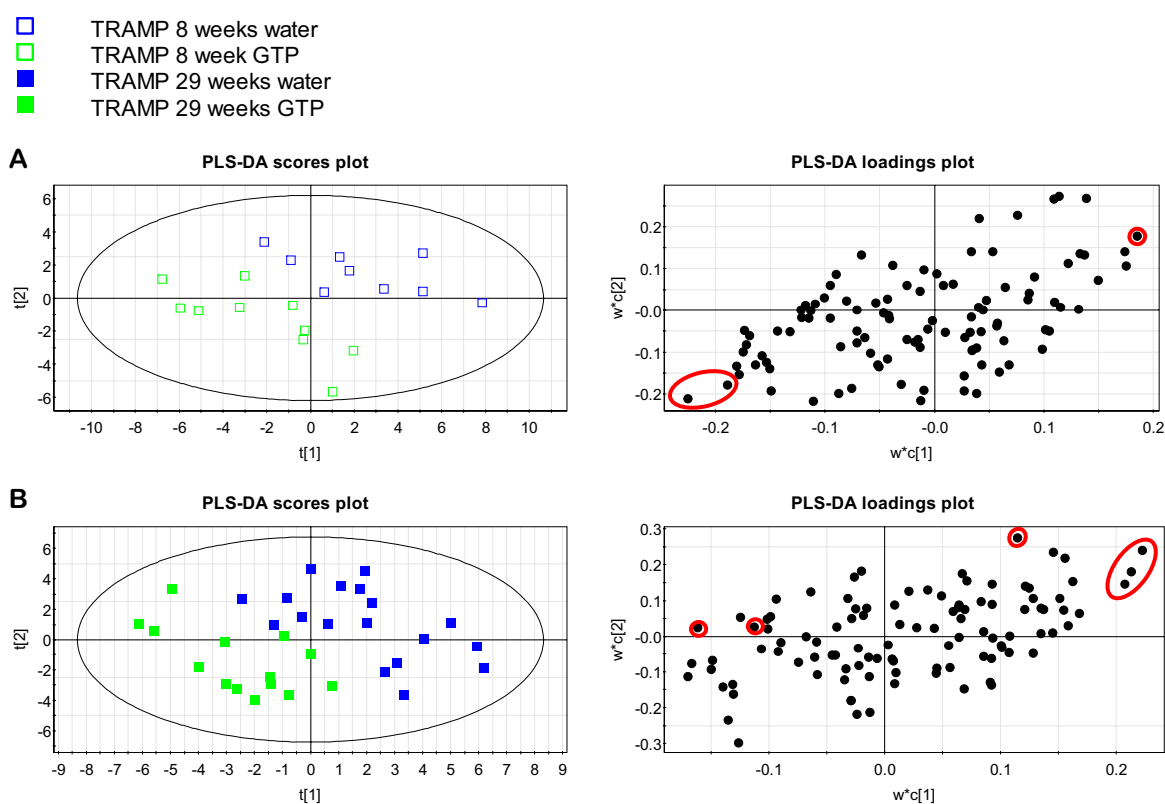


**Figure 5.18** Scores and loadings plots of PLS-DA models for maximal separation between GTP- and water-fed TRAMP mice at (A) 8 and (B) 29 weeks of age. The dots in red marked areas of the loadings plots are m/z ratios which were significantly different between the groups. The data are scaled to unit variance.

**Table 5.5** Significant changes in urinary peptide profile of GTP-fed TRAMP mice compared to age matched water-fed TRAMP mice

<b>Change in GTP-fed vs. water-fed TRAMP mice</b>		<b>Change in GTP-fed vs. water-fed TRAMP mice</b>	
<i>8 weeks</i>		<i>29 weeks</i>	
m/z		m/z	
1455.3	-15%	1132.0	-36%
1927.9	+22%	1618.9	-16%
1977.1	+143%	1733.1	-31%
		2506.0	-39%
		1977.1	+62%
		2159.0	+47%

The urinary peptide profiles of water-fed TRAMP and wild mice were evaluated using PLS-DA models in order to compare results with those reported in Chapter 4. For both time points a valid model could be generated. The significant changes are summarised in table 5.6. In the present study m/z 1743.9 was decreased in old TRAMP compared to age-matched wild type mice. In the TRAMP study described in Chapter 4 an ion at m/z 1744.0 was found to be decreased in young TRAMP mice compared to young wild type mice.

As in the preceding TRAMP study (Chapter 4), no differentiating ion was common to both age groups. The observed differences in the urinary peptide profile can therefore not be unequivocally assigned as markers of early malignancy or TRAMP carcinogenesis.

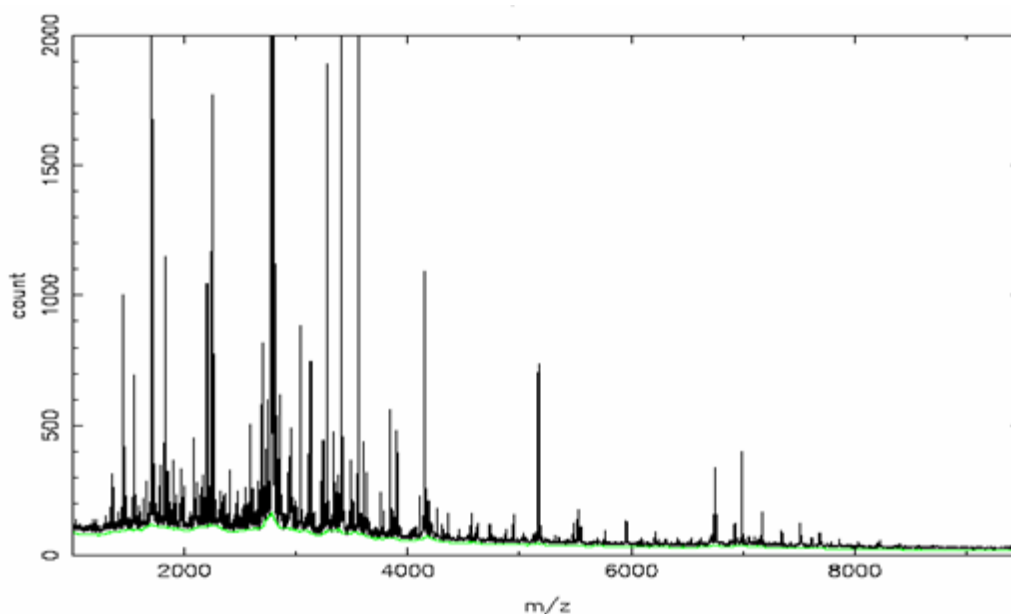
**Table 5.6** Significant changes in urinary peptide profile of TRAMP mice compared to age matched wild type mice

<b>Change in TRAMP vs. wild type</b>		<b>Change in TRAMP vs. wild type</b>	
<i>8 weeks</i>		<i>29 weeks</i>	
m/z		m/z	
1026.9	+80%	1335.0	+30%
1138.0	+39%	1601.9	+48%
1262.9	+63%	1686.4	-40%
1373.2	+86%	1695.3	-42%
1390.4	+80%	1743.9	-48%
1455.3	+57%	1751.3	-25%
1586.4	+64%	1759.9	-47%
1699.3	+108%	1942.0	-30%
1703.9	+34%	2035.9	-49%
1733.1	+42%		
1819.0	+69%		

In summary, GTP consumption had no overall effect on the urinary peptide profile of TRAMP and wild type mice at either age. Some TRAMP specific changes seemingly related to GTP feeding were detected using PLS-DA (table 5.5). However, only one ion (m/z 1455.3) was also found to be differentiating between TRAMP and wild type mice in the water-fed groups (table 5.6).

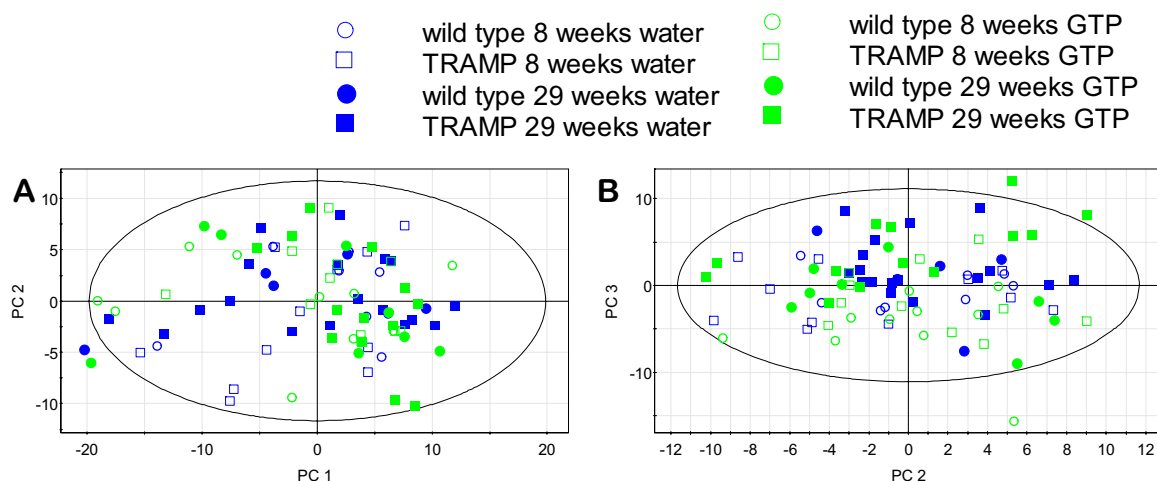
### 5.4.2 Peptidomic profiling of plasma

Figure 5.19 shows the binned, combined mass spectra of all plasma samples with the green line indicating the unresolved background continuum which was subtracted before data evaluation. From the background-subtracted spectrum 192 significant peaks were extracted for further analysis.



**Figure 5.19** Combined and binned mass spectra of all mouse plasma samples analysed by MALDI-MS. The green line indicates the unresolved background continuum which is subtracted prior to data evaluation.

Figure 5.20 shows the PCA scores plot of all analysed plasma samples. The major source of variation (first principal component) is unrelated to age, genotype or treatment. In the third principal component a trend of age separation is visible. Further data evaluation was carried out for each age group separately.



**Figure 5.20** PCA scores plots of all plasma samples analysed by MALDI-MS showing (A) the first and second and (B) the second and third principal component (PC). The data are scaled to unit variance.

As described in the preceding sections, an attempt was made to establish the overall effect of GTP on the TRAMP phenotype using PLS-DA models for the separation of TRAMP and wild type mice regardless of treatment. At neither time point did the generated models pass the validation test (see section 5.1.3) and they were therefore not used. Instead, loadings plots of PLS-DA and difference/correlation plots maximising the separation between GTP- and water-fed TRAMP mice were examined. Figure 5.21 shows the PLS-DA scores and loadings plots for each age group. At neither time point were the group differences great enough to produce a valid PLS-DA model. Significant differences are marked red in the loadings plots and summarised in table 5.7. There were no overlaps of differentiating ions between the TRAMP mice at 8 and 29 weeks of age. The ion at  $m/z$  3421.0 was also found to be decreased in young and old wild type mice receiving GTP compared to water fed controls, indicating that this might be a general GTP effect. However, no valid PLS-DA model for the separation of tea- and

water-fed mice could be generated at either time point, indicating that GTP consumption did not exert a global effect on the plasma peptide profile.

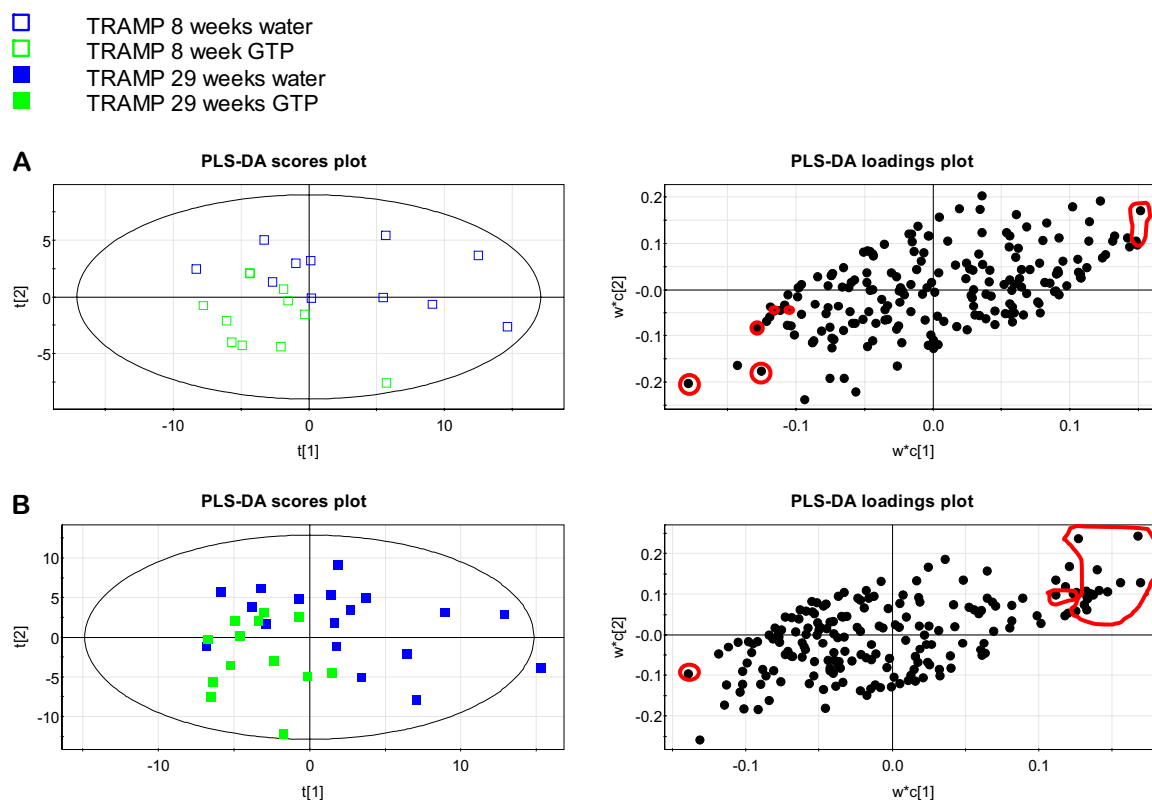


**Figure 5.21** Scores and loadings plots of PLS-DA models for maximal separation between GTP- and water-fed TRAMP mice at (A) 8 and (B) 29 weeks of age. The dots in red marked areas of the loadings plots are  $m/z$  ratios which were significantly different between the groups. The data are scaled to unit variance.

**Table 5.7** Significant changes in plasma peptide profile of GTP-fed TRAMP mice compared to age matched water-fed TRAMP mice

<b>Change in GTP-fed vs. water-fed TRAMP mice</b>		<b>Change in GTP-fed vs. water-fed TRAMP mice</b>	
<b>m/z</b>		<b>m/z</b>	
<i>8 weeks</i>		1919.9	-19%
1420.2	+14%	2031.9	-38%
2236.1	+15%	2181.1	-38%
2535.0	+19%	2450.0	-8%
2581.0	+40%	2977.1	-33%
2592.9	+18%	3133.1	-46%
1468.1	-34%	3339.9	-41%
3421.0	-20%	3437.1	-31%
<i>29 weeks</i>		3493.9	-46%
1895.0	+14%	3509.0	-31%
1169.1	-26%	3769.0	-48%
1444.4	-43%	3782.9	-56%
1700.2	-40%	3882.0	-58%

PLS-DA analysis could not generate a valid model for the separation of water-fed TRAMP and wild type mice at either time point. The number of discriminating ions was minimal (table 5.8). The ion at m/z 2535.0 was also found to be significantly different between the GTP- and water-fed young TRAMP mice. No overlaps in differentiating ions were found between the two TRAMP studies.

**Table 5.8** Significant changes in plasma peptide profile of TRAMP mice compared to age matched wild type mice

Change in TRAMP vs. wild type		Change in TRAMP vs. wild type	
<i>8 weeks</i>		<i>29 weeks</i>	
m/z		m/z	
1241.3	+13%	2169.1	+152%
1312.3	+57%	2375.9	-10%
2535.0	-17%	2493.0	-22%

### 5.4.3 Discussion

Peptidomic profiling could not detect an overall effect of GTP consumption on the composition of the urine or plasma peptide profile of TRAMP and wild type mice. PLS-DA analysis revealed some ions which were significantly different between GTP- and water-fed TRAMP mice in urine and plasma at both time points. However, with regard to the fact that most of these ions did not discriminate between TRAMP and wild type mice and that no overall GTP effect was observed, the differences between GTP- and water-fed TRAMP mice cannot be regarded as markers of chemopreventive activity of GTP. This conclusion is in agreement with the fact that no conclusive evidence for chemopreventive efficacy of GTP in TRAMP mice was found in this study (see section 5.1). As discussed earlier this may be due to the relatively low dose of GTP used.

Comparison of ions discriminating between TRAMP and wild type mice in the previous study (Chapter 4) with those found in this study showed no overlap. The reason for this observation may be due to the fact that sample collection was different for both studies (see sections 2.2.1.4, 2.2.1.5 and 3.1). The lack of common discriminatory ions between the studies again highlights the importance of pre-analytical sample handling discussed in sections 1.4.2, 3.1 and 4.4.3.

## **5.5 Effect of GTP on levels of urinary 8-oxodG**

Levels of 8-oxodG and creatinine were determined in urine of 8 and 29 week old TRAMP and wild type mice as described in sections 2.2.3.4, 2.2.3.5 and 2.2.3.7. The data are described using the median, and statistical significance was established using the Mann-Whitney U-test with  $p < 0.05$ .

### **5.5.1 Results**

As in the study described in Chapter 4, for evaluation of the results, creatinine-normalised data (marked yellow) were used. Tables 5.9 and 5.10 list the median values of urinary 8-oxodG levels and percent group differences, respectively. Treatment with GTP did not have a significant effect on the levels of renally excreted 8-oxodG. However, the findings from the study investigating carcinogenesis in TRAMP mice (see Chapter 4) were confirmed. The presence of the TRAMP genotype did not have any effect on urinary 8-oxodG levels at either time point, with or without GTP treatment. Older animals excreted higher levels of 8-oxodG, although the comparison between young and old wild type mice receiving water was not quite statistical significant (table 5.10). This lack of significance might be due to the fact that there are only four old wild type mice and there is one high outlier in the young wild type group (figure 5.22).

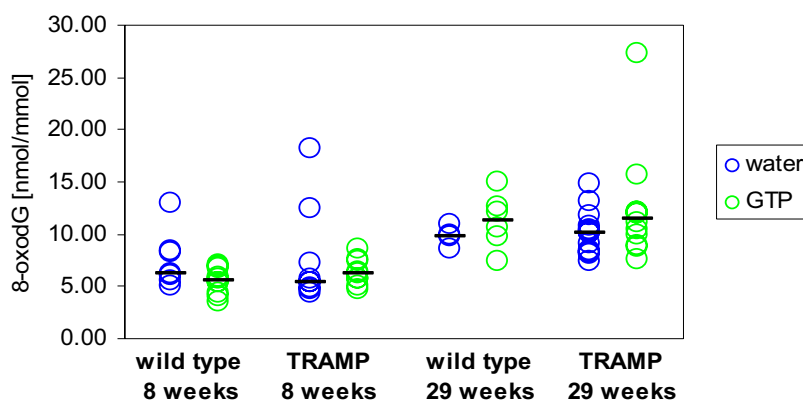


**Figure 5.22** Urinary 8-oxodG levels for individual animals normalised to creatinine. The black bars indicate the median value for each group.

**Table 5.9** Median values for urinary 8-oxodG using different data normalisation techniques.

	unnormalised [pmol/ml]	creatinine- normalised [nmol/mmol]	SG-normalised [pmol/ml]	SG- & weight- normalised [fmol/ml/g]
wild type 8 weeks water	10.83 (4.45/13.88) (n=7)	6.18 (5.03/12.90) (n=7)	9.02 (6.35/16.33) (n=7)	354 (254/763) (n=7)
wild type 8 weeks green tea	9.18 (2.14/17.23) (n=10)	5.55 (3.56/7.07) (n=10)	8.15 (5.39/11.13) (n=10)	365 (247/515) (n=9)
TRAMP 8 weeks water	6.56 (4.35/11.37) (n=10)	5.38 (4.38/18.15) (n=10)	7.61 (5.44/22.74) (n=10)	325 (218/947) (n=9)
TRAMP 8 weeks green tea	7.53 (5.57/12.32) (n=9)	6.17 (4.76/8.55) (n=9)	8.75 (5.87/11.58) (n=9)	381 (258/495) (n=9)
wild type 29 weeks water	20.73 (20.01/26.59) (n=4)	9.80 (8.64/10.99) (n=4)	20.49 (14.29/24.17) (n=4)	632 (371/739) (n=4)
wild type 29 weeks green tea	24.47 (9.38/37.34) (n=6)	11.35 (7.49/14.94) (n=6)	18.25 (11.03/27.66) (n=6)	542 (363/758) (n=6)
TRAMP 29 weeks water	18.79 (11.76/32.09) (n=17)	10.19 (7.34/15.80) (n=17)	21.52 (14.65/33.55) (n=17)	632 (401/948) (n=16)
TRAMP 29 weeks green tea	29.35 (19.69/47.12) (n=12)	11.47 (7.59/27.26) (n=12)	20.10 (14.58/33.70) (n=12)	580 (393/1087) (n=12)

The numbers in brackets are the minima and maxima; n is the number of animals per group.

**Table 5.10** Changes in 8-oxodG levels with respect to GTP treatment, transgenesis, and age

Effect of		unnormalised [pmol/ml]	creatinine- normalised [nmol/mmol]	SG- normalised [pmol/ml]	SG- & weight- normalised [fmol/ml/g]
GTP	WT 8 wks water vs. WT 8 wks GTP	-15% (p=0.558)	-10% (p=0.097)	-10% (p=0.380)	+3% (p=0.370)
	TRAMP 8 wks water vs. TRAMP 8 wks GTP	+14% (p=0.142)	+15% (p=0.348)	+15% (p=0.514)	+17% (p=0.200)
	WT 29 wks water vs. WT 29 wks GTP	+18% (p=1.000)	+16% (p=0.286)	-11% (p=0.831)	-14% (p=0.521)
	TRAMP 29 wks water vs. TRAMP 29 wks GTP	+56% (p=0.005)	+13% (p=0.309)	-7% (p=0.825)	-8% (p=0.710)
TRANSGENESIS	WT 8 wks water vs. TRAMP 8 wks water	-39% (p=0.051)	-13% (p=0.205)	-16% (p=0.495)	-8% (p=0.340)
	WT 8 wks GTP vs. TRAMP 8 wks GTP	-18% (p=0.568)	+11% (p=0.165)	+7% (p=0.414)	+4% (p=0.480)
	WT 29 wks water vs. TRAMP 29 wks water	-9% (p=0.591)	+4% (p=0.788)	+5% (p=0.720)	0% (p=0.850)
	WT 29 wks GTP vs. TRAMP 29 wks GTP	+20% (p=0.349)	+1% (p=0.925)	+10% (p=0.574)	+7% (0.454)
AGE	WT 8 wks water vs. WT 29 wks water	+91% (p=0.008)	+59% (p=0.059)	+127% (p=0.014)	+79% (p=0.131)
	TRAMP 8 wks water vs. TRAMP 29 wks water	+186% (p<0.0001)	+89% (p=0.006)	+183% (p=0.001)	+94% (p=0.002)
	WT 8 wks GTP vs. WT 29 wks GTP	+167% (p=0.007)	+105% (p=0.001)	+124% (p=0.002)	+48% (p=0.013)
	TRAMP 8 wks GTP vs. TRAMP 29 wks GTP	+290% (p<0.001)	+86% (p<0.001)	+130% (p<0.001)	+52% (p<0.001)

### 5.5.2 Discussion

The TRAMP mouse model has been widely employed in the field of preclinical chemoprevention research, including numerous studies investigating the effect of green tea or compounds therefrom (see Chapter 1, section 1.3.1). In human subjects green tea has been shown to reduce the excretion of urinary 8-oxodG (Hakim *et al.*, 2003; Luo *et al.*, 2006). Tam *et al.* have shown that a 13 week treatment of TRAMP mice with EGCG eliminated immunohistochemical staining for 8-oxodG from the ventral prostate and decreased it in the other prostate lobes (Tam *et al.*, 2006). A slight reduction of plasma peroxide levels in TRAMP mice after 13 weeks of EGCG treatment has also been observed (Nyska *et al.*, 2003). These studies provide evidence that green tea has antioxidant properties in TRAMP mice. However, these findings are not supported by decreased urinary levels of 8-oxodG in the study described here. GTP did not elicit an effect on 8-oxodG in TRAMP or in wild type mice after 4 or 24 weeks of treatment. This observation is consistent with findings described in the preceding sections of this Chapter. Again the low dose of GTP used is a possible explanation. The animals in the studies published by Tam *et al.* and Nyska *et al.* received 200mg EGCG/kg. That equals 5mg for a mouse weighing 25g. In order to consume the same amount of total polyphenols, a 25g mouse in the present study would need to drink 10ml per day. The estimated water intake, however, is only about 4ml (Wolfensohn and Lloyd, 1998). The intake of polyphenols in this study was therefore less than half compared to that for other studies. However, four cups of green tea, which is equivalent to approximately 850mg of polyphenols (Harbowy and Balentine, 1997), have been shown to decrease the urinary 8-oxodG levels in human smokers (Hakim *et al.*, 2003). Assuming that the average person weighs 70kg, this dose is equivalent to 12mg/kg. Luo *et al.* have tested doses of 29 and 58mg/kg (Luo *et al.*, 2006) in humans at high risk of developing liver

cancer and also observed reductions in levels of urinary 8-oxodG. The estimated dose for the animals in this study (80mg/kg) was higher than those in both human studies. It is conceivable that the dose response differs between the mice and humans. Also, as discussed in section 5.1.4, the possibility of lowered GTP concentration in the drinking bottles has to be considered.

### **5.6 Summary**

Overall, the study presented here did not provide sufficient evidence for chemopreventive activity of GTP in the TRAMP mouse model. Nevertheless, slightly less pronounced focal hyperplasia in young TRAMP mice and lower plasma lipid levels were observed in young GTP-fed mice compared to the water-fed controls. These observations might reflect trends of chemopreventive activity and effects on energy metabolism, both of which could potentially be linked. The reason for the poor chemopreventive activity observed in this study is likely to be due to the low dose of GTP given.

# Chapter 6

## 6. Effects of tea constituents on patients with benign prostatic hyperplasia

This experiment was carried out as part of the analysis of the clinical trial conducted by James Thorpe in our laboratory (see section 2.2.1.6). It was undertaken with the aim of investigating whether the main polyphenolic compounds derived from either green or black tea have an effect on urinary and plasma metabolic and peptide profiles and whether they could alter levels of 8-oxodG in urine of patients diagnosed with benign prostatic hyperplasia (BPH). It was also intended to compare possible effects of green tea polyphenols (GTP) on humans with their effect in TRAMP mice.

Urine and plasma samples from patients with BPH receiving either 1g of GTP per day, 1g of black tea theaflavins (BTT) per day or no treatment (control), were collected before and after the four week intervention period.

### 6.1 Effects of tea polyphenols on the urinary and plasma metabolome

#### 6.1.1 $^1\text{H}$ -NMR metabolic profiling of urine

Sample preparation and analysis are described in sections 2.2.4.1, 2.2.4.5 and 2.2.4.6. Spectral assignments were made by comparison with the literature (Bollard *et al.*, 2005; Nicholson *et al.*, 1989), the BMRB database (<http://www.bmrw.wisc.edu/>) (Seavey *et al.*, 1991) and personal communication with Dr Hector Keun (Imperial College, London). Due to insufficient suppression of the water signal one spectrum from the GTP pre-treatment group was excluded from the analysis. Figure 6.1 shows a typical  $^1\text{H}$ -NMR urine spectrum from a patient after four weeks of GTP intervention. PCA analysis showed that the variation in the data set is dominated by physiological variation rather than the consumption of GTP or BTT. Only in the fourth and fifth principal component does a separation of GTP and BTT samples occur; more pronounced for the GTP samples than the BTT samples (figure 6.2).

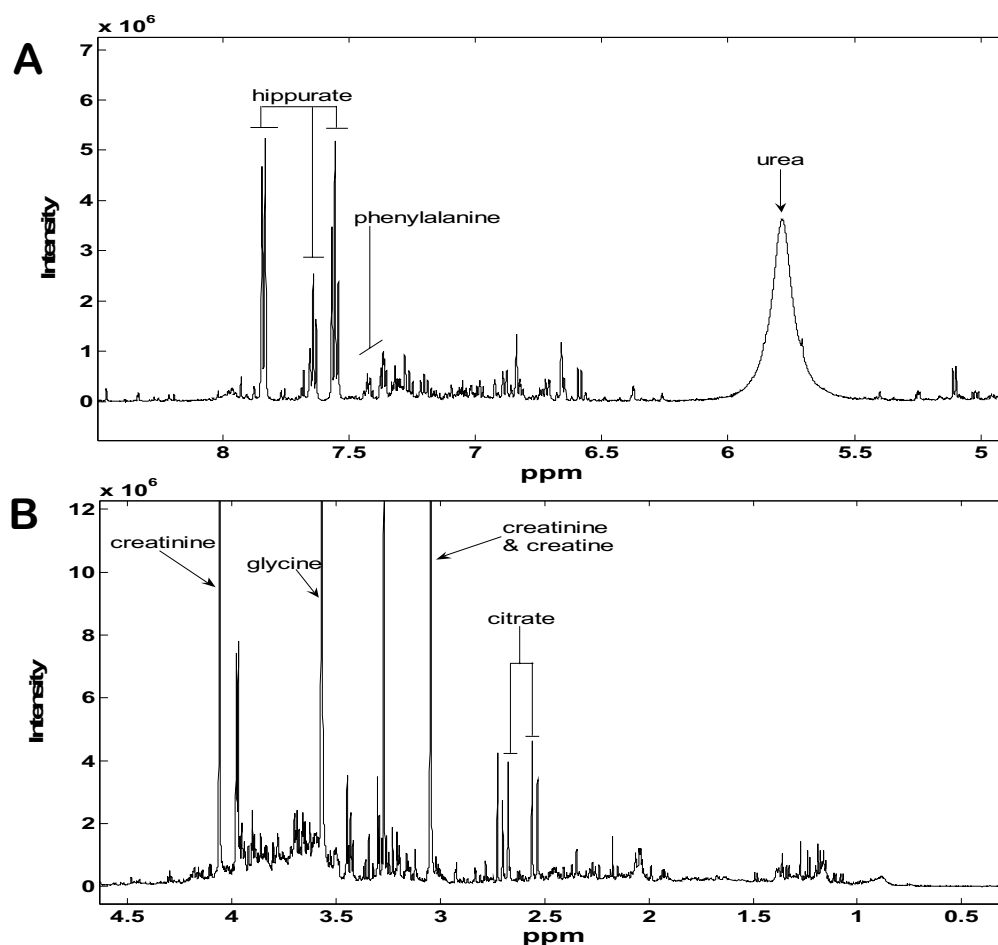


**Figure 6.1** Typical  $^1\text{H-NMR}$  urine spectrum from a patient with BPH after one four weeks intervention with GTP. **A:** aromatic region; **B:** aliphatic region

For the identification of metabolites altered by GTP or BTT consumption loadings plots of PLS-DA models generated to maximise the separation between GTP or BTT and controls (all untreated samples), respectively, were used. The model for the GTP and control samples, but not the BTT and control samples, passed the validation test. In addition overlaid spectra, coloured according to groups, were compared. Another data mining approach employed was the inspection of PLS-DA loadings and difference/correlation spectra comparing control with GTP or BTT samples following the subtraction of the pre-dose spectrum from the post-dose spectrum for each patient.

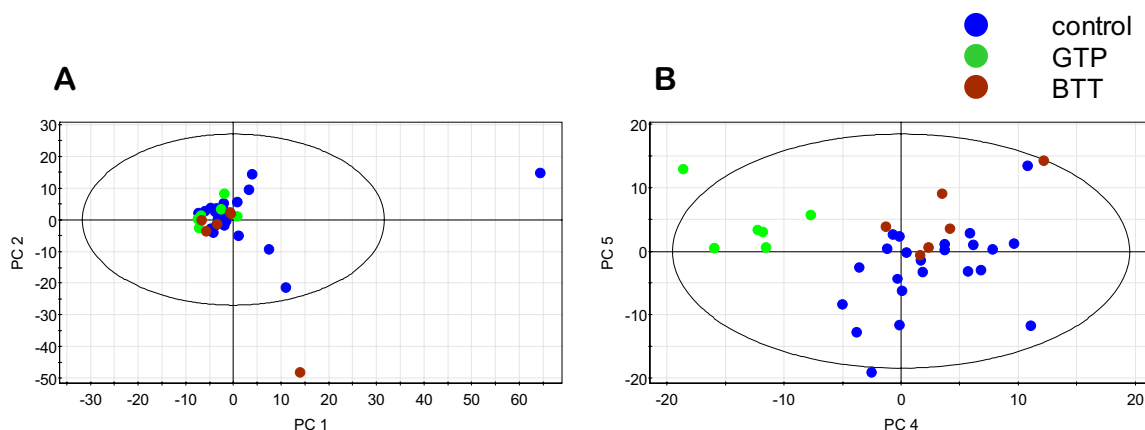


**Figure 6.2** PCA scores plots of all urine samples analysed by  $^1\text{H-NMR}$  showing (A) the first and second and (B) fourth and fifth Principal Component (PC). Samples labelled as control include all non-treatment samples. The data are scaled to unit variance.

For samples from patients on GTP but not for BTT samples, excretion of aromatic metabolites, probably GTP metabolites, were detected (figure 6.3). These metabolites were mainly responsible for the separation of the GTP samples. Van Dorsten *et al.* have also described aromatic metabolites in the same region after green tea but not black tea consumption (van Dorsten *et al.*, 2006).

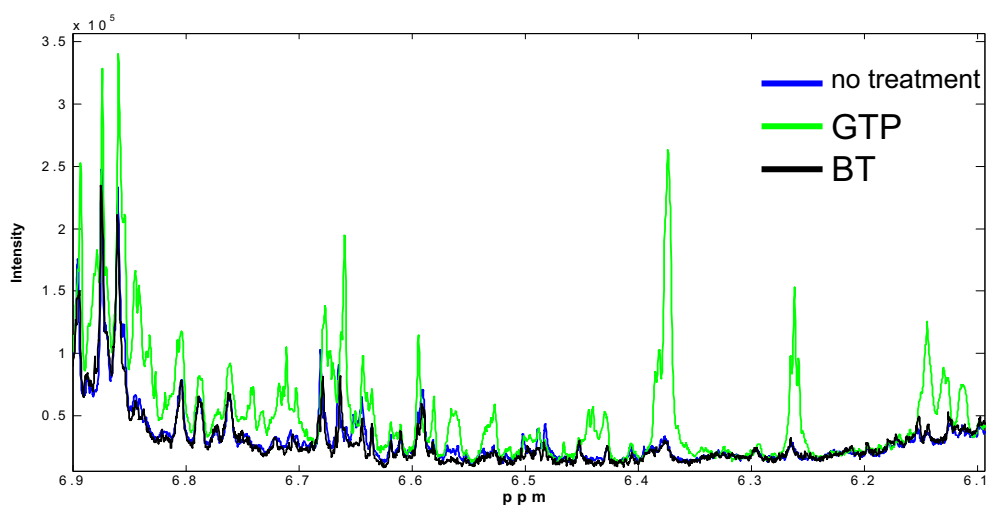


**Figure 6.3** Median urine spectra of control, GTP and BTT samples zoomed in on the region of suspected GTP metabolites.

The statistical significance of potential markers of intervention other than the suspected GTP metabolites was tested using the Wilcoxon-test for paired samples in each group. Table 6.1 lists metabolites or spectral regions that were characterised by a significance level of  $p < 0.05$  in the Wilcoxon test in any of the three groups. All the metabolites which showed a significant difference in the control group were not further considered as markers of GTP or BTT effect. In the case of acetyl-carnitine, however, it should be noted that the change observed in the GTP group was an increase by 31% while the second urine sample set in the control group exhibited a 27% lower level. The doublet at 5.41ppm was decreased in GTP and BTT post-dose samples by 34 and 35%, respectively, as compared to pre-dose samples. The singlet at 5.40ppm was 26% lower in the GTP samples. Although not significant, the BTT samples showed a similar trend (-28%). Phenylalanine levels were 77% higher in the GTP post-dose samples. Other metabolites which were changed in the GTP post-dose samples with a significance level of  $p < 0.1$  (Wilcoxon test) were alanine (-18%, d 1.47ppm), beta-hydroxybutyrate (+41%, d 1.20ppm) and trimethylamine-N-oxide (TMAO; +51%, s 3.27ppm). All differences were calculated with respect to the group medians. Figure 6.4 shows the levels of the above mentioned metabolites in individual samples. The trend of increased phenylalanine excretion was the only common alteration between the TRAMP (Chapter 5) and human GTP intervention study.

**Table 6.1** Levels of significance of urinary metabolite changes within one treatment group (Wilcoxon test)

<i>metabolite or spectral region</i>	<i>Wilcoxon test control group</i>	<i>Wilcoxon test GTP group</i>	<i>Wilcoxon test BTT group</i>
dimethylamine (s 2.73ppm)	p=0.0277* ↑	p=0.2249	p=0.0464* ↑
carnitine (s 3.23ppm)	p=0.0277* ↓	p=0.2249	p=0.7532
acetyl-carnitine (s 3.19ppm)	p=0.0277* ↓	p=0.0431* ↑	p=0.3454
d 5.41ppm	p=0.6002	p=0.0796	p=0.0277* ↓
s 5.40ppm	p=0.3454	p=0.0431* ↓	p=0.1159
creatinine (s 3.05ppm)	p=0.0277* ↑	p=0.2249	p=0.4631
phenylalanine (m 7.42ppm)	p=0.9165	p=0.0431* ↑	p=0.6002

ppm values in brackets denote spectral region used for integration. \* indicate statistical significance according to the Wilcoxon test with  $p < 0.05$ . Arrows indicate direction of change.

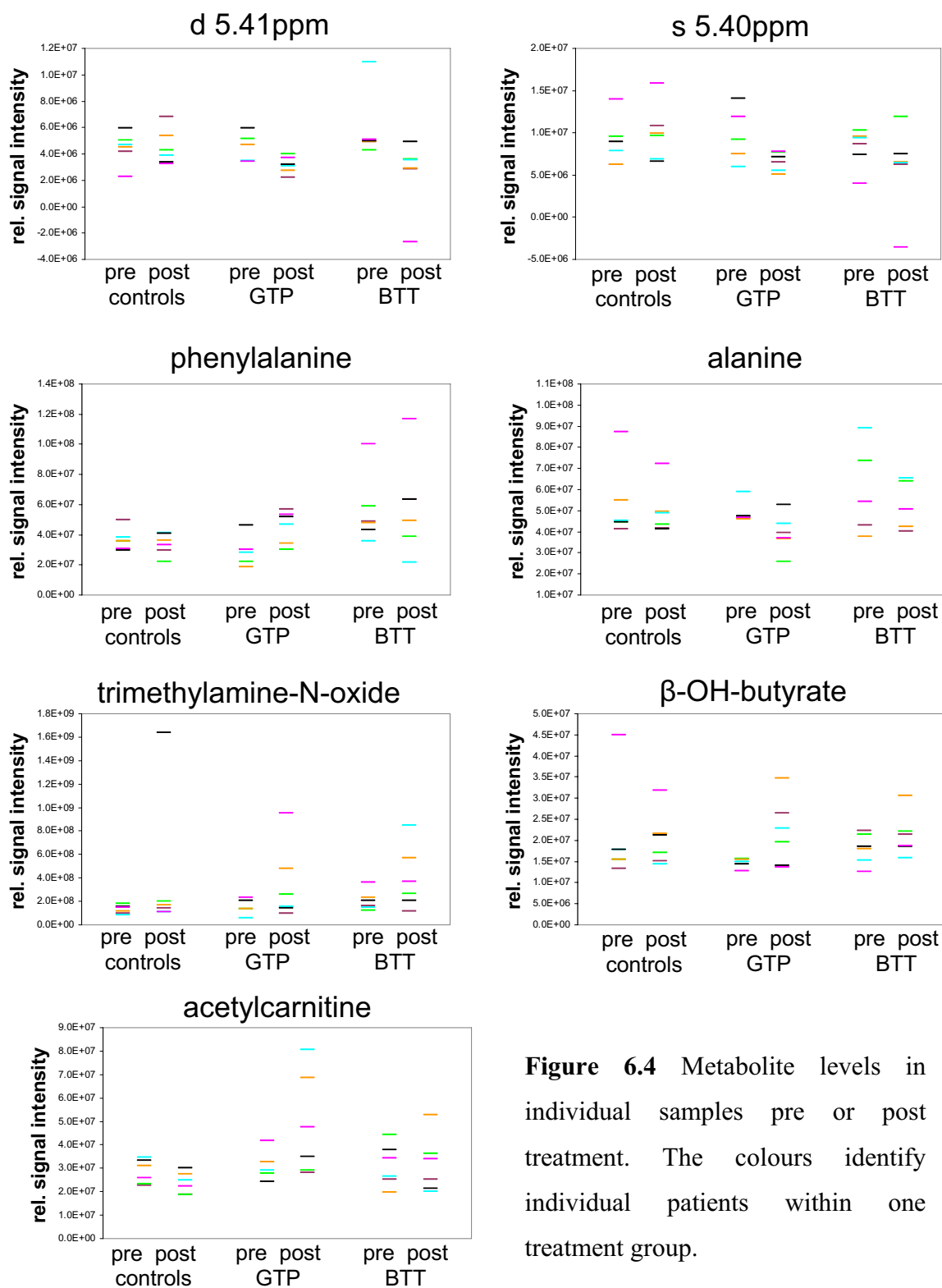


**Figure 6.4** Metabolite levels in individual samples pre or post treatment. The colours identify individual patients within one treatment group.

### 6.1.2 $^1\text{H}$ -NMR metabolic profiling of plasma

Samples were prepared and analysed as described in sections 2.2.4.2, 2.2.4.5 and 2.2.4.6. Figure 6.5 shows a typical  $^1\text{H}$ -NMR spectrum of a plasma sample acquired using a CPMG pulse sequence.

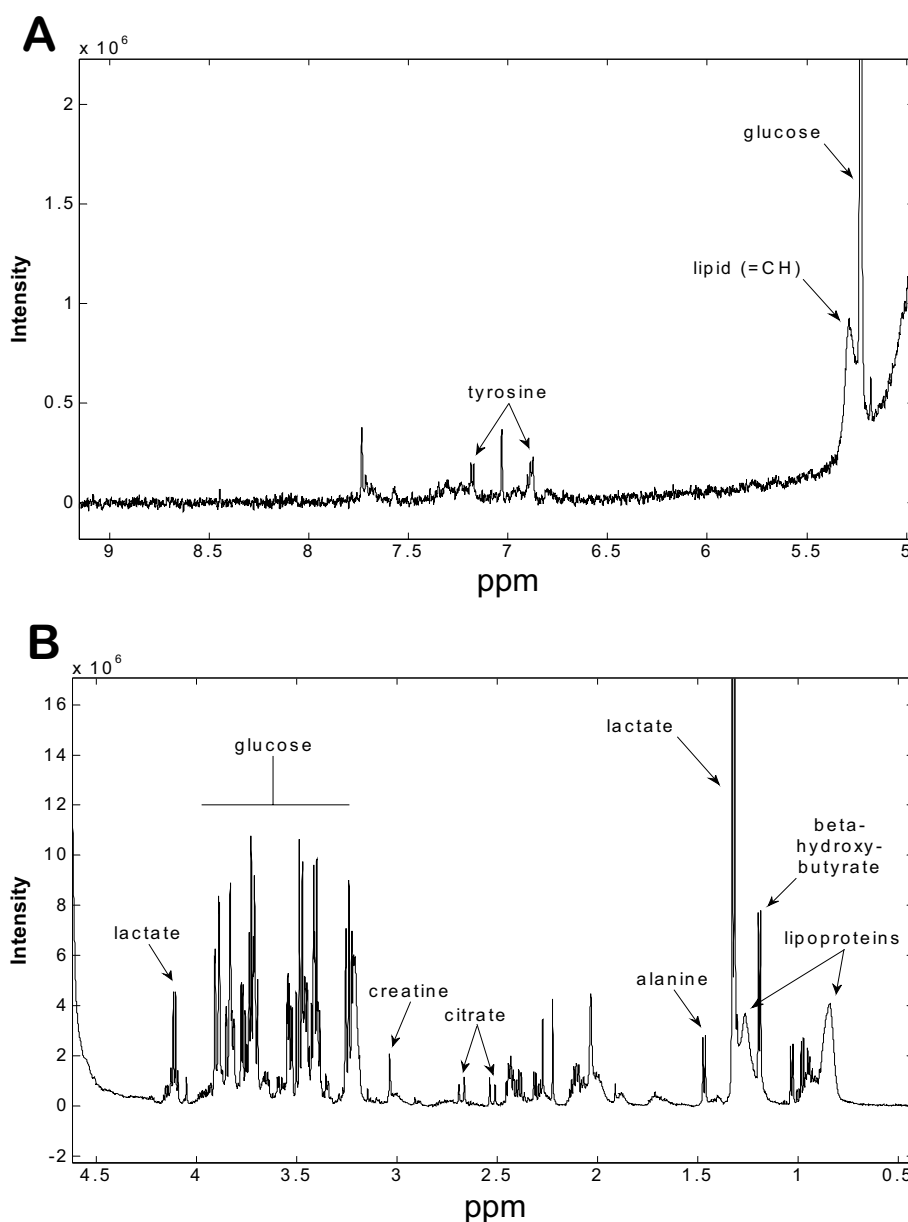


**Figure 6.5**  $^1\text{H}$ -NMR spectrum of plasma from a patient with BPH after four weeks of GTP intervention. **A:** aromatic region; **B:** aliphatic region

The same data mining techniques and statistical tools as described in section 6.1.1 were used to identify GTP and BTT mediated changes in the plasma metabolic profile. PLS-DA models for the separation of control and GTP or BTT samples did not pass the validation test. Figure 6.6 shows the PCA scores plot of all plasma samples analysed by NMR. The PCA model did not reveal any group-related clustering in any of the components.

Table 6.2 lists metabolites or spectral regions that were characterised by a significance level of  $p < 0.05$  in the Wilcoxon test in either of the three groups. All those metabolites which showed a significant difference in the control group were not further considered as markers of a GTP or BTT effect. Alanine and the doublet at 1.13ppm were decreased by 16% and 15%, respectively, in the post-dose GTP samples compared to pre-dose samples.

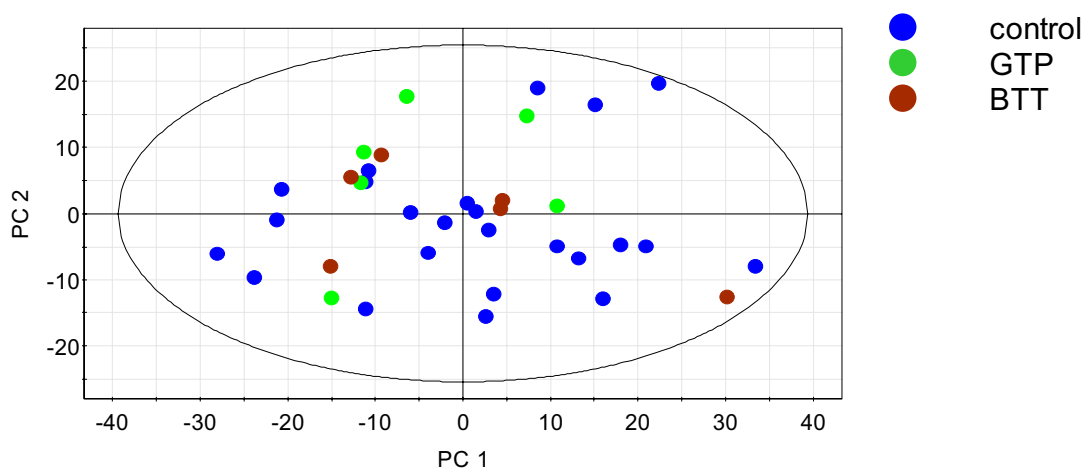


**Figure 6.6** PCA scores plots of all plasma samples analysed by  $^1\text{H-NMR}$  showing the first and second a principal component (PC). Samples labelled as control include all non-treatment samples. The data are scaled to unit variance.

**Table 6.2** Levels of significance of plasma metabolite changes within one treatment group (Wilcoxon test)

<i>metabolite or spectral region</i>	<i>Wilcoxon test control group</i>	<i>Wilcoxon test GTP group</i>	<i>Wilcoxon test BTT group</i>
alanine (d1.47ppm)	p=0.3454	p=0.0464* ↓	p=0.2489
lipids CH <sub>3</sub> a (m 0.81ppm)	p=0.0464* ↓	p=0.0464* ↓	p=0.6002
lipids CH <sub>3</sub> b (m 0.87ppm)	p=0.0277* ↓	p=0.1730	p=0.4631
unsat. lipids (m 5.31ppm)	p=0.0464* ↓	p=0.0277* ↓	p=0.6002
lipoproteins (m 1.25ppm)	p=0.0464* ↓	p=0.0464* ↓	p=0.7532
d 1.13ppm	p=0.2489	p=0.0464* ↓	p=0.2489
valine (d 1.03ppm)	p=0.0464* ↓	p=0.3454	p=0.9165
s 3.92ppm	p=0.0277* ↓	p=0.1159	p=0.4631

ppm values in brackets denote spectral region used for integration. \* indicate statistical significance according to the Wilcoxon test with  $p < 0.05$ . Arrows indicate direction of change.

Figure 6.7 shows the median plasma NMR spectra of the three treatment groups in the region of the CH<sub>3</sub> groups of plasma lipids (mainly lipoproteins). In the GTP group as well as the control group the post treatment samples exhibited lower lipoprotein levels. In figure 6.8 the individual levels of alanine and the doublet at 1.13ppm for all samples are depicted.

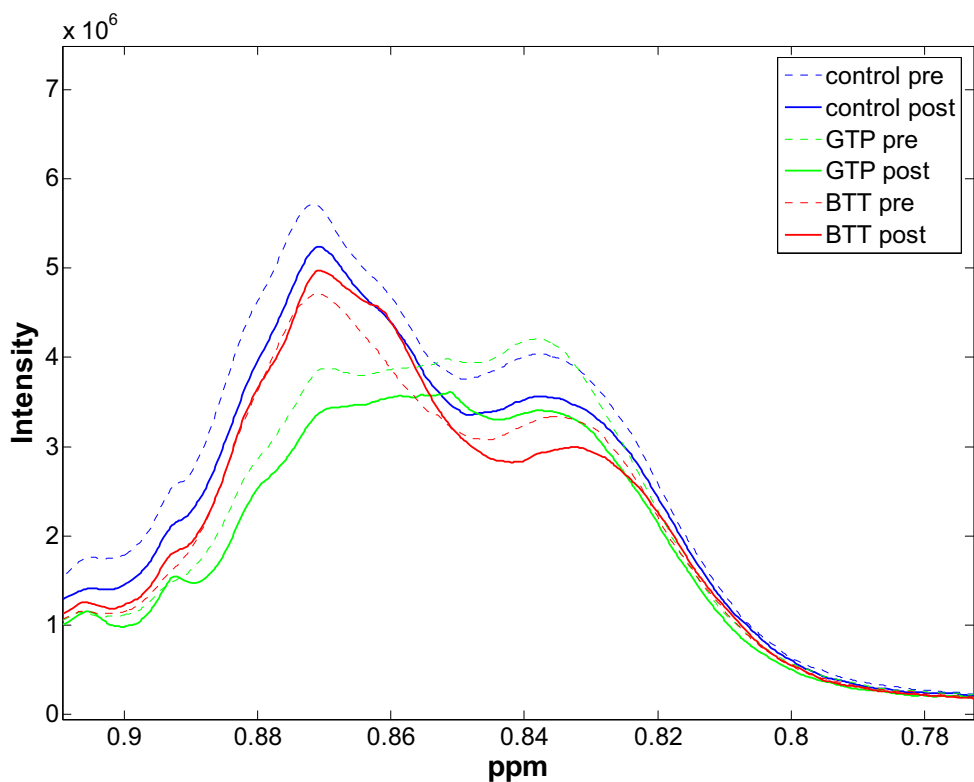


**Figure 6.7** Median NMR spectra of all treatment groups pre and post intervention zoomed in on the signal of CH<sub>3</sub> groups of the plasma lipids.

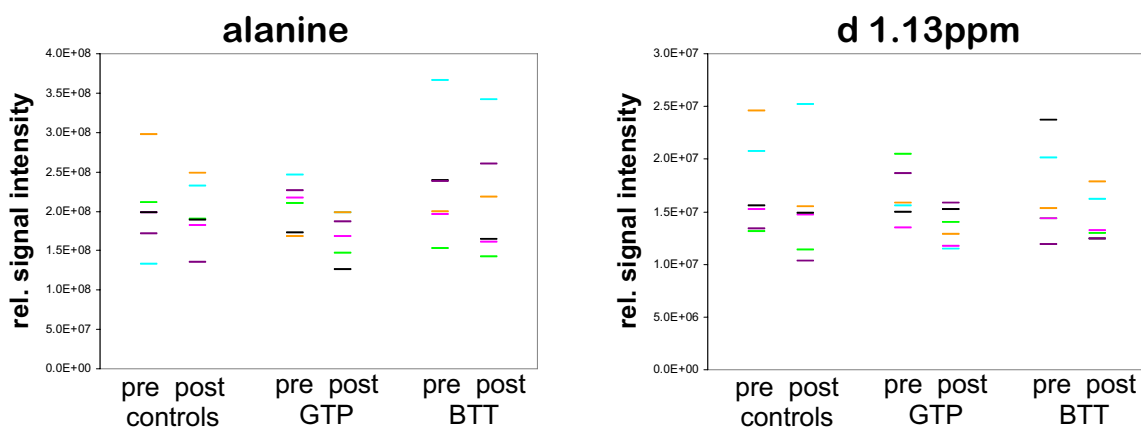


**Figure 6.8** Metabolite levels in individual samples pre or post treatment. The colours identify individual patients within one treatment group.

### 6.1.3 Discussion

NMR analysis could not detect major changes in the endogenous urinary or plasma metabolic profile following four weeks of intervention with either GTP or BTT. In the case of urine, PCA analysis showed a separation of GTP samples from control and BTT samples which was due to the urinary excretion of aromatic metabolites. The only valid PLS-DA model for the separation of GTP or BTT from controls that could be generated for urinary GTP and control samples, was again due to the excreted aromatic metabolites. The reason for the lack of separation of the BTT samples probably lies in the fact that patients were not asked to refrain from tea consumption over the period of intervention. Nearly every patient reported consumption of black tea, the average being three cups per day. Another factor that may have compromised the evaluation of any GTP or BTT effects is the time of sample collection. The pre-dose samples were obtained from patients during normal doctors appointments, while the post-dose samples were collected on the day of the operation for prostatectomy, prior to which patients were asked to fast from 12am the night before. Diurnal and fasting effects on urinary metabolite profiles have previously been reported for healthy humans and rodents (Bollard *et al.*, 2001; Gavaghan *et al.*, 2002; Lenz *et al.*, 2003; Maher *et al.*, 2007), and it seems likely that such effects would also occur in these patients.

In the plasma samples a decrease of lipoprotein signals was observed in both the GTP and control post-dose samples (figure 6.7), which confounds the ability to draw any conclusions about possible effects of GTP on that region. Apart from the general lack of information about sampling times, the medication regime of the patients introduces another variability. Although the prescribed medication (including anti-hypertension and hypolipidemic drugs) would have been the same for each patient before and after the intervention, no record was kept about the time these drugs were taken with regard

to the time of sample collection. Neither was the use of any over-the-counter drugs recorded. All these factors may have contributed to the fact that only a few metabolic changes related to GTP or BTT intervention could be detected. In urine, tea-specific changes were decreased signals at 5.41 (doublet) and 5.40ppm (singlet), probably sugar-related compounds. To the best of my knowledge these signals have not been previously associated with tea consumption. No further BTT effects on the metabolic profile could be identified. Upon GTP intervention patients presented with increased TMAO excretion, which may be due to alterations in the gut microflora (Nicholls *et al.*, 2003), an effect which tea polyphenols have previously been shown to exert (Lee *et al.*, 2006). The GTP group further exhibited increased excretion of acetylcarnitine and  $\beta$ -OH-butyrate, two metabolites which have been shown to be excreted at higher levels after 24h of fasting, due to elevated  $\beta$ -oxidation of fatty acids (Bales *et al.*, 1986; Hoppel and Genuth, 1980). However, increased levels of the other ketone bodies (acetate and acetoacetate) could not be detected in the present study. Green tea has previously been shown to stimulate fatty acid oxidation (Harada *et al.*, 2005; Murase *et al.*, 2005; Ota *et al.*, 2005; Shimotoyodome *et al.*, 2005) and it is therefore conceivable that the increased levels of  $\beta$ -OH-butyrate and acetylcarnitine reflect this effect of GTP. Furthermore, the observed decrease in urinary and plasma levels of alanine might reflect a shift towards metabolic features observed in prolonged fasting. In the initial phase of fasting, glucose is generated from liver glycogen and increased amino acid oxidation, but after that, a switch to protein conservation results in fat utilisation for energy generation (Saudek and Felig, 1976). In the state of protein-sparing metabolism circulating levels of alanine are significantly decreased, because the alanine-glucose cycle of gluconeogenesis (figure 6.9) becomes less and less significant. Lower levels of plasma alanine, and

increased levels of ketone bodies have also been previously associated with green tea consumption (van Dorsten *et al.*, 2006).

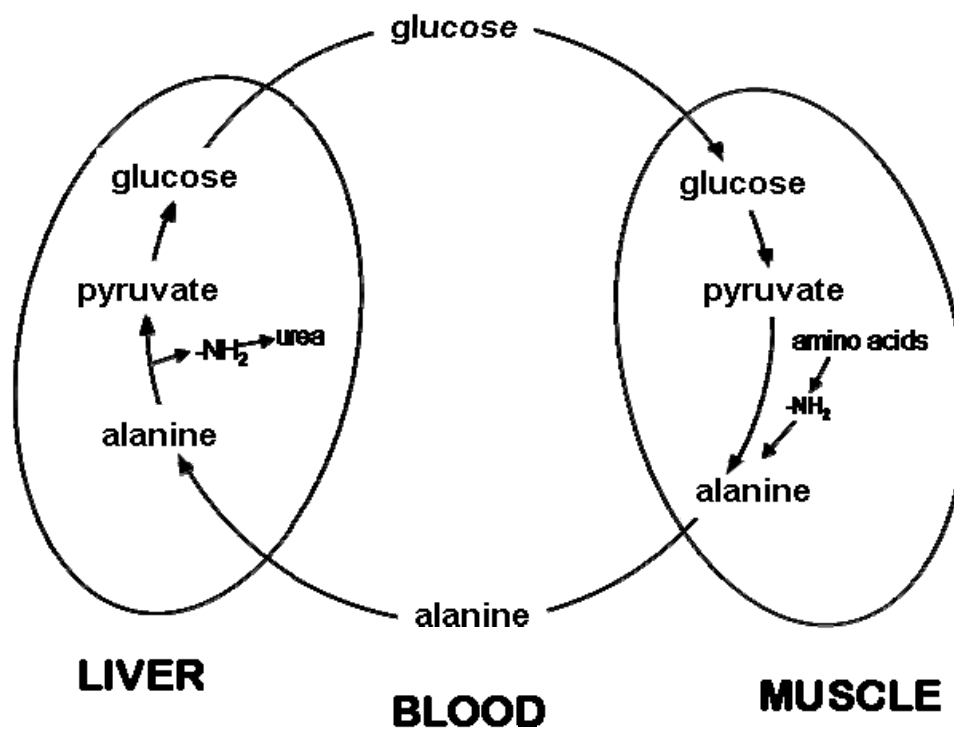


**Figure 6.9** Glucose-alanine-cycle

A link between cancer chemopreventive properties of GTP and its effects on energy metabolism may be provided by the IGF-1 signalling pathway. Green tea has been shown to significantly decrease IGF-1 levels (Adhami *et al.*, 2004) and IGF-1 is also known to be down-regulated in fasting (Ross, 2000). It is conceivable that either the down-regulation of IGF-1 or the increased  $\beta$ -oxidation of fatty acids initiates the other event. Equally, both effects could occur independently and synergise each other.

It should be stressed that the observed changes in urinary and plasma metabolite levels can only be understood as trends, because the study design was not optimised towards

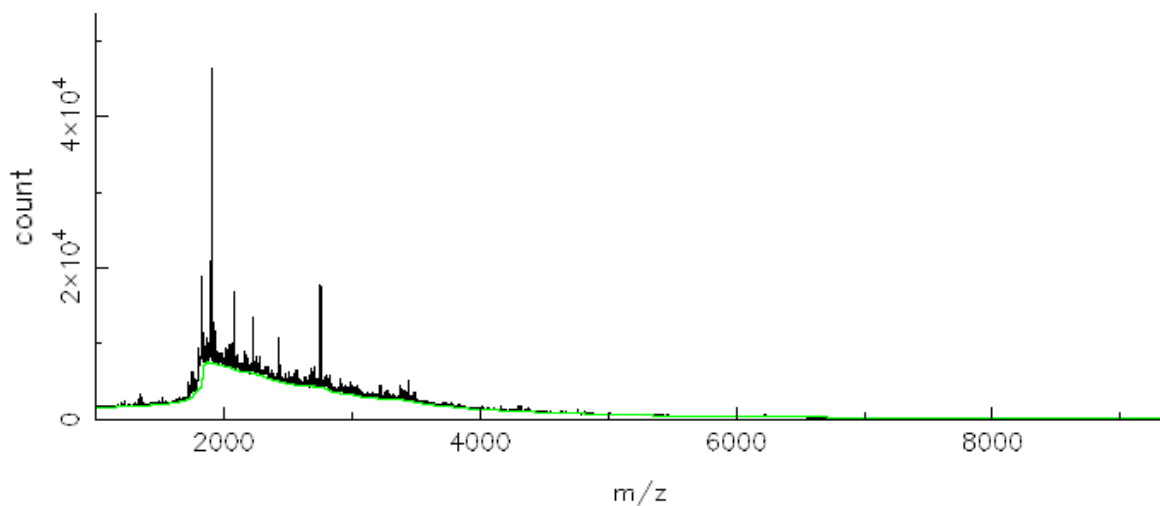
the determination of metabolic changes (discussed above), and also the study population was too small to make definitive claims. GTP intervention has shown promising trends with regard to its effects on energy metabolism, but further investigations are required to fully explain these trends.

## 6.2 Effects of tea polyphenols on the urinary and plasma peptidome

Samples were prepared and analysed as described in sections 2.2.2.4, 2.2.2.5 and 2.2.2.8. Data reduction and normalisation are described in section 2.2.2.9. The obtained peak lists were exported to SIMCA and MatLab software for detailed evaluation.

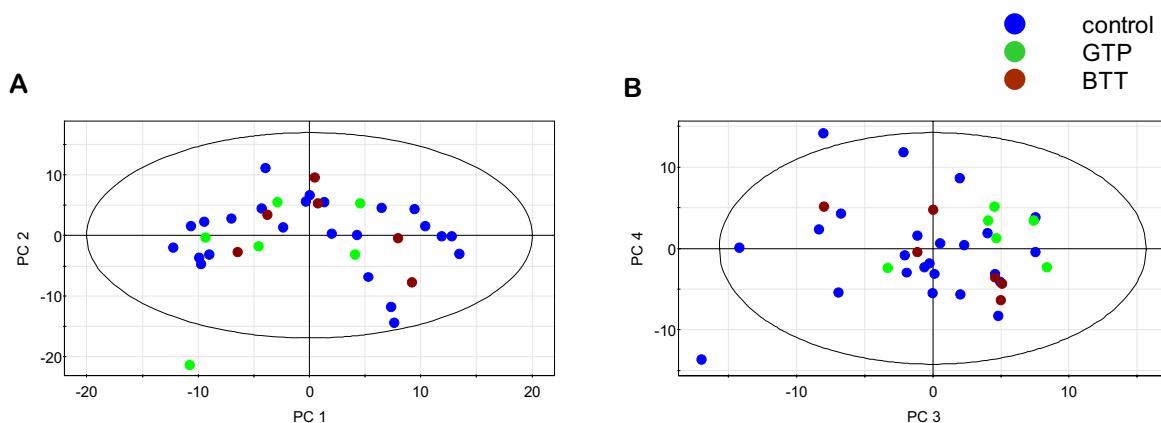
### 6.2.1 Peptide profiling of urine

Figure 6.10 shows the bucketed, combined mass spectra of all urine samples with the green line indicating the background continuum which was subtracted before data evaluation. From the background-subtracted spectrum 363 significant peaks were extracted for further analysis.



**Figure 6.10** Combined and bucketed mass spectra of all urine samples analysed by MALDI-MS. The green line indicates the unresolved background spectrum which is subtracted prior to data evaluation.

PCA analysis did not show group specific clustering in any components of the model, indicating that physiological and analytical variation had a greater effect on the urinary peptide profile than GTP or BTT intervention (figure 6.11).



**Figure 6.11** PCA scores plots of all urine samples analysed by MALDI-MS showing (A) the first and second and (B) third and fourth Principal Component (PC). The data are scaled to unit variance.

Data mining techniques for the identification of ions, which were altered after GTP or BTT intervention, included PLS-DA loadings and difference/correlations plots for models, generated to maximise the separation between i) all untreated samples and GTP or BTT samples, ii) pre- and post-dose samples from the GTP or BTT group and iii) the control and GTP or BTT group following the subtraction of the pre-dose peak list from the post-dose peak list for each patient. None of the PLS-DA models passed the validation test, indicating that tea polyphenol-related differences in peptide patterns were subtle. Figure 6.12 shows the difference/correlation plot for control vs. GTP samples after subtraction of the pre-dose peak list from the post-dose peak list for each sample. Some ions which were identified using this data mining approach are marked in the figure.

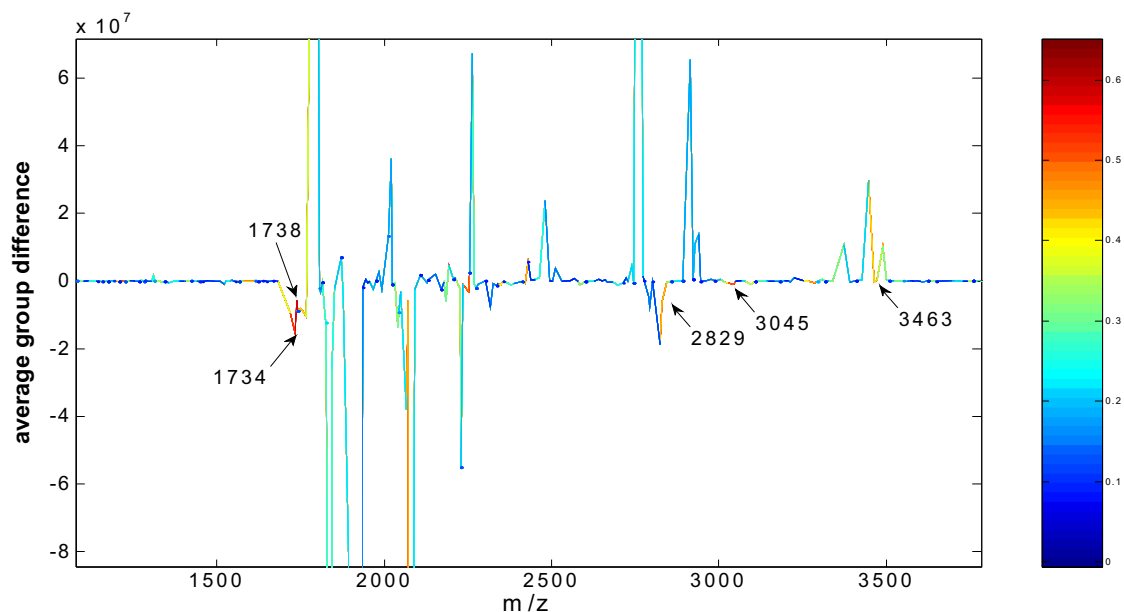


**Figure 6.12** Section of difference/correlation plot of GTP and control samples after subtraction of the pre-dose from the post dose peak list for each individual sample

Significance of potential marker ions was tested using the Wilcoxon test for paired samples in each treatment group with  $p < 0.05$ . Ions which differed in the control group with a significance level of  $p < 0.2$  were not considered further. This restriction led to the exclusion of five ions. Table 6.3 lists  $m/z$  values of peptides which were differentially excreted in urine after GTP or BTT intervention. The only commonly affected ion in the GTP and BTT group was at  $2601.9m/z$ . While this ion was present at lower levels in the GTP post treatment samples, it was more abundant after BTT treatment. Comparison with changes observed in the urinary peptide profile of TRAMP mice treated with GTP (see Chapter 5, section 5.4.1) did not show any commonly altered ions.

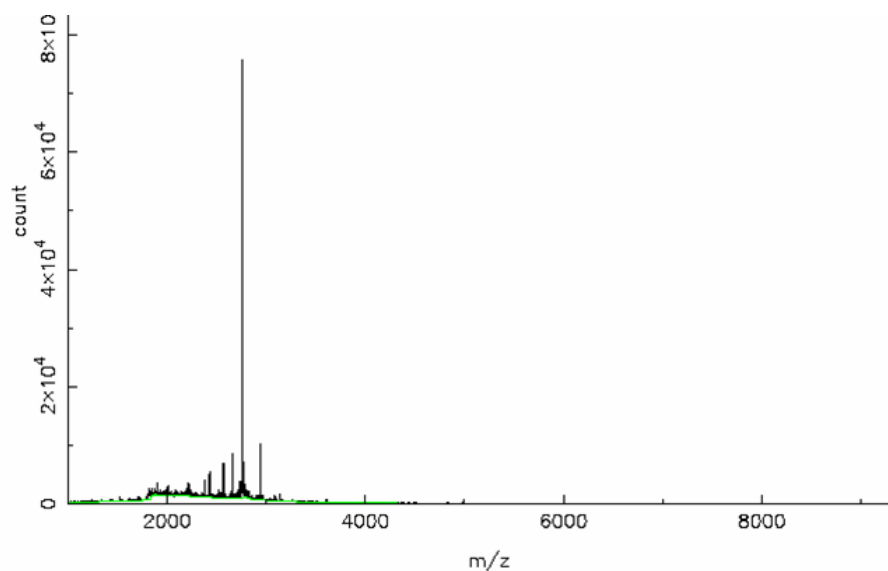
**Table 6.3** Statistically significant changes in the urinary peptide profile after four weeks of GTP or BTT intervention

<i>m/z</i>	<i>change in post- vs. pre-dose</i>	<i>m/z</i>	<i>change in post- vs. pre-dose</i>
<b>GTP</b>		2828.9	-55%
1034.2	-55%	3027.0	-39%
1052.3	-69%	3045.0	-26%
1054.9	-44%	3463.1	-62%
1135.0	-23%	3880.0	+52%
1153.9	-35%	3890.9	+39%
1222.1	-43%	4130.0	+229%
1283.1	-51%	4729.9	+70%
1289.0	+89%	<b>BTT</b>	
1325.0	+24%	1152.1	+85%
1537.9	-39%	1319.9	-9%
1579.0	-53%	1349.0	+52%
1600.1	-77%	1423.9	+89%
1717.9	-80%	1799.9	+63%
1734.1	-84%	2128.0	+90%
1738.1	-77%	2601.9	+63%
1742.9	-88%	2893.0	+16%
1751.1	-77%	3571.0	-28%
2568.1	-32%	3590.1	-25%
2601.9	-38%	6216.0	+2%

Changes were calculated from group medians. Significance was established with the Wilcoxon test with  $p < 0.05$ .

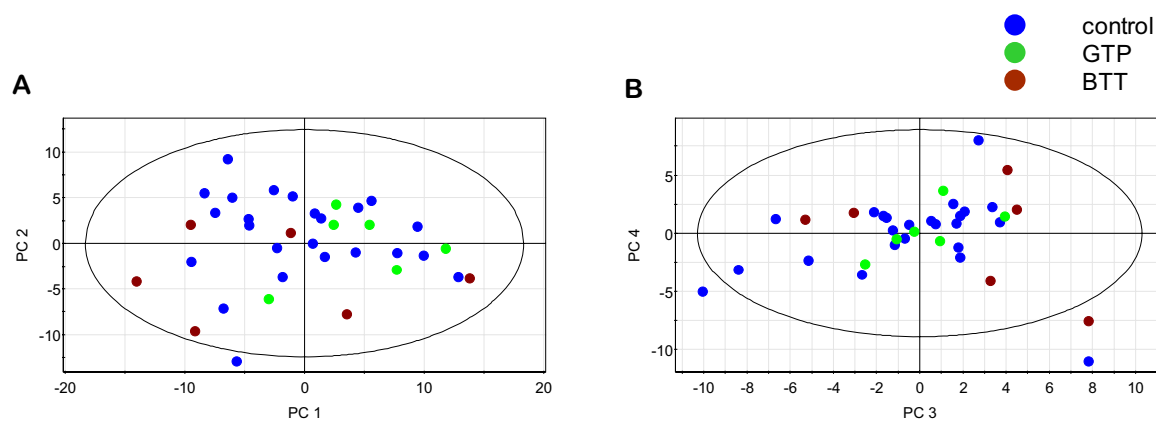
### 6.2.2 Peptide profiling of plasma

Figure 6.13 shows the bucketed, combined mass spectra of all plasma samples with the green line indicating the background continuum which was subtracted before data evaluation. From the background-subtracted spectrum 162 significant peaks were extracted for further analysis.



**Figure 6.13** Combined and bucketed mass spectra of all plasma samples analysed by MALDI-MS. The green line indicates the unresolved background spectrum which is subtracted prior to data evaluation.

PCA analysis showed that variation unrelated to intervention dominated the data set (figure 6.14).



**Figure 6.14** PCA scores plots of all plasma samples analysed by MALDI-MS showing (A) the first and second and (B) third and fourth Principal Component (PC). The data are scaled to unit variance.

The same data mining techniques and exclusion criteria as described in section 6.2.1 were used to identify ions with different abundance before and after GTP or BTT intervention. Only one ion had to be excluded due to variation in the control group. As for the urine data, none of the plasma PLS-DA models passed the validation test. Table 6.4 lists all the ions which were found to be statistically changed in abundance after GTP or BTT intervention. The ion with  $m/z$  1700.9 was reduced after both GTP and BTT intervention. No overlaps were found between the present study and the TRAMP mouse GTP prevention study (see Chapter 5, section 5.4.2).

**Table 6.4** Statistically significant changes in the plasma peptide profile after four weeks of GTP or BTT intervention

<i>m/z</i>	<i>change in post- vs. pre-dose</i>	<i>m/z</i>	<i>change in post- vs. pre-dose</i>
<b>GTP</b>		1317.8	-28%
1656.0	-37%	1435.1	-13%
1700.9	-25%	1618.8	-22%
2268.0	+26%	1700.9	-9%
3003.0	-1%	1718.8	-34%
3878.9	+15%	1901.9	-25%
<b>BTT</b>		2066.1	+25%
1034.3	-24%	2185.9	-31%
1134.8	-21%	3432.1	+130%
1152.2	-17%		

Changes were calculated from group medians. Significance was established using the Wilcoxon test with  $p < 0.05$ .

### 6.2.3 Discussion

Both the urinary and plasma peptide profile showed changes after a four week intervention with either GTP or BTT. PLS-DA analysis, however, could not generate predictive models. This lack of robust overall changes may be explained by the heterogeneity of individual responses to the intervention and the small number of patients enrolled in this trial. In order to determine the effects of compounds derived from natural products at the peptidomic and metabonomic levels, larger study populations are probably required, since the effect of natural occurring compounds with little or no side effects, such as tea polyphenols, in humans is likely to be less pronounced than that of pharmaceutical drugs, administered at a known effective dose.

Furthermore, healthy individuals should be included as controls. The present study only investigated the effect of tea polyphenols on patients with BPH, a condition which may in itself alter the response to chemopreventive agents such as tea polyphenols. The comparison of intervention effects between healthy and diseased individuals could provide valuable information about the mechanism of action of the investigated chemopreventive agent as well as underlying molecular processes of the disease.

The changes which were observed in this study indicate that GTP and BTT do exert an effect on the peptide composition of both plasma and urine. However, no overlaps were found between the TRAMP and human study, although both BPH patients and TRAMP mice received the same GTP. The reason for this observation may lie in the fact that GTP administration did not show an overall effect in the TRAMP study (see Chapter 5).

In summary, the data presented here provide evidence that the human urine and plasma peptidome undergoes changes following chemopreventive intervention with tea polyphenols and can therefore be used to discover pathways and mechanisms of chemoprevention. However, larger study populations are required in order to determine more robust changes. At present, the possibility that similar changes can be observed in mice and humans cannot be excluded and has to be further investigated with studies designed to carefully consider the equality of compound dose and mode of application.

### **6.3 Effects of tea polyphenols on urinary 8-oxodG levels**

8-oxodG and creatinine concentrations were determined as described in sections 2.2.3.4, 2.2.3.5 and 2.2.3.7. 8-oxodG values were normalised to creatinine rather than specific gravity since this study is a follow up of individuals and creatinine is a relative stable feature, as it is mostly dependent on the muscle mass (Narayanan and Appleton, 1980).

#### **6.3.1 Results**

Levels of urinary 8-oxodG were determined in 18 patients diagnosed with BPH and awaiting prostatectomy. These patients received GTP, BTT or no treatment for four weeks prior to surgery. Urine samples were collected before and after treatment (see section 2.2.1.6).

In none of the three groups could a significant change in 8-oxodG concentration be observed (table 6.5). Figure 6.15 shows the values for the measured 8-oxodG concentrations across all three groups with a colour code according to each patient. It is evident that in most cases urinary 8-oxodG levels are relatively stable. The maximal intra-person variation was 0.79nmol 8-oxodG/mmol creatinine, while the maximal inter-person variation amounted to 2.68 nmol 8-oxodG/mmol creatinine. Due to the lack of data about the weight or height of the patients, it was not possible to evaluate a correlation of these measurements or the Body Mass Index (BMI) to urinary 8-oxodG. The age of the patients enrolled in the study ranged from 51-79 years. There was no correlation between age and 8-oxodG.

**Table 6.5** Median values for urinary 8-oxodG expressed in nmol/mmol creatinine and percent changes after tea polyphenol intervention

controls		GTP		BTT	
pre	post	pre	post	pre	post
2.42	2.53	1.70	1.56	2.18	2.21
(1.94/3.49)	(1.60/3.29)	(1.12/1.85)	(1.14/2.17)	(0.81/3.11)	(0.75/3.49)
difference pre → post		difference pre → post		difference pre → post	
+5%		-8%		+1%	
(p=0.674)		(p=0.753)		(p=0.528)	

Values in brackets denote the minima and maxima for each group. Significance was established using the Wilcoxon signed-rank test for paired samples.

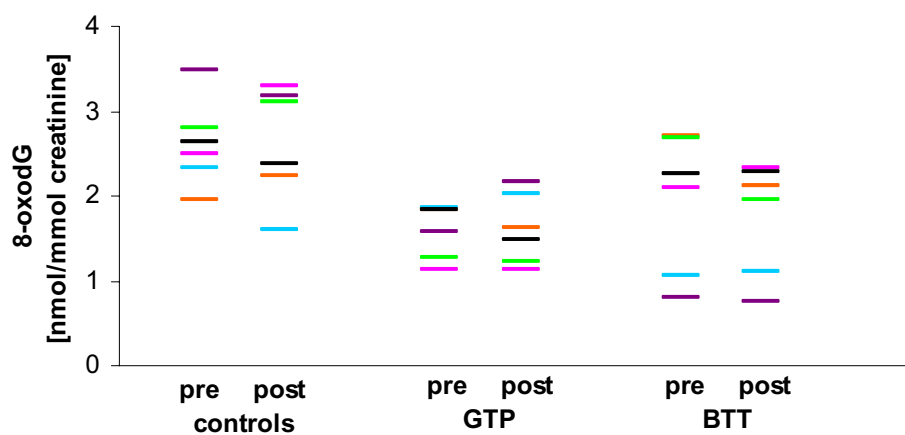


**Figure 6.15** Concentrations of urinary 8-oxodG measured in patients with BPH before and after treatment with GTP, BTT, or no treatment. All values are normalised to creatinine. The colours identify individual patients within one treatment group.

### 6.3.2 Discussion

Epidemiological and preclinical investigations have long suggested that GTP is a good chemopreventive agent for prostate cancer (see Introduction). The clinical studies are not as numerous, but even so, there is good evidence that green tea indeed has protective properties against this cancer. A case control study from China, based on patient interviews and multivariate logistic regression, adjusting for several confounding factors, such as physical features, dietary habits, and social environment, showed a significant decrease in prostate cancer risk for regular tea drinkers with a significant dose response relationship (Jian *et al.*, 2004). The preventive effect of GTP in men with high-grade prostate intraepithelial neoplasia was recently shown by Bettuzzi *et al.* The consumption of 600mg of GTP per day over a period of one year reduced the occurrence of a tumour to 3% compared to 30% in the placebo group (Bettuzzi *et al.*, 2006). The reports on the effects of green tea on the levels of urinary 8-oxodG are equivocal. But in general there was a decrease of 8-oxodG observed whenever the intervention was three months or longer (Hakim *et al.*, 2003; Luo *et al.*, 2006), but not after only one month or less (Luo *et al.*, 2006) (Young *et al.*, 2002). The exception is one study in which a decrease was observed after only 7 days (Klaunig *et al.*, 1999). No change of urinary 8-oxodG was seen after a four months intervention with black tea (Hakim *et al.*, 2003). The pilot study described here investigated the effect of 1gram GTP or BTT per day administered over a period of four weeks (see section 2.2.1.6). Neither GTP nor BTT had a significant effect on levels of urinary 8-oxodG. It can be argued that four weeks was not long enough to produce significant changes in the amount of 8-oxodG excreted. The same argument is of course also valid for the BTF. However, in contrast to green tea, black tea has failed to show antioxidant effects as previously measured by urinary excretion of 8-oxodG (Hakim *et al.*, 2003).

On the statistical side it has to be taken into account that the number of enrolled patients, only six per arm, is very small. For results to be significant it would require very clear-cut differences. Another factor that might not have been optimally handled in this study is the urine collection. Random creatinine corrected spot urine samples have been shown to have a much higher intra-individual variation than 24h urine samples or morning spot urine samples (Miwa *et al.*, 2004). The fact that all urine samples in this study were collected during the first half of the day, though they were not necessarily the first morning urine, might explain the relative good intra-subject reproducibility (see figure 6.15). However, by using 24h samples or, for easier study conduct and sample cooling, strictly only first morning urine samples, the variation could possibly be further reduced and thus less obfuscation of possible changes may result.

In summary, the study conducted here failed to show an effect of either GTP or BTT on urinary 8-oxodG levels. The results are in general agreement with the literature, and this study is not arguing against the antioxidant properties of green tea. It also can not be excluded that the study design confounded the detection of significant changes.

#### **6.4 Summary**

Metabolic profiling of plasma and urine in humans has shown trends for the effects of GTP consumption on energy metabolism introducing alterations similar to those seen in prolonged starvation. However, due to sub-optimal study design, the changes observed can only be interpreted cautiously. Peptidomic profiling has provided evidence for an effect of tea polyphenols on the peptidome so rendering it suitable for the investigation of such effects. Intervention with tea polyphenols over a period of four weeks did not prompt any alterations in levels of urinary 8-oxodG which may be related to the relative short intervention period.

# Chapter 7

## **7. Final discussion**

The work described in this thesis was aimed at detecting biomarkers of carcinogenesis and GTP-mediated chemoprevention in the TRAMP mouse model using metabonomic and peptidomic profiling approaches as well as the measurement of urinary 8-oxodG. Although TRAMP and GTP-group-specific metabonomic and peptidomic changes were found in plasma and urine, none of these metabolites or peptides could unambiguously be identified as biomarkers of carcinogenesis or GTP efficacy. Possible confounding factors and observed trends have already been discussed in the respective chapters. In the following, the wider implications of the results for potential future work are discussed.

### **7.1 The use of TRAMP mice for chemoprevention studies**

#### **7.1.1 General aspects**

Metabonomic profiling of TRAMP mouse tumours (see Chapter 4, section 4.1) has revealed that, in the advanced stages of carcinogenesis, phospholipid metabolism is affected differently to that observed in human prostate tumours. The TRAMP mouse exhibits lower levels of choline, phosphocholine and glycerophosphocholine in tumours compared to normal prostate, while in human prostate tumours choline metabolites are relatively more abundant than in normal prostate (discussed in section 4.1.6). These findings are indicative of great differences in tumour characteristics, and therefore growth mechanisms, between humans and TRAMP mice. However, in young TRAMP mice, which presented with early proliferative lesions, a decrease in the GPC/PC ratio was observed. This finding is consistent with changes demonstrated in human prostate cancer (Swanson *et al.*, 2008), suggesting that at an early stage of

carcinogenesis TRAMP mice may be subject to metabolic alterations similar to those observed in the human disease. In order to obtain results more relevant to humans, it seems appropriate to restrict the use of the TRAMP mouse model for assessment of the chemopreventive efficacy of a given compound to early stages of carcinogenesis with minor proliferative lesions.

Furthermore, the lobe specific evaluation of chemopreventive efficacy in the TRAMP mouse model should be envisaged for future studies. When the protein expression of ChK was investigated, it was found that there were great differences in levels between the different lobes. Pronounced expression was only found in the ventral parts of the healthy prostate (see Chapter 4, section 4.1.4). Previously published work has also pointed out the lobe specific effect of different chemopreventive agents in TRAMP mice (Nyska *et al.*, 2003).

### **7.1.2 GTP efficacy in the TRAMP mouse model**

Intervention with 0.05% GTP in the drinking water did not prevent development of prostate cancer in the TRAMP mouse model (see Chapter 5). This dose was chosen as it complemented a TRAMP study in our laboratory in which effects of GTP and BTT at this dose in drinking water were compared. This dose failed to exhibit major effects on tumour progression in contrast to other researchers who observed efficacy using GTP doses of 0.1% or 0.3% in drinking water (Gupta *et al.*, 2001 and Caporali *et al.*, 2004, see Introduction, section 1.3.1). It has been discussed earlier that the discrepancy between the published studies and the results described here may stem from the substantially lower dose that has been given in this study. It is conceivable that this observation reflects a real dose-response effect. Ideally though, to ascertain dose-

response relationships, experimental setups with multiple doses are required. The comparison of studies from different laboratories does not allow conclusions to be drawn in this respect. On the one hand it is possible that TRAMP mice in different laboratories exhibit different genotypes and phenotypes due to genetic drift in the colony (Stevens *et al.*, 2007). This can lead to different responsiveness of mice to intervention. Alteration in the gut microbial composition may also be a cause of differences in chemopreventive activity of GTP in TRAMP mice in different laboratories (discussed in section 7.2). On the other hand it has to be taken into account that the GTP extracts used by different laboratories are often not the same. Table 7.1 gives an overview of the composition the GTP extracts used in the respective studies.

**Table 7.1** Composition of GTP used in TRAMP chemoprevention studies

<b>Studies</b>	<b>Total GTP content</b>	<b>EGCG</b>	<b>ECG</b>	<b>EGC</b>	<b>EC</b>	<b>caffeine</b>
Gupta <i>et al.</i> (2001) Adhami <i>et al.</i> (2004) Saleem <i>et al.</i> (2005)	> 95%	62%	24%	5%	6%	~ 1%
Caporali <i>et al.</i> (2004) Scaltriti <i>et al.</i> (2006)	76%	52%	6%	6%	12%	> 1%
Present study (from Bonoli <i>et al.</i> , 2002)	72%	39%	10%	12%	6%	> 0.1%

The work described in Chapter 5 was designed to investigate effects of GTP treatment on the urinary and plasma peptidomic and metabonomic profile with the aim to discover potential biomarkers of GTP efficacy. As discussed in Chapter 5, no definitive marker of GTP could be identified due to the lack of an overall effect. For biomarker discovery future studies should incorporate a dose which has a clear effect on cancer development and can be assessed by pathological means. It is important to be able to relate a possible biomarker to a primary outcome, otherwise the usefulness of the marker is questionable. Changes in the metabolic or peptide profiles related to carcinogenesis or GTP intervention were not the same between age groups. As discussed in Chapter 4, the investigation of smaller time windows than those chosen in the present study would be beneficial to identify and follow up markers of carcinogenesis. This notion can in principle also be applied to the investigation of markers of GTP activity. Not only may the response to an intervention change with progressing disease, but it may also be possible to identify markers of success or failure of intervention before a correlation with primary outcome is apparent. In order to be able to discover such markers, it is vital to show that the marker changes over time as well as is correlating with the primary outcome.

## **7.2 The role of the gut microflora in chemoprevention**

Global profiling approaches like peptidomics and metabonomics are non-hypothesis driven and therefore allow detection of changes which may fall beyond the anticipated range. Metabonomic profiling of urine from 8 week old TRAMP and wild type mice (see Chapter 4, section 4.2) indicated that there was a difference in the composition of the gut microflora between the transgenic mice and their non-transgenic littermates. At

28 weeks of age this difference was no longer noticeable, and the separation between TRAMP and wild type mice was less pronounced, indicating that the gut microflora perhaps had a greater influence on the urinary metabolic profile than the presence of prostate tumours. In the second TRAMP study no evidence was found for a difference in gut microflora between 8 week old TRAMP and wild type mice (see Chapter 5, section 5.2). The TRAMP phenotype can therefore be excluded as an intrinsic cause of gut microbial alterations, and other factors such as a different microenvironment have to be considered. It is for example conceivable that the position of the TRAMP and wild type mouse cages in the isolator had an effect on the gut microflora. The fact that both spatial and temporal separation lead to changes in the composition of the gut microflora is well established (Robosky *et al.*, 2005; Rohde *et al.*, 2007). The fact that the impact of gut microbes on the urinary composition is not minor has several implications for the design and set up of biomarker studies. When profiling of urine is employed for the discovery of biomarkers, either of disease or intervention, a great deal of consideration should be directed towards possible effects caused by the intestinal microbiome. Every effort should be made to avoid unintentional treatment- or disease-group-specific differences in the gut microflora. In pre-clinical studies animals should not be housed in group-specific areas, which may be easier for the animal house personnel, but in randomly assigned spaces within the same room or isolator. It is also important to ensure that control and test animals are derived from the same colony, with generations being as close together as possible. As such factors are not controllable in human studies, all emphasis has to be put into randomisation of patients. Factors that may play a role in the composition of the metabolome (not limited to microbiota) and therefore should be considered include gender, age, ethnicity, country or region of residence, diet, smoking habits, medical conditions other than the investigated one and medication,

including over-the-counter-drugs. The time points and conditions of sample collection have to be the same for pre and post treatment samples (Lenz *et al.*, 2003; 2004c; Phipps *et al.*, 1998).

Apart from being a possible confounding factor in the search for biomarkers, the gut microflora may even play a role in the chemopreventive activity itself. A trend of increased excretion of TMAO after intervention with GTP was observed, which could be attributed to alterations in the gut microflora (see Chapter 6, section 6.1). It is known that the gut microflora is generally influenced by diet and varies between populations (Dumas *et al.*, 2006; Lee *et al.*, 2006; Li *et al.*, 2008; Zanchi *et al.*, 2008). But the host-microbiome-axis is not a one way street: Intestinal bacteria and dietary compound can affect each other. The bioavailability of polyphenols is affected by microbial metabolism in the intestine (Xu *et al.*, 1995) and therefore the extent of chemopreventive activity may be influenced by the composition of the gut microflora. This concept has already been proposed for the chemopreventive activity of soy isoflavones, in particular daidzein (Yuan *et al.*, 2007). The ability to convert daidzein to equol, a metabolite with stronger estrogenic properties, is dependant on the composition of the intestinal microflora. A link between the ability to produce equol and a lower incidence of prostate cancer has been suggested (Akaza *et al.*, 2004). In addition, it has been noticed that the percentage of “equol-producers” is significantly higher in Asians as compared to Americans. Whether similar mechanisms would also apply to GTP is currently not known. Further research is required to establish whether metabolites of GTP are important for their chemopreventive properties, and what the role of gut micro-organisms may be. In the light of the observations described above, it also seems expedient to consider the assessment of potential chemopreventive agents specific to ethnic and regional subgroups, as this could shed additional light on the mechanisms by

which they act. Furthermore, a link between the composition of the gut microflora and chemopreventive efficacy of the agent in question, such as GTP, would allow the design of personalised chemoprevention (Nicholson *et al.*, 2005).

### **7.3 Implications for clinical intervention studies**

Differences in response to chemopreventive intervention may also stem from sources other than the gut microflora. The pharmacokinetic characteristics of a drug or chemopreventive agent are determined by physiology of an individual, interaction with other pharmaceuticals or nutrients, as well as the enzyme complement available for metabolism. Polymorphisms or altered activity in metabolising enzymes may affect the composition of metabolites or parent compounds available in the biophase to act as chemopreventives. It is therefore advisable to take levels of chemopreventive parent compounds and metabolites into account, when the success of an intervention is judged by primary outcome. Correlations that may or may not exist between dose/metabolite levels and primary outcome or other biomarkers can help to shed further light on mechanisms of action and also provide information on which metabotype may be sensitive to chemopreventive intervention.

## 7.4 Summary

The work described in this thesis was designed to investigate markers of carcinogenesis and GTP chemoprevention in the TRAMP mouse model of prostate cancer. Metabolic profiling of TRAMP mouse prostate tumours provided evidence that the phospholipid metabolism in late stage TRAMP mouse tumours greatly differs from that observed in humans. It was therefore concluded that the TRAMP model should be used with caution and that the assessment of chemopreventive drugs should be restricted to early stages of carcinogenesis in that model. In order to discover and develop biomarkers of GTP intervention in the TRAMP model it is important to investigate narrower time windows of intervention as well as choosing at least one dose level that shows effects that can be assessed by pathological means and used as primary outcome.

Although the studies failed to unambiguously identify markers of carcinogenesis or GTP chemoprevention, valuable lessons were learned for future studies. Especially for approaches using urinary profiling, the effect of the gut microflora has to be considered, as the urinary composition is heavily influenced by the gut microflora. Furthermore, the mutual interactions of gut microbes and GTP have been highlighted. In clinical GTP chemoprevention studies the relationship between actual levels of chemopreventive parent compound or metabolites and the primary outcome or biomarkers should be investigated.

Taking gut microfloral interactions and dose/metabolite-response relationships into account may ultimately lead to a better understanding of mechanisms of action of GTP and the possibility of offering personalised chemoprevention strategies.

# Metabolic Profiling of Transgenic Adenocarcinoma of Mouse Prostate (TRAMP) Tissue by <sup>1</sup>H-NMR Analysis: Evidence for Unusual Phospholipid Metabolism

Friederike Teichert,<sup>1</sup> Richard D. Verschoyle,<sup>1</sup> Peter Greaves,<sup>1</sup>  
Richard E. Edwards,<sup>2</sup> Orla Teahan,<sup>3</sup> Donald J.L. Jones,<sup>1</sup> Ian D. Wilson,<sup>4</sup>  
Peter B. Farmer,<sup>1</sup> William P. Steward,<sup>1</sup> Timothy W. Gant,<sup>2</sup>  
Andreas J. Gescher,<sup>1</sup> and Hector C. Keun<sup>3\*</sup>

<sup>1</sup>Cancer Biomarkers and Prevention Group, University of Leicester, Leicester, UK

<sup>2</sup>Medical Research Council Toxicology Unit, University of Leicester, Leicester, UK

<sup>3</sup>Biomolecular Medicine, Division of Surgery, Oncology, Reproductive Biology and Anaesthetics, Faculty of Medicine, Imperial College, London, UK

<sup>4</sup>Department of Drug Metabolism and Pharmacokinetics, Astra Zeneca, Alderley Park, Macclesfield, UK

**BACKGROUND.** The TRansgenic Adenocarcinoma of the Mouse Prostate (TRAMP) mouse model has frequently been used in preclinical studies with chemotherapeutic/chemopreventive rationales. Here the hypothesis was tested using <sup>1</sup>H-NMR-based metabolic profiling that the TRAMP tumor metabolic phenotype resembles that reported for human prostate cancer.

**METHODS.** Aqueous extracts or intact tissues of normal prostate from 8- ("young") or 28- ("old") week-old C57BL/6J wild-type mice or of prostate tumor from age-matched TRAMP mice were analyzed by <sup>1</sup>H-NMR. Results were compared with immunohistochemical findings. Expression of choline kinase was studied at the protein and mRNA levels.

**RESULTS.** In young TRAMP mice presenting with zonal hyperplasia, the ratio of glycerophosphocholine (GPC) to phosphocholine (PC) was 22% below that in wild-type mice ( $P < 0.05$ ). In old TRAMP mice with well-defined malignancy, reduced tumor levels of citrate (49%), choline (33%), PC (57%), GPC (66%), and glycerophosphoinositol (61%) were observed relative to normal prostate ( $P < 0.05$ ). Hierarchical cluster analysis of metabolite levels distinguished between normal and malignant tissue in old but not young mice. While the reduction in tissue citrate resembles human prostate cancer, low levels of choline species in TRAMP tumors suggest atypical phospholipid metabolism as compared to human prostate cancer. TRAMP tumor and normal prostate tissues did not differ in expression of choline kinase, which is overexpressed in human prostate cancer.

**CONCLUSION.** Although prostate cancer in TRAMP mice shares some metabolic features with that in humans, it differs with respect to choline phospholipid metabolism, which could impact upon the interpretation of results from biomarker or chemotherapy/chemoprevention studies. *Prostate* 68: 1035–1047, 2008. © 2008 Wiley-Liss, Inc.

**KEY WORDS:** <sup>1</sup>H-NMR analysis; metabonomics; metabolomics; choline metabolism; prostate cancer

Grant sponsor: Cancer Research UK; Grant number: C325/A6691;  
Grant sponsor: UK Medical Research Council; Grant numbers:  
G0100874UK, G0100873UK.

\*Correspondence to: Hector C. Keun, Biomolecular Medicine,  
Division of Surgery, Oncology, Reproductive Biology and  
Anaesthetics, Faculty of Medicine, Imperial College, Sir Alexander

Fleming Building, Exhibition Rd, South Kensington, London, UK.  
E-mail: h.keun@imperial.ac.uk

Received 12 December 2007; Accepted 4 February 2008  
DOI 10.1002/pros.20761

Published online 5 May 2008 in Wiley InterScience  
(www.interscience.wiley.com).

## INTRODUCTION

Prostate cancer is the second most common cause of male cancer deaths in most developed countries, and the incidence has increased significantly over recent years [1]. Rodent models of prostate carcinogenesis are useful for the discovery of disease biomarkers and in the development of novel chemopreventive or chemotherapeutic interventions. One well established example is the "TRansgenic Adenocarcinoma of the Mouse Prostate" (TRAMP) mouse, in which the prostate-specific expression of Simian virus 40 (SV40) early-region tumor antigens (T and t antigen) drives prostate neoplasia culminating in well and poorly differentiated adenocarcinomas with metastases in lung and pelvic lymph nodes [2,3]. The TRAMP phenotype is thought to be the result of inactivated p53 and Rb gene products, which have also been associated with human prostate cancer [4,5]. The TRAMP model has been frequently used in preclinical studies of cancer chemopreventive or therapeutic interventions [6–9]. Currently, the most common way to assess outcome of intervention in TRAMP mice is by weight of the urogenital tract combined with histopathology. However, malignant cells are also characterized by altered metabolism as compared to their non-malignant counterparts [10–13], and this fact is exploited in the diagnosis and therapy of many cancers, including prostate cancer. Among metabolic features of human prostate tumors, which differ from normal prostate, are decreased levels of citrate [14] and increased levels of phosphocholine (PC) and total choline-containing metabolites [15–17]. Choline kinase (ChK), which catalyzes the phosphorylation of choline, is overexpressed in human prostate cancer, and plays a major role in the mechanism leading to elevated levels of choline-derived species in malignant tissue [18]. Tumor levels of PC have been shown to be a pharmacodynamic marker of the chemotherapeutic efficacy of choline kinase inhibitors in experimental human breast and colon cancer models [19]. Measurement of citrate and total choline species *in vivo* has been used clinically in the diagnosis of prostate cancer [20–22].

Metabolic profiling (metabonomics/metabolomics) of intact tissue or tissue extracts allows measurement of several metabolites simultaneously, rendering it an attractive tool for the comprehensive assessment of the metabolome associated with the malignant phenotype. In the work described here <sup>1</sup>H-NMR-based metabonomics has been employed to test the following hypotheses in TRAMP mice: (i) metabolic differences between normal and malignant prostate tissue reflect differences discernible by histopathology and (ii) the metabolic phenotype of TRAMP tumors resembles that

reported for human prostate cancer. When choline metabolism in TRAMP tumors was found to differ from that in humans, the expression of ChK and other enzymes involved in choline metabolism was studied to help interpret underlying mechanistic differences.

## MATERIALS AND METHODS

### Materials

Solvents were purchased from Fisher Scientific, Inc. (Loughborough, UK) and chemicals from Sigma-Aldrich Company Ltd (Gillingham, UK). Polyclonal antibodies against murine choline kinases ChK- $\alpha$  and ChK- $\beta$  were kindly provided by Dr G Wu (Department of Biochemistry, University of Alberta, Canada).

### Animal Experimental Design

Experiments were carried out under UK Home Office animal project license PPL 40/2496. The experimental design met the standards required by the UKCCCR guidelines [23]. Mice were bred in the Leicester University Biomedical Services facility using female hemizygous transgenic mice on a C57BL/6J background, originally obtained from the NCI Mouse Repository (NCI Frederick) and male wild-type C57BL/6J mice. Mice had unlimited access to AIN93g standard diet (Dyets, Inc., Bethlehem, PA) and water. TRAMP genotype was established by PCR analysis of an ear punch sample taken at approximately 3 weeks of age. Each TRAMP mouse was paired with a C57BL/6J wild-type control from the same litter or from a litter with the same father. At 4 weeks of age the animals were weaned and received AIN93g standard diet. At 8 or 28 weeks of age mice were killed by cardiac exsanguination under terminal isoflurane anesthesia. Analyses were performed on four groups of mice: (1) wild-type 8 weeks of age, (2) wild-type 28 weeks of age, (3) TRAMP 8 weeks of age, (4) TRAMP 28 weeks of age.

### Prostate Tissue Preparation

Prostates from ten 8-week-old and eight 28-week-old C57BL/6J wild-type mice and prostate tumors from ten 8-week-old and nine 28-week-old TRAMP mice were dissected out from surrounding tissues also avoiding the seminal vesicles. Each tissue was divided in two parts. One part was snap-frozen (liquid nitrogen) and stored at  $-80^{\circ}\text{C}$  prior to homogenization and extraction for <sup>1</sup>H-NMR analysis. The other part was fixed in neutral buffered formalin, processed, sectioned, and stained with hematoxylin and eosin for histopathological assessment applying criteria outlined in the Bar Harbor classification [24].

Tissue parts for  $^1\text{H-NMR}$  analysis were selected randomly without any bias for specific lobes. A lymph node metastasis was dissected from one TRAMP mouse. For  $^1\text{H-NMR}$  analysis two separate tumor samples per mouse, rather than one, were used in the case of three out of the nine 28-week-old TRAMP mice. Total sample number per group was between 8 and 12. Aliquots (20–40 mg) of frozen tissue were homogenized in 300  $\mu\text{l}$  of a mixture of chloroform and methanol (2:1). After addition of 300  $\mu\text{l}$  water and further mixing, the homogenate was centrifuged (5 min, 15,000g, room temperature). Aqueous and organic phases were separated, and the tissue pellet was re-extracted. Both aqueous phases were combined, freeze-dried and re-dissolved in buffer [575  $\mu\text{l}$   $\text{D}_2\text{O}$  with 8 mM  $\text{NaH}_2\text{PO}_4$ , 40 mM  $\text{Na}_2\text{HPO}_4$ , 1.4 mM sodium 3-(trimethylsilyl)-2,2,3,3- $^2\text{H}_4$ )-1-propionate (TSP), 0.58 mM sodium azide, 5%  $\text{H}_2\text{O}$ ].

For High-Resolution Magic Angle Spinning (HRMAS)  $^1\text{H-NMR}$  analyses of intact tissue, samples (30–50 mg) of prostate or prostate tumor from three TRAMP and five wild-type mice (28 weeks of age) were used. Tissues were dipped in  $\text{D}_2\text{O}$  and placed into a 3 mm zirconium rotor prior to analysis.

#### NMR Data Acquisition and Processing

$^1\text{H-NMR}$  spectra of aqueous extracts were acquired using a Bruker DRX600 spectrometer (Bruker BioSpin GmbH, Rheinstetten, Germany) operating at a frequency of 600.13 MHz and a temperature of 300 K. Tissue extracts were analyzed in a standard 5 mm probe.  $^1\text{H}$  spectra were acquired using a 1D-NOESY pulse sequence ( $\text{RD-90}^\circ\text{-t}_1\text{-90}^\circ\text{-}\tau_m\text{-90}^\circ\text{-acquire}$ ) with  $t_1 = 3 \mu\text{s}$  and  $\tau_m = 100 \text{ ms}$ . Intact tissue was analyzed using a Magic Angle Spinning (MAS) probe with rotation speed set at 5 kHz.  $^1\text{H}$  spectra were acquired using a Carr-Purcell-Meiboom-Gill (CPMG) pulse sequence ( $\text{RD-90}^\circ\text{-}\{\tau\text{-180}^\circ\text{-}\tau\}_n\text{-acquire}$ ) with  $n = 250$  and  $\tau = 400 \mu\text{s}$ . For all spectra, 128 free induction decays (FIDs) were collected into 32 K complex data points, using a spectral width of 12,019 Hz and a 2 s relaxation delay (RD) between pulses. A water pre-saturation pulse was applied throughout the RD. All FIDs were zero filled by a factor of 2 and multiplied by an exponential weighting function equivalent to a line broadening of 1 Hz prior to Fourier transformation (XWINNMR, Bruker). All subsequent data processing and analysis, unless specifically stated otherwise, was conducted using in-house software developed in MATLAB (Mathworks) written and compiled by TMD Ebbels, HC Keun, JT Pearce, and O Cloarec (Imperial College, London). The acquired spectra were corrected for phase and baseline distortions and referenced internally to the anomeric proton signal of

$\alpha$ -glucose at  $\delta$  5.23 or to TSP at  $\delta$  0. Spectra were interpolated to a common ppm scale from 32 to 42 K data points prior to visualization and integration. Spectral assignments were made by a combination of 2D homonuclear experiments, 1D NMR of authentic standards, literature data [25,26], and the Biological Magnetic Resonance Bank (BMRB, <http://www.bmrb.wisc.edu/>) [27]. Glycerophosphoinositol (GPI) was assigned by additional analysis of extracts by  $^1\text{H-}^{31}\text{P}$  correlation spectroscopy (HMQC) using a QXI probe and a Bruker Avance 800 MHz spectrometer, and by comparison to spectra of phosphoinositol standards and literature data [28]. UDP-linked sugars were assigned by data provided by M Coen (Imperial College, London).

#### Spectral Integration and Statistical Analyses

Spectra obtained from aqueous extracts of all groups were averaged to generate an overall median spectrum (reference spectrum). Each individual spectrum was then divided by the reference spectrum to obtain the fold change for each spectral data point. The median of these fold changes was used to normalize each individual spectrum [29]. HRMAS  $^1\text{H-NMR}$  spectra were normalized to creatine (singlet at 3.04 ppm). For quantitation of individual metabolites, signals were integrated at the following resonance frequencies (values in ppm): citrate 2.55 (doublet), choline 3.21 (singlet), phosphocholine (PC) 3.23 (singlet), glycerophosphocholine (GPC) 3.24 (singlet), creatine 3.04 (singlet), GPI 4.27 (triplet), taurine 3.43 (triplet), UDP-linked sugars (UDP $\times$ ) 7.96 (doublet), tyrosine 6.90 (doublet), glucose 5.23 (doublet), aspartate 2.82 (doublet), alanine 1.48 (doublet), lactate 1.33 (doublet), glutamate 2.36 (triplet of doublets). Table I shows the median, minimal, and maximal integration units for each group of mice. Statistical significance was established by Mann–Whitney  $U$ -test. For pattern recognition analysis by hierarchical clustering, data were mean-centered and scaled to unit variance. Single linkage analysis was applied. The software used was written by TMD Ebbels (Imperial College, London) using MATLAB.

#### Immunohistochemical Analysis

Formalin-fixed, paraffin sections (5  $\mu\text{m}$ ) of prostate and a lymph node metastasis were de-waxed in xylene and taken to water through descending concentrations of industrial methylated spirit. They were then placed in citrate buffer (pH 6.0) and microwaved (20 min, 700 W). Sections were placed in distilled water, and endogenous peroxidase activity was blocked with 3% (v/v)  $\text{H}_2\text{O}_2$  in water (20 min). ChK was detected using polyclonal antibodies for murine ChK- $\alpha$  and ChK- $\beta$

**TABLE I. Median Relative Metabolite Peak Areas (A) and Median Metabolite Ratios (B) in Prostate Tissues of C57BL/6J Wild-Type or TRAMP Mice Aged 8 or 28 Weeks**

Metabolite	Relative peak area (min / max)				
	Wild-type 8 weeks	TRAMP 8 weeks	Wild-type 28 weeks	TRAMP 28 weeks	
citrate	1.21 x10 <sup>9</sup> (0.54 x10 <sup>9</sup> / 1.76 x10 <sup>9</sup> )	1.27 x10 <sup>9</sup> (0.52 x10 <sup>9</sup> / 2.14 x10 <sup>9</sup> )	1.72 x10 <sup>9</sup> (0.58 x10 <sup>9</sup> / 2.61 x10 <sup>9</sup> )	0.88 x10 <sup>9</sup> (0.33 x10 <sup>9</sup> / 1.61 x10 <sup>9</sup> )	**
choline	1.13 x10 <sup>9</sup> (0.32 x10 <sup>9</sup> / 2.72 x10 <sup>9</sup> )	0.87 x10 <sup>9</sup> (0.47 x10 <sup>9</sup> / 1.65 x10 <sup>9</sup> )	0.81 x10 <sup>9</sup> (0.57 x10 <sup>9</sup> / 0.96 x10 <sup>9</sup> )	0.54 x10 <sup>9</sup> (0.13 x10 <sup>9</sup> / 0.93 x10 <sup>9</sup> )	*
PC	2.36 x10 <sup>9</sup> (1.60 x10 <sup>9</sup> / 4.31 x10 <sup>9</sup> )	3.44 x10 <sup>9</sup> (1.53 x10 <sup>9</sup> / 4.87 x10 <sup>9</sup> )	5.90 x10 <sup>9</sup> (2.62 x10 <sup>9</sup> / 6.78 x10 <sup>9</sup> )	2.53 x10 <sup>9</sup> (0.39 x10 <sup>9</sup> / 6.44 x10 <sup>9</sup> )	**
GPC	5.22 x10 <sup>9</sup> (2.92 x10 <sup>9</sup> / 10.44 x10 <sup>9</sup> )	6.34 x10 <sup>9</sup> (1.34 x10 <sup>9</sup> / 9.87 x10 <sup>9</sup> )	8.02 x10 <sup>9</sup> (4.92 x10 <sup>9</sup> / 11.23 x10 <sup>9</sup> )	2.75 x10 <sup>9</sup> (0.39 x10 <sup>9</sup> / 5.44 x10 <sup>9</sup> )	**
GPI	2.87 x10 <sup>8</sup> (2.30 x10 <sup>8</sup> / 5.45 x10 <sup>8</sup> )	3.34 x10 <sup>8</sup> (1.87 x10 <sup>8</sup> / 5.76 x10 <sup>8</sup> )	5.24 x10 <sup>8</sup> (4.13 x10 <sup>8</sup> / 5.80 x10 <sup>8</sup> )	2.07 x10 <sup>8</sup> (1.16 x10 <sup>8</sup> / 4.07 x10 <sup>8</sup> )	**
taurine	3.07 x10 <sup>9</sup> (1.64 x10 <sup>9</sup> / 4.72 x10 <sup>9</sup> )	3.03 x10 <sup>9</sup> (1.37 x10 <sup>9</sup> / 4.16 x10 <sup>9</sup> )	2.75 x10 <sup>9</sup> (1.87 x10 <sup>9</sup> / 3.28 x10 <sup>9</sup> )	3.50 x10 <sup>9</sup> (1.40 x10 <sup>9</sup> / 6.10 x10 <sup>9</sup> )	
lactate	2.52 x10 <sup>9</sup> (1.28 x10 <sup>9</sup> / 4.61 x10 <sup>9</sup> )	2.88 x10 <sup>9</sup> (1.01 x10 <sup>9</sup> / 3.90 x10 <sup>9</sup> )	1.90 x10 <sup>9</sup> (1.44 x10 <sup>9</sup> / 3.27 x10 <sup>9</sup> )	1.96 x10 <sup>9</sup> (1.08 x10 <sup>9</sup> / 3.47 x10 <sup>9</sup> )	
glucose	0.84 x10 <sup>8</sup> (0.45 x10 <sup>8</sup> / 1.88 x10 <sup>8</sup> )	0.70 x10 <sup>8</sup> (0.52 x10 <sup>8</sup> / 1.13 x10 <sup>8</sup> )	0.83 x10 <sup>8</sup> (0.60 x10 <sup>8</sup> / 1.22 x10 <sup>8</sup> )	0.38 x10 <sup>8</sup> (0.18 x10 <sup>8</sup> / 0.59 x10 <sup>8</sup> )	**
tyrosine	3.82 x10 <sup>7</sup> (2.54 x10 <sup>7</sup> / 5.33 x10 <sup>7</sup> )	3.11 x10 <sup>7</sup> (2.10 x10 <sup>7</sup> / 4.51 x10 <sup>7</sup> )	2.79 x10 <sup>7</sup> (2.20 x10 <sup>7</sup> / 4.91 x10 <sup>7</sup> )	3.57 x10 <sup>7</sup> (2.02 x10 <sup>7</sup> / 7.60 x10 <sup>7</sup> )	
aspartate	1.78 x10 <sup>8</sup> (1.17 x10 <sup>8</sup> / 2.26 x10 <sup>8</sup> )	1.71 x10 <sup>8</sup> (1.42 x10 <sup>8</sup> / 2.25 x10 <sup>8</sup> )	1.80 x10 <sup>8</sup> (1.44 x10 <sup>8</sup> / 1.93 x10 <sup>8</sup> )	2.02 x10 <sup>8</sup> (1.58 x10 <sup>8</sup> / 3.63 x10 <sup>8</sup> )	*
glutamate	7.91 x10 <sup>8</sup> (5.84 x10 <sup>8</sup> / 9.25 x10 <sup>8</sup> )	7.40 x10 <sup>8</sup> (5.44 x10 <sup>8</sup> / 9.03 x10 <sup>8</sup> )	5.99 x10 <sup>8</sup> (4.81 x10 <sup>8</sup> / 7.19 x10 <sup>8</sup> )	8.32 x10 <sup>8</sup> (4.68 x10 <sup>8</sup> / 12.73 x10 <sup>8</sup> )	
alanine	7.25 x10 <sup>8</sup> (3.90 x10 <sup>8</sup> / 8.99 x10 <sup>8</sup> )	6.07 x10 <sup>8</sup> (3.28 x10 <sup>8</sup> / 8.36 x10 <sup>8</sup> )	4.16 x10 <sup>8</sup> (3.93 x10 <sup>8</sup> / 6.03 x10 <sup>8</sup> )	4.90 x10 <sup>8</sup> (3.07 x10 <sup>8</sup> / 7.15 x10 <sup>8</sup> )	
UDP-sugars	0.59 x10 <sup>8</sup> (0.07 x10 <sup>8</sup> / 1.53 x10 <sup>8</sup> )	0.58 x10 <sup>8</sup> (0.08 x10 <sup>8</sup> / 1.26 x10 <sup>8</sup> )	0.63 x10 <sup>8</sup> (0.41 x10 <sup>8</sup> / 1.51 x10 <sup>8</sup> )	0.34 x10 <sup>8</sup> (0.14 x10 <sup>8</sup> / 0.59 x10 <sup>8</sup> )	*
creatine	1.73 x10 <sup>9</sup> (0.66 x10 <sup>9</sup> / 3.28 x10 <sup>9</sup> )	1.76 x10 <sup>9</sup> (0.66 x10 <sup>9</sup> / 2.96 x10 <sup>9</sup> )	1.56 x10 <sup>9</sup> (1.03 x10 <sup>9</sup> / 2.74 x10 <sup>9</sup> )	2.10 x10 <sup>9</sup> (0.39 x10 <sup>9</sup> / 8.42 x10 <sup>9</sup> )	

TABLE I. (Continued)

Metabolite pair	Peak area ratio (min / max)			
	Wild-type 8 weeks	TRAMP 8 weeks	Wild-type 28 weeks	TRAMP 28 weeks
Cho/Cit	0.79 (0.36 / 5.07)	0.88 (0.22 / 3.20)	0.50 (0.24 / 0.98)	0.56 (0.25 / 1.12)
tCho/Cit	9.35 (4.30 / 16.06)	9.03 (3.96 / 13.35)	9.17 (4.17 / 20.48)	6.76 (2.73 / 16.89)
GPC/PC	2.40 (1.23 / 3.55)	1.88 (0.87 / 2.36)	1.33 (0.92 / 3.33)	1.03 (0.42 / 2.23)
aspartate/PC	0.062 (0.052 / 0.11)	0.056 (0.041 / 0.11)	0.032 (0.027 / 0.055)	0.075 (0.056 / 0.46)
GPI/glutamate	0.48 (0.28 / 0.61)	0.42 (0.26 / 0.69)	0.89 (0.69 / 1.08)	0.25 (0.18 / 0.32)

Values are the median of between 8 and 12 tissue samples, animal groups size was 8–10. Asterisks suggest that differences between median metabolite levels or ratios were significant by Mann–Whitney *U*-test.

\**P* < 0.05.

\*\**P* < 0.01; \*\*\**P* < 0.001. Values in brackets show the minimum and maximum, respectively, for each group.

[30] at a dilution of 1:800. For control staining normal rabbit serum lacking ChK reactivity was used. The primary antibodies were applied to sections and incubated at room temperature (3 hr). Detection was by the DAKO Duet detection system (DAKO, Ely, UK) using 3,3'-diaminobenzidine for visualization. Sections were counterstained with hematoxylin prior to dehydration and mounting.

#### RNA Extraction

Total RNA (duplicate samples) was extracted from prostate tumors from four TRAMP mice, a lymph node metastasis from one TRAMP mouse and normal prostates from two C57BL/6J wild-type mice, all 28 weeks of age. In the case of three tumors and both normal prostates, tissue was taken from two different sites, yielding seven tumor and four normal samples in total. Tissue aliquots (40–60 mg) were homogenized (1 ml TRI reagent) according to the manufacturer's instructions (Sigma-Aldrich Company Ltd). RNA pellets were re-dissolved in water containing diethylpyrocarbonate (0.1%).

#### Real Time PCR Analysis

Primers were designed to cross exon-exon boundaries to eliminate the detection of any contaminating genomic DNA using Primer Express software v2.0 (Applied Biosystems, Warrington, UK). Total RNA (500 ng) was reverse-transcribed using Superscript III RT (Invitrogen, Paisley, UK). The resulting cDNA product was amplified with SYBR Green Mastermix (Applied Biosystems) using an ABI PRISM 7700 RT-PCR Sequence Detection System (Applied Biosystems) and the following optimized primers: 900 nM forward primer and 900 nM reverse primer for ChK- $\alpha$  or ChK- $\beta$  and 900 and 300 nM of forward and reverse primer for  $\beta$ -actin, respectively. The sequences (forward primer/reverse primer) were CTCCCTGC-CAGACTCCATAGC/CTCATCTTTAAGATTGCCC-CATAGAG for ChK- $\alpha$  and CTAGGGCCCCAGCTT-TACG/CCGGCTTGGGAGGTACTGT for ChK- $\beta$ . Expression levels were normalized to those of  $\beta$ -actin. Relative quantification of ChK gene expression was performed with the comparative cycle threshold

method (Applied Biosystems, User Bulletin no 2, 1997). The mean expression level of ChK- $\alpha$  or ChK- $\beta$  in normal prostate samples was used as calibrator.

### cDNA Microarray Analysis

cDNA microarrays were made on aldehyde slides (Genetix, New Milton, UK) using a Stanford type microarray spotter. Targets were the MEEBO set designed in the laboratory of Alizadeh (<http://alizadehlab.stanford.edu/>) and obtained from Invitrogen. Targets were printed from a 10  $\mu$ M solution in 1.5 M Betaine/3X SSC. After printing microarrays were processed according to the manufacturer's (Invitrogen) instructions. RNA (10  $\mu$ g) was labeled using an indirect technique of incorporation of aminoallyl-dUTP (Ambion, Warrington, UK) in the reverse transcription reactions, which were primed using both a locked oligodT<sub>25</sub> primer and pentadecamers. Superscript III (Invitrogen) was used to generate cDNA. After synthesis of labeled cDNA, it was coupled to the Alexa 555 or 647 dyes (Invitrogen). Labeling efficiency was checked using a Nanodrop spectrophotometer. Hybridization was performed under coverslips in a humidified chamber (Genetix) at 42°C in a hybridization buffer, which contained 50% deionized formamide. After hybridization overnight, microarrays were washed to a stringency of 0.05X SSC before drying by centrifugation and scanning using an Axon 4200A scanner and GenePix 5.10.19 (Molecular Devices Coop, Sunnyvale, CA). Data were acquired from the image using GenePix. Data were processed using NorTT and statistical methods published previously [31].

## RESULTS

### Histopathology of TRAMP Prostate Tumor

Normal prostate tissue from C57BL/6J wild-type mice or malignant prostate from TRAMP mice of

8 weeks (in the following referred to as "young") or 28 weeks of age (in the following referred to as "old") were subjected to histopathological investigation. While prostates from wild-type mice did not present with any discernible malignant change, prostate glands from young TRAMP mice showed minimal focal neoplasia (Fig. 1a). Glands in old TRAMP mice were characterized by varying degrees of glandular hyperplasia and atypical hyperplasia (prostatic intraepithelial neoplasia, PIN), carcinomas with microinvasion through to overtly invasive well-differentiated adenocarcinomas (Fig. 1b), which tended to be accompanied by lung metastases. Although within each sample there was a heterogeneous pattern of pathology the assignment of stage was based on the predominant and most advanced pathology, notably whether hyperplasia or well differentiated adenocarcinoma. Some very poorly differentiated tumors were also observed, usually associated with lymph node deposits.

### Comparison of Metabolites in Normal and Malignant Prostate

Extracts of prostate and prostate tumor tissue were subjected to <sup>1</sup>H-NMR analysis. Figure 2A shows a representative <sup>1</sup>H-NMR spectrum of a prostate tissue extract from an old wild-type mouse. Visual comparison of spectra of tissue extracts from wild-type and TRAMP mice suggested differences in resonance intensity between the four groups of mice for citrate, choline, PC, GPC, GPI, lactate, taurine, glucose, tyrosine, aspartate, glutamate, alanine and UDP sugar conjugates (UDP<sub>x</sub>). Metabolite peaks were integrated for comparative quantitative evaluation. There was no significant difference in single metabolite level between young TRAMP and wild-type mice (Table I). In contrast, old TRAMP mice presented with levels of citrate, choline, PC and GPC which were decreased by 49%, 33%, 57%, and 66%, respectively, as compared to normal prostate in age-matched wild-type mice

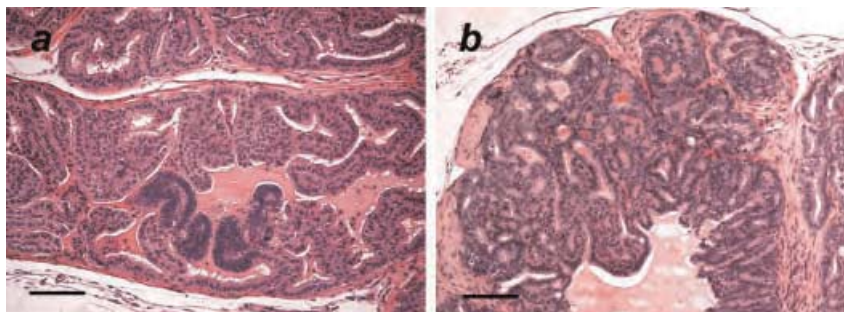


**Fig. 1.** Prostatic tissue from TRAMP mice of 8 (a) or 28 weeks of age (b) stained with hematoxylin and eosin. Dark staining reflects elevated chromatin levels indicating an above-average cell division rate. Note early focal zone of hyperplasia in (a), and edge of a large well differentiated carcinoma showing microinvasion at the periphery in (b). Bar: 100  $\mu$ m. [Color figure can be viewed in the online issue, which is available at [www.interscience.wiley.com](http://www.interscience.wiley.com).]

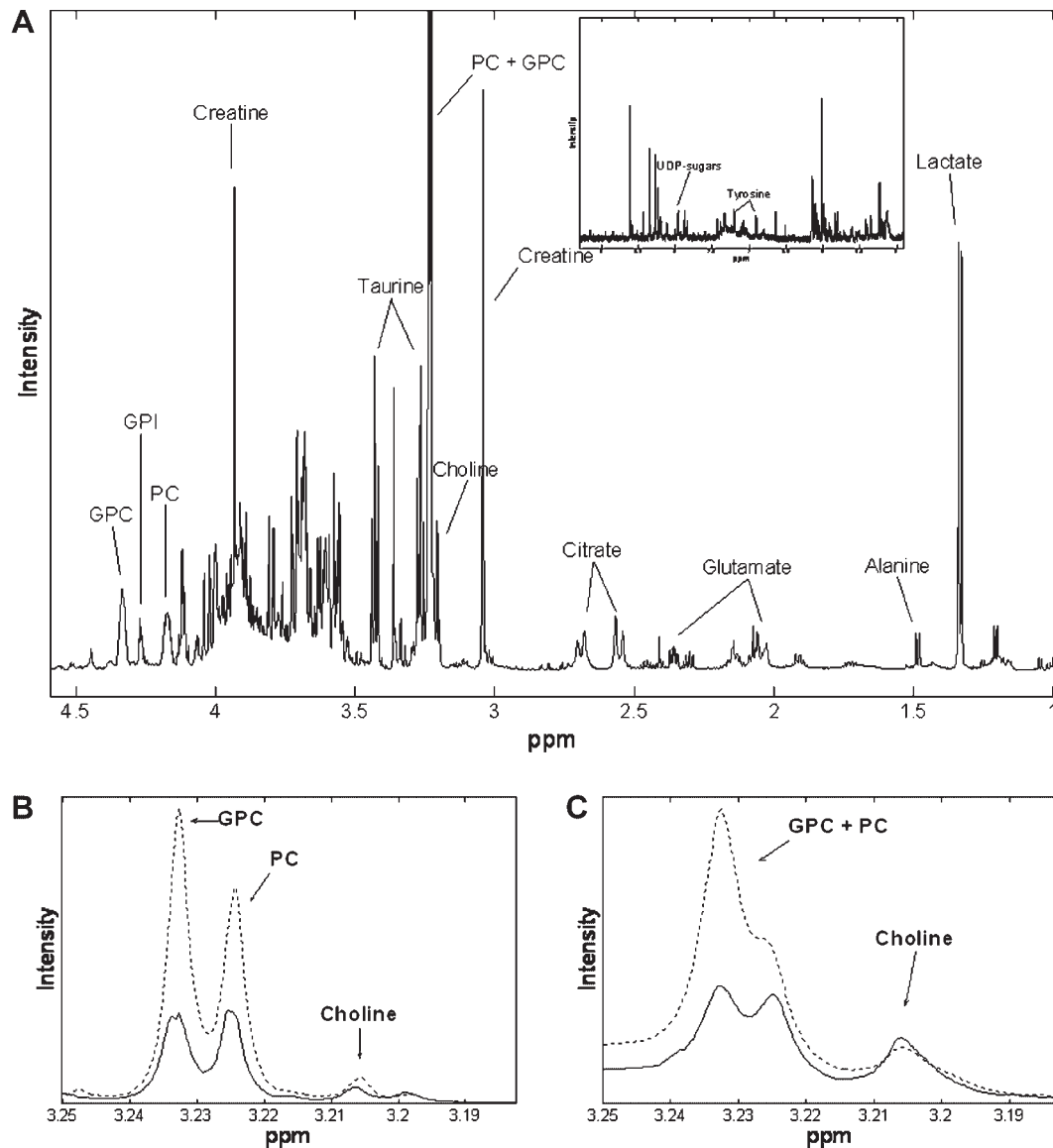


**Fig. 2.**  $^1\text{H}$ -NMR analyses of prostate tissue from 28-week-old mice. **A:** Typical spectrum of the aliphatic and aromatic (insert) regions of an aqueous extract of prostate tissue from a C57BL/6j wild-type mouse. **B,C:** Median  $^1\text{H}$ -NMR spectra of aqueous tissue extracts (B) or median HRMAS NMR spectra of intact tissue (C) of normal prostate from C57BL/6j wild-type mice (broken line) or TRAMP mouse tumors (solid lines). Spectra in (B) and (C) focus on the choline metabolite region.

(Fig. 2B, Table I). GPI in tumor tissue was 61% below normal tissue levels (Table I). Tumor levels of taurine, tyrosine, alanine, glutamate and aspartate were 27%, 28%, 18%, 39%, and 12%, respectively, above those in control prostate, although the difference was significant only in the case of aspartate (Table I). Levels of glucose and UDPx in tumor were decreased by 54% and 45%, respectively, compared to normal tissue. There were no differences between groups in lactate levels (Table I). Although there was a clear difference between normal and TRAMP prostate, there was no correlation between tumor stage and metabolic profile (data not shown). It is conceivable that pathological

assessment was done at a tumor site not exactly identical with that selected for biochemical analysis, particularly in view of the histological heterogeneity within each prostate

Peak intensity ratios of choline to citrate (Cho/Cit) and total choline (choline + PC + GPC) to citrate (tCho/Cit) are commonly used to distinguish normal from malignant prostate tissue in humans [20]. Significant changes in these metabolite ratios were not observed between TRAMP and wild-type mice at either age. However, the GPC to PC ratio (GPC/PC) was decreased by 22% in young TRAMP mice compared to age-matched wild-type mice. There was no significant

difference in this ratio between old TRAMP and wild-type mice (Table I).

Hierarchical clustering analysis of metabolite levels showed that among old mice prostate profiles in wild-type animals formed a cluster distinct from TRAMP tumor profiles (Fig. 3A). In this analysis metabolites separated into two main groups. One group included phospholipid-related species (GPC, PC, GPI, choline), citrate, UDPx and glucose and exhibited lower abundance in tumor tissue than in normal prostate. The other group contained amino acid metabolites, which were more abundant in tumor tissue than in normal prostate. Hierarchical clustering analysis of tissue extracts from young animals did not reveal group-specific clustering (Fig. 3B), hence the clustering between metabolites at this time point was largely driven by normal physiological variation and

not by the presence of malignancy. The pattern of clustering of metabolites at each time point was broadly similar, with the exception of glucose and aspartate. These two species appeared to change clusters depending on presence or absence of malignancy, which suggests that they are related to different metabolites in malignant as compared to normal prostate. This apparent shift in metabolism was also observed when inter-metabolite correlations for TRAMP mice were compared with those in wild-type mice (Fig. 3C,D). These correlations were calculated using data from young and old mice combined, hence patterns obtained reflect variation due to the normal process of aging in wild-type mice and to tumorigenesis in TRAMP mice. This analysis suggests that normal prostate tissue development is accompanied by positive correlation between levels of aspartate and citrate, with both

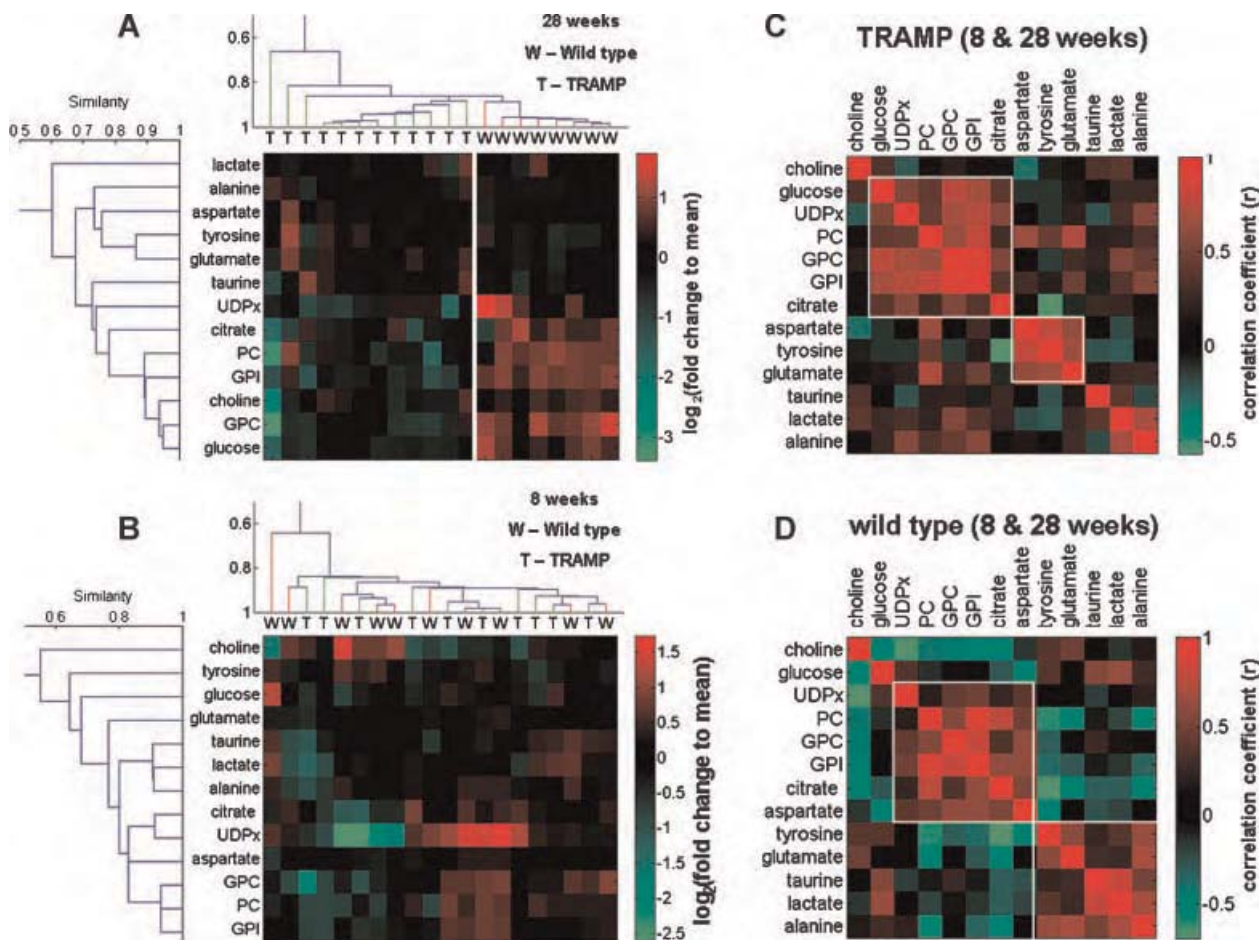


**Fig. 3.** Pattern recognition analyses of variation in metabolite levels in aqueous extracts of prostate tumor tissue or normal prostate tissue from TRAMP or C57BL/6J wild-type mice, respectively, of 8 or 28 weeks of age. **A,B:** Hierarchical clustering of metabolite levels showing that TRAMP and wild-type mice can be distinguished by prostate metabolic profile at 28 weeks of age (A) but not at 8 weeks of age (B). Data are presented as mean-centered  $\log_2$  values, such that a value of 1 indicates a twofold change from the average amount of each metabolite across all samples from the same age group. **C,D:** Matrices of correlation coefficients ( $r$ ) between metabolite levels in extracts of prostate from TRAMP mice at either age (C), or in extracts of normal prostate from wild-type mice at either age (D), showing a difference in metabolite clustering between prostate carcinogenesis and normal prostate aging. [Color figure can be viewed in the online issue, which is available at [www.interscience.wiley.com](http://www.interscience.wiley.com).]

metabolites sharing a common correlation pattern, and by negative correlation between levels of citrate and glucose. The reverse scenario was observed in TRAMP mice, in which there was a positive correlation between levels of citrate and glucose, and both constituted part of the same cluster. In TRAMP mice aspartate was not correlated to citrate and clustered with other amino acids.

We tested the hypothesis that ratios of metabolites allow better discrimination between TRAMP and wild-type animals than levels of individual metabolites. Hierarchical clustering analysis suggests that metabolites from each cluster provides similar information regarding presence of malignancy, and hence that the evaluation of combinations of metabolites from different clusters could be potentially more informative. For example the aspartate/PC ratio was completely discriminatory between the two groups, whereas levels of the individual species were not (Table I). GPI levels separated between old TRAMP and wild-type mice, but the GPI/glutamate ratio improved separation considerably: for GPI alone the difference between the lowest value for wild-type tissue and the highest value for tumor tissue was only 1.3% of the combined wild-type and tumor tissue value range, whilst for the GPI/glutamate ratio this value is 41.1% (Table I). Collectively, the results of the metabolite ratio and clustering analyses provide evidence for an effect of malignancy on the production and/or utilization of metabolites, even when the difference in absolute concentration between wild-type and TRAMP mice was not statistically significant.

The results for choline species obtained in tissue extracts were corroborated by HRMAS <sup>1</sup>H-NMR analysis using intact tissue samples from old mice. Median levels of PC plus GPC as reflected by relative peak areas were 4.33 in tumor samples (minimum 3.21, maximum 4.93) and 9.41 in normal prostate (minimum 2.77, maximum 15.79,  $P=0.101$ , Fig. 2C), suggesting tumor levels were 54% below controls, even though the difference was not significant. There was no discrepancy in choline levels between normal and malignant tissue (Table I).

Results very similar to those shown in Table I were obtained when metabolite levels were related to creatine (singlet 3.04 ppm; results not shown), which has been used previously to normalize metabolite data in human studies [32]. This finding reflects the robustness of the method of normalization used here for data interpretation.

#### Choline Kinase (ChK) Expression in Prostate Tumor

Elevated PC levels and its regulation by ChK has been linked to malignancy [33]. Therefore we tested the

hypothesis that the difference in PC levels observed by <sup>1</sup>H-NMR analysis between normal prostate in C57BL/6J wild-type mice and malignant prostate in TRAMP mice was related to differential ChK expression. Immunohistochemistry of sections of normal or malignant prostate from old mice suggests expression of ChK- $\beta$  protein in the cytoplasm of glandular epithelial cells in the prostate gland (Fig. 4a). In wild-type animals, the staining intensity varied between different lobes of the gland; intense expression was only seen in ventral regions. Hyperplastic glands and well-differentiated carcinomas generally showed low expression (Fig. 4b). Even less or no expression of ChK- $\beta$  was seen in poorly differentiated carcinomas, either in primary tumors or in a lymph node metastasis (Fig. 4C,D). The antibody against ChK- $\alpha$  failed to generate significant staining in any of the tissues studied.

There was no difference in mean expression levels of *ChK- $\alpha$*  or *ChK- $\beta$*  mRNA between wild-type prostate and TRAMP prostate tumor tissue as determined by RT-PCR. In contrast, in the lymph node metastasis sample *ChK- $\alpha$*  and *- $\beta$*  mRNA levels were only 8% and 50%, respectively, of those in normal tissue (result not shown).

#### Kennedy Pathway Gene Expression in Prostate Tumor

cDNA microarray analysis focused on changes in genes specifically linked to metabolic pathways related to phosphatidylcholine synthesis and degradation (Kennedy pathway). In prostate tumor tissue of old TRAMP mice, mRNA expression levels of choline phosphotransferase 1 (*Chpt1*) and lysophospholipase 3 (*Lypla3*) were reduced as compared to normal prostate. Fold reduction was 0.47 for *Chpt1* ( $n=5$  TRAMP and 4 wild-type,  $P=0.008$ ) and 0.57 for *Lypla3* ( $n=7$  TRAMP and 4 wild-type,  $P=0.028$ ). Other significant changes in the expression of genes germane to these pathways, including *ChK*, were not observed, consistent with the results obtained by RT-PCR. Figure 5 illustrates and integrates the findings in TRAMP mouse prostate described here for metabolite and enzyme components of the Kennedy pathway.

#### DISCUSSION

This is the first report of the tumor metabolome in the TRAMP murine model of prostate cancer. When compared to normal prostate, tumor tissue displayed decreased levels of citrate, choline, PC and GPC, GPI and increased levels of taurine, aspartate, tyrosine, and glutamate. These changes were observed in old mice, which presented with histopathologically well established tumors. In young mice, in which histopathological investigation detected subtle preneoplastic

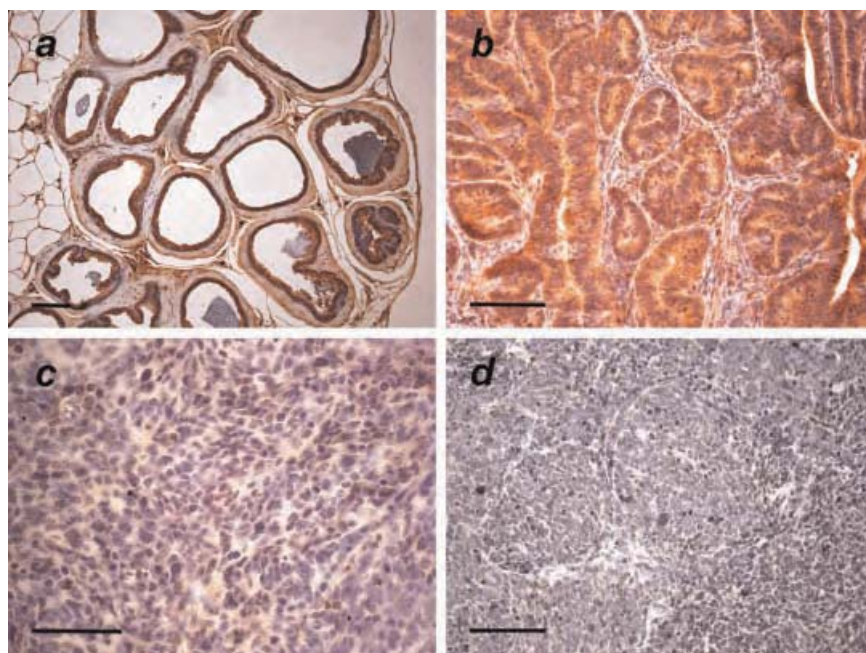


**Fig. 4.** Immunohistochemical staining for ChK- $\beta$  in normal ventral prostate (a) of C57BL/6J wild-type mice, and in prostate tumors, well-differentiated (b) and poorly differentiated (c), or in a pelvic lymph node metastasis (d) in TRAMP mice. All mice were 28 weeks of age. Brown staining intensity reflects presence of enzyme. Bar: 100  $\mu$ m. For details of immunohistochemical analysis see Materials and Methods Section. [Color figure can be viewed in the online issue, which is available at [www.interscience.wiley.com](http://www.interscience.wiley.com).]

lesions, the only metabolic feature which allowed discrimination between TRAMP and wild-type mice was a reduction in the GPC/PC ratio. In the following, the differences in levels of metabolites between TRAMP tumors and normal prostate described here are juxtaposed with those reported in humans.

#### Amino Acids and Citrate

The changes in citrate and taurine in TRAMP tumors described above mimic those reported in humans [14]. In healthy human prostate tissue zinc accumulates and inhibits *m*-aconitase, an enzyme which recycles citrate to oxaloacetate in the Krebs cycle. Thus, in normal prostate, the cycle is truncated resulting in net citrate synthesis [14,34,35]. In prostate cancer such truncation does not exist, which explains why it harbors lower citrate levels than normal prostate. The decrease in citrate observed here in TRAMP tumors is consistent with results in the murine DU-145 prostate xenograft and PB-ErbB-2 $\Delta$ xPten<sup>+/-</sup> models [36,37]. Reduced recycling of citrate in normal prostate means that alternative sources for oxaloacetate are utilized, namely *via* transamination of aspartate, hence prostate tissue contains high levels of this metabolite [13]. According to the results described above, in normal prostate tissue from C57BL/6J mice aspartate concentrations were directly correlated to citrate levels, whilst in TRAMP tumor tissue aspartate was increased and

citrate reduced. These observations suggest that in TRAMP tumors a greater proportion of citrate produced from aspartate is consumed by the Krebs cycle than in normal prostate, mimicking the biochemistry of the human counterpart. The observed increase in other amino acids in tumor, relative to normal prostate, is consistent with a general enhancement in amino acid catabolism *via* the Krebs cycle.

#### Choline Species

Human prostate cancer is characterized by increased choline and choline metabolites when compared to healthy prostate [38,39]. Total choline species (choline, PC plus GPC), and its individual components (choline and PC plus GPC), were reported to be elevated in human prostate samples containing at least 20% malignant tissue, and these measures have been suggested to serve as markers of prostate cancer progression [32]. In contrast to human prostate cancer, prostate tumors from old TRAMP mice with well-established malignancy are shown here to harbor lower choline, PC and GPC than normal prostate. Furthermore, the GPC/PC and total choline/citrate species ratios did not differ between the two tissue types. These results are consistent with a recent analysis in which the total choline/citrate species ratio was measured in TRAMP mouse tumor using <sup>1</sup>H-MR spectroscopic imaging, which did not resolve individual choline

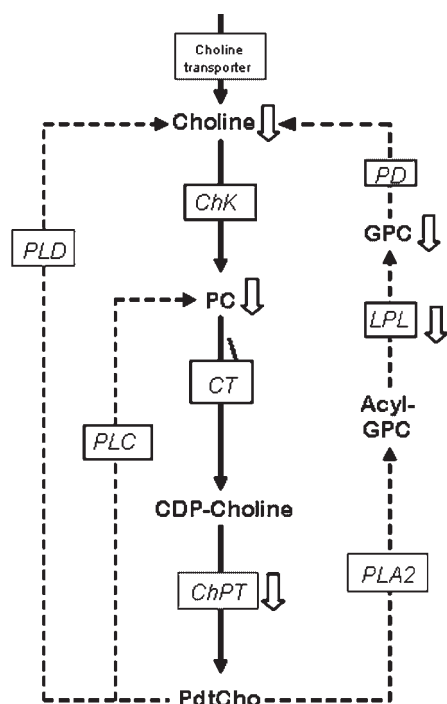


**Fig. 5.** Pathways of phosphatidylcholine synthesis (solid arrows) and degradation (broken arrows). Block arrows indicate changes described here for TRAMP tumor compared to normal prostate in levels of metabolites measured by  $^1\text{H-NMR}$  or of mRNA expression. PC = phosphocholine; GPC = glycerophosphocholine; PtdCho = phosphatidylcholine, *Chk* = choline kinase (E.C. 3.1.4.2), *CT* = CTP:phosphocholine cytidyltransferase (E.C. 2.7.7.15), *ChPT* = choline phosphotransferase (E.C. 2.7.8.2), *PLC* = phospholipase C (E.C. 3.1.4.3), *PLD* = phospholipase D (E.C. 3.1.4.4), *PLA2* = phospholipase A2 (E.C. 3.1.1.4), *LPL* = lysophospholipase (E.C. 3.1.1.5), *PD* = glycerophosphocholine diesterase (E.C. 3.1.4.2).

species [36]. These authors report that in contrast to the finding in TRAMP mice, in PB-ErbB-2 $\Delta$ xPten $^{+/-}$  mouse tumors the total choline/citrate species ratio was increased, consistent with observations in human prostate cancer.

The observed decrease in GPC/PC ratio in young TRAMP mice, which showed only minor signs of dysplasia, is consistent with changes demonstrated in human cancer [15]. This finding suggests that at an early stage of carcinogenesis TRAMP mice may be subject to metabolic alterations similar to those observed in the human disease. However, as carcinogenesis progresses, secondary processes are engaged, which differ between TRAMP mice and humans.

### GPI

Altered levels of GPI have hitherto not been associated with prostate cancer, and the finding presented here, that levels of GPI in TRAMP tumors were lower than in normal prostate, is novel. GPI is

generated by deacylation of membrane phosphoinositides (PIs). PIs occur at micromolar concentrations in most cell types [40,41]. GPI has been found to be elevated in Ras-transformed cell lines [40,42], and exposure to exogenous GPI inhibits tumor cell invasion of the extracellular matrix [43]. The difference in GPI levels observed here between murine prostate and prostate tumor was strongly correlated to differences in levels of PC and GPC, implying commonality in the source of variation or mechanism of regulation. The phospholipid metabolism profile in TRAMP tumors, in which malignancy is driven by SV40 T/t-antigen mediated inactivation of p53 and Rb, may conceivably be influenced by events associated with p53 and/or Rb inactivation. Loss of normal p53 function has been shown to increase glycolysis [44,45], and our observation that TRAMP tumors had lower glucose levels than normal prostate is consistent with this finding.

### Enzymes Affecting Choline Metabolite Levels

Altered choline phospholipid metabolism in human prostate cancer, as compared to normal tissue, has been linked to overexpression of *ChK* [18], and overexpression of *ChK* has been postulated to be a critical requirement for malignant disease progression in breast cancer [33]. Here *ChK* overexpression, or a link between *ChK* expression and PC levels, was not found in TRAMP mice. Regional or lobe-specific differences in enzyme expression might have confounded detection of subtle differences. Our results are consistent with a recent gene expression study, in which *ChK* expression was demonstrated to be decreased in advanced stage TRAMP tumors [46]. These results imply that *ChK* overexpression is not a necessary consequence of, nor a requirement for, TRAMP tumor development, as suggested for mammary tumors [33]. The decrease in GPC observed here in TRAMP tumor as compared to normal prostate might be explained by transcriptional down-regulation of lysophospholipase *Lypla3* (Fig. 5). Malignancy-related underexpression of lysophospholipase has been demonstrated in breast cancer cells [47]. The underexpression of choline phosphotransferase *Chpt1* mRNA shown here in TRAMP tumor, compared to normal prostate, contrasts with overexpression of this enzyme reported in mammary tumors [48,49].

In conclusion, the work described here highlights the potential utility of metabolic profiling in the evaluation of tumor models. The results show both similarities and differences between metabolic profiles associated with prostate cancer in humans and in TRAMP mice. Whilst perturbation in prostate-specific citrate metabolism seems to be conserved in prostate

tumors between rodent prostate carcinogenesis models including TRAMP and humans, regulation of choline metabolism differs between them. NMR methodology has been used before to show that cancer chemotherapeutic intervention changes choline phospholipid metabolite levels [19], and choline kinase inhibition has been suggested as potential prostate cancer chemotherapeutic approach [18]. Hence, the observations presented here imply that the TRAMP model may respond to chemotherapeutic or chemopreventive strategies impinging on choline phospholipid metabolism in a fashion which differs from other rodent models and humans. The results shown here demonstrate that NMR spectroscopy is an eminently suitable tool for the detection of metabolic differences between normal prostate and prostate tumors and for the characterization of biochemical connections between these differences. The results also exemplify the power of the profiling approach, which allows combined measurement of two or more species and their correlation, as it can provide more discriminatory and process-specific biomarkers than single metabolites. Metabolomic profiling by NMR as exemplified by the work shown here may in the future aid cancer detection, patient stratification and pharmacodynamic assessment of cancer chemopreventive or chemotherapeutic interventions.

#### ACKNOWLEDGMENTS

This study was supported by Cancer Research UK program grant C325/A6691 and UK Medical Research Council program grants G0100874UK and G0100873UK. We thank Dr. C Aoyama, Dr. A Ohtani, Dr. K Ishidate (Medical Research Institute, Tokyo Medicinal and Dental University, Japan), Dr. G Wu and Dr. D Vance (Department of Biochemistry, University of Alberta, Canada) for providing antibodies against ChK and Dr. R Davis, JM Edwards, K Phillips, J Riley (MRC Toxicology Unit, Leicester UK), TMD Ebbels, P Simpson (Imperial College London, UK) and S Euden (University of Leicester, UK) for technical assistance.

#### REFERENCES

- Mazhar D, Waxman J. Prostate cancer. *Postgrad Med J* 2002;78: 590–595.
- Greenberg NM, DeMayo F, Finegold MJ, Medina D, Tilley WD, Aspinall JO, Cunha GR, Donjacour AA, Matusik RJ, Rosen JM. Prostate cancer in a transgenic mouse. *Proc Natl Acad Sci USA* 1995;92:3439–3443.
- Gingrich JR, Barrios RJ, Morton RA, Boyce BF, DeMayo FJ, Finegold MJ, Angelopoulou R, Rosen JM, Greenberg NM. Metastatic prostate cancer in a transgenic mouse. *Cancer Res* 1996;56:4096–4102.
- Bookstein R, Rio P, Madreperla SA, Hong F, Allred C, Grizzle WE, Lee WH. Promoter deletion and loss of retinoblastoma gene expression in human prostate carcinoma. *Proc Natl Acad Sci USA* 1990;87:7762–7766.
- Rubin SJ, Hallahan DE, Ashman CR, Brachman DG, Beckett MA, Virudachalam S, Yandell DW, Weichselbaum RR. Two prostate carcinoma cell-lines demonstrate abnormalities in tumor suppressor genes. *J Surg Oncol* 1991;46:31–36.
- Verschoyle RD, Greaves P, Cai H, Edwards RE, Steward WP, Gescher AJ. Evaluation of the cancer chemopreventive efficacy of rice bran in genetic mouse models of breast, prostate and intestinal carcinogenesis. *Br J Cancer* 2007;96:248–254.
- Gupta S, Hastak K, Ahmad N, Lewin JS, Mukhtar H. Inhibition of prostate carcinogenesis in TRAMP mice by oral infusion of green tea polyphenols. *Proc Natl Acad Sci USA* 2001;98:10350–10355.
- Raghow S, Hooshdaran MZ, Katiyar S, Steiner MS. Toremifene prevents prostate cancer in the transgenic adenocarcinoma of mouse prostate model. *Cancer Res* 2002;62:1370–1376.
- Morales PR, Dillehay DL, Moody SJ, Pallas DC, Pruet S, Allgood JC, Symolon H, Merrill AH. Safingol toxicology after oral administration to TRAMP mice: Demonstration of safingol uptake and metabolism by N-acylation and n-methylation. *Drug Chem Toxicol* 2007;30:197–216.
- Warburg O, Wind F, Negelein E. Ueber den Stoffwechsel von Tumoren im Koerper. *Klin Wochenschr* 1926;5:829–832.
- Modica-Napolitano JS, Singh KK. Mitochondrial dysfunction in cancer. *Mitochondrion* 2004;4:755–762.
- Baggetto LG. Deviant energetic metabolism of glycolytic cancer cells. *Biochimie* 1992;74:959–974.
- Costello LC, Franklin RB. 'Why do tumour cells glycolyse?': From glycolysis through citrate to lipogenesis. *Mol Cell Biochem* 2005;280:1–8.
- Costello LC, Franklin RB. The clinical relevance of the metabolism of prostate cancer; zinc and tumor suppression: Connecting the dots. *Mol Cancer* 2006 [Serial on the Internet] 5: 17.
- Glunde K, Serkova NJ. Therapeutic targets and biomarkers identified in cancer choline phospholipid metabolism. *Pharmacogenomics* 2006;7:1109–1123.
- Griffin JL, Kauppinen RA. Tumour metabolomics in animal models of human cancer. *J. Proteome Res* 2007;6:498–505.
- Griffin JL, Shockcor JP. Metabolic profiles of cancer cells. *Nat Rev Cancer* 2004;4:551–561.
- Ramírez de Molina A, Rodríguez-González A, Gutiérrez R, Martínez-Pineiro L, Sanchez JJ, Bonilla F, Rosell R, Lacal JC. Overexpression of choline kinase is a frequent feature in human tumor-derived cell lines and in lung, prostate, and colorectal human cancers. *Biochem Biophys Res Commun* 2002;296:580–583.
- Al-Saffar NMS, Troy H, Ramírez de Molina A, Jackson LE, Madhu B, Griffiths JR, Leach MO, Workman P, Lacal JC, Judson IR, Chung YL. Noninvasive magnetic resonance spectroscopic pharmacodynamic markers of the choline kinase inhibitor MN58b in human carcinoma models. *Cancer Res* 2006;66:427–434.
- Kurhanewicz J, Vigneron DB, Hricak H, Narayan P, Carroll P, Nelson SJ. Three-dimensional H-1 MR spectroscopic imaging of the in situ human prostate with high (0.24–0.7-cm(3)) spatial resolution. *Radiology* 1996;198:795–805.
- Schick F, Bongers H, Kurz S, Jung WI, Pfeffer M, Lutz O. Localized proton MR spectroscopy of citrate in vitro and of the human prostate in vivo at 1.5 T. *Magn Reson Med* 1993; 29:38–43.

22. Cheng LL, Burns MA, Taylor JL, He WL, Halpern EF, McDougal WS, Wu CL. Metabolic characterization of human prostate cancer with tissue magnetic resonance spectroscopy. *Cancer Res* 2005;65:3030–3034.
23. Workman P, Twentyman P, Balkwill F, Balmain A, Chaplin D, Double J, Embleton J, Newell D, Raymond R, Stables J, Stephens T, Wallace J. United Kingdom Co-ordinating Committee on Cancer Research (UKCCCR) guidelines for the welfare of animals in experimental neoplasia (second edition). *Br J Cancer* 1998;77:1–10.
24. Shappell SB, Thomas GV, Roberts RL, Herbert R, Ittmann MM, Rubin MA, Humphrey PA, Sundberg JP, Rozengurt N, Barrios R, Ward JM, Cardiff RD. Prostate pathology of genetically engineered mice: Definitions and classification. The consensus report from the Bar Harbor meeting of the mouse models of human cancer consortium prostate pathology committee. *Cancer Res* 2004;64:2270–2305.
25. Fan WMT. Metabolite profiling by one- and two-dimensional NMR analysis of complex mixtures. *Prog NMR Spectrosc* 1996;28:161–219.
26. Nicholson JK, Foxall PJD, Spraul M, Farrant RD, Lindon JC. 750 MHz <sup>1</sup>H and <sup>1</sup>H-<sup>13</sup>C NMR spectroscopy of human blood plasma. *Anal Chem* 1995;67:793–811.
27. Seavey BR, Farr EA, Westler WM, Markley JL. A relational database for sequence-specific protein NMR data. *J Biomol NMR* 1991;1:217–236.
28. van der Rest B, Boisson AM, Gout E, Bligny R, Douce R. Glycerophosphocholine metabolism in higher plant cells. Evidence of a new glyceryl-phosphodiester phosphodiesterase. *Plant Physiol* 2002;130:244–255.
29. Dieterle F, Ross A, Schlotterbeck G, Senn H. Probabilistic quotient normalization as robust method to account for dilution of complex biological mixtures. Application in <sup>1</sup>H NMR metabonomics. *Anal Chem* 2006;78:4281–4290.
30. Aoyama C, Ohtani A, Ishidate K. Expression and characterization of the active molecular forms of choline/ethanolamine kinase- $\alpha$  and - $\beta$  in mouse tissues, including carbon tetrachloride-induced liver. *Biochem J* 2002;363:777–784.
31. Zhang SD, Gant TW. A statistical framework for the design of microarray experiments and effective detection of differential gene expression. *Bioinformatics* 2004;20:2821–2828.
32. Swanson MG, Vigneron DB, Tabatabai ZL, Males RG, Schmitt L, Carroll PR, James JK, Hurd RE, Kurhanewicz J. Proton HR-MAS spectroscopy and quantitative pathologic analysis of MRI/3D-MRSI-targeted postsurgical prostate tissues. *Magn Reson Med* 2003;50:944–954.
33. Ramírez de Molina A, Báñez-Coronel M, Gutiérrez R, Rodríguez-González A, Olmeda D, Megías D, Lacal JC. Choline kinase activation is a critical requirement for the proliferation of primary human mammary epithelial cells and breast tumor progression. *Cancer Res* 2004;64:6732–6739.
34. Costello LC, Franklin RB. Bioenergetic theory of prostate malignancy. *Prostate* 1994;25:162–166.
35. Costello LC, Franklin RB. The metabolism of prostate malignancy: Insight into the pathogenesis of prostate cancer and new approaches for its diagnosis and treatment. *Oncol Spectr* 2001;2:452–457.
36. Fricke ST, Rodriguez O, VanMeter J, Dettin LE, Casimiro M, Chien CD, Newell T, Johnson K, Ileva L, Ojeifo J, Johnson MD, Albanese C. In vivo magnetic resonance volumetric and spectroscopic analysis of mouse prostate cancer models. *Prostate* 2006;66:708–717.
37. Kurhanewicz J, Dahiya R, MacDonald JM, Chang L-H, James TL, Narayan P. Citrate alterations in primary and metastatic human prostatic adenocarcinomas: <sup>1</sup>H magnetic resonance spectroscopy and biochemical study. *Magn Reson Med* 1993;29:149–157.
38. Kurhanewicz J, Vigneron DB, Nelson SJ. Three-dimensional magnetic resonance imaging of brain and prostate cancer. *Neoplasia* 2000;2:166–189.
39. Jana S, Blaurock MD. Nuclear medicine studies of the prostate, testes, and bladder. *Semin Nucl Med* 2006;36:51–72.
40. Alonso T, Morgan RO, Marvizon JC, Zarbl H, Santos E. Malignant transformation by ras and other oncogenes produces common alterations in inositol phospholipid signaling pathways. *Proc Natl Acad Sci USA* 1988;85:4271–4275.
41. Falasca M, Carvelli A, Iurisci C, Qiu RG, Symons MH, Corda D. Fast receptor-induced formation of glycerophosphoinositol-4-phosphate, a putative novel intracellular messenger in the Ras pathway. *Mol Biol Cell* 1997;8:443–453.
42. Valitutti S, Cucchi P, Colletta G, Di Filippo C, Corda D. Transformation by the K-ras oncogene correlates with increases in phospholipase A2 activity, glycerophosphoinositol production and phosphoinositide synthesis in thyroid cells. *Cell Signal* 1991;3:321–332.
43. Buccione R, Baldassarre M, Trapani V, Catalano C, Pompeo A, Brancaccio A, Giavazzi R, Luini A, Corda D. Glycerophosphoinositols inhibit the ability of tumour cells to invade the extracellular matrix. *Eur J Cancer* 2005;41:470–476.
44. Bensaad K, Tsuruta A, Selak MA, Vidal MNC, Nakano K, Bartrons R, Gottlieb E, Vousden KH. TIGAR, a p53-inducible regulator of glycolysis and apoptosis. *Cell* 2006;126:107–120.
45. Matoba S, Kang JG, Patino WD, Wragg A, Boehm M, Gavrilova O, Hurley PJ, Bunz F, Hwang PM. p53 regulates mitochondrial respiration. *Science* 2006;312:1650–1653.
46. Morgenbesser SD, McLaren RP, Richards B, Zhang M, Akmaev VR, Winter SF, Mineva ND, Kaplan-Lefko PJ, Foster BA, Cook BP, Dufault MR, Cao X, Wang CJ, Teicher BA, Klinger KW, Greenberg NM, Madden SL. Identification of genes potentially involved in the acquisition of androgen-independent and metastatic tumor growth in an autochthonous genetically engineered mouse prostate cancer model. *Prostate* 2006;67:83–106.
47. Glunde K, Jie C, Bhujwala ZM. Molecular causes of the aberrant choline phospholipid metabolism in breast cancer. *Cancer Res* 2004;64:4270–4276.
48. Akech J, Roy SS, Das SK. Modulation of cholinephosphotransferase activity in breast cancer cell lines by Ro5-4864, a peripheral benzodiazepine receptor agonist. *Biochem Biophys Res Commun* 2005;333:35–41.
49. Ghosh A, Akech J, Mukherjee S, Das SK. Differential expression of cholinephosphotransferase in normal and cancerous human mammary epithelial cells. *Biochem Biophys Res Commun* 2002;297:1043–1048.

# Investigation of analytical variation in metabonomic analysis using liquid chromatography/mass spectrometry

Tim P. Sangster<sup>1\*</sup>, Julie E. Wingate<sup>2</sup>, Lyle Burton<sup>3</sup>, Friederike Teichert<sup>4</sup> and Ian D. Wilson<sup>5</sup>

<sup>1</sup>Huntingdon Life Science, East Millstone, NJ 08875-2360, USA

<sup>2</sup>Applied Biosystems, Toronto, Canada

<sup>3</sup>MDS Sciex, Toronto, Canada

<sup>4</sup>Cancer Biomarkers and Prevention Group, Department of Cancer Studies and Molecular Medicine, University of Leicester, Leicester, UK

<sup>5</sup>AstraZeneca, Department of Drug Metabolism and Pharmacokinetics, Alderley Park, Macclesfield, Cheshire SK10 4TG, UK

Received 9 April 2007; Revised 28 June 2007; Accepted 29 June 2007

**Sources of analytical variation in high-performance liquid chromatography/mass spectrometry (HPLC/MS), such as changes in retention, mass accuracy or signal intensity, have been investigated to assess their importance as a variable in the metabonomic analysis of human urine. In this study chromatographic retention and mass accuracy were found to be quite reproducible with the most significant source of analytical variation in the data sets obtained being the result of changes in detector response. Depending on the signal intensity threshold used to define the presence of a peak a sample component could be present in some replicate injections and absent in others within the same run. The implementation of a more sophisticated data software analysis package was found to greatly reduce the impact of detector response variability resulting in improved data analysis. Copyright © 2007 John Wiley & Sons, Ltd.**

Metabonomics and metabolomics investigations are based on the ability of the analyst to obtain robust and comprehensive global metabolite profiles from complex biological samples such as plasma, urine and tissue extracts.<sup>1–3</sup> Currently, a range of analytical methods are used to interrogate such samples including liquid chromatography/mass spectrometry (LC/MS), gas chromatography/mass spectrometry (GC/MS), capillary electrophoresis/mass spectrometry (CE/MS) and nuclear magnetic resonance (NMR) spectroscopy (recently reviewed in<sup>4</sup>). There are many sources of confounding variables that can be encountered in such studies, many of which result from differences in, e.g., factors such as diet, diurnal variation, strain, gender, age, disease state, drug treatment, etc., and often such factors dominate the final metabolite profile.<sup>5–8</sup> Assuming that such variables can be controlled, or at least monitored, the next important source of variability comes from the analytical method itself. A number of studies have now been published that have emphasized the analytical reproducibility of NMR spectroscopic methods,<sup>9,10</sup> but, no doubt as a result of its relatively recent application as a tool in this area, this is not yet the case for LC/MS. Indeed, it is our experience that a major difficulty, when chromatographic techniques are employed, is ensuring that the analytical reproducibility of the method is acceptable. Variability in the analytical method (as opposed to the biological variability found in the samples) can result from a variety of sources. Thus, methods for endogenous metabolites that employ either high-performance liquid chromatography (HPLC), or particularly

GC/MS, generally require some sample preparation. In the case of GC-based analysis such sample preparation is often extensive and multi-step,<sup>11</sup> introducing the potential for numerous sources of irreproducibility. The subsequent chromatographic separation, and then detection using MS, can also provide much potential for variability. Chromatographic techniques are liable to degradation over time due to column contamination whilst the response of the mass spectrometer can also decline as contamination builds up. As we have discussed elsewhere these factors can be controlled to some extent using internal standards and quality control samples.<sup>12</sup> However, as LC/MS evolves from an experimental to a routine metabolomic/metabonomics tool, there will be an increasing emphasis on producing robust, reproducible and validated methods (e.g. see<sup>13–15</sup>).

Here we describe the results of investigations into the causes and importance of particular aspects of analytical variability in the collection and analysis of global metabolite profiling data and techniques to minimize their effects.

## EXPERIMENTAL

### Materials

All solvents used were of HPLC grade and obtained from Fisher Scientific (Loughborough, UK). Water (18.2 MΩ) was obtained from a Purelab Ultra system (Elga, Bucks, UK). All reagents were of analytical or higher grade and were obtained from Fisher Scientific or Sigma-Aldrich (Dorset, UK).

\*Correspondence to: T. P. Sangster, Huntingdon Life Science, East Millstone, NJ 08875-2360, USA.  
E-mail: Sangstert@princeton.huntingdon.com

## Sample preparation

Mouse and human urine samples were stored frozen at  $-80^{\circ}\text{C}$  and  $-20^{\circ}\text{C}$ , respectively, until analysis. For HPLC/MS the samples were subjected to minimal sample pre-treatment involving dilution with 0.1% aqueous formic acid in a ratio 1:5 v/v. These diluted samples were transferred into autosampler vials and then vortex mixed. The vials were then centrifuged at 3000 rpm for 2 min prior to analysis. The use of these samples is described more fully in the text.

## HPLC/MS

Chromatography was performed on a  $3.5\ \mu\text{m}$  Symmetry C18  $100 \times 2.1\ \text{mm}$  HPLC column (Waters, Milford, MA, USA) using gradient elution with a mobile phase of 0.1% formic acid in acetonitrile and 0.1% formic acid aq. at a flow rate of  $0.4\ \text{mL}/\text{min}$ . The HPLC system consisted of a CTC Pal autosampler (CTC Analytics, Zwingen, Switzerland) connected to a PE200 micro binary solvent delivery system (Perkin Elmer Ltd., Norwalk, CT, USA). Mass spectrometry was carried out using a 4000 QTRAP<sup>®</sup> mass spectrometer (Applied Biosystems, Concord, ON, Canada), with the Turbo Ion Spray<sup>®</sup> inlet in positive ion mode. Analysis was performed using a linear reversed-phase gradient elution, starting at 5% acetonitrile and rising to 95% acetonitrile over 10 min. Mouse urine samples were analyzed in negative ion mode. A similar LC method was used. Initial conditions were 100% A and remained at 100% A for 0.5 min. This then increased gradually to 20% B at 4 min and 95% B at 8 min. The mobile phase remained at 95% B for a further 1 min before returning to the starting conditions.

## Data analysis

All mass spectrometric data were acquired using Analyst<sup>®</sup> 1.4.1 and the initial metabolomic interpretation was performed using Markerview<sup>™</sup> software versions 1.0.0.3 and 1.1.0.1. As described in the text, experience with the first software version led to the development of the second version, which allowed peak re-integration directly from the raw data (see later) and permits the data from several samples to be compared so that differences can be identified. This is done by applying principal components analysis (PCA) to discover groupings and relationships between both the samples and the variables (LC/MS peaks consisting of retention, mass and intensity data). However, before PCA can be applied, the data must first be transformed into a two-dimensional (2D) format containing peak responses or areas with the distinct variables or peaks as one dimension and the individual samples as the other dimension. The general process used by the software is illustrated in Fig. 1 and is discussed more fully in the Results and Discussion section, where appropriate.

## RESULTS AND DISCUSSION

Small variations between runs are to be expected in any LC/MS-based procedure and, as a result, in conventional bioanalysis, internal standards and quality control (QC) samples are routinely used. As we have discussed elsewhere<sup>12</sup> it is difficult to do this in metabolomics because the

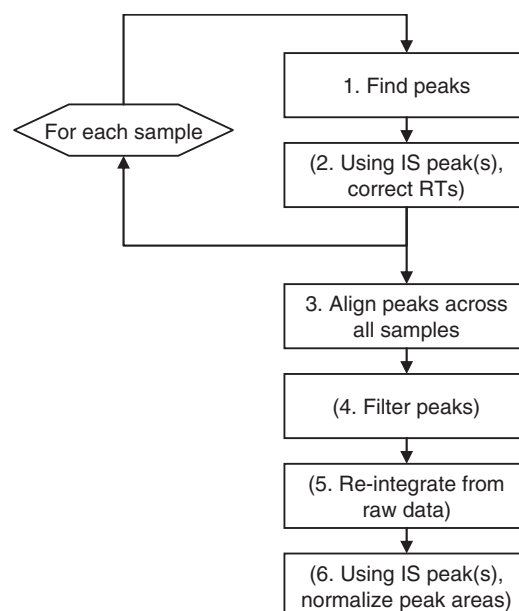


**Figure 1.** Peak finding and subsequent processing takes place in the order shown in the flowchart. The steps shown in parentheses are optional within the software; for this work steps 2 and 6 were not performed. For details of each step, see the main text.

identities of many of the analytes that are likely to be present in the sample are currently unknown. However, a simple and pragmatic approach is to use a 'standard' sample of the biofluid under investigation as a QC sample and analyze it on multiple occasions through the run. After the run is completed PCA can be performed and the tightness with which the 'QC' samples cluster provides an indication of the analytical variation in the system; this can be used to assess the 'process' as opposed to the biological variability and gives an indication of the quality of the data. This is illustrated in Fig. 2 where a 'test' set of mouse urine samples have been analyzed together with multiple injections of a urine sample prepared by mixing aliquots of all of the test samples to make a pool which was used as a 'QC' sample, as described elsewhere.<sup>12</sup> As can be seen from this figure, there is variation between the replicate analyses of the pooled urine QC sample, shown as stars near the centre of the figure. As these samples are identical this result can only be attributed to analytical (process) variation. As we have described elsewhere,<sup>12,15</sup> some of the variation in the first few injections seen with such QC samples was due to changes in chromatographic retention time as the chromatographic system stabilizes (presumably as the result of the need to 'condition' the system by masking active sites such as, e.g., silanols on the stationary phase). However, once the system had achieved chromatographic equilibrium, indicated by the relatively tight clustering of seven of the eight QC samples shown in Fig. 2, we have found that retention times are generally quite stable.<sup>15</sup> However, to eliminate the variability in the first few samples due to this system conditioning, it is our standard practice to run several QC samples prior to the start of the main run.<sup>12,15</sup> The remaining variability, however, is due to other causes and further investigations were undertaken with the aim of reducing,

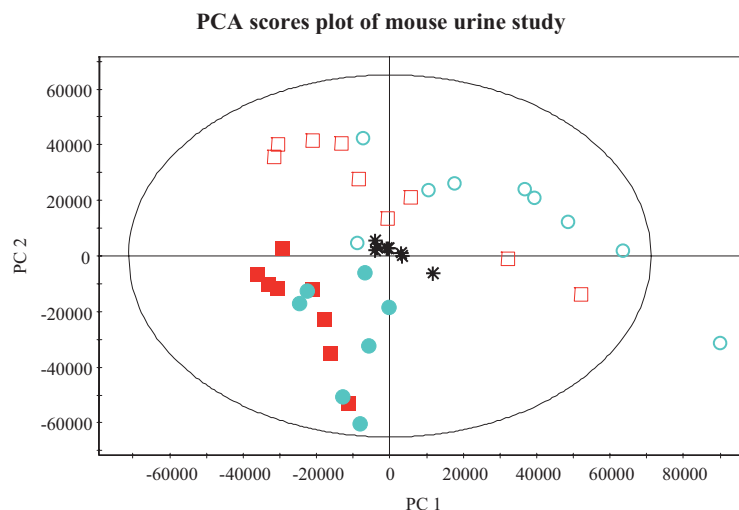


**Figure 2.** PCA scores plot of a metabolomics study on mouse urine (four groups). The coloured circles and squares represent individual samples; the black stars represent repeated injections of the QC sample. Data were centred and Pareto scaled prior to PCA (SIMCA-P+, Umetrix).

controlling and understanding its causes. This was undertaken in the belief that, by reducing the process variation as much as possible, there would be reduced noise within the data set and, hence, the statistical analysis would be less complex and more likely to give interpretable data.

We therefore further investigated variability in some of the important parameters such as peak picking, chromatographic retention, mass accuracy and signal intensity, which are used in data processing. Thus, the first major step in constructing the 2D data sets used for PCA is to find the individual LC/MS peaks for each sample. It is important that these variables represent the same compound in every sample, so the next major step is alignment, which ensures that this is the case by adjusting the data for small variations in mass and retention time. Figure 1 shows the order for the peak-finding and other processing steps (note that although present in the software, steps 2 and 6 were not used in this study). These steps are considered in detail below.

Peaks are found in the LC/MS data using an algorithm known as 'Enhance', which processes each of the mass spectra for a given run in order of increasing scan number. The algorithm first locates crude peak 'clusters' or 'islands' as follows: Each spectrum is background subtracted. For this work, the current spectrum to be processed was subtracted by the spectrum ten scans earlier, with the intensities of the background spectrum first multiplied by a factor of 1.3 (the very first ten spectra are not processed). This procedure prevents the algorithm reporting multiple peaks for noisy background ions. A threshold (here  $2.5 \times 10^4$  counts/s) was applied to the spectra such that {mass, intensity} data points with intensity less than the threshold are removed from the spectrum. This threshold intensity was chosen pragmatically as being close to the limits of detection for analyte peaks that are generally observed in urine samples under these analytical conditions. Working from low  $m/z$  to high  $m/z$ , each consecutive run of non-zero intensity (i.e. one spectral

peak or group of overlapping peaks) in the current spectrum is treated as a potential cluster. If the mass range overlaps that of any currently active cluster within an absolute or relative error (here 0.25 Da) the run is merged into that cluster, otherwise it defines a new cluster. Merging means that the run, treated as a limited mass-range mini-spectrum, is added to the current mini-spectrum for the cluster.

After each spectrum has been processed, any active clusters which have no data merged from the current spectrum are considered to be finished and no longer active. Clusters for which both the mass and retention time ranges of data merged that are larger than specified minima (here 0.5 Da and 2 cycles) are kept for further processing, otherwise they are discarded.

Once all spectra for the sample have been processed, the net result is a collection of clusters which are (essentially) limited mass-range spectra summed over the cycle range for the corresponding LC peak.

For high-resolution instruments, each cluster will generally correspond to one particular isotopic form of a given compound. However, for quadrupole data such as used here, the cluster may correspond to a mass range comprising some or all adjacent isotopic forms – depending on whether the 'dip' between spectral peaks is above or below the threshold (here  $2.5 \times 10^4$  counts/s) mentioned above. For this reason, a spectral-only peak finder was applied to the limited mass-range spectra for each cluster to (potentially) break the cluster into separate peaks corresponding to each isotope.

The final result for each sample was a collection of peaks comprising a retention time range and a mass range (i.e. a start and stop RT and mass) with a peak area. The centroid mass and the retention time of the largest cluster originally merged into the peak were also tracked.

Taking the thought experiment that assumes that the peak-picking software itself is reliable and reproducible, then, if the analytical data presented to it from a number of

repeat analyses of the same sample are identical (as a result of perfect analytical reproducibility), then all of the samples should cluster together. This assumption was tested by using the data from a single sample and replicating it ten times on the computer, thereby providing a 'perfect' data set free from analytical variation. When this perfect electronic data set was processed through the software via PCA it unsurprisingly showed the data clustering as a single point. This result was then compared against the data derived from the repeated LC/MS analysis of a urine sample and processed using the same peak-picking software. For this analysis a retention time window of 0.3 min was selected for chromatographic retention times within the peak-picking method, so that any shifts in retention greater than this window would be expected to result in significant analytical variation. This corresponds to step 3 of Fig. 1 where peaks are aligned across all samples. A mass tolerance of 0.4 Da was also used. Thus cross-sample alignment was performed to determine if two {mass, RT} peaks found in different samples represent the same underlying chemical component or not. If their masses and retention times are both within specific absolute or relative tolerances this was assumed to be the case. This alignment procedure was also applied within one sample. If a single noisy chromatographic peak was initially found as two or more separate entities, this procedure allowed them to be recombined into a single peak. The extracted ion chromatograms (XICs) from samples were examined and the retention times compared throughout the repeated analysis of the same sample with the result that over 100 replicate runs of a single human urine sample, none of the selected marker ions moved outside of the 0.3 min retention window set in the peak-picking parameters (data not shown). The change in mass accuracy throughout the analysis was monitored for a selection of analytes and, although the mass accuracy was not absolute, it did allow the markers to be correctly assigned within the analysis (data not shown). However, despite this acceptable chromatographic and mass accuracy performance, the real data sets, as illustrated in Fig. 3, showed significant differences between replicate injections within the analysis and did not cluster as a single point, unlike the 'perfect' electronic data set. The differences seen in the real data set, which are attributable to analytical variation, must (if not the result of mass or retention time variability) be due to some other factor. This observation led us to consider the effects of changes in peak intensity as a variable. This is potentially a very important factor as one of the steps in the data-processing software for peak picking enables the aligned peak list to be optionally

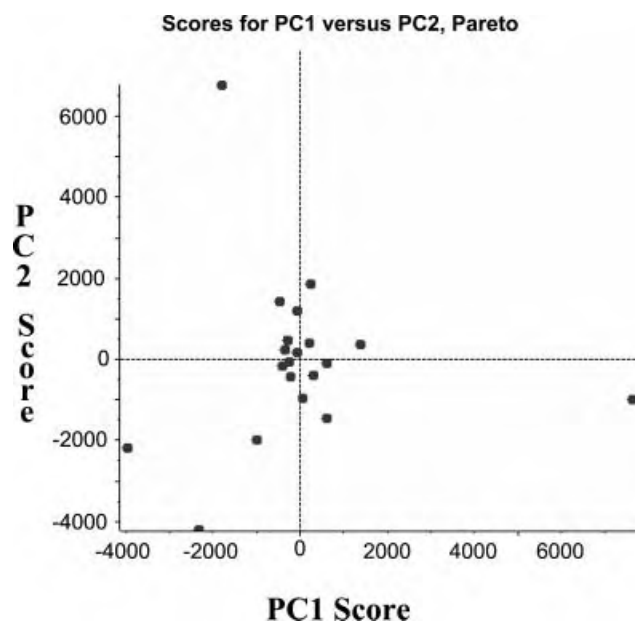


**Figure 3.** Principal components analysis of the single sample of human urine analysis from repeat analysis.

filtered to remove specific entries. In particular, peaks for which the maximum peak height (for all samples) is below a threshold, in this instance  $5e4$  counts/s, as well as known background peaks with specific  $m/z$  and RT, and peaks outside a specific retention time range are automatically removed. It is also possible to limit the total number of peaks by removing the smallest ones. To investigate the change in intensities between samples the XICs from the samples were examined and the intensity compared throughout the analysis. The peak area reported from the peak picking was also examined once markers had been assigned within the software.

A change in signal intensity was indeed observed in both the XICs and the mass chromatograms between samples. This is not unexpected, as signal intensity in the mass spectrometer using electrospray can be subject to variation. Examination of the reported peak areas (see Table 1 for an example of a small subset of the data) showed that, for a selection of the replicates, there are markers where no peak area has been reported, giving rise to zero values in the table, despite the fact that these compounds must have been present as they were detected in the remaining samples. On investigation it was found that, although no peak area had been reported, there were indeed detectable peaks for these

**Table 1.** Excerpt of the Marker list from two-subject experiment. Mass charge ratio vs. retention time vs. area (counts)

Mass/charge ratio ( $m/z$ )	Retention time (min)	Subject 1 Injection 2	Subject 2 Injection 2	Subject 1 Injection 3	Subject 2 Injection 3
674.4	6.4	0	0	0	0
674.7	10.0	60114000	67521000	83911000	56053000
675.3	1.4	2199700	10638000	2662300	0
675.5	3.3	0	31289000	0	4420800
680.0	5.0	0	0	0	0
684.0	6.4	0	0	0	0
685.1	1.3	0	0	0	0
686.4	3.3	492510	71193000	0	19692000

analytes but in some analyses the intensities were below that set for the threshold value used in the peak picking. However, simply reducing the threshold was not a practical solution to 'recovering' these peaks as this just moved the problem to a different set of markers. Eliminating the threshold value resulted in the data becoming completely unusable due to the increased number of markers, which

were difficult to distinguish from noise. This illustrates one of the problems associated with a pure peak-finding approach, namely that small or noisy peaks which are present for a particular sample may be missed. Using the algorithm described here, this will be the case for peaks below the initial threshold; the assumption is that such peaks are of limited importance, but this may not always be the

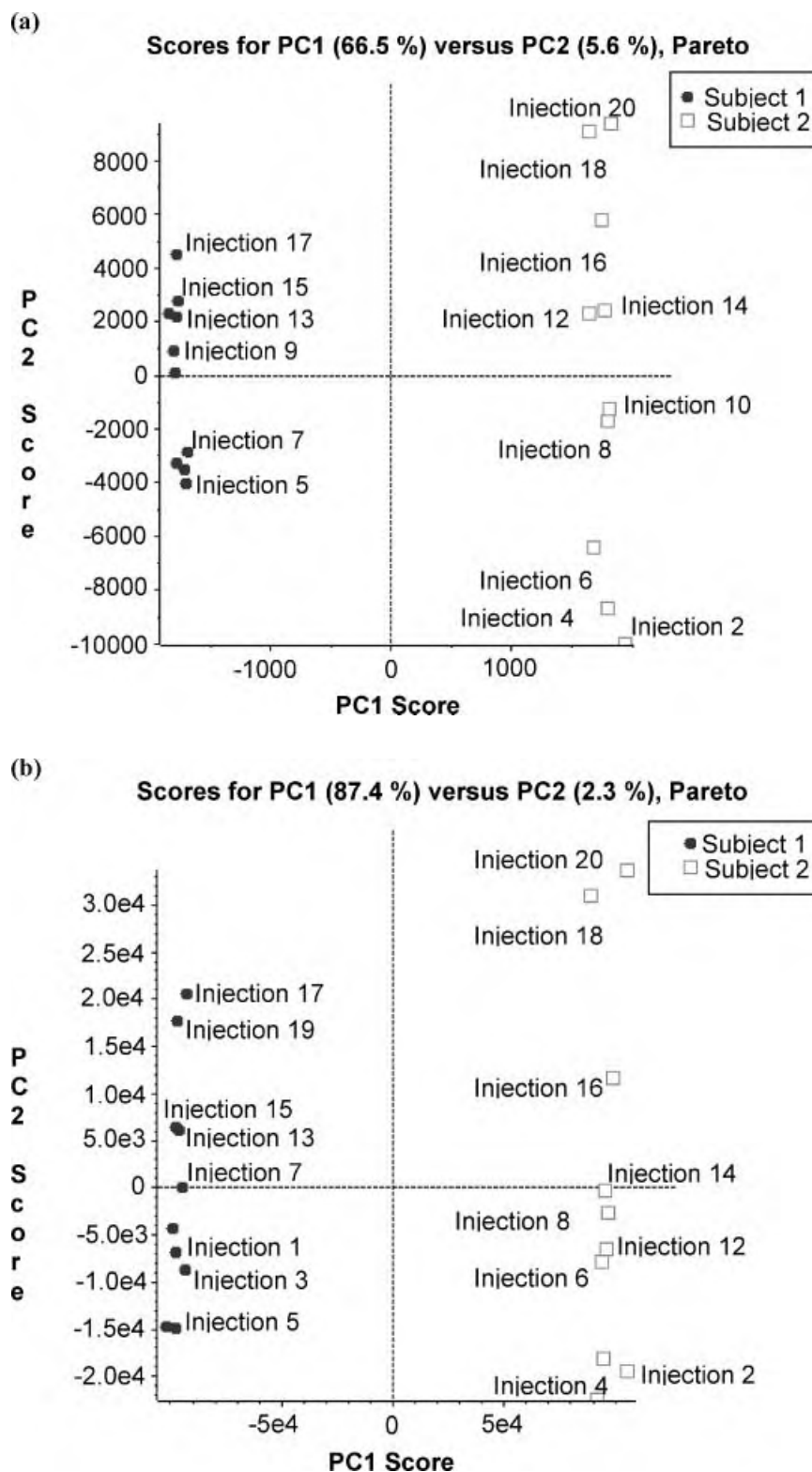


**Figure 4.** Principal components analysis of a two-subject data set using the original peak-finding algorithm (a) and the two-step algorithm (b).

case. No matter how good an ideal threshold-free peak-finding algorithm, this would presumably always be an issue for peaks close to the signal/noise ratio.

The solution to the problem was to approach the peak picking from a different angle, to use an initial threshold value to discover potential markers and then remove the threshold and use the defined marker list to go back to the original data and extract values for those markers that fell below the initial threshold and thereby characterize the sample set.

Thus, the software was modified such that the peak areas could be optionally recalculated for each sample as follows: For each aligned peak, mass and retention time ranges were calculated. The start mass for the range was the lowest start mass for each of the original peaks for all samples which aligned to the current peak and the end mass was the corresponding highest end mass. The retention time range was calculated analogously. The net result was the smallest {mass, RT} 'rectangle' which enclosed the original peaks found for the samples corresponding to the current aligned peak. For each aligned peak for each sample, the intensities for each {mass, intensity, RT} data point for the current sample with mass and retention time within the current peak's ranges were summed. Note that if internal standards are used to correct retention times (step 2), the retention time range for each aligned peak would be adjusted for each sample. The adjustment converts back from the corrected retention times to the original retention times for the sample.

This procedure ultimately ensures that all peaks are treated equally, regardless of how well the original peak finding worked. Using the new algorithm the data obtained from the repeat analysis of human urine from two subjects was analyzed with both the original peak-picking software and the new two-stage process. The results of the PCA of these data are shown in Figs. 4(a) and 4(b), respectively, and the improvement in clustering of the urine for the two subjects using the latter approach is clear when the percentage of the total variation accounted for by PC1 is examined. (Note that PC1 accounts for the differences between the two subjects, while the remaining PCs account for other sources of variation due to various sources of noise.) Thus, without the use of the two-step data-processing methodology, PC1 only accounts for some 66.5% of the variation in the data, with PC2 a further 5.6% (Fig. 4(a)). Employing the two-step process meant that PC1 now accounted for 87.4%, and PC2 2.3%, of the data (Fig. 4(b)). In addition, the new marker list (data not shown) produced by the improved software was found to have no markers without an area value, in contrast to the previous example (e.g. Table 1). Comparison of markers between the two methods of peak picking shows that the change did not affect which markers were detected but rather allowed the peak to be defined in all cases.

## CONCLUSIONS

Whilst there is no doubt that it is possible to use post-data collection statistical methods to accommodate some of the observed analytical variation (e.g. see<sup>13,16–18</sup>), a good case can be made to reduce the need for this as much as possible by ruthlessly going after the causes of analytical variation. This can only be done by first understanding the causes of the variation and then controlling them. Whilst both chromatographic or mass accuracy variation could have been expected to contribute to analytical variation, the most significant factor emerging from this study was the change in intensities between analyses. Applying the new algorithm enabled the effects of this variability to be dramatically reduced.

## Acknowledgements

The authors would like to thank the following people for their support during this research: Toby Athersuch, Gareth Booth, Rebecca Bradley, Chris Smith, Paula Wiebkin and A. J. Wilson.

## REFERENCES

- Robertson D, Lindon JC, Nicholson JK, Holmes E (eds). *Metabonomics in Toxicity Assessment*. CRC Press: Boca Raton, 2005.
- Brindle JT, Antti H, Holmes E, Tranter G, Nicholson JK, Bethell HWL, Clarke S, Schofield PM, McKilligin E, Mosedale DE, Grainger DJ. *Nat. Med.* 2002; **8**: 1439.
- Lindon JC, Nicholson JK, Holmes E. *The Handbook of Metabonomics and Metabolomics*. Elsevier: Amsterdam, 2007.
- Lenz E, Wilson ID. *J. Proteome Res.* 2007; **6**: 443.
- Lenz EM, Bright J, Wilson ID, Hughes A, Morrison J, Lindberg H, Lockton A. *J. Pharm. Biomed. Anal.* 2004; **36**: 841.
- Gavaghan CL, Wilson ID, Nicholson JK. *FEBS Lett.* 2002; **530**: 191.
- Bollard ME, Holmes E, Lindon JC, Mitchell SC, Branstetter D, Zhang W, Nicholson JK. *Anal. Biochem.* 2001; **295**: 194.
- Plumb R, Granger J, Stumpf C, Wilson ID, Evans JA, Lenz E. *The Analyst* 2003; **128**: 819.
- Dumas ME, Maibaum EC, Teague C, Ueshima H, Zhou B, Lindon JC, Nicholson JK, Stamler J, Elliot P, Chan Q, Holmes E. *Anal. Chem.* 2006; **78**: 2199.
- Maher AD, Zirah SFM, Holmes E, Nicholson JK. *Anal. Chem.* 2007; in press.
- Fiehn O, Kopka J, Dormann P, Altmann T, Trethewey RN, Willmitzer L. *Nat. Biotechnol.* 2000; **18**: 1157.
- Sangster T, Major H, Plumb R, Wilson AJ, Wilson ID. *Analyst* 2006; **131**: 1075.
- Wagner S, Scholz K, Donegan M, Burton L, Wingate J, Volkel W. *Anal. Chem.* 2006; **79**: 1296.
- Bottcher C, Roepenack-Lahaye Ev, Willscher E, Scheel D, Clemens S. *Anal. Chem.* 2007; **79**: 1507.
- Gika HG, Theodoridis GA, Wingate JE, Wilson ID. *J. Proteome Res.* 2007; in press.
- Trygg J, Lundstedt T. In *The Handbook of Metabonomics and Metabolomics*, Lindon J, Nicholson JK, Holmes E (eds). Elsevier: Amsterdam, 2007; 171–200.
- Trygg J, Holmes E, Lundstedt T. *J. Proteome Res.* 2007; **6**: 469.
- Bijlsma S, Bobeldjik I, Verheij ER, Ramaker R, Kochhar S, Macdonald IA, van Ommen B, Smilde AK. *Anal. Chem.* 2006; **78**: 567.

# Bibliography

**Adam, B. L., Qu, Y. S., Davis, J. W., Ward, M. D., Clements, M. A., Cazares, L. H., Semmes, O. J., Schellhammer, P. F., Yasui, Y., Feng, Z. D. and Wright, G. L.** Serum protein fingerprinting coupled with a pattern-matching algorithm distinguishes prostate cancer from benign prostate hyperplasia and healthy men. *Cancer Research* 62, 3609-3614 (2002)

**Adhami, V. M., Siddiqui, I. A., Ahmad, N., Gupta, S. and Mukhtar, H.** Oral consumption of green tea polyphenols inhibits Insulin-like growth factor-I-induced signaling in an autochthonous mouse model of prostate cancer. *Cancer Research* 64, 8715-8722 (2004)

**Akaza, H., Miyanaga, N., Takashima, N., Naito, S., Hirao, Y., Tsukamoto, T., Fujioka, T., Mori, M., Kim, W. J., Song, J. M. and Pantuck, A. J.** Comparisons of percent equol producers between prostate cancer patients and controls: Case-controlled studies of isoflavones in Japanese, Korean and American residents. *Japanese Journal of Clinical Oncology* 34, 86-89 (2004)

**Akech, J., Roy, S. S. and Das, S. K.** Modulation of cholinephosphotransferase activity in breast cancer cell lines by Ro5-4864, a peripheral benzodiazepine receptor agonist. *Biochemical and Biophysical Research Communications* 333, 35-41 (2005)

**Al-Saffar, N. M. S., Troy, H., Ramírez de Molina, A., Jackson, L. E., Madhu, B., Griffiths, J. R., Leach, M. O., Workman, P., Lacal, J. C., Judson, I. R. and Chung, Y. L.** Noninvasive magnetic resonance spectroscopic pharmacodynamic markers of the choline kinase inhibitor MN58b in human carcinoma models. *Cancer Research* 66, 427-434 (2006)

**Alonso, T., Morgan, R. O., Marvizon, J. C., Zarbl, H. and Santos, E.** Malignant transformation by ras and other oncogenes produces common alterations in inositol phospholipid signaling pathways. *Proceedings of the National Academy of Sciences of the United States of America* 85, 4271-4275 (1988)

**Ames, B. N., Shigenaga, M. K. and Hagen, T. M.** Oxidants, antioxidants, and the degenerative diseases of aging. *Proceedings of the National Academy of Sciences of the United States of America* 90, 7915-22 (1993)

**Aoyama, C., Ohtani, A. and Ishidate, K.** Expression and characterization of the active molecular forms of choline/ethanolamine kinase-alpha and -beta in mouse tissues, including carbon tetrachloride-induced liver. *Biochemical Journal* 363, 777-784 (2002)

**Baggerly, K. A., Morris, J. S. and Coombes, K. R.** Reproducibility of SELDI-TOF protein patterns in serum: Comparing datasets from different experiments. *Bioinformatics* 20, 777-785 (2004)

**Bala, L., Ghoshal, U. C., Ghoshal, U., Tripathi, P., Misra, A., Gowda, G. A. N. and Khetrpal, C. L.** Malabsorption syndrome with and without small intestinal bacterial overgrowth: A study on upper-gut aspirate using  $^1\text{H}$  NMR spectroscopy. *Magnetic Resonance in Medicine* 56, 738-744 (2006)

**Bales, J. R., Bell, J. D., Nicholson, J. K. and Sadler, P. J.**  $^1\text{H}$  NMR studies of urine during fasting - Excretion of ketone bodies and acetylcarnitine. *Magnetic Resonance in Medicine* 3, 849-856 (1986)

**Banez, L. L., Prasanna, P., Sun, L., Ali, A., Zou, Z. Q., Adam, B. L., McLeod, D. G., Moul, J. W. and Srivastava, S.** Diagnostic potential of serum proteomic patterns in prostate cancer. *Journal of Urology* 170, 442-446 (2003)

**Banks, R. E., Stanley, A. J., Cairns, D. A., Barrett, J. H., Clarke, P., Thompson, D. and Selby, P. J.** Influences of blood sample processing on low-molecular-weight proteome identified by surface-enhanced laser desorption/ionization mass spectrometry. *Clinical Chemistry* 51, 1637-1649 (2005)

**Bensaad, K., Tsuruta, A., Selak, M. A., Vidal, M. N. C., Nakano, K., Bartrons, R., Gottlieb, E. and Vousden, K. H.** TIGAR, a p53-inducible regulator of glycolysis and apoptosis. *Cell* 126, 107-120 (2006)

**Bessho, T., Tano, K., Kasai, H., Ohtsuka, E. and Nishimura, S.** Evidence for two DNA repair enzymes for 8-hydroxyguanine (7,8-dihydro-8-oxoguanine) in human cells. *Journal of Biological Chemistry* 268, 19416-19421 (1993)

**Bettuzzi, S., Brausi, M., Rizzi, F., Castagnetti, G., Peracchia, G. and Corti, A.** Chemoprevention of human prostate cancer by oral administration of green tea catechins in volunteers with high-grade prostate intraepithelial neoplasia: A preliminary report from a one-year proof-of-principle study. *Cancer Research* 66, 1234-1240 (2006)

**Boiteux, S. and Radicella, J. P.** Base excision repair of 8-hydroxyguanine protects DNA from endogenous oxidative stress. *Biochimie* 81, 59-67 (1999)

**Bollard, M. E., Holmes, E., Lindon, J. C., Mitchell, S. C., Branstetter, D., Zhang, W. and Nicholson, J. K.** Investigations into biochemical changes due to diurnal variation and estrus cycle in female rats using high-resolution <sup>1</sup>H NMR spectroscopy of urine and pattern recognition. *Analytical Biochemistry* 295, 194-202 (2001)

**Bollard, M. E., Keun, H. C., Beckonert, O., Ebbels, T. M. D., Antti, H., Nicholls, A. W., Shockcor, J. P., Cantor, G. H., Stevens, G., Lindon, J. C., Holmes, E. and Nicholson, J. K.** Comparative metabolomics of differential hydrazine toxicity in the rat and mouse. *Toxicology and Applied Pharmacology* 204, 135-151 (2005)

**Bongaerts, G. P. A., Tolboom, J. J. M., Naber, A. H. J., Sperl, W. J. K., Severijnen, R., Bakkeren, J. and Willems, J. L.** Role of bacteria in the pathogenesis of short bowel syndrome-associated D-lactic acidemia. *Microbial Pathogenesis* 22, 285-293 (1997)

**Bonoli, M., Pelillo, M., Toschi, T. G. and Lercker, G.** Analysis of green tea catechins: Comparative study between HPLC and HPCE. *Food Chemistry* 81, 631-638 (2003)

**Bookstein, R., Shew, J. Y., Chen, P. L., Scully, P. and Lee, W. H.** Suppression of tumorigenicity of human prostate carcinoma cells by replacing a mutated Rb gene. *Science* 247, 712-715 (1990)

**Bratt, O.** What should a urologist know about hereditary predisposition to prostate cancer? *BJU International* 99, 743-747 (2007)

**Brindle, J. T., Antti, H., Holmes, E., Tranter, G., Nicholson, J. K., Bethell, H. W., Clarke, S., Schofield, P. M., McKilligin, E., Mosedale, D. E. and Grainger, D. J.** Rapid and noninvasive diagnosis of the presence and severity of coronary heart disease using  $^1\text{H}$  NMR-based metabonomics. *Nature Medicine* 8, 1439-44 (2002)

**Buccione, R., Baldassarre, M., Trapani, V., Catalano, C., Pompeo, A., Brancaccio, A., Giavazzi, R., Luini, A. and Corda, D.** Glycerophosphoinositols inhibit the ability of tumour cells to invade the extracellular matrix. *European Journal of Cancer* 41, 470-476 (2005)

**Cani, P. D. and Delzenne, N. M.** Gut microflora as a target for energy and metabolic homeostasis. *Current Opinion in Clinical Nutrition and Metabolic Care* 10, 729-734 (2007)

**Caporali, A., Davalli, P., Astancolle, S., D'Arca, D., Brausi, M., Bettuzzi, S. and Corti, A.** The chemopreventive action of catechins in the TRAMP mouse model of prostate carcinogenesis is accompanied by clusterin over-expression. *Carcinogenesis* 25, 2217-2224 (2004)

**Check, E.** Proteomics and cancer: Running before we can walk? *Nature* 429, 496-497 (2004)

**Cheng, L. L., Burns, M. A., Taylor, J. L., He, W. L., Halpern, E. F., McDougal, W. S. and Wu, C. L.** Metabolic characterization of human prostate cancer with tissue magnetic resonance spectroscopy. *Cancer Research* 65, 3030-3034 (2005)

**Chiou, C. C., Chang, P. Y., Chan, E. C., Wu, T. L., Tsao, K. C. and Wu, J. T.** Urinary 8-hydroxydeoxyguanosine and its analogs as DNA marker of oxidative stress: Development of an ELISA and measurement in both bladder and prostate cancers. *Clinica Chimica Acta* 334, 87-94 (2003)

**Choan, E., Segal, R., Jonker, D., Malone, S., Reaume, N., Eapen, L. and Gallant, V.** A prospective clinical trial of green tea for hormone refractory prostate cancer: An evaluation of the complementary/alternative therapy approach. *Urologic Oncology* 23, 108-113 (2005)

**Clarke, W., Silverman, B. C., Zhang, Z., Chan, D. W., Klein, A. S. and Molmenti, E. P.** Characterization of renal allograft rejection by urinary proteomic analysis. *Annals of Surgery* 237, 660-664 (2003)

**Cloarec, O., Dumas, M. E., Trygg, J., Craig, A., Barton, R. H., Lindon, J. C., Nicholson, J. K. and Holmes, E.** Evaluation of the orthogonal projection on latent structure model limitations caused by chemical shift variability and improved visualization of biomarker changes in <sup>1</sup>H NMR spectroscopic metabonomic studies. *Analytical Chemistry* 77, 517-26 (2005)

**Cooke, M. S., Evans, M. D., Dove, R., Rozalski, R., Gackowski, D., Siomek, A., Lunec, J. and Olinski, R.** DNA repair is responsible for the presence of oxidatively damaged DNA lesions in urine. *Mutation Research* 574, 58-66 (2005)

**Cooke, M. S., Evans, M. D. and Lunec, J.** DNA repair: Insights from urinary lesion analysis. *Free Radical Research* 36, 929-932 (2002)

**Cooke, M. S., Singh, R., Hall, G. K., Mistry, V., Duarte, T. L., Farmer, P. B. and Evans, M. D.** Evaluation of enzyme-linked immunosorbent assay and liquid chromatography-tandem mass spectrometry methodology for the analysis of 8-oxo-7,8-dihydro-2'-deoxyguanosine in saliva and urine. *Free Radical Biology and Medicine* 41, 1829-1836 (2006a)

**Cooke, M. S., Rozalski, R., Dove, R., Gackowski, D., Siomek, A., Evans, M. D. and Olinski, R.** Evidence for attenuated cellular 8-oxo-7,8-dihydro-2'-deoxyguanosine removal in cancer patients. *Biological Chemistry* 387, 393-400 (2006b)

**Costello, L. C. and Franklin, R. B.** Bioenergetic theory of prostate malignancy. *Prostate* 25, 162-166 (1994)

**Costello, L. C. and Franklin, R. B.** The metabolism of prostate malignancy: Insight into the pathogenesis of prostate cancer and new approaches for its diagnosis and treatment. *Oncology Spectrums* 2, 452-457 (2001)

**Costello, L. C. and Franklin, R. B.** 'Why do tumour cells glycolyse?': From glycolysis through citrate to lipogenesis. *Molecular and Cellular Biochemistry* 280, 1-8 (2005)

**Costello, L. C. and Franklin, R. B.** The clinical relevance of the metabolism of prostate cancer; zinc and tumor suppression: connecting the dots. *Molecular Cancer [serial on the internet]* 5, Available from:  
<http://www.pubmedcentral.nih.gov/articlerender.fcgi?artid=1481516> (2006)

**Croteau, D. L. and Bohr, V. A.** Repair of oxidative damage to nuclear and mitochondrial DNA in mammalian cells. *Journal of Biological Chemistry* 272, 25409-25412 (1997)

**Cummings, J. H. and Macfarlane, G. T.** Role of intestinal bacteria in nutrient metabolism. *Clinical Nutrition* 16, 3-11 (1997)

**de Hoffmann, E. and Stroobant, V.** Mass Spectrometry: Principles and Applications, second Edition, *John Wiley & Sons, Ltd* (2002).

**DeMarzo, A. M., Nelson, W. G., Isaacs, W. B. and Epstein, J. I.** Pathological and molecular aspects of prostate cancer. *Lancet* 361, 955-964 (2003)

**Desouki, M. M., Geradts, J., Milon, B., Franklin, R. B. and Costello, L. C.** hZip2 and hZip3 zinc transporters are down regulated in human prostate adenocarcinomatous glands. *Molecular Cancer [serial on the internet]* 6, available from:  
<http://www.molecular-cancer.com/content/6/1/37> (2007)

**Diamandis, E. P.** Proteomic patterns in biological fluids: Do they represent the future of cancer diagnostics? *Clinical Chemistry* 49, 1272-1275 (2003)

**Diamandis, E. P.** Analysis of serum proteomic patterns for early cancer diagnosis: Drawing attention to potential problems. *Journal of the National Cancer Institute* 96, 353-356 (2004)

**Dieterle, F., Ross, A., Schlotterbeck, G. and Senn, H.** Probabilistic quotient normalization as robust method to account for dilution of complex biological mixtures. Application in  $^1\text{H}$  NMR metabonomics. *Analytical Chemistry* 78, 4281-4290 (2006)

**Dumas, M. E., Maibaum, E. C., Teague, C., Ueshima, H., Zhou, B. F., Lindon, J. C., Nicholson, J. K., Stamler, J., Elliott, P., Chan, Q. and Holmes, E.** Assessment of analytical reproducibility of  $^1\text{H}$  NMR spectroscopy based metabonomics for large-scale epidemiological research: The INTERMAP study. *Analytical Chemistry* 78, 2199-2208 (2006)

**Ellison, L. F.** Tea and other beverage consumption and prostate cancer risk: a Canadian retrospective cohort study. *European Journal of Cancer Prevention* 9, 125-130 (2000)

**Eriksson, L., Johansson, N., Kettaneh-Wold, N. and Wold, S.** Multi- and Megavariate Data Analysis - Principles and Applications, *Umetrics AB* (2001).

**Evans, M. D., Dizdaroglu, M. and Cooke, M. S.** Oxidative DNA damage and disease: induction, repair and significance. *Mutation Research* 567, 1-61 (2004)

**Falasca, M., Carvelli, A., Iurisci, C., Qiu, R. G., Symons, M. H. and Corda, D.** Fast receptor-induced formation of glycerophosphoinositol-4-phosphate, a putative novel intracellular messenger in the Ras pathway. *Molecular Biology of the Cell* 8, 443-453 (1997)

**Findeisen, P., Sismanidis, D., Riedl, M., Costina, V. and Neumaier, M.** Preanalytical impact of sample handling on proteome profiling experiments with matrix-assisted laser desorption/ionization time-of-flight mass spectrometry. *Clinical Chemistry* 51, 2409-2411 (2005)

**Fleshner, N. and Zlotta, A. R.** Prostate cancer prevention - Past, present, and future. *Cancer* 110, 1889-1899 (2007)

**Fraga, C. G., Shigenaga, M. K., Park, J. W., Degan, P. and Ames, B. N.** Oxidative damage to DNA during aging - 8-hydroxy-2'-deoxyguanosine in rat organ DNA and urine. *Proceedings of the National Academy of Sciences of the United States of America* 87, 4533-4537 (1990)

**Franklin, R. B., Feng, P., Milon, B., Desouki, M. M., Singh, K. K., Kajdacsy-Balla, A., Bagasra, O. and Costello, L. C.** hZIP1 zinc uptake transporter down regulation and zinc depletion in prostate cancer. *Molecular Cancer [serial on the internet]* 4, available from: <http://www.pubmedcentral.nih.gov/articlerender.fcgi?artid=1243239> (2005)

**Fricke, S. T., Rodriguez, O., VanMeter, J., Dettin, L. E., Casimiro, M., Chien, C. D., Newell, T., Johnson, K., Ileva, L., Ojeifo, J., Johnson, M. D. and Albanese, C.** In vivo magnetic resonance volumetric and spectroscopic analysis of mouse prostate cancer models. *Prostate* 66, 708-717 (2006)

**Friedberg, E. C.** How nucleotide excision repair protects against cancer. *Nature Reviews Cancer* 1, 22-33 (2001)

**Gavaghan, C. L., Wilson, I. D. and Nicholson, J. K.** Physiological variation in metabolic phenotyping and functional genomic studies: Use of orthogonal signal correction and PLS-DA. *Febs Letters* 530, 191-196 (2002)

**Ghosh, A., Akech, J., Mukherjee, S. and Das, S. K.** Differential expression of cholinephosphotransferase in normal and cancerous human mammary epithelial cells. *Biochemical and Biophysical Research Communications* 297, 1043-1048 (2002)

**Gleason, D. F. and Mellinger, G. T.** Prediction of prognosis for prostatic adenocarcinoma by combined histological grading and clinical staging. *Journal of Urology* 111, 58-64 (1974)

**Glunde, K., Jacobs, M. A. and Bhujwala, Z. M.** Choline metabolism in cancer: implications for diagnosis and therapy. *Expert Review of Molecular Diagnostics* 6, 821-829 (2006)

**Glunde, K., Jie, C. and Bhujwala, Z. M.** Molecular causes of the aberrant choline phospholipid metabolism in breast cancer. *Cancer Research* 64, 4270-4276 (2004)

**Glunde, K. and Serkova, N. J.** Therapeutic targets and biomarkers identified in cancer choline phospholipid metabolism. *Pharmacogenomics* 7, 1109-1123 (2006)

**Greenberg, N. M., Demayo, F., Finegold, M. J., Medina, D., Tilley, W. D., Aspinall, J. O., Cunha, G. R., Donjacour, A. A., Matusik, R. J. and Rosen, J. M.** Prostate cancer in a transgenic mouse. *Proceedings of the National Academy of Sciences of the United States of America* 92, 3439-3443 (1995)

**Griffin, J. L. and Shockcor, J. P.** Metabolic profiles of cancer cells. *Nature Reviews Cancer* 4, 551-561 (2004)

**Grollman, A. P. and Moriya, M.** Mutagenesis by 8-oxoguanine - An enemy within. *Trends in Genetics* 9, 246-249 (1993)

**Gronberg, H.** Prostate cancer epidemiology. *Lancet* 361, 859-864 (2003)

**Gupta, S., Hastak, K., Ahmad, N., Lewin, J. S. and Mukhtar, H.** Inhibition of prostate carcinogenesis in TRAMP mice by oral infusion of green tea polyphenols. *Proceedings of the National Academy of Sciences of the United States of America* 98, 10350-10355 (2001)

**Gutierrez, S., Chernokalskaya, E., Dedeo, A., Lazarev, A. and Leonard, J.** Purification of peptides from serum and cell lysates for mass spectrometry. *Millipore - Technical Library* available from:  
<http://www.millipore.com/publications.nsf/docs/ps2003enus>, (2003)

**Haghdoost, S., Czene, S., Naslund, I., Skog, S. and Harms-Ringdahl, M.** Extracellular 8-oxo-dG as a sensitive parameter for oxidative stress in vivo and in vitro. *Free Radical Research* 39, 153-162 (2005)

**Haghdoost, S., Sjolander, L., Czene, S. and Hanns-Ringdahl, M.** The nucleotide pool is a significant target for oxidative stress. *Free Radical Biology and Medicine* 41, 620-626 (2006)

**Hakim, I. A., Harris, R. B., Brown, S., Chow, H. H. S., Wiseman, S., Agarwal, S. and Talbot, W.** Effect of increased tea consumption on oxidative DNA damage among smokers: A randomized controlled study. *Journal of Nutrition* 133, 3303S-3309S (2003)

**Halliwell, B. and Cross, C. E.** Oxygen-derived species: Their relation to human disease and environmental stress. *Environmental Health Perspectives* 102 Supplement 10, 5-12 (1994)

**Halliwell, B. and Gutteridge, J. M.** Oxygen toxicity, oxygen radicals, transition metals and disease. *Biochemical Journal* 219, 1-14 (1984)

**Hamdan, M. and Righetti, P. G.** Proteomics today: Protein assessment and biomarkers using mass spectrometry, 2D electrophoresis, and microarray technology, *Wiley-Interscience* (2005).

**Hamilton, M. L., Van Remmen, H., Drake, J. A., Yang, H., Guo, Z. M., Kewitt, K., Walter, C. A. and Richardson, A.** Does oxidative damage to DNA increase with age? *Proceedings of the National Academy of Sciences of the United States of America* 98, 10469-10474 (2001)

**Hampel, D. J., Sansome, C., Sha, M., Brodsky, S., Lawson, W. E. and Goligorsky, M. S.** Toward proteomics in uroscopy: Urinary protein profiles after radiocontrast medium administration. *Journal of the American Society of Nephrology* 12, 1026-1035 (2001)

- Harada, U., Chikama, A., Saito, S., Takase, H., Nagao, T., Hase, T. and Tokimitsu, I.** Effects of the long-term ingestion of tea catechins on energy expenditure and dietary fat oxidation in healthy subjects. *Journal of Health Science* 51, 248-252 (2005)
- Harbowy, M. E. and Balentine, D. A.** Tea chemistry. *Critical Reviews in Plant Sciences* 16, 415-480 (1997)
- Harper, C. E., Patel, B. B., Wang, J., Eltoum, I. A. and Lamartiniere, C. A.** Epigallocatechin-3-gallate suppresses early stage, but not late stage prostate cancer in TRAMP mice: Mechanisms of action. *Prostate* 67, 1576-1589 (2007)
- Harwood, L. M. and Claridge, T. D. W.** Introduction to organic spectroscopy, *Oxford University Press* (1997).
- Haskins, N. J.** The application of stable isotopes in biomedical research. *Biomedical Mass Spectrometry* 9, 269-77 (1982)
- Hayakawa, H., Taketomi, A., Sakumi, K., Kuwano, M. and Sekiguchi, M.** Generation and elimination of 8-oxo-7,8-dihydro-2'-deoxyguanosine 5'-triphosphate, a mutagenic substrate for DNA-synthesis, in human cells. *Biochemistry* 34, 89-95 (1995)
- Heavner, D. L., Morgan, W. T., Sears, S. B., Richardson, J. D., Byrd, G. D. and Ogden, M. W.** Effect of creatinine and specific gravity normalization techniques on xenobiotic biomarkers in smokers' spot and 24-h urines. *Journal of Pharmaceutical and Biomedical Analysis* 40, 928-942 (2006)
- Heerschap, A., Jager, G. J., van der Graaf, M., Barentsz, J. O., DelaRosette, J., Oosterhof, G. O. N., Ruijter, E. T. G. and Ruijs, S. H. J.** In vivo proton MR spectroscopy reveals altered metabolite content in malignant prostate tissue. *Anticancer Research* 17, 1455-1460 (1997)
- Heilbrun, L. K., Nomura, A. and Stemmermann, G. N.** Black tea consumption and cancer risk: A prospective study. *British Journal of Cancer* 54, 677-683 (1986)

**Hoppel, C. L. and Genuth, S. M.** Carnitine metabolism in normal-weight and obese human subjects during fasting. *American Journal of Physiology* 238, E409-E415 (1980)

**Hortin, G. L., Meilinger, B. and Drake, S. K.** Size-selective extraction of peptides from urine for mass spectrometric analysis. *Clinical Chemistry* 50, 1092-1095 (2004)

**Houten, S. M., Watanabe, M. and Auwerx, J.** Endocrine functions of bile acids. *Embo Journal* 25, 1419-1425 (2006)

**Huffman, D. M., Johnson, M. S., Watts, A., Elgavish, A., Eltoun, I. A. and Nagy, T. R.** Cancer progression in the transgenic adenocarcinoma of mouse prostate mouse is related to energy balance, body mass, and body composition, but not food intake. *Cancer Research* 67, 417-424 (2007)

**Husková, R., Chrastina, P., Adam, T. and Schneiderka, P.** Determination of creatinine in urine by tandem mass spectrometry. *Clinica Chimica Acta* 350, 99-106 (2004)

**Isaacs, W. B., Carter, B. S. and Ewing, C. M.** Wild-type p53 suppresses growth of human prostate cancer cells containing mutant p53 alleles. *Cancer Research* 51, 4716-4720 (1991)

**Jaffé, M. Z.** Über den Niederschlag welchen Pikrinsäure in normalem Harn erzeugt und über neue Reaktionen des Kreatinins *Zeitschrift für Physiologische Chemie* 10, 391-400 (1886)

**Jain, M. G., Hislop, G. T., Howe, G. R., Burch, J. D. and Ghadirian, P.** Alcohol and other beverage use and prostate cancer risk among Canadian men. *International Journal of Cancer* 78, 707-711 (1998)

**Jaiswal, M., Lipinski, L. J., Bohr, V. A. and Mazur, S. J.** Efficient in vitro repair of 7-hydro-8-oxodeoxyguanosine by human cell extracts: involvement of multiple pathways. *Nucleic Acids Research* 26, 2184-2191 (1998)

**Jatoi, A., Ellison, N., Burch, P. A., Sloan, J. A., Dakhil, S. R., Novotny, P., Tan, W., Fitch, T. R., Rowland, K. M., Young, C. Y. F. and Flynn, P. J.** A phase II trial of green tea in the treatment of patients with androgen independent metastatic prostate carcinoma. *Cancer* 97, 1442-1446 (2003)

**Jian, L., Xie, L. P., Lee, A. H. and Binns, C. W.** Protective effect of green tea against prostate cancer: A case-control study in southeast China. *International Journal of Cancer* 108, 130-135 (2004)

**Joenje, H.** Genetic toxicology of oxygen. *Mutation Research* 219, 193-208 (1989)

**Kaighn, M. E., Narayan, K. S., Ohnuki, Y., Lechner, J. F. and Jones, L. W.** Establishment and characterization of a human prostatic carcinoma cell line (PC-3). *Investigative Urology* 17, 16-23 (1979)

**Kasai, H.** Analysis of a form of oxidative DNA damage, 8-hydroxy-2'-deoxyguanosine, as a marker of cellular oxidative stress during carcinogenesis. *Mutation Research* 387, 147-63 (1997)

**Kasper, S., Sheppard, P. C., Yan, Y. L., Pettigrew, N., Borowsky, A. D., Prins, G. S., Dodd, J. G., Duckworth, M. L. and Matusik, R. J.** Development, progression, and androgen-dependence of prostate tumors in probasin-large T antigen transgenic mice: A model for prostate cancer. *Laboratory Investigation* 78, 319 (1998)

**Kim, J. K., Kim, D. Y., Lee, Y. H., Sung, N. K., Chung, D. S., Kim, O. D. and Kim, K. B.** In vivo differential diagnosis of prostate cancer and benign prostatic hyperplasia: Localized proton magnetic resonance spectroscopy using external-body surface coil. *Journal of Magnetic Resonance Imaging* 16, 1281-1288 (1998)

**Kind, T., Tolstikov, V., Fiehn, O. and Weiss, R. H.** A comprehensive urinary metabolomic approach for identifying kidney cancer. *Analytical Biochemistry* 363, 185-195 (2007)

**Klaunig, J. E., Xu, Y., Han, C., Kamendulis, L. M., Chen, J. S., Heiser, C., Gordon, M. S. and Mohler, E. R.** The effect of tea consumption on oxidative stress in smokers and nonsmokers. *Proceedings of the Society for Experimental Biology and Medicine* 220, 249-254 (1999)

**Kurhanewicz, J., Dahiya, R., MacDonald, J. M., Chang, L.-H., James, T. L. and Narayan, P.** Citrate alterations in primary and metastatic human prostatic adenocarcinomas: <sup>1</sup>H magnetic resonance spectroscopy and biochemical study. *Magnetic Resonance in Medicine* 29, 149-157 (1993)

**Kurhanewicz, J., Swanson, M. G., Nelson, S. J. and Vigneron, D. B.** Combined magnetic resonance imaging and spectroscopic imaging approach to molecular imaging of prostate cancer. *Journal of Magnetic Resonance Imaging* 16, 451-463 (2002)

**Kurhanewicz, J., Vigneron, D. B., Hricak, H., Narayan, P., Carroll, P. and Nelson, S. J.** Three-dimensional <sup>1</sup>H MR spectroscopic imaging of the in situ human prostate with high (0.24-0.7-cm<sup>3</sup>) spatial resolution. *Radiology* 198, 795-805 (1996)

**Lavecchia, C., Negri, E., Franceschi, S., Davanzo, B. and Boyle, P.** Tea Consumption and Cancer Risk. *Nutrition and Cancer* 17, 27-31 (1992)

**Lee, H. C., Jenner, A. M., Low, C. S. and Lee, Y. K.** Effect of tea phenolics and their aromatic fecal bacterial metabolites on intestinal microbiota. *Research in Microbiology* 157, 876-884 (2006)

**Lenz, E. M., Bright, J., Knight, R., Wilson, I. D. and Major, H.** Cyclosporin A - induced changes in endogenous metabolites in rat urine: A metabonomic investigation using high field <sup>1</sup>H NMR spectroscopy, HPLC-TOF/MS and chemometrics. *Journal of Pharmaceutical and Biomedical Analysis* 35, 599-608 (2004a)

**Lenz, E. M., Bright, J., Knight, R., Wilson, I. D. and Major, H.** A metabonomic investigation of the biochemical effects of mercuric chloride in the rat using <sup>1</sup>H NMR and HPLC-TOF/MS: Time dependant changes in the urinary profile of endogenous metabolites as a result of nephrotoxicity. *Analyst* 129, 535-541 (2004b)

**Lenz, E. M., Bright, J., Wilson, I. D., Hughes, A., Morrisson, J., Lindberg, H. and Lockton, A.** Metabonomics, dietary influences and cultural differences: a  $^1\text{H}$  NMR-based study of urine samples obtained from healthy British and Swedish subjects. *Journal of Pharmaceutical and Biomedical Analysis* 36, 841-849 (2004c)

**Lenz, E. M., Bright, J., Wilson, I. D., Morgan, S. R. and Nash, A. F. P.** A  $^1\text{H}$  NMR-based metabonomic study of urine and plasma samples obtained from healthy human subjects. *Journal of Pharmaceutical and Biomedical Analysis* 33, 1103-1115 (2003)

**Lenz, E. M. and Wilson, I. D.** Analytical strategies in metabonomics. *Journal of Proteome Research* 6, 443-458 (2007)

**Levine, L. and Fahy, J. P.** Evaluations of urinary lead determinations. 1. Significance of specific gravity. *Journal of Industrial Hygiene and Toxicology* 27, 217-23 (1945)

**Li, M., Wang, B. H., Zhang, M. H., Rantalainen, M., Wang, S. Y., Zhou, H. K., Zhang, Y., Shen, J., Pang, X. Y., Zhang, M. L., Wei, H., Chen, Y., Lu, H. F., Zuo, J., Su, M. M., Qiu, Y. P., Jia, W., Xiao, C. N., Smith, L. M., Yang, S. L., Holmes, E., Tang, H. R., Zhao, G. P., Nicholson, J. K., Li, L. J. and Zhao, L. P.** Symbiotic gut microbes modulate human metabolic phenotypes. *Proceedings of the National Academy of Sciences of the United States of America* 105, 2117-2122 (2008)

**Lim, L. S. and Sherin, K.** Screening for prostate cancer in US men - ACPM position statement on preventive practice. *American Journal of Preventive Medicine* 34, 164-170 (2008)

**Lin, H. S., Jenner, A. M., Ong, C. N., Huang, S. H., Whiteman, M. and Halliwell, B.** A high-throughput and sensitive methodology for the quantification of urinary 8-hydroxy-2'-deoxyguanosine: Measurement with gas chromatography-mass spectrometry after single solid-phase extraction. *Biochemical Journal* 380, 541-548 (2004)

**Lindon, J. C., Holmes, E. and Nicholson, J. K.** Metabonomics in pharmaceutical R & D. *FEBS Journal* 274, 1140-1151 (2007)

**Lippman, S. M., Benner, S. E. and Hong, W. K.** Cancer chemoprevention. *Journal of Clinical Oncology* 12, 851-873 (1994)

**Loft, S. and Poulsen, H. E.** Cancer risk and oxidative DNA damage in man. *Journal of Molecular Medicine* 74, 297-312 (1996)

**Luo, H. T., Tang, L. L., Tang, M., Billam, M., Huang, T. R., Yu, J. H., Wei, Z. L., Liang, Y. Q., Wang, K. B., Zhang, Z. Q., Zhang, L. S. and Wang, J. S.** Phase IIa chemoprevention trial of green tea polyphenols in high-risk individuals of liver cancer: Modulation of urinary excretion of green tea polyphenols and 8-hydroxydeoxyguanosine. *Carcinogenesis* 27, 262-268 (2006)

**M'Koma, A. E., Blum, D. L., Norris, J. L., Koyama, T., Billheimer, D., Motley, S., Ghiassi, M., Ferdowsi, N., Bhowmick, I., Chang, S. S., Fowke, J. H., Caprioli, R. M. and Bhowmick, N. A.** Detection of pre-neoplastic and neoplastic prostate disease by MADI profiling of urine. *Biochemical and Biophysical Research Communications* 353, 829-834 (2007)

**Maher, A. D., Zirah, S. F. M., Holmes, E. and Nicholson, J. K.** Experimental and analytical variation in human urine in <sup>1</sup>H NMR spectroscopy-based metabolic phenotyping studies. *Analytical Chemistry* 79, 5204-5211 (2007)

**Margison, G. P. and Santibanez-Koref, M. F.** O-6-alkylguanine-DNA alkyltransferase: Role in carcinogenesis and chemotherapy. *Bioessays* 24, 255-266 (2002)

**Maroulakou, I. G., Anver, M., Garrett, L. and Green, J. E.** Prostate and mammary adenocarcinoma in transgenic mice carrying a rat C3(1) Simian-Virus-40 large tumor-antigen fusion gene. *Proceedings of the National Academy of Sciences of the United States of America* 91, 11236-11240 (1994)

**Martin, F. P., Dumas, M. E., Wang, Y., Legido-Quigley, C., Yap, I. K., Tang, H., Zirah, S., Murphy, G. M., Cloarec, O., Lindon, J. C., Sprenger, N., Fay, L. B., Kochhar, S., van Bladeren, P., Holmes, E. and Nicholson, J. K.** A top-down systems biology view of microbiome-mammalian metabolic interactions in a mouse model. *Molecular Systems Biology* 3, 112 (2007)

**Masumori, N., Thomas, T. Z., Chaurand, P., Case, T., Paul, M., Kasper, S., Caprioli, R. M., Tsukamoto, T., Shappell, S. B. and Matusik, R. J.** A probasin-large T antigen transgenic mouse line develops prostate adenocarcinoma and neuroendocrine carcinoma with metastatic potential. *Cancer Research* 61, 2239-2249 (2001)

**Matoba, S., Kang, J. G., Patino, W. D., Wragg, A., Boehm, M., Gavrilova, O., Hurley, P. J., Bunz, F. and Hwang, P. M.** p53 regulates mitochondrial respiration. *Science* 312, 1650-1653 (2006)

**Mazhar, D. and Waxman, J.** Prostate cancer. *Postgraduate Medical Journal* 78, 590-595 (2002)

**McCabe, M. T., Low, J. A., Daignault, S., Imperiale, M. J., Wojno, K. J. and Day, M. L.** Inhibition of DNA methyltransferase activity prevents tumorigenesis in a mouse model of prostate cancer. *Cancer Research* 66, 385-392 (2006)

**McLerran, D., Grizzle, W. E., Feng, Z., Bigbee, W. L., Banez, L. L., Cazares, L. H., Chan, D. W., Diaz, J., Izbicka, E., Kagan, J., Malehorn, D. E., Malik, G., Oelschlager, D., Partin, A., Randolph, T., Rosenzweig, N., Srivastava, S., Srivastava, S., Thompson, I. M., Thornquist, M., Troyer, D., Yasui, Y., Zhang, Z., Zhu, L. and Semmes, O. J.** Analytical validation of serum proteomic profiling for diagnosis of prostate cancer: Sources of sample bias. *Clinical Chemistry* 54, 44-52 (2008a)

**McLerran, D., Grizzle, W. E., Feng, Z. D., Thompson, I. M., Bigbee, W. L., Cazares, L. H., Chan, D. W., Dahlgren, J., Diaz, J., Kagan, J., Lin, D. W., Malik, G., Oelschlager, D., Partin, A., Randolph, T. W., Sokoll, L., Srivastava, S., Srivastava, S., Thornquist, M., Troyer, D., Wright, G. L., Zhang, Z., Zhu, L. and Semmes, O. J.** SELDI-TOF MS whole serum proteomic profiling with IMAC surface does not reliably detect prostate cancer. *Clinical Chemistry* 54, 53-60 (2008b)

**Mecocci, P., Fano, G., Fulle, S., MacGarvey, U., Shinobu, L., Polidori, M. C., Cherubini, A., Vecchiet, J., Senin, U. and Beal, M. F.** Age-dependent increases in oxidative damage to DNA, lipids, and proteins in human skeletal muscle. *Free Radical Biology and Medicine* 26, 303-308 (1999)

**Miura, Y., Chiba, T., Tomita, I., Koizumi, H., Miura, S., Umegaki, K., Hara, Y., Ikeda, M. and Tomita, T.** Tea catechins prevent the development of atherosclerosis in apoprotein E-deficient mice. *Journal of Nutrition* 131, 27-32 (2001)

**Miwa, M., Matsumaru, H., Akimoto, Y., Naito, S. and Ochi, H.** Quantitative determination of urinary 8-hydroxy-2-deoxyguanosine level in healthy Japanese volunteers. *Biofactors* 22, 249-253 (2004)

**Miyake, H., Hara, I., Kamidono, S. and Eto, H.** Oxidative DNA damage in patients with prostate cancer and its response to treatment. *Journal of Urology* 171, 1533-1536 (2004)

**Mobley, J. A., Lam, Y. W., Lau, K. M., Pais, V. M., L'Esperance, J. O., Steadman, B., Fuster, L. M. B., Blute, R. D., Taplin, M. E. and Ho, S. M.** Monitoring the serological proteome: The latest modality in prostate cancer detection. *Journal of Urology* 172, 331-337 (2004)

**Morgenbesser, S. D., McLaren, R. P., Richards, B., Zhang, M., Akmaev, V. R., Winter, S. F., Mineva, N. D., Kaplan-Lefko, P. J., Foster, B. A., Cook, B. P., Dufault, M. R., Cao, X., Wang, C. J., Teicher, B. A., Klinger, K. W., Greenberg, N. M. and Madden, S. L.** Identification of genes potentially involved in the acquisition of androgen-independent and metastatic tumor growth in an autochthonous genetically engineered mouse prostate cancer model. *Prostate* 67, 83-106 (2006)

**Murase, T., Haramizu, S., Shimotoyodome, A., Nagasawa, A. and Tokimitsu, I.** Green tea extract improves endurance capacity and increases muscle lipid oxidation in mice. *American Journal of Physiology. Regulatory Integrative and Comparative Physiology* 288, R708-R715 (2005)

**Nakabeppu, Y., Kajitani, K., Sakamoto, K., Yamaguchi, H. and Tsuchimoto, D.** MTH1, an oxidized purine nucleoside triphosphatase, prevents the cytotoxicity and neurotoxicity of oxidized purine nucleotides. *DNA Repair* 5, 761-72 (2006)

**Narayanan, S. and Appleton, H. D.** Creatinine - A Review. *Clinical Chemistry* 26, 1119-1126 (1980)

**Nicholls, A. W., Mortishire-Smith, R. J. and Nicholson, J. K.** NMR spectroscopic-based metabonomic studies of urinary metabolite variation in acclimatizing germ-free rats. *Chemical Research in Toxicology* 16, 1395-1404 (2003)

**Nicholson, J. K., Foxall, P. J. D., Spraul, M., Farrant, R. D. and Lindon, J. C.** 750-MHz  $^1\text{H}$  and  $^1\text{H} - ^{13}\text{C}$  NMR spectroscopy of human blood plasma. *Analytical Chemistry* 67, 793-811 (1995)

**Nicholson, J. K., Higham, D. P., Timbrell, J. A. and Sadler, P. J.** Quantitative high resolution  $^1\text{H}$  NMR urinalysis studies on the biochemical effects of cadmium in the rat. *Molecular Pharmacology* 36, 398-404 (1989)

**Nicholson, J. K., Holmes, E. and Wilson, I. D.** Gut microorganisms, mammalian metabolism and personalized health care. *Nature Reviews Microbiology* 3, 431-438 (2005)

**Nicholson, J. K. and Wilson, I. D.** Understanding 'global' systems biology: Metabonomics and the continuum of metabolism. *Nature Reviews Drug Discovery* 2, 668-676 (2003)

**Nyska, A., Suttie, A., Bakshi, S., Lomnitski, L., Grossman, S., Bergman, M., Ben-Shaul, V., Crocket, P., Haseman, J. K., Moser, G., Goldsworthy, T. L. and Maronpot, R. R.** Slowing tumorigenic progression in TRAMP mice and prostatic carcinoma cell lines using natural anti-oxidant from spinach, NAO - A comparative study of three anti-oxidants. *Toxicologic Pathology* 31, 39-51 (2003)

**Odunsi, K., Wollman, R. M., Ambrosone, C. B., Hutson, A., McCann, S. E., Tammela, J., Geisler, J. P., Miller, G., Sellers, T., Cliby, W., Qian, F., Keitz, B., Intengan, M., Lele, S. and Alderfer, J. L.** Detection of epithelial ovarian cancer using <sup>1</sup>H NMR-based metabonomics. *International Journal of Cancer* 113, 782-788 (2005)

**Ota, N., Soga, S., Shimotoyodome, A., Haramizu, S., Inaba, M., Murase, T. and Tokimitsu, I.** Effects of combination of regular exercise and tea catechins intake on energy expenditure in humans. *Journal of Health Science* 51, 233-236 (2005)

**Pan, Y. Z., Xiao, X. Y., Zhao, D., Zhang, L., Ji, G. Y., Li, Y., Yang, B. X., He, D. C. and Zhao, X. J.** Application of surface-enhanced laser desorption/ionization time-of-flight-based serum proteomic array technique for the early diagnosis of prostate cancer. *Asian Journal of Andrology* 8, 45-51 (2006)

**Petricoin, E. F., Ardekani, A. M., Hitt, B. A., Levine, P. J., Fusaro, V. A., Steinberg, S. M., Mills, G. B., Simone, C., Fishman, D. A., Kohn, E. C. and Liotta, L. A.** Use of proteomic patterns in serum to identify ovarian cancer. *Lancet* 359, 572-577 (2002a)

**Petricoin, E. F., Ornstein, D. K., Paweletz, C. P., Ardekani, A., Hackett, P. S., Hitt, B. A., Velasco, A., Trucco, C., Wiegand, L., Wood, K., Simone, C. B., Levine, P. J., Linehan, W. M., Emmert-Buck, M. R., Steinberg, S. M., Kohn, E. C. and Liotta, L. A.** Serum proteomic patterns for detection of prostate cancer. *Journal of the National Cancer Institute* 94, 1576-1578 (2002b)

**Phipps, A. N., Stewart, J., Wright, B. and Wilson, I. D.** Effect of diet on the urinary excretion of hippuric acid and other dietary-derived aromatics in rat. A complex interaction between diet, gut microflora and substrate specificity. *Xenobiotica* 28, 527-537 (1998)

**Pilger, A., Germadnik, D., Riedel, K., Meger-Kossien, I., Scherer, G. and Rudiger, H. W.** Longitudinal study of urinary 8-hydroxy-2'-deoxyguanosine excretion in healthy adults. *Free Radical Research* 35, 273-280 (2001)

**Plumb, R., Granger, J., Stumpf, C., Wilson, I. D., Evans, J. A. and Lenz, E. M.** Metabonomic analysis of mouse urine by liquid-chromatography- time of flight mass spectrometry (LC-TOFMS): Detection of strain, diurnal and gender differences. *Analyst* 128, 819-823 (2003)

**Plumb, R. S., Johnson, K. A., Rainville, P., Shockcor, J. P., Williams, R., Granger, J. H. and Wilson, I. D.** The detection of phenotypic differences in the metabolic plasma profile of three strains of Zucker rats at 20 weeks of age using ultra-performance liquid chromatography/orthogonal acceleration time-of-flight mass spectrometry. *Rapid Communications in Mass Spectrometry* 20, 2800-2806 (2006)

**Poulsen, H. E., Loft, S., Prieme, H., Vistisen, K., Lykkesfeldt, J., Nyssonen, K. and Salonen, J. T.** Oxidative DNA damage in vivo: Relationship to age, plasma antioxidants, drug metabolism, glutathione-S-transferase activity and urinary creatinine excretion. *Free Radical Research* 29, 565-571 (1998)

**Pourcelot, S., Faure, H., Firoozi, F., Ducros, V., Tripier, M., Hee, J., Cadet, J. and Favier, A.** Urinary 8-oxo-7,8-dihydro-2'-deoxyguanosine and 5-(hydroxymethyl) uracil in smokers. *Free Radical Research* 30, 173-180 (1999)

**Qu, Y. S., Adam, B. L., Yasui, T., Ward, M. D., Cazares, L. H., Schellhammer, P. F., Feng, Z. D., Semmes, O. J. and Wright, G. L.** Boosted decision tree analysis of surface-enhanced laser desorption/ionization mass spectral serum profiles discriminates prostate cancer from noncancer patients. *Clinical Chemistry* 48, 1835-1843 (2002)

**Ramírez de Molina, A., Báñez-Coronel, M., Gutiérrez, R., Rodríguez-González, A., Olmeda, D., Megías, D. and Lacal, J. C.** Choline kinase activation is a critical requirement for the proliferation of primary human mammary epithelial cells and breast tumor progression. *Cancer Research* 64, 6732-6739 (2004)

**Ramírez de Molina, A., Rodríguez-González, A., Gutiérrez, R., Martínez-Pineiro, L., Sanchez, J. J., Bonilla, F., Rosell, R. and Lacal, J. C.** Overexpression of choline kinase is a frequent feature in human tumor-derived cell lines and in lung, prostate, and colorectal human cancers. *Biochemical and Biophysical Research Communications* 296, 580-583 (2002)

**Rantalainen, M., Cloarec, O., Beckonert, O., Wilson, I. D., Jackson, D., Tonge, R., Rowlinson, R., Rayner, S., Nickson, J., Wilkinson, R. W., Mills, J. D., Trygg, J., Nicholson, J. K. and Holmes, E.** Statistically integrated metabonomic-proteomic studies on a human prostate cancer xenograft model in mice. *Journal of Proteome Research* 5, 2642-2655 (2006)

**Reardon, J. T., Bessho, T., Kung, H. C., Bolton, P. H. and Sancar, A.** In vitro repair of oxidative DNA damage by human nucleotide excision repair system: Possible explanation for neurodegeneration in Xeroderma pigmentosum patients. *Proceedings of the National Academy of Sciences of the United States of America* 94, 9463-9468 (1997)

**Rikitake, K., Oka, I., Ando, M., Yoshimoto, T. and Tsuru, D.** Creatinine amidohydrolase (creatininase) from *Pseudomonas putida* - Purification and some properties. *Journal of Biochemistry* 86, 1109-1117 (1979)

**Robosky, L. C., Wells, D. F., Egnash, L. A., Manning, M. L., Reily, M. D. and Robertson, D. G.** Metabonomic identification of two distinct phenotypes in Sprague-Dawley (CrI:CD(SD)) rats. *Toxicological Sciences* 87, 277-84 (2005)

**Rogers, M. A., Clarke, P., Noble, J., Munro, N. P., Paul, A., Selby, P. J. and Banks, R. E.** Proteomic profiling of urinary proteins in renal cancer by surface enhanced laser desorption ionization and neural-network analysis: Identification of key issues affecting potential clinical utility. *Cancer Research* 63, 6971-6983 (2003)

**Rohde, C. M., Wells, D. F., Robosky, L. C., Manning, M. L., Clifford, C. B., Reily, M. D. and Robertson, D. G.** Metabonomic evaluation of schaedler altered microflora rats. *Chemical Research in Toxicology* 20, 1388-1392 (2007)

**Ross, R. J. M.** GH, IGF-I and binding proteins in altered nutritional states. *International Journal of Obesity* 24, S92-S95 (2000)

**Roy-Burman, P., Wu, H., Powell, W. C., Hagenkord, J. and Cohen, M. B.** Genetically defined mouse models that mimic natural aspects of human prostate cancer development. *Endocrine-Related Cancer* 11, 225 - 254 (2004)

**Saleem, M., Adhami, V. M., Ahmad, N., Gupta, S. and Mukhtar, H.** Prognostic significance of metastasis-associated protein S100A4 (Mts1) in prostate cancer progression and chemoprevention regimens in an autochthonous mouse model. *Clinical Cancer Research* 11, 147-153 (2005)

**Saleem, M., Adhami, V. M., Siddiqui, I. A. and Mukhtar, H.** Tea beverage in chemoprevention of prostate cancer: A mini- review. *Nutrition and Cancer-an International Journal* 47, 13-23 (2003)

**Sangster, T. P., Wingate, J. E., Burton, L., Teichert, F. and Wilson, I. D.** Investigation of analytical variation in metabonomic analysis using liquid chromatography/mass spectrometry. *Rapid Communications in Mass Spectrometry* 21, 2965-2970 (2007)

**Santin, A. D., Zhan, F., Cane, S., Bellone, S., Palmieri, M., Thomas, M., Burnett, A., Roman, J. J., Cannon, M. J., Shaughnessy, J. and Pecorelli, S.** Gene expression fingerprint of uterine serous papillary carcinoma: identification of novel molecular markers for uterine serous cancer diagnosis and therapy. *British Journal of Cancer* 92, 1561-1573 (2005)

**Saudek, C. D. and Felig, P.** The metabolic events of starvation. *The American Journal of Medicine* 60, 117-26 (1976)

**Scaltriti, M., Belloni, L., Caporali, A., Davalli, P., Remondini, D., Rizzi, F., Astancolle, S., Corti, A. and Bettuzzi, S.** Molecular classification of green tea catechin-sensitive and green tea catechin-resistant prostate cancer in the TRAMP mice model by quantitative real-time PCR gene profiling. *Carcinogenesis* 27, 1047-1053 (2006)

**Schaub, S., Rush, D., Wilkins, J., Gibson, I. W., Weiler, T., Sangster, K., Nicolle, L., Karpinski, M., Jeffry, J. and Nickerson, P.** Proteomic-based detection of urine proteins associated with acute renal allograft rejection. *Journal of the American Society of Nephrology* 15, 219-227 (2004)

**Seavey, B. R., Farr, E. A., Westler, W. M. and Markley, J. L.** A relational database for sequence-specific protein NMR data. *Journal of Biomolecular NMR* 1, 217-236 (1991)

**Semmes, O. J., Feng, Z., Adam, B. L., Banez, L. L., Bigbee, W. L., Campos, D., Cazares, L. H., Chan, D. W., Grizzle, W. E., Izbicka, E., Kagan, J., Malik, G., McLerran, D., Moul, J. W., Partin, A., Prasanna, P., Rosenzweig, J., Sokoll, L. J., Srivastava, S., Thompson, I., Welsh, M. J., White, N., Winget, M., Yasui, Y., Zhang, Z. and Zhu, L.** Evaluation of serum protein profiling by surface-enhanced laser desorption/ionization time-of-flight mass spectrometry for the detection of prostate cancer: I. Assessment of platform reproducibility. *Clinical Chemistry* 51, 102-112 (2005)

**Seraglia, R., Ragazzi, E., Vogliardi, S., Allegri, G., Pucciarelli, S., Agostini, M., Lise, M., Nitti, D., Urso, E. D. and Traldi, P.** Search of plasma markers for colorectal cancer by matrix- assisted laser desorption/ionization mass spectrometry. *Journal of Mass Spectrometry* 40, 123-126 (2005)

**Shigenaga, M. K., Gimeno, C. J. and Ames, B. N.** Urinary 8-Hydroxy-2'-Deoxyguanosine as a Biological Marker of Invivo Oxidative DNA Damage. *Proceedings of the National Academy of Sciences of the United States of America* 86, 9697-9701 (1989)

**Shimotoyodome, A., Haramizu, S., Inaba, M., Murase, T. and Tokimitsu, I.** Exercise and green tea extract stimulate fat oxidation and prevent obesity in mice. *Medicine and Science in Sports and Exercise* 37, 1884-1892 (2005)

**Singh, R., McEwan, M., Lamb, J. H., Santella, R. M. and Farmer, P. B.** An improved liquid chromatography/tandem mass spectrometry method for the determination of 8-oxo-7,8-dihydro-2'-deoxyguanosine in DNA samples using immunoaffinity column purification. *Rapid Communications in Mass Spectrometry* 17, 126-134 (2003)

**Siomek, A., Gackowski, D., Rozalski, R., Dziaman, T., Szpila, A., Guz, J. and Olinski, R.** Higher leukocyte 8-oxo-7,8-dihydro-2'-deoxyguanosine and lower plasma ascorbate in aging humans? *Antioxidants & Redox Signaling* 9, 143-150 (2007)

**Skytt, A., Thysell, E., Stattin, P., Stenman, U. H., Antti, H. and Wikstrom, P.** SELDI-TOF MS versus prostate specific antigen analysis of prospective plasma samples in a nested case-control study of prostate cancer. *International Journal of Cancer* 121, 615-620 (2007)

**Slattery, M. L. and West, D. W.** Smoking, alcohol, coffee, tea, caffeine, and theobromine - Risk of prostate cancer in Utah (United States). *Cancer Causes & Control* 4, 559-563 (1993)

**Smith, C. A., O'Maille, G., Want, E. J., Qin, C., Trauger, S. A., Brandon, T. R., Custodio, D. E., Abagyan, R. and Siuzdak, G.** METLIN: a metabolite mass spectral database. *Therapeutic Drug Monitoring* 27, 747-51 (2005)

**Smith, J. R., Freije, D., Carpten, J. D., Gronberg, H., Xu, J. F., Isaacs, S. D., Brownstein, M. J., Bova, G. S., Guo, H., Bujnovszky, P., Nusskern, D. R., Damber, J. E., Bergh, A., Emanuelsson, M., Kallioniemi, O. P., WalkerDaniels, J., BaileyWilson, J. E., Beaty, T. H., Meyers, D. A., Walsh, P. C., Collins, F. S., Trent, J. M. and Isaacs, W. B.** Major susceptibility locus for prostate cancer on chromosome 1 suggested by a genome-wide search. *Science* 274, 1371-1374 (1996)

**Sohal, R. S., Agarwal, S., Candas, M., Forster, M. J. and Lal, H.** Effect of age and caloric restriction on DNA oxidative damage in different tissues of C57BL/6 mice. *Mechanisms of Ageing and Development* 76, 215-224 (1994)

**Solanky, K. S., Bailey, N. J., Beckwith-Hall, B. M., Bingham, S., Davis, A., Holmes, E., Nicholson, J. K. and Cassidy, A.** Biofluid <sup>1</sup>H NMR-based metabonomic techniques in nutrition research metabolic effects of dietary isoflavones in humans. *Journal of Nutritional Biochemistry* 16, 236-244 (2005)

**Solanky, K. S., Bailey, N. J. C., Beckwith-Hall, B. M., Davis, A., Bingham, S., Holmes, E., Nicholson, J. K. and Cassidy, A.** Application of biofluid <sup>1</sup>H nuclear magnetic resonance-based metabonomic techniques for the analysis of the biochemical effects of dietary isoflavones on human plasma profile. *Analytical Biochemistry* 323, 197-204 (2003a)

**Solanky, K. S., Bailey, N. J. C., Holmes, E., Lindon, J. C., Davis, A. L., Mulder, T. P. J., Van Duynhoven, J. P. M. and Nicholson, J. K.** NMR-based metabonomic studies on the biochemical effects of epicatechin in the rat. *Journal of Agricultural and Food Chemistry* 51, 4139-4145 (2003b)

**Sporn, M. B., Dunlop, N. M., Newton, D. L. and Smith, J. M.** Prevention of chemical carcinogenesis by Vitamin A and its synthetic analogs (Retinoids). *Federation Proceedings* 35, 1332-1338 (1976)

**Stevens, J. C., Banks, G. T., Festing, M. F. W. and Fischer, E. M. C.** Quiet mutations in inbred strains of mice. *Trends in Molecular Medicine* 13, 512-519 (2007)

**Swanson, M. G., Zektzer, A. S., Tabatabai, Z. L., Simko, J., Jarso, S., Keshari, K. R., Schmitt, L., Carroll, P. R., Shinohara, K., Vigneron, D. B. and Kurhanewicz, J.** Quantitative analysis of prostate metabolites using <sup>1</sup>H HR-MAS spectroscopy. *Magnetic Resonance in Medicine* 55, 1257-64 (2006)

**Swanson, M. G., Keshari, K. R., Tabatabai, Z. L., Simko, J. P., Shinohara, K., Carroll, P. R., Zektzer, A. S. and Kurhanewicz, J.** Quantification of choline- and ethanolamine-containing metabolites in human prostate tissues using  $^1\text{H}$  HR-MAS total correlation spectroscopy. *Magnetic Resonance in Medicine* 60, 33-40 (2008)

**Swanson, M. G., Vigneron, D. B., Tabatabai, Z. L., Males, R. G., Schmitt, L., Carroll, P. R., James, J. K., Hurd, R. E. and Kurhanewicz, J.** Proton HR-MAS spectroscopy and quantitative pathologic analysis of MRI/3D-MRSI-targeted postsurgical prostate tissues. *Magnetic Resonance in Medicine* 50, 944-954 (2003)

**Tabaqchali, S., Hatzioannou, J. and Booth, C. C.** Bile-salt deconjugation and steatorrhoea in patients with the stagnant-loop syndrome. *Lancet* 2, 12-6 (1968)

**Takahashi, N., Boysen, G., Li, F., Li, Y. and Swenberg, J. A.** Tandem mass spectrometry measurements of creatinine in mouse plasma and urine for determining glomerular filtration rate. *Kidney International* 71, 266-271 (2007)

**Tam, N. N. C., Nyska, A., Maronpot, R. R., Kissling, G., Lomnitski, L., Suttie, A., Bakshi, S., Bergman, M., Grossman, S. and Ho, S. M.** Differential attenuation of oxidative/nitrosative injuries in early prostatic neoplastic lesions in TRAMP mice by dietary antioxidants. *Prostate* 66, 57-69 (2006)

**Tammen, H., Zucht, H. D. and Budde, P.** Oncopeptidomics - A commentary on opportunities and limitations. *Cancer Letters* 249, 80-86 (2007)

**Teahan, O., Gamble, S., Holmes, E., Waxman, J., Nicholson, J. K., Bevan, C. and Keun, H. C.** Impact of analytical bias in metabolomic studies of human blood serum and plasma. *Analytical Chemistry* 78, 4307-4318 (2006)

**Theodorescu, D., Fliser, D., Wittke, S., Mischak, H., Krebs, R., Walden, M., Ross, M., Eltze, E., Bettendorf, O., Wulfing, C. and Semjonow, A.** Pilot study of capillary electrophoresis coupled to mass spectrometry as a tool to define potential prostate cancer biomarkers in urine. *Electrophoresis* 26, 2797-2808 (2005)

**Thompson, I. M. and Ankerst, D. P.** Prostate-specific antigen in the early detection of prostate cancer. *Canadian Medical Association Journal* 176, 1853-1858 (2007)

**Thompson, I. M., Goodman, P. J., Tangen, C. M., Lucia, M. S., Miller, G. J., Ford, L. G., Lieber, M. M., Cespedes, R. D., Atkins, J. N., Lippman, S. M., Carlin, S. M., Ryan, A., Szczepanek, C. M., Crowley, J. J. and Coltman, C. A.** The influence of finasteride on the development of prostate cancer. *New England Journal of Medicine* 349, 215-224 (2003)

**Thorpe, J., Jain, S., Marcylo, T., Gescher, A., Steward, W. and Mellon, J. K.** Theaflavins inhibit prostate carcinogenesis in the TRAMP mouse model. *Journal of Urology* 175, 81-81 (2006)

**Thürmer, R., Meisenbach, M., Echner, H., Weiler, A., Al-Qawasmeh, R. A., Voelter, W., Korff, U. and Schmitt-Sody, W.** Monitoring of liquid-phase peptide synthesis on soluble polymer supports via matrix-assisted laser desorption/ionization time-of-flight mass spectrometry. *Rapid Communications in Mass Spectrometry* 12, 398-402 (1998)

**Tomlins, A. M., Foxall, P. J. D., Lindon, J. C., Lynch, M. J., Spraul, M., Everett, J. R. and Nicholson, J. K.** High resolution magic angle spinning <sup>1</sup>H nuclear magnetic resonance analysis of intact prostatic hyperplastic and tumour tissues. *Analytical Communications* 35, 113-115 (1998)

**Tsuzuki, T., Egashira, A., Igarashi, H., Iwakuma, T., Nakatsura, Y., Tominaga, Y., Kawate, H., Nakao, K., Nakamura, K., Ide, F., Kura, S., Nakabeppu, Y., Katsuki, M., Ishikawa, T. and Sekiguchi, M.** Spontaneous tumorigenesis in mice defective in the MTH1 gene encoding 8-oxo-dGTPase. *Proceedings of the National Academy of Sciences of the United States of America* 98, 11456-11461 (2001)

**Valitutti, S., Cucchi, P., Colletta, G., Di Filippo, C. and Corda, D.** Transformation by the K-ras oncogene correlates with increases in phospholipase A2 activity, glycerophosphoinositol production and phosphoinositide synthesis in thyroid cells. *Cell Signalling* 3, 321-332 (1991)

**van der Rest, B., Boisson, A. M., Gout, E., Bligny, R. and Douce, R.** Glycerophosphocholine metabolism in higher plant cells. Evidence of a new glyceryl-phosphodiester phosphodiesterase. *Plant Physiology* 130, 244-255 (2002)

**van Dorsten, F. A., Daykin, C. A., Mulder, T. P. J. and van Duynhoven, J. P. M.** Metabonomics approach to determine metabolic differences between green tea and black tea consumption. *Journal of Agricultural and Food Chemistry* 54, 6929-6938 (2006)

**Venkateswaran, V., Xu, H. Y., Fleshner, N. and Klotz, L.** Inhibition of prostate carcinogenesis in lady TRAMP mice by the administration of dietary antioxidants: Protein profiling by SELDI mass spectrometry. *Journal of Urology* 169, S194 (2003)

**Villanueva, J., Philip, J., Entenberg, D., Chaparro, C. A., Tanwar, M. K., Holland, E. C. and Tempst, P.** Serum peptide profiling by magnetic particle-assisted, automated sample processing and MALDI-TOF mass spectrometry. *Analytical Chemistry* 76, 1560-70 (2004)

**Villanueva, J., Shaffer, D. R., Philip, J., Chaparro, C. A., Erdjument-Bromage, H., Olshen, A. B., Fleisher, M., Lilja, H., Brogi, E., Boyd, J., Sanchez-Carbayo, M., Holland, E. C., Cordon-Cardo, C., Scher, H. I. and Tempst, P.** Differential exoprotease activities confer tumor-specific serum peptidome patterns. *Journal of Clinical Investigation* 116, 271-284 (2006)

**Vlahou, A., Schellhamrner, P. F., Mendrinos, S., Patel, K., Kondylis, F. I., Gong, L., Nasim, S. and Wright, G. L.** Development of a novel proteomic approach for the detection of transitional cell carcinoma of the bladder in urine. *American Journal of Pathology* 158, 1491-1502 (2001)

**Want, E. J., Smith, C. A., Qin, C. A., VanHorne, K. C. and Siuzdak, G.** Phospholipid capture combined with non-linear chromatographic correction for improved serum metabolite profiling. *Metabolomics* 2, 145-154 (2006)

**Waters.** Therapeutic peptides: oxytocin and angiotensin I and II (Guideline for peptides), p152. *Oasis*<sup>®</sup> *Applications Notebook* available from:

<http://www.waters.com/WatersDivision/pdfs/720000609EN.pdf>, (2003)

**Weaver, R. and Riley, R. J.** Identification and reduction of ion suppression effects on pharmacokinetic parameters by polyethylene glycol 400. *Rapid Communications in Mass Spectrometry* 20, 2559-2564 (2006)

**Weber, J. A. and Vanzanten, A. P.** Interferences in Current Methods for Measurements of Creatinine. *Clinical Chemistry* 37, 695-700 (1991)

**Williams, R., Lenz, E. M., Wilson, A. J., Granger, J., Wilson, I. D., Major, H., Stumpf, C. and Plumb, R.** A multi-analytical platform approach to the metabonomic analysis of plasma from normal and Zucker (fa/fa) obese rats. *Molecular Biosystems* 2, 174-183 (2006)

**Willingale, R., Jones, D. J. L., Lamb, J. H., Quinn, P., Farmer, P. B. and Ng, L. L.** Searching for biomarkers of heart failure in the mass spectra of blood plasma. *Proteomics* 6, 5903-5914 (2006)

**Wilson, I. D., Plumb, R., Granger, J., Major, H., Williams, R. and Lenz, E. A.** HPLC-MS-based methods for the study of metabonomics. *Journal of Chromatography B-Analytical Technologies in the Biomedical and Life Sciences* 817, 67-76 (2005)

**Wolfensohn, S. and Lloyd, M.** Handbook of laboratory animal management and welfare, second Edition, *Blackwell Science* (1998).

**Wolk, A.** Diet, lifestyle and risk of prostate cancer. *Acta Oncologica* 44, 277-281 (2005)

**Wu, L. L., Chiou, C. C., Chang, P. Y. and Wu, J. T.** Urinary 8-OHdG: A marker of oxidative stress to DNA and a risk factor for cancer, atherosclerosis and diabetics. *Clinica Chimica Acta* 339, 1-9 (2004)

**Xu, X., Harris, K. S., Wang, H. J., Murphy, P. A. and Hendrich, S.** Bioavailability of soybean isoflavones depends upon gut microflora in women. *Journal of Nutrition* 125, 2307-2315 (1995)

**Ye, B., Skates, S., Mok, S. C., Horick, N. K., Rosenberg, H. F., Vitonis, A., Edwards, D., Sluss, P., Han, W. K., Berkowitz, R. S. and Cramer, D. W.** Proteomic-based discovery and characterization of glycosylated eosinophil-derived neurotoxin and COOH-terminal osteopontin fragments for ovarian cancer in urine. *Clinical Cancer Research* 12, 432-441 (2006)

**Young, J. F., Dragsted, L. O., Haraldsdottir, J., Daneshvar, B., Kall, M. A., Loft, S., Nilsson, L., Nielsen, S. E., Mayer, B., Skibsted, L. H., Huynh-Ba, T., Hermetter, A. and Sandstrom, B.** Green tea extract only affects markers of oxidative status postprandially: lasting antioxidant effect of flavonoid-free diet. *British Journal of Nutrition* 87, 343-355 (2002)

**Yuan, J. P., Wang, J. H. and Liu, X.** Metabolism of dietary soy isoflavones to equol by human intestinal microflora - implications for health. *Molecular Nutrition & Food Research* 51, 765-781 (2007)

**Zanchi, R., Canzi, E., Molteni, L. and Scozzoli, M.** Effect of *Camellia sinensis* L. whole plant extract on piglet intestinal ecosystem. *Annals of Microbiology* 58, 147-152 (2008)

**Zhang, S. D. and Gant, T. W.** A statistical framework for the design of microarray experiments and effective detection of differential gene expression. *Bioinformatics* 20, 2821-2828 (2004)

**Zhang, X., Leung, S.-M., Morris, C. R. and Shigenaga, M. K.** Evaluation of a novel, integrated approach using functionalized magnetic beads, bench-top MALDI-Tof-MS and pattern recognition software for profiling potential biomarkers in human plasma. *Journal of Biomolecular Techniques* 15, 167-175 (2004)